MACROPHAGE PHENOTYPE AND FUNCTION IN PRIMARY LUNG CANCER

[Saleh Abdulrahman Al Matroodi]

[Master of Laboratory Medicine]

Submitted in fulfilment of the requirements for the degree of Doctor of Philosophy

School of Medical Sciences

College of Science Engineering and Health

RMIT University

[January, 2015]

Supervisors:

Dr. Dodie Pouniotis

Prof. Christine McDonald

A/Prof. Ian Darby

Declaration

I certify that except where due acknowledgement has been made, the work is that of the author alone; the work has not been submitted previously, in whole or in part, to qualify for any other academic award; the content of the thesis/project is the result of work which has been carried out since the official commencement date of the approved research program; any editorial work, paid or unpaid, carried out by a third party is acknowledged; and, ethics procedures and guidelines have been followed.

Saleh Abdulrahman Al Matroodi

19/07/15

Keywords

Alveolar macrophages; Bronchoalveolar lavage fluid; Blood; Cytometric bead array; Cytokines; Chemokines; Deoxyribonucleic acid; Function; Flow cytometry; Genes; Human Lung; Lung cancer; Macrophage; Monocyte; M1 classical macrophage; M2 alternative macrophage; Non-small cell lung carcinoma; Peripheral blood monocyte; Phenotype; Polarisation; Plasma; Proteomics; Proteins; Real-time polymerase chain reaction; Tumour environment; Tumour microenvironment; Tumour progression; Tumour regression

Abstract

Background: Lung cancer is one of the most commonly reported cancers, and is known to be associated with a poor prognosis. The role of macrophages in lung cancer, including alveolar macrophages (AMs), tumour-associated macrophages (TAMs) and monocytes, is multifaceted and the literature shows conflicting roles. In the lungs, macrophages are termed AMs and are located both in the air spaces of the lungs and in the lower airways. AMs play a vital role in the lung microenvironment and have been used to investigate cellular changes within the lung environment in different pulmonary diseases, including lung cancer. Similar to TAMs, two distinct phenotypes of AMs have been identified within the lungs, the M1 (classically activated) and M2 (alternatively activated) macrophage subsets. TAMs are a cell type belonging to the macrophage lineage and are known to be located near or within tumour masses. They have been considered to be a better macrophage type to study in cancer research, because of their location within tumour microenvironment and interaction with cancer cells. Similarly, monocytes play an essential role in the immune response against tumour cells in the systemic environment. Monocytes have been shown to have similar phenotypes to those seen in the M1 and M2 TAMs population in tumour microenvironments. Although macrophage subsets have been well characterised in many cancers, their phenotype and function in lung cancer still needs further investigation. **Aims**: (I) To characterise the M1 and M2 macrophage populations within the AM population using flow cytometry and real-time quantitative polymerase chain reaction (RT-PCR) in patients with non-small lung carcinoma (NSCLC) compared to non-cancer controls; (II) To evaluate the M1 and M2 monocyte populations (macrophage precursors) in patients with NSCLC compared to non-cancer controls using flow cytometry. In addition, Th1 and Th2 cytokine levels that contribute to the differentiation of these populations will be analysed in the serum of patients

with NSCLC versus non-cancer controls; (III) To use quantitative proteomics to investigate the up-regulation of novel proteins in bronchoalveolar lavage (BAL) fluid from patients with primary lung adenocarcinoma to potentially identify new potential biomarkers expressed by AMs; and (IV) To characterise the M1 and M2 macrophage populations within TAMs in different subtypes of NSCLC compared to non-cancer lung tissue. **Methods and materials**: AMs were obtained from patients with NSCLC and non-cancer control subjects and analysed for surface marker differences using flow cytometry. The mRNA expression of IL-6, IL-12, IL-10 and MMP-9 cytokines was measured using RT-PCR. Freshly prepared peripheral blood mononuclear cell (PBMC) samples were also obtained from patients with NSCLC and from non-cancer controls. Flow cytometry was performed to investigate the expression of M1 and M2 markers on peripheral monocytes (classical monocytes CD14^{++}, CD45^{+} and CD16^{-}). The Th1 and Th2 cytokine levels were analysed in serum samples using the cytometric bead array (CBA) and the Bio-Plex, MAGPIC-Luminex system, respectively. In addition, BAL fluid samples from subjects with and without primary lung adenocarcinoma were analysed using quantitative proteomics. Finally, TAMs subsets from non-tumour and tumour tissues were analysed using immunohistochemistry (IHC). **Results**: The expression of M2 marker CD163 as well as CD71 and CD44 was greater on AMs from patients with NSCLC compared to non-cancer controls. However, there were no significant differences in the surface expression (%SE) of M1 marker HLA-DR (Human leukocyte antigen-D related) and myeloid marker CD11b in NSCLC patients compared to non-cancer controls. The mRNA expression levels of IL-10 and MMP-9 were increased in AMs from NSCLC patients compared to non-cancer controls. In contrast, the expression of IL-6 and IL-12 was not significantly different in NSCLC patients compared to non-cancer controls. There were no significant differences in the expression of M1 (HLA-DR) and/or M2 markers (CD163 and CD36) on classical monocytes in patients with NSCLC compared to non-cancer controls. The expression of

CD11b, CD11c, CD71 and CD44 were also shown to be similar in patients with NSCLC compared to non-cancer controls. The Th1 and Th2 cytokines levels in serum revealed no significant difference between patients with NSCLC (undifferentiated NSCLC, lung adenocarcinoma and squamous cell lung carcinoma) and non-cancer controls. However, the expression of IL-1β, IL-4, IL-6 and IL-8 was found to be significantly increased in serum of patients with large cell lung carcinoma but not in other lung cancer subtypes compared to non-cancer controls using the Bio-Plex, MAGPIC-Luminex assay. For proteomic analysis, 1,100 proteins were identified and 33 of these were found to be consistently over-expressed in the BAL fluid of adenocarcinoma samples compared to non-cancer controls. These proteins included S100-A8, annexin A1, annexin A2, thymidine phosphorylase (TP) and transglutaminase 2 (TG2) which have been shown previously to be related to cancer progression. Other over-expressed identified proteins such as chloride intracellular channel protein 1, transgelin-2, catalase, carbonic anhydrase II, galectin-1, and Lamin-B1 have been shown to be promising new lung cancer biomarkers. For the TAMs investigation, the expression of CD68 and M2 marker CD163 was found to be significantly increased in all NSCLC subtypes (adenocarcinoma, squamous cell lung carcinoma and large cell lung carcinoma) compared to non-tumour tissues. In contrast, the expression of iNOS (M1 marker) was significantly decreased in the tumour tissue of patients with adenocarcinoma and squamous cell lung carcinoma but not in large cell lung carcinoma compared to non-tumour tissue. **Conclusion**: The results of the AM study (aim I) suggested that NSCLC has the ability to alter AMs function and play a role in changing their phenotype. Different markers and cytokines such as CD163, CD71, CD44, IL-10 and MMP-9 were found to be altered in patients with NSCLC compared to non-cancer controls. It also indicated that AMs express more M2 phenotype in NSCLC patients compared to non-cancer controls. Moreover, the result of the monocyte study (aim II) showed no alteration in classical peripheral blood

monocyte phenotype and function in patients with NSCLC compared to non-cancer controls. Therefore, these results suggested that there is no systemic impairment in monocyte phenotype and function in patients with NSCLC compared to non-cancer controls. The Th1/Th2 cytokine levels were also found to not be affected by the presence of NSCLC (except large cell lung carcinoma) compared to non-cancer controls. The expression of some Th1 and Th2 cytokines (IL-1β, IL-4, IL-6 and IL-8) were altered in patients with large cell lung carcinoma, which indicates the ability of this lung cancer subtype to manipulate cytokine expression in the systemic environment. In addition, the results of the proteomics study (aim III) demonstrated an overexpression of a number of novel proteins in BAL fluid of adenocarcinoma patients may be utilised as potential biomarkers. These proteins included S100-A8, annexin A1, annexin A2, thymidine phosphorylase (TP) and transglutaminase 2 (TG2) which are known to be related to cancer progression. The last aim results (TAM study) suggested that NSCLC has the ability to alter TAMs phenotype. The expression of M2 marker CD163 was found to be significantly increased in all NSCLC subtypes compared to non-tumour tissues. In contrast, the expression of iNOS (M1 marker) was significantly decreased in the tumour tissue of patients with adenocarcinoma and squamous cell lung carcinoma but not in large cell lung carcinoma compared to non-tumour tissues. These results indicated that TAMs express more M2 phenotype in NSCLC patients compared to non-tumour tissues. Taken together, the results of this thesis indicate that NSCLC might have the ability to alter phenotype and function within the lung tumour areas in the local environment (AMs and TAMs) but not in the bloodstream in the systemic environment (monocytes and serum). The thesis outcomes support the previous suggestion regarding the importance of potentially targeting M2 macrophages for future therapeutic agents and aim to skew macrophage populations back to M1 subsets to stimulate anti-tumour effects within the tumour microenvironment.

Table of Contents

List of Abbreviations

AMs: Alveolar macrophages

ATS: American Thoracic Society

BA: Basophil

BAL fluid: Bronchoalveolar lavage fluid

bFGF: Basic fibroblast growth factor

BSA: Bovine serum albumin

cAMP: Cyclic adenosine monophosphate

CBA: Cytometric bead array

CBC: Complete blood count

cDNA: Complementary deoxyribonucleic acid

COPD: Chronic obstructive pulmonary disease

DC: Dendritic cells

DMSO: Dimethyl sulfoxide

DNA: Deoxyribonucleic acid

ECM: Extracellular matrix

EGFR: Epidermal growth factor receptor

ELISA: Enzyme-linked immunosorbent assay

EO: Eosinophil

ERS: European Respiratory Society

FITC: Fluorescein isothiocyanate

FBS: Fetal bovine serum

FI: Fluorescence intensity

FSC: Forward scatter

GA: Golgi apparatus

GM-CSF: Granulocyte-macrophage colony-stimulating factor

HLA-DR: Human leukocyte antigen-D related

HIF-1α: Hypoxia-inducible factor 1-alpha

IASLC: International Association for the Study of Lung Cancer

ICAM-1: Intracellular adhesion molecule

IFN-γ: Interferon gamma

IHC: Immunohistochemistry

IL-: Interleukin-

IL-1β: Interleukin-1 beta

IL-2: Interleukin-2

IL-4: Interleukin-4

IL-5: Interleukin-5

IL-6: Interleukin-6

IL-8: Interleukin-8

IL-10: Interleukin-10

IL-12: Interleukin-12

iNOS: Inducible nitric oxide synthase

IP-10: IFN-γ inducible protein 10

KRAS: Kirsten rat sarcoma viral oncogene homolog

LPS: Lipopolysaccharide

LY: Lymphocyte

MO: Monocyte

M1: Classically activated macrophages

M2: Alternatively activated macrophages

MCP-1: Monocyte chemoattractant protein-1

M-CSF: Macrophage colony-stimulating factor

MHC: Major histocompatibility complex

MFI: Mean fluorescence intensity

MMPs: Matrix metalloproteinases

MMP-9: Matrix metalloproteinases-9

MMP-12: Matrix metalloproteinases-12

mRNA: Messenger ribonucleic acid

MW: Molecular weight

NK: Natural killer cells

NOS: Nitric oxide synthase

NF-κB: Nuclear factor-κB

p38 MAPK: p38 mitogen-activated protein kinases

PBMC: Peripheral blood mononuclear cells

PBS: Phosphate buffered saline

PDGF: Platelet derived growth factor

PE: Phycoerythrin

NE: Neutrophil

NSCLC: Non-small cell lung carcinoma

RBC: Red blood cell

RER: Rough endoplasmic reticulum

RFTs: Respiratory function tests

RNA: Ribonucleic acid

RNS: Reactive nitrogen species

ROS: Reactive oxygen species

RT-PCR: Real-time polymerase chain reaction

SD: Standard deviation

%SE: Surface expression

SEM: Standard error of the mean

SSC: Side scatter

TAMs: Tumour-associated macrophages

TCEP: Tris2-carboxyethyl phosphine

TEAB: Triethyl ammonium bicarbonate

TGF: Transforming growth factor

TGF-β: Transforming growth factor-β

TLRs: Toll-like receptor

TNM: Tumour, node, metastases staging system

TNF: Tumour necrosis factor

TNF-α: Tumour necrosis factor alpha

TNF-β: Tumour necrosis factor beta

VEGF: Vascular endothelial growth factor

WBC: White blood cell

WHO: World Health Organisation

List of Tables

List of Figures

Acknowledgements

Conference Contributions

Conferences

- Australian Flow Cytometry Group (AFCC) 34th annual meeting, "Using flow cytometry to characterise M1 and M2 phenotypes in alveolar macrophages from primary lung cancer patients", Tasmania, Australia 2011.

- RMIT University, College of Science Engineering and Health Higher Degree Research Student Conference, "Macrophage polarisation in primary lung cancer", Melbourne, Australia 2011.

- Australian Lung Cancer Conference, "Monocyte polarisation in primary lung cancer", 23 - 25 August 2012 Adelaide Convention Centre Adelaide, Australia.

- Austin Health, Research week, "Macrophage / monocyte polarisation in primary lung cancer", Melbourne, Australia 2012; 18 October.

- College of Science Engineering and Health Higher Degree Research Student Conference, "Macrophage polarisation in primary lung cancer", Melbourne, Australia 2012, 19 October.

- Austin Health, Research week, "Macrophage / monocyte polarisation in primary lung cancer", Melbourne, Australia 2013; November.

- RMIT University, College of Science Engineering and Health Higher Degree Research Student Conference, "Quantitative Proteomics of Bronchoalveolar Lavage Fluid in Lung Adenocarcinoma", Melbourne, Australia 2014.

Published Contributions

Papers

- ≠ Saleh A. Almatroodi, Christine F. McDonald, and Dodie S. Pouniotis, "Alveolar Macrophage Polarisation in Lung Cancer," Lung Cancer International, vol. 2014, Article ID 721087, 9 pages, 2014. doi: 10.1155/2014/721087.

- ≠ Almatroodi SA, McDonald CF, Collins AL, Darby IA, Pouniotis DS. Blood classical monocytes phenotype is not altered in primary non-small cell lung cancer. World journal of clinical oncology. 2014; 5(5): 1078-87.

- ≠ Almatroodi SA, McDonald CF, Collins AL, Darby IA, Pouniotis DS. Quantitative Proteomics of Bronchoalveolar Lavage Fluid in Lung Adenocarcinoma. Cancer genomics & proteomics. 2015; 12(1): 39-48.

- ≠ Almatroodi SA, McDonald CF, Collins AL, Darby IA, Pouniotis DS. Alveolar Macrophage Polarisation and Function is Altered in Primary Lung Cancer (Manuscript in preparation, to be submitted 2015).

- ≠ Almatroodi SA, McDonald CF, Collins AL, Darby IA, Pouniotis DS. Characterisation of M1 and M2 Tumour-Associated Macrophages (TAMs) in Patients with NSCLC (Manuscript in preparation, to be submitted 2015).

Chapter 1 Literature Review

1.1. Introduction

The human lungs are highly vascularised in order to facilitate their main role of gas exchange (1). They are exposed to numerous substances from the external environment, which can cause lung injury and eventually may lead to lung tumour initiation (2, 3). Lung cancer is a malignant tumour that generally initiates in the tissue of the lungs. It arises when lung cells convert from a normal to an abnormal state and then start to grow leading to the tumour mass origination (4). Lung cancer is one of the most common cancers worldwide and in the Western World particularly it has a high incidence (Fig. 1) (5). It has also been recognised to be the leading cause of cancer mortality worldwide with approximately 1 million deaths annually (6-8). In Australia, males with lung cancer have a worse prognosis than patients with other frequently diagnosed cancers. In particular, the 5-year relative survival for male lung cancer patients is shown to be 6 to 8 times lower than males with melanoma, prostate cancer, bowel cancer and lymphoid cancers. In addition, the 5-year relative survival for females diagnosed with lung cancer was about 4 to 6 times worse than for female patients who were diagnosed with melanoma, breast cancer, lymphoid cancers and bowel cancer (Fig. 2) (5). Despite the development of new treatments, lung cancer still has, in general, a poor prognosis and short patient survival time (9).
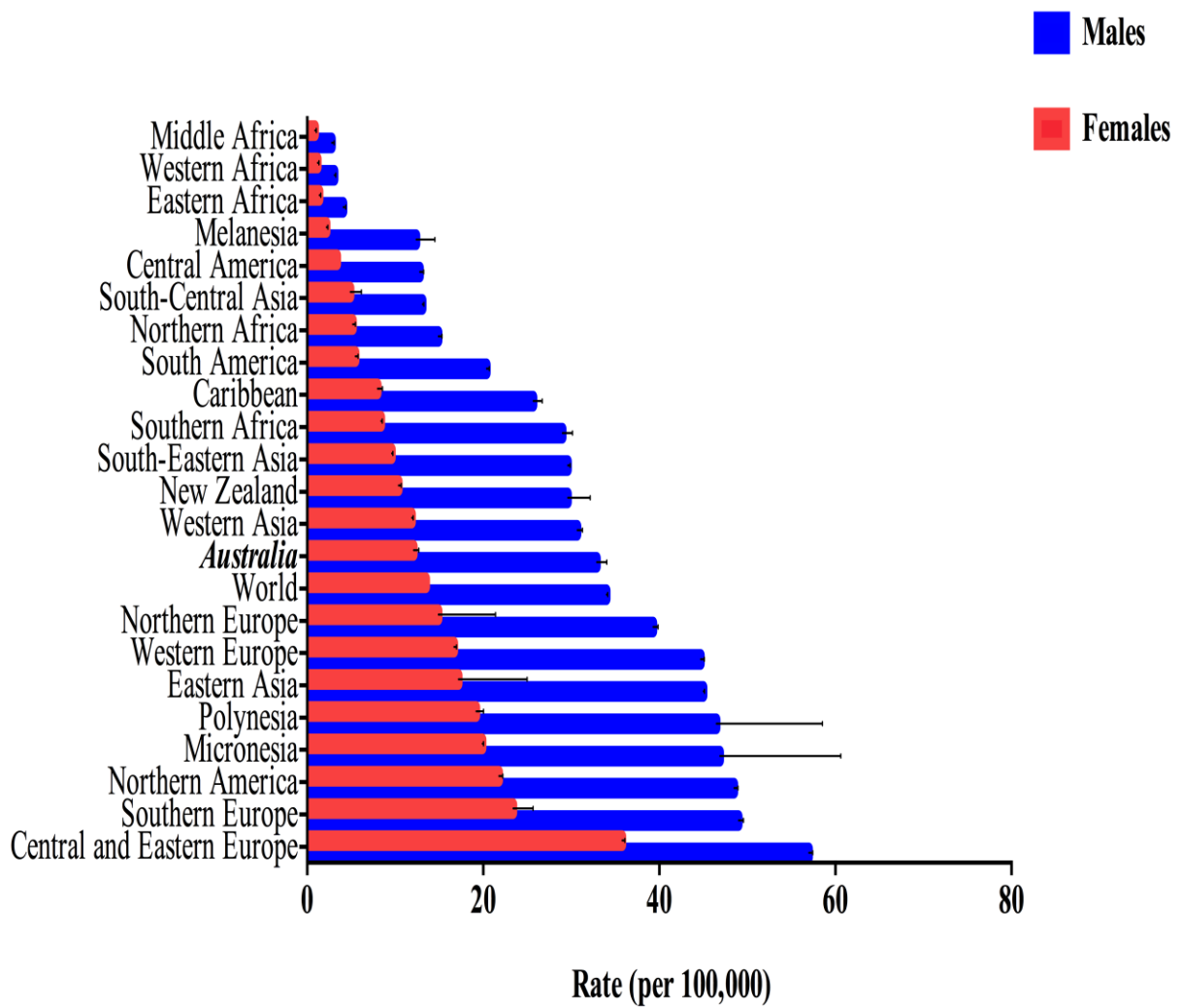
Figure 1: International comparison of estimated incidence of lung cancer, males and females, 2008. The incidence rate of lung cancer is high in developed regions including Australia, Europe and North America (5).
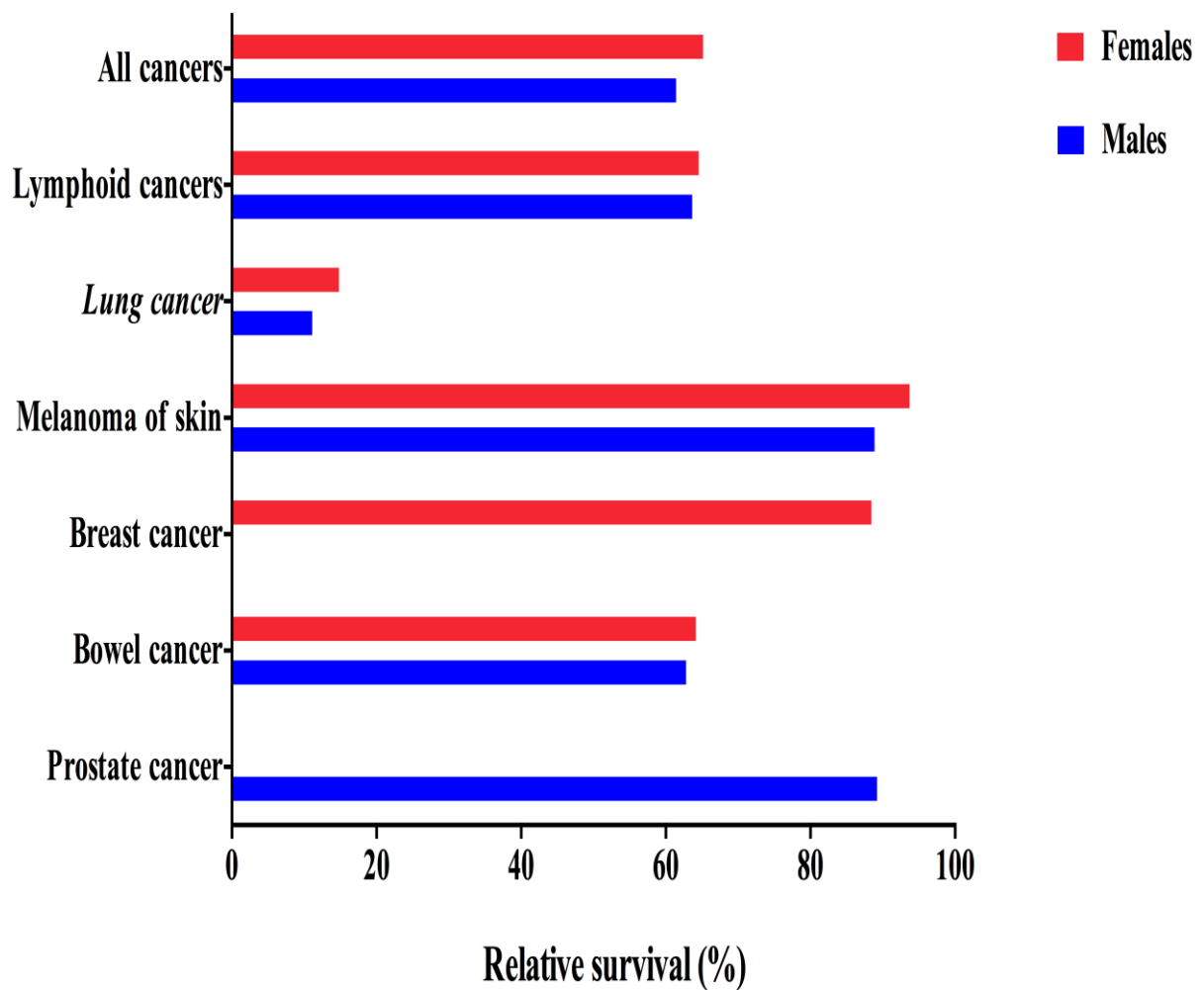
Figure 2: Five-year relative survival for most commonly diagnosed cancers in Australia from 2000 to 2007. This graph indicates that lung cancer patients, both males and females, have a poor prognosis in comparison to people with other frequently diagnosed cancers (5).

The human immune system is known to play a role in local and systemic defence that eventually inhibits tumour growth in most scenarios. Human immune system components such as macrophages are essential to control and prevent the initiation of cancer. They are also involved in cancer immunoediting through the innate and adaptive immune systems (10, 11). However, it has been shown that the human immune system may play a dual role in both eliminating and promoting human tumours. Thus, the human immune system has been described as a double-edged sword in regard to its interaction with tumour microenvironments (12). In particular, the role of macrophages in lung cancer is multifaceted and conflicting. They have the ability to produce pro-inflammatory factors that have been found to enhance anti-tumour functions. In contrast, pro-tumour functions of macrophages in lung cancer have also been reported. Thus, a dual role of macrophages is suggested in the lung cancer microenvironment (13).

Monocytes are a macrophage precursor and identified to be the leading source of recruited tissue macrophages (12). Macrophages can then migrate to local sites of injury, disorder and infection, where their presence leads to acute and chronic inflammation either in the local or systemic environment (14). In human lungs, alveolar macrophages (AMs) are located in the air spaces of the lungs and in the lower airways (15). AMs perform a vital role in the lung microenvironment and have been used to investigate cellular changes within the lung environment in a variety of pulmonary diseases, including lung cancer (16). Two distinct phenotypes of tumour-associated macrophages (TAMs) have been identified within the lungs; the classically activated macrophages (M1) and the alternatively activated macrophages (M2). Similar to macrophages, monocytes (macrophage precursors) play a vital role in the immune response against tumour cells. Monocytes have also been shown to have similar phenotypes (M1 and M2) in the blood stream to those shown by TAMs in the tumour microenvironments (17). The M1 macrophages are activated by IFN-γ with or without LPS

and TNF-α. They are generally suggested to be associated with anti-tumour functions and extended survival time in patients with non-small cell lung carcinoma (NSCLC) (18, 19). In contrast, the M2 macrophages have three well-defined forms: M2a which are induced by IL-4 or IL-13; M2b which are initiated by exposure to immune complexes and agonists of toll-like receptor (TLRs); and M2c which are induced by IL-10 and glucocorticoids. M2 are known to be related to tumour initiation, tumour growth, poor prognosis and tumour metastasis (18, 19).

It has been shown previously that there are many differences between polarised subsets of macrophages (M1 and M2) in terms of cytokine and chemokine secretion, cytokine and chemokine receptor, expression of surface markers and effector molecules (20). Each macrophage subset expresses distinct molecules under the influence of various macrophage activators (19). For instance, the cytokines and enzymes that have been described as inhibitors of tumour cell proliferation, such as IL-1, TNF-α (tumour necrosis factor alpha), ROS (reactive oxygen species) and NOS (nitric oxide synthase), are associated with the M1 subset. Conversely, M2 are associated with a low expression of such tumour inhibitor enzymes (e.g. iNOS) and produce factors such as IL-10 that are associated with tumour cell proliferation (19, 20). It has also been hypothesised that changes in the tumour microenvironment such as alterations in glucose levels and pH as well as the development of hypoxia may arise in the transition from an early to an advanced tumour stage (21). These factors could mediate macrophage phenotype alteration within the local or systemic environment.

Studies that have examined the role of macrophages in lung cancer have provided inconsistent results. Although some studies report increased cytotoxic activity and anti-tumour effects of these immune effector cells, others have reported decreased cytotoxic activity and pro-tumour effects (13, 22-27). A dual role for macrophages in lung cancer has

therefore been suggested, with the idea that they may both inhibit and/or promote tumour progression (13). Further investigation of macrophages is highly desirable in order to advance our understanding of these important components of the human immune system and their connection to the lung cancer microenvironment. This thesis aims to determine the influence of NSCLC on the phenotype and function of macrophages in their local (AMs and TAMs) and systemic (circulating classical blood monocytes and serum) environments. Samples used in this study were collected from patients with NSCLC and then compared to non-cancer controls. The resident AMs, circulating classical blood monocytes and serum were collected from bronchoalveolar lavage (BAL) fluid and blood, respectively. Various indicators and techniques were used in this study to illuminate the impact of NSCLC on macrophage (AMs, TAMs and monocytes) phenotype and function including flow cytometry, real-time quantitative polymerase chain reaction (RT-PCR), quantitative proteomics, cytometric bead array (CBA), Bio-Plex assay and immunohistochemistry (IHC).

1.2. The human lungs

The human lungs are surrounded by visceral pleura and they fill the pleural cavities. The lungs comprise approximately 80% air, 10% blood, 3% conductive airways and blood vessels, and only 3% is alveolar tissue. The lungs are divided into upper and lower lobes by oblique fissures and five lobar bronchi are divided from the main bronchi (Fig. 3) (28). The human lungs are highly vascularised to facilitate their main function of gas exchange. The adult human lungs have a surface area of approximately 150 m^2 that enables inhalation of about 10,000 – 15,000 litres of air every day (1). This exposes the lung to numerous toxic substances from the external environment with possible resulting lung injury. However, the respiratory tract has various defence mechanisms to overcome the inhalation of some external particles such as chemicals and microorganisms (2, 3). These mechanisms include coughing and sneezing when particles lodge and irritate the upper respiratory tract. In the lower respiratory tract, there are two main clearance methods, the mucociliary and phagocytic systems. The mucociliary system clears larger particles (<5 µm) from the trachea-bronchial airway while smaller particles (<0.1 µm) are removed by the phagocytic system, which is mainly mediated by resident AMs (2). However, repeated chronic lung injury can result in lung cancer initiation, which stimulates the creation of reactive oxygen and nitrogen species (ROS and RNS) and other pro-inflammatory chemokines and cytokines through the involvement of different inflammatory cells in the lung including macrophages (3, 29).
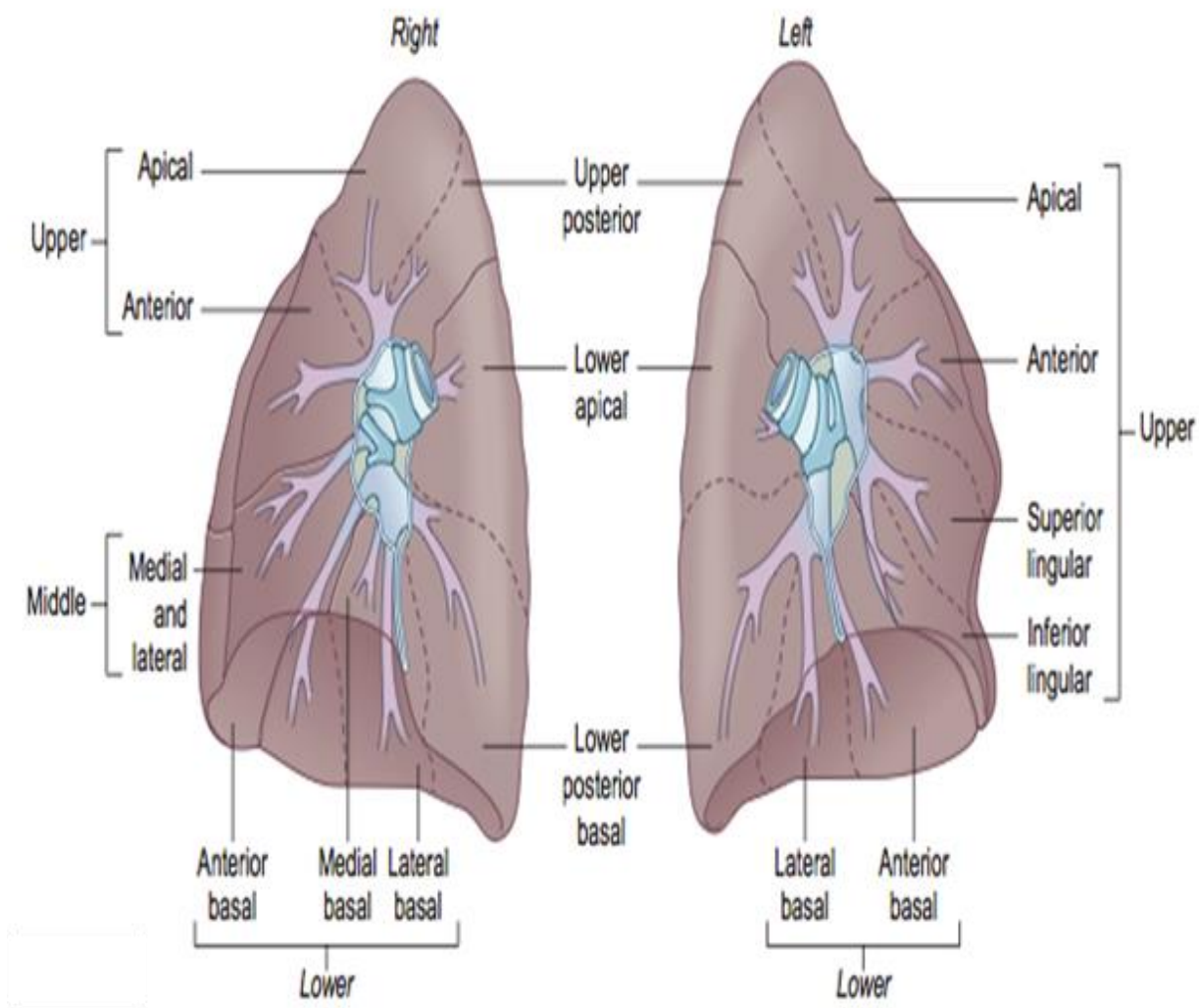
Figure 3: The normal structure of the human lungs. This image shows the structure of the normal human lungs. They are divided into upper and lower lobes by oblique fissures (28).

1.3. Histology of the normal human lungs and airways

The bronchial wall contains a thin mucosa and a large submucosal layer. The mucosa has respiratory epithelium lying on a basement membrane and under that a supportive connective tissue. Between the mucosa and the submucosa, there is no clear boundary. The submucosal coat is known to contain muscle, glands and cartilage (28, 30). The basement membrane consists of three layers: a lamina lucida, which makes contact with epithelial cells, a lamina densa and a lamina reticularis, the latter only present in adults. Epithelial cells overlay the basement membrane and are held together by desmosomes, gap junctions and terminal bars that block excessive fluid movement across the epithelium (30). The morphology and function of the individual epithelial cells will not be discussed here, except to mention that the main epithelial cells include ciliated cells, mucous cells, submucosal glands, neuroendocrine cells and basal cells (28, 31). Alveoli are present in large numbers and in diverse arrangement on respiratory bronchioles and alveolar ducts. In the alveolar duct system, alveoli are arranged to facilitate their functions in expiration and inspiration. In the human adult lungs, there are around 300-500 million alveoli (28, 32). Each alveolus measures about 250μm in diameter when expanded, although sizes vary with those in the upper parts of the lung described as being larger than those in the lower parts of the lung as a result of gravitational forces (28, 33). Alveolar tissue contains different types of cells that are known to assist various functions in the lung. The alveolar epithelium is one example, which consists of two cell types, the alveolar epithelial type I and II cells. The alveolar epithelial type I cells have limited cytoplasmic organelles, but are significant for their attenuated cytoplasm. As a result they extend long distances from the nuclear zone of the cell, and have been described as covering up to 5,000 μm^2 of the alveolar surface (32, 34). These cells function to provide a comprehensive thin covering and prevent fluid loss, however they also enable rapid gas exchange. The alveolar epithelial type II cell is taller compared to the type I cell. However, it

only covers 7% of the alveolar surface. It is often present in the corners of alveoli and is covered with the type I cell. The function of alveolar epithelial type II cell is to differentiate into a type I cell and to remodel the alveolar wall in the case of injury. The alveolar epithelial type I cells are connected together and also to type II epithelial cells via tight junctions (32). Other cells including interstitial cells and the immune effector cells considered in this study will be discussed in detail later.

1.4. Lung cancer

Lung cancer is a malignant tumour, which originates in lung tissue. It can arise anywhere in the lungs, including the trachea, bronchi, bronchioles and alveoli. It grows when the lung cells become abnormal and ultimately lead to the development of a tumour mass (4). Lung cancer is one of the most common cancers in the Western World and is the primary source of cancer mortality with approximately 1 million deaths annually (6-8). It is associated with a short survival time (10-15% of patients survive 5 years or longer) and an ineffective treatment strategy (9). It is well known that the survival rate of lung cancer is related to the age of diagnosis (Fig. 4 and Fig. 5). In Australia, more than 9,000 people are diagnosed with lung cancer every year. The incidence rate of lung cancer in Australia has decreased by 32% in men (from 85 to 58 cases per 100,000), but in women it is rising by 72% (from 18 to 31 cases per 100,000); a phenomenon which has been explained as being due to women taking up smoking later than men (Fig. 6) (35). Lung cancer was the leading cause of cancer deaths in both men and women in Australia in 2007. On average, 13 men and eight women die from lung cancer every day in Australia (with a total of 7626 deaths from lung cancer in 2007) (5).
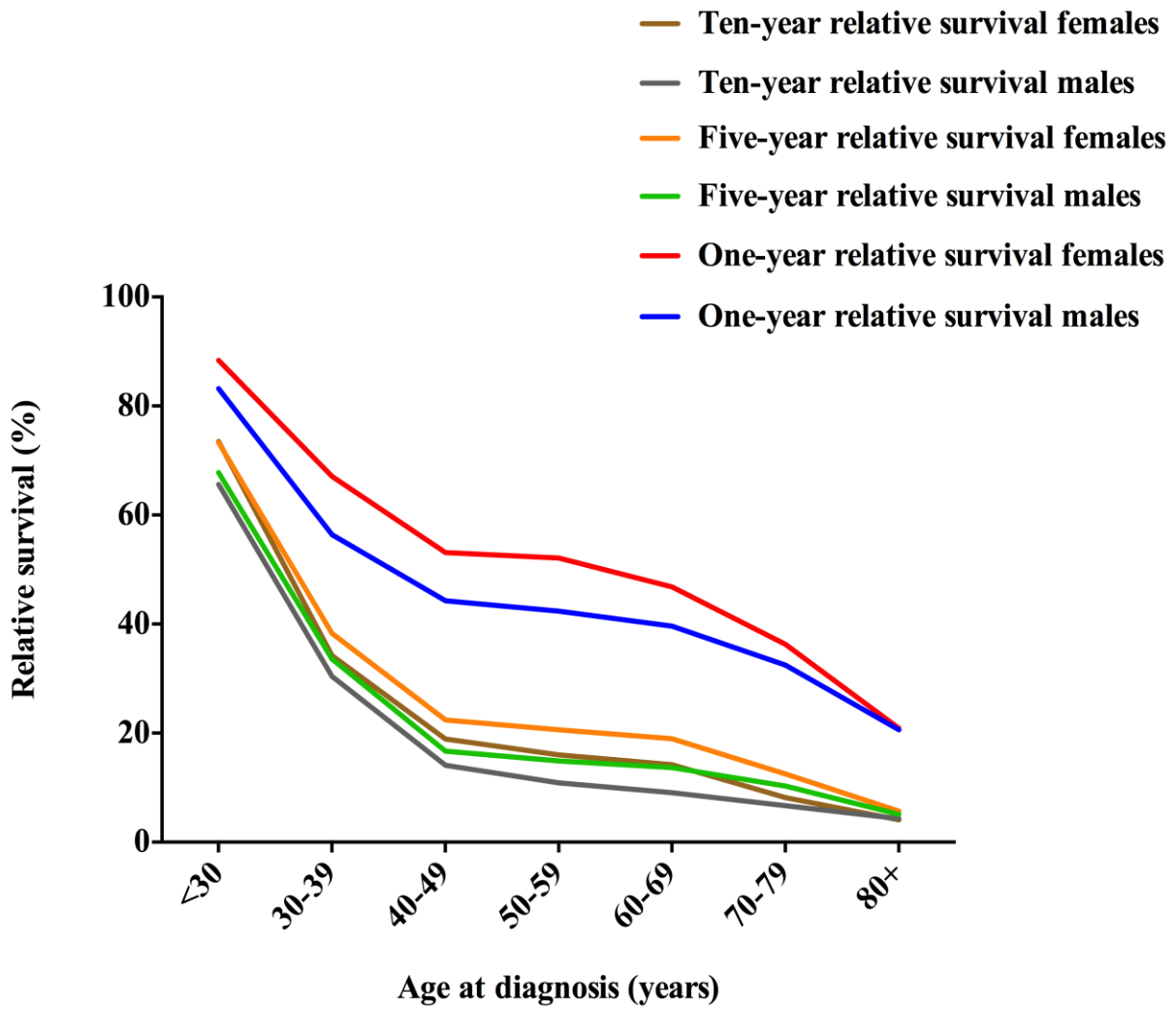
Figure 4: Relative survival for lung cancer per 100,000, for males and females in Australia. The graph shows that the relative survival rates are different depending on the age of diagnosis and these results confirm the importance of early diagnosis (5).
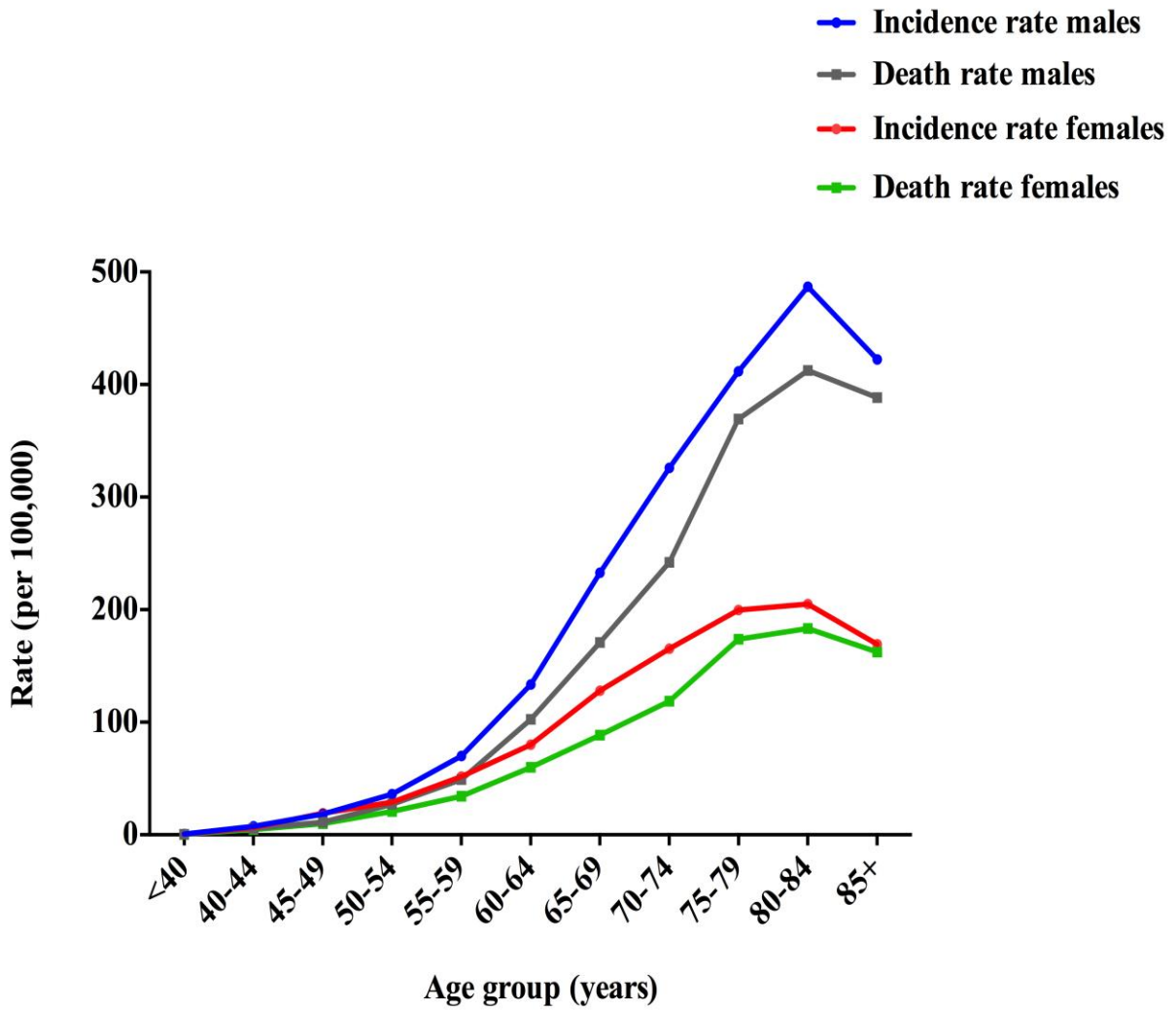
Figure 5: Incidence and death rates for lung cancer per 100,000, for males and females in Australia. The graph displays the incidence and death rate of lung cancer in Australian males and females in 2007 (5).
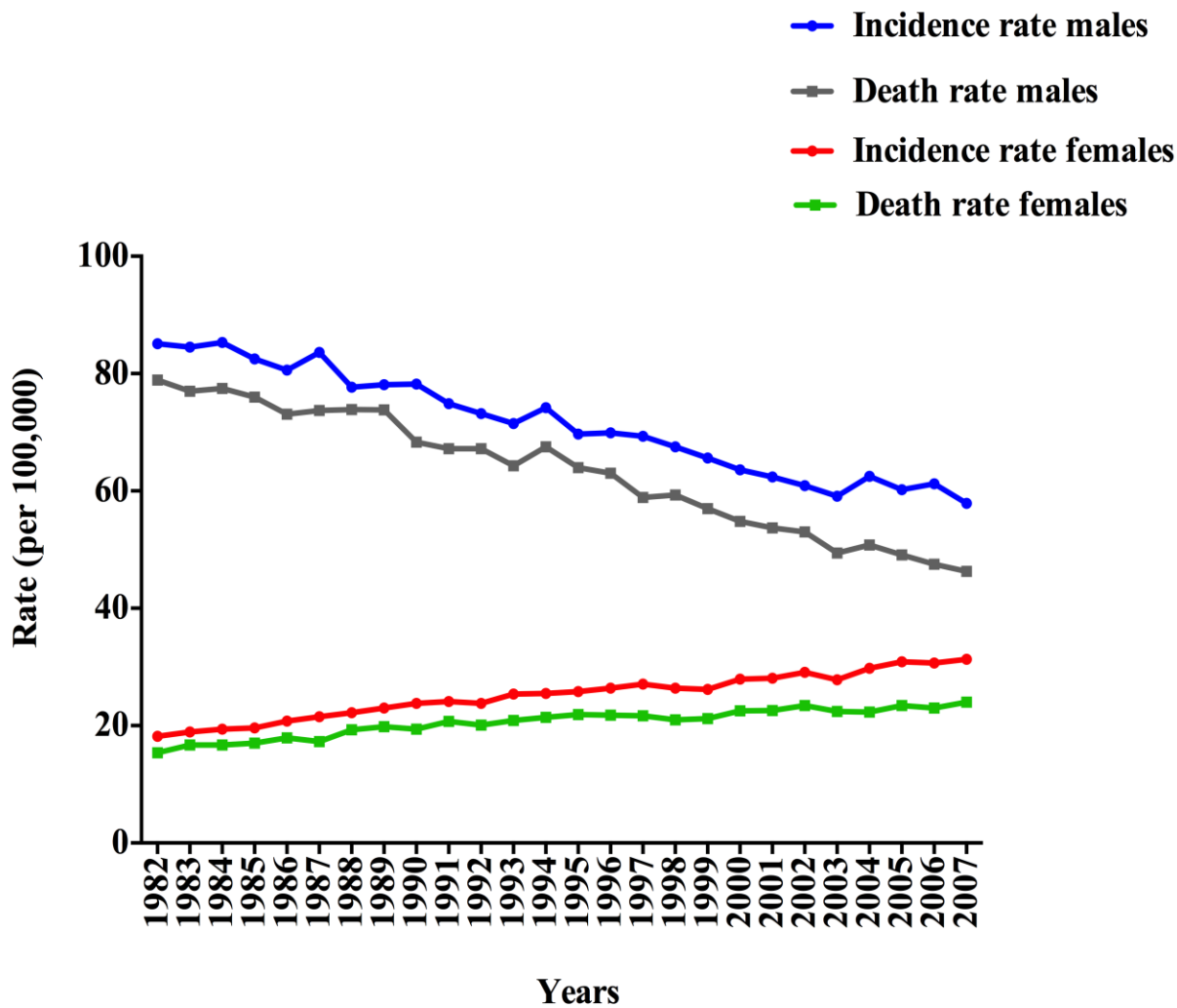
Figure 6: Incidence and death rates for lung cancer per 100,000, for males and females in Australia. The graph exhibits the incidence and death rates of lung cancer from 1982 to 2007 in Australia (5).

It is well established that smoking is the leading cause (80-90%) of lung cancer cases (36, 37). However, accumulating evidence strongly suggests that there are other factors that might increase the susceptibility of humans to lung cancer. These include air pollution, a family history of lung tumours, chronic lung disorders, gender and race (Fig. 7). An example of the influence of gender is that female smokers are found to be more vulnerable to developing lung cancer than men, and this is believed to be a result of the higher level of aromatic DNA adducts (deoxyribonucleic acid) (indicating DNA damage) in females. Another example where race appears to be a factor is that African Americans are found to be at higher risk of lung cancer, with a 1.8 times greater risk than that of their Caucasian counterparts (38, 39).

The majority of lung cancer is primary lung cancer, which initiates from the lung. The main subtypes of primary lung cancer are small cell lung carcinoma and non-small cell lung carcinoma (NSCLC). The progression of primary lung cancer is based on clinical stages and lung cancer subtypes. Approximately 85-90% of diagnosed lung cancers are NSCLC. NSCLC is differentiated into squamous cell lung carcinoma, adenocarcinoma and large cell lung carcinoma mainly based on their histological features (40). These NSCLC subclasses have different tumour cell size and shape, but they were grouped together because of their approach to treatment and the prognosis is very similar. However, recently it has been recognised that different lung cancer subtypes respond differently to treatment. For example, metastatic lung adenocarcinoma that expresses epidermal growth factor receptor (EGFR) or KRAS (kirsten rat sarcoma viral oncogene homolog) can be treated with biological agents that are not helpful as yet for other subtypes, e.g. squamous cell lung carcinoma (41, 42).

LIFESTYLE FACTORS	ENVIRONMENTAL FACTORS	BIOMEDICAL FACTORS
• Tobacco smoking	• Passive smoking • Occupational exposure • Air pollution	• Family history of lung cancer • Chronic lung disorders
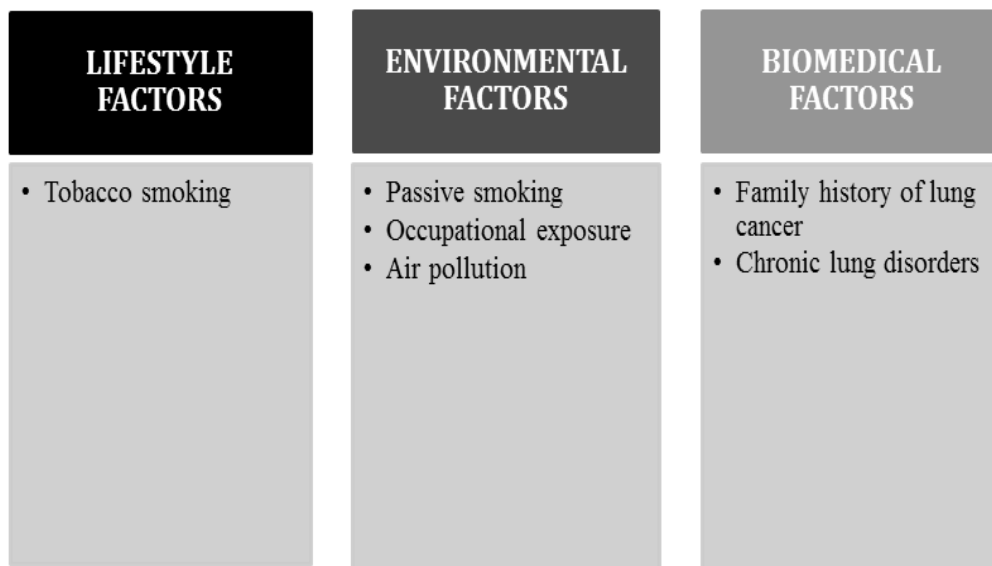
Figure 7: This diagram summarises the main risk factors of lung cancer. Cigarette smoking has been confirmed to be the leading cause of lung cancer. Other factors have also been suggested to be associated with lung cancer occurrence, in particular air pollution and chronic lung diseases (5).

1.5. Classification of lung cancer

The classification of lung cancers has been updated and adjusted several times. The lung cancer typing is mainly based on histological features. Thus, lung cancer types are named depending on the initial tumour cell type (43). In some lung tumour environments, there are mixed cell types or the cell might change during the cancer progression and treatment (44-46). This has led some researchers to suggest that all pulmonary carcinomas arise from a common stem cell that has the ability to display various pathways (47). However, the different tumour subtypes can be clearly differentiated based on their clinical behaviour and the way they respond to treatment. Lung cancer typing is negatively impacted by the small size of fibreoptic bronchoscopic biopsy specimens, the reliability of pathologist identification of histology and methodological limitations. A study on pathologists' examination and classification showed that they agreed on the classification of 72% of small cell lung carcinomas, 56% of adenocarcinomas, 48% of squamous cell lung carcinomas and only 5% of large cell lung carcinomas (48). This study has shown that there is considerable variability in the classification of the lung cancer subtypes (47). However, the World Health Organisation (WHO) classified lung cancer into (I) NSCLC and (II) small cell lung carcinoma. NSCLC is categorised into squamous cell lung carcinoma, adenocarcinoma and large cell lung carcinoma and a few other less common subtypes e.g. adenosquamous carcinoma and sarcomatoid carcinoma. NSCLC is known to be the most common lung cancer and accounts for 85% of all lung cancer cases (5, 47). In Australia, approximately 64% of lung cancers in males and 61% in females were reported to be NSCLC (Fig. 8). For males and females, adenocarcinoma was the most reported type of NSCLC, though the adenocarcinoma incidence rate was lower in males than females (26% vs. 34%). However, the incidence rate of squamous cell lung carcinoma was higher in males than in females, being 20% versus 10%, respectively. The percentage of lung cancers that were classified as

large cell lung carcinoma was around 17% for both males and females. Moreover, the percentage of lung cancers that were categorised as small cell lung carcinoma was 11% for males and 13% for females. Finally, other specified carcinoma types and unspecified malignant neoplasms accounted for 25% of lung cancers in males and 26% in females (Fig. 8) (5). This statistical fact was the main factor that led us to concentrate on NSCLC and try to add additional knowledge to this field. The following paragraphs will briefly discuss the three NSCLC subtypes, including squamous cell lung carcinoma, adenocarcinoma and large cell lung carcinoma.
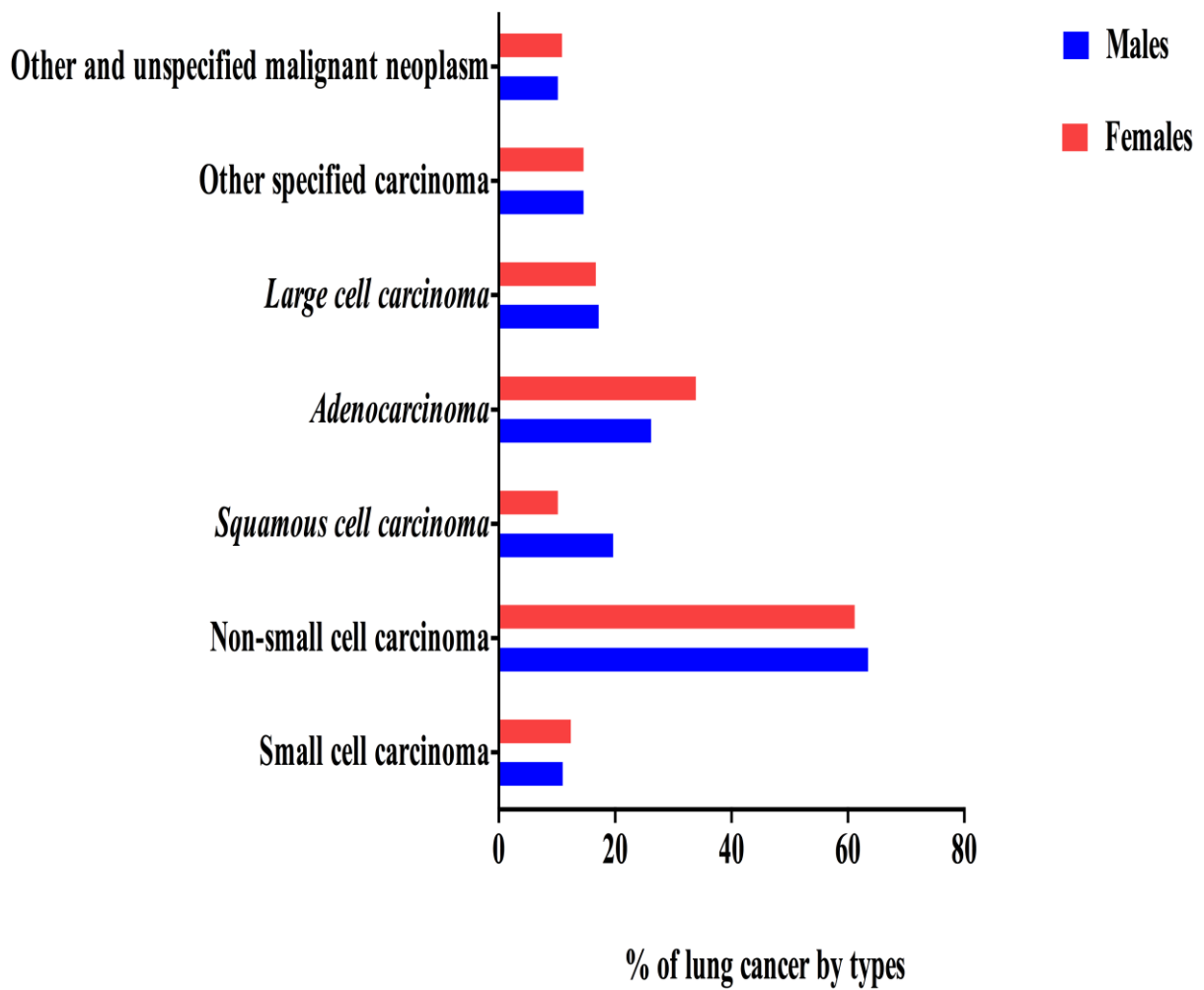
Figure 8: The percentage of lung cancer incidence by type in Australia, 2007. This graph displays that NSCLC is the most common lung cancer (5).

Firstly, squamous cell lung carcinoma has typically been considered as a tumour of the central bronchi but recently there has been a decrease in the number of central tumours and an increase in tumours initiated from peripheral areas (49). Squamous cell lung carcinoma was known to be the most common type in many countries but adenocarcinoma is increasing and is now the commonest NSCLC type (50, 51). The decline in squamous cell lung carcinoma incidence might be because of the decrease in the percentage of smokers since the 1950s and the skew to low-tar filter cigarettes. Squamous cell lung carcinoma accounts for 25–30% of all lung cancer (52). It can be diagnosed histologically from uneven nests and tumour cells separated by varying amounts of fibrous stroma. This kind of tumour cell has large irregular nuclei, clumped chromatin and nucleoli of varying size and differentiated squamous cell lung carcinomas show noticeable keratinization (47). The WHO classification describes four different subtypes of squamous cell lung carcinoma: papillary, clear cell, small cell and basaloid (47).

Next, adenocarcinoma incidence shows an increase in many countries and is now the most frequent NSCLC and it accounts for 35–40% of lung cancers overall (47, 50, 53). The reason behind the increase in the number of patients with adenocarcinoma is believed to be the growing popularity of filter-tipped cigarettes. The majority of patients with pulmonary adenocarcinoma are elderly smokers, but there is a high number of adenocarcinoma in non-smokers and the young (54, 55). Most of the adenocarcinomas arise from the periphery of the lung or what has been called the terminal respiratory unit. The WHO classification of lung tumours names five different subtypes of adenocarcinoma (acinar, papillary, bronchiolo-alveolar, solid with mucin production and mixed). Recently several researchers have suggested the existence of other growth patterns; papillary with a prominent "morular" component, micropapillary, secretory endometrioid-like, adenocarcinoma with massive lymphocyte infiltration, basaloid and those showing enteric differentiation (56, 57). These

classification changes have guided the International Association for the Study of Lung Cancer (IASLC), the American Thoracic Society (ATS) and European Respiratory Society (ERS) to suggest adjustments to the WHO classification (47).

Finally, large cell lung carcinoma subtype is a less common lung cancer in comparison to other NSCLC subtypes; it accounts for 10–15% of lung cancers (47). This subtype is an aggressive tumour and is usually centrally located and frequently displays an exophytic, endobronchial pattern of growth and a well-defined edge (52, 58). The large lung carcinoma cells are arranged in monotonous fields and can be distinguished from small cell carcinoma through cytological features. The features of this cancer are the large size of the tumour cell and the nuclear detail; they also have a moderate amount of cytoplasm, chromatin that is clumped at the periphery of the nucleus and a prominent nucleolus (59, 60). Five subtypes of large cell lung carcinomas have been documented: clear cell, neuroendocrine (the tumour of middle-aged or elderly cigarette smokers that arises in central bronchi) basaloid, lymphoepithelioma-like and rhabdoid (47).

1.6. Cancer immunoediting and lung stromal cells

The term "immunoediting" is used to describe the changes in immunogenicity of tumours due to the anti-tumour response of the immune system. It contains three phases: elimination, equilibrium, and escape. The elimination phase contains four different phases, including (I) the initiation of the anti-tumour immune response, (II) tumour death induced through interferon gamma (IFN-γ), (III) more tumour killing by natural killer cells (NK) and macrophages, and (IV) the specific anti-tumour function via CD4$^+$ and CD8$^+$ T cells. The tumour cells that successfully survive the elimination phase might proceed to the equilibrium phase where the immune system is able to control their growth but cannot completely destroy them. The tumour cells may overcome all these phases and enter the escape phase where they start to progress and metastasise to other organs (61).

The human immune system exhibits local and systemic functions that ultimately inhibit tumour growth. Several studies have shown that the components of the immune system are not just important in controlling and preventing the initiation of cancer, but that they are involved in cancer immunoediting through the innate and adaptive immune systems (10, 11). Such immunoediting can occur through a number of different mechanisms, including via the presence of inflammatory cells (macrophages, NK, dendritic cells and lymphocytes) and their secretion of various immunological factors such as chemokines and cytokines that are known to increase the host's defence against tumours (e.g. IFN-γ, IL-12 and IL-1) (12).

However, the immune system has been shown to exhibit a dual role in both eliminating and promoting human tumours, thus sometimes being described as a double-edged sword in the way it interacts in tumour microenvironments (12). A number of studies have shown that components of the immune system (innate and adaptive) are associated with tumour growth and poor prognosis in cancer patients (62-64). In particular, macrophages have been

suggested to promote tumour growth, invasion and metastasis through the secretion of different chemokines, cytokines and other factors such as IL-10, matrix metalloproteinases (MMPs), vascular endothelial growth factor (VEGF) and transforming growth factor-β (TGF-β) (62). Macrophages are known to be the first cells to arrive at the tumour site and perform various functions that can inhibit tumour growth, while other macrophages may encourage tumour cell survival and escape (Fig. 9) (12, 65). All these reasons make macrophages (AMs, TAMs and monocytes) crucial fundamental cells to be intensely investigated in order to understand the association between these cells and tumour initiation, growth and metastasis.
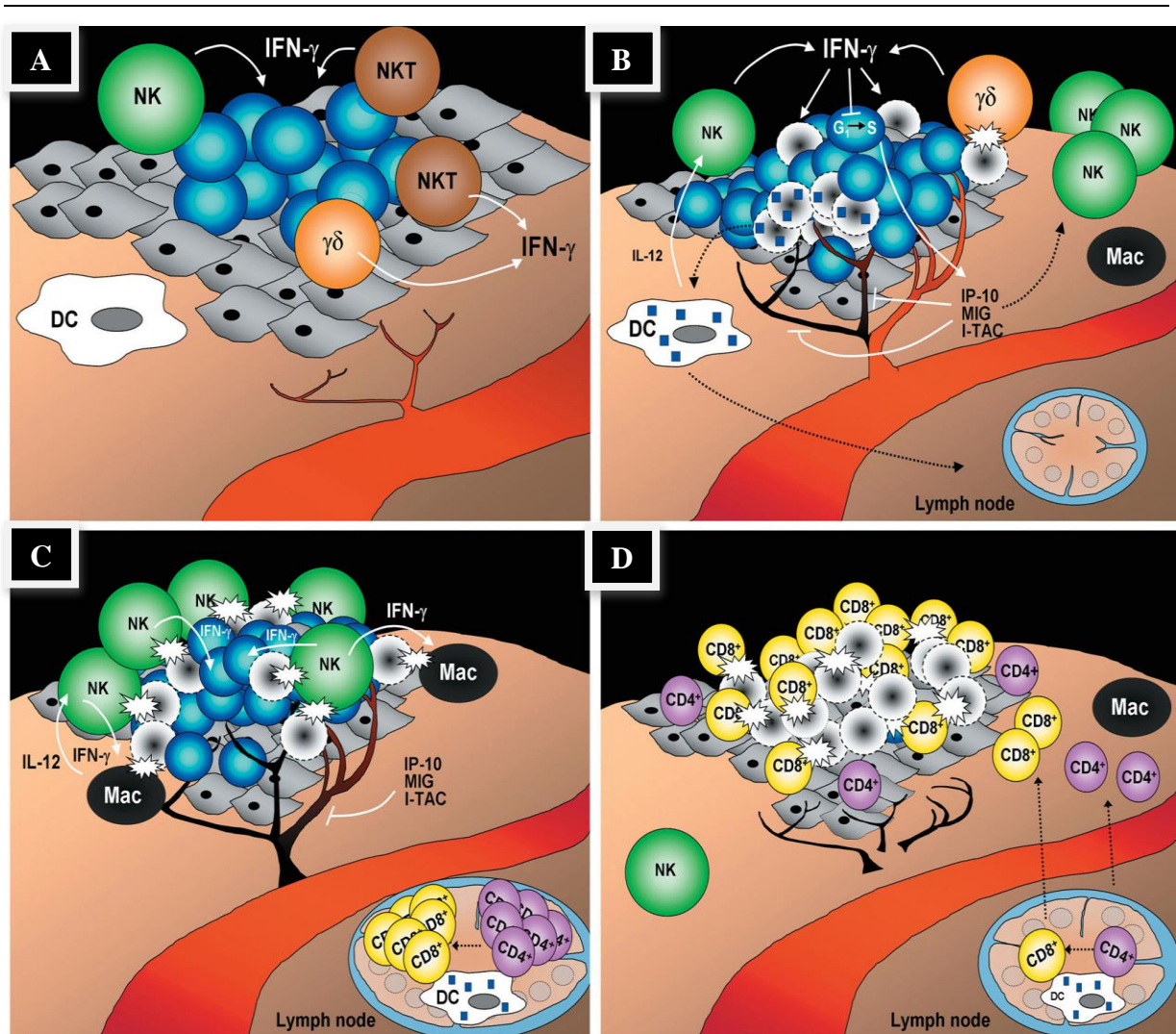
Figure 9: The process of cancer immunoediting. (A) This figure shows how the elimination process begins with the recognition of transformed cells through lymphocytes, which is then stimulated to produce IFN-γ. (B) The expression of IFN-γ leads to stimulation of the innate immune system response and then recruitment of NK, DC and macrophages. (C) NK cells and macrophages attack tumour cells while CD4$^+$ and CD8$^+$ T cells develop in the lymph node. (D) Tumour-specific T cells (CD4$^+$ and CD8$^+$) then migrate into the tumour site where they start recognising and destroying tumour cells. Blue: Tumour cells; grey: non-transformed cells; white surrounded by a dashed black line: dead tumour cells; DC: dendritic cells; NK: natural killer cells and Mac: macrophages (12).

Lung tumours are composed of tumour cells and surrounding connective tissue and cells, which make up the tumour stroma (Fig. 10). The interaction between tumour cells and stromal cells as well as the extracellular matrix (ECM) plays a vital role in tumour growth and progression (66). Tumour cells have the ability to interact and alter the function of surrounding connective tissue to support and maintain their proliferation and progression (67). The tumour stroma possesses several cellular compartments, including fibroblasts/myofibroblasts, smooth muscle cells, endothelial cells, dendritic cells, macrophages and other inflammatory cells. They can interact with each other through the secretion of growth factors, chemokines, proteases and ECM components (67-69). Macrophages are one of the most important types of stromal cells that have been shown to be associated with both tumour progression and tumour regression. Macrophages (AMs and TAMs) and their precursor cell, monocytes, will be studied in detail here in order to examine their potential role in patients with NSCLC. AMs, TAMs and monocytes are attractive cells to be targeted to find new biomarkers, treatment targets, prognostic and diagnostic indicators.
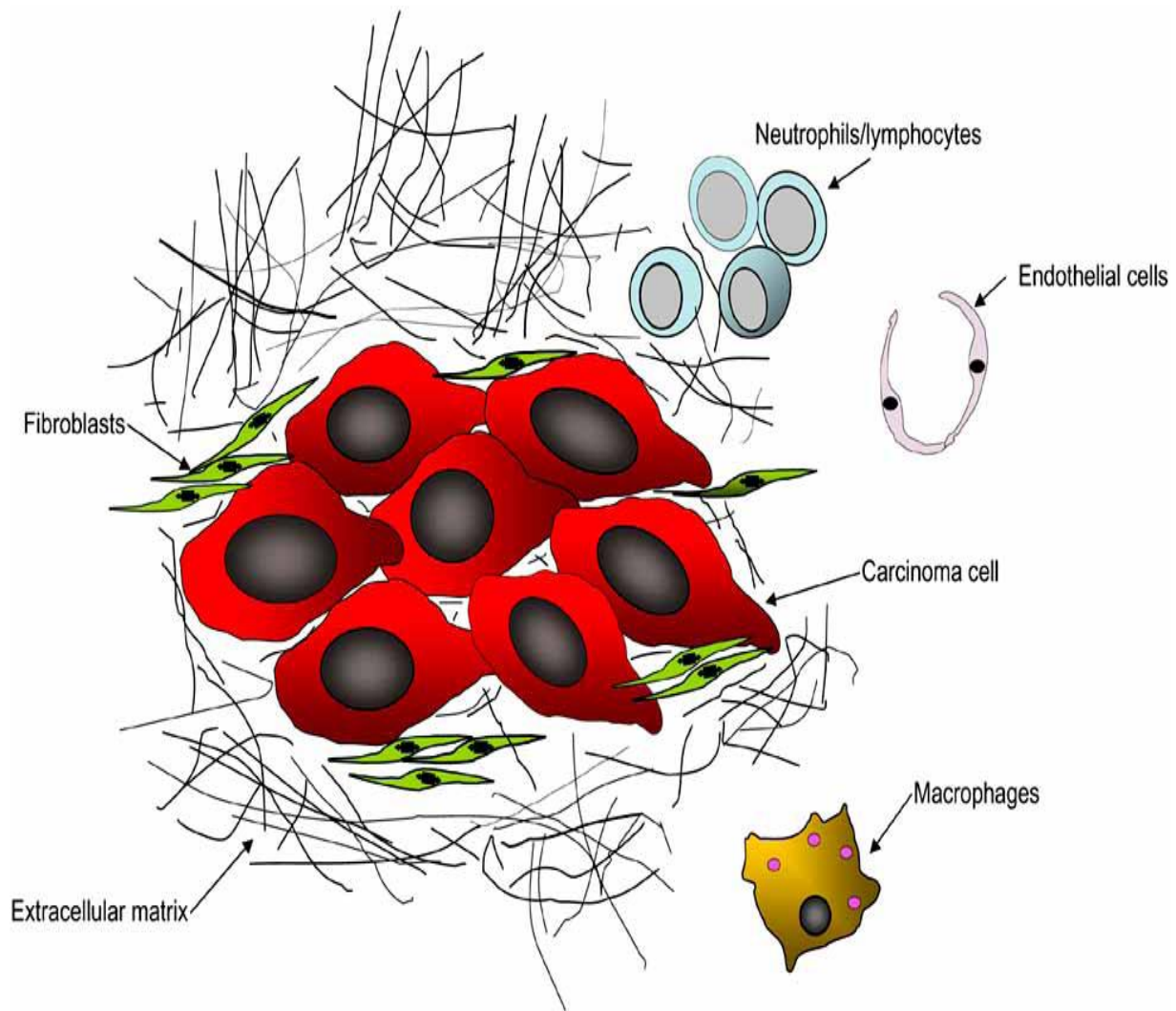
Figure 10: The interaction between tumour cells and tumour stroma. The tumour cells are able to alter the function of stromal cells and utilise their expression to survive, grow, invade and migrate. Stromal cells, including macrophages, endothelial cells, neutrophils, lymphocytes and fibroblasts, as well as the extracellular matrix compartment, surround and interact with the tumour cells. This drawing shows the vital location and the significant role of macrophages, which allows them to be active in controlling tumour cell growth and/or support tumour growth and metastasis (70).

1.7. Macrophage phenotype and function

Macrophages and monocytes both have similar features to granulocytes, in particular with neutrophils. They both have the ability to migrate through several body compartments, including bone marrow, blood, lymphoid, and all non-hematopoietic tissues (Fig. 11) (14, 71). Monocytes are the main source of recruited tissue macrophages in several conditions such as infection, granulomata, atherosclerosis and tumours. Macrophages then migrate to sites of injury and infection, where their presence leads to acute and chronic inflammation either in the local or systemic environment (14).

Monocytes are an important part of the innate immune response to cancer. The notion that the immune system has a protective role in tumour development is well established (12), with recent work also suggesting a converse role in promoting tumour initiation and progression (72). Previous studies looking at monocytes in a range of different cancer types have demonstrated conflicting results regarding monocyte phenotype and function in different cancer microenvironments. Studies in patients with lung, breast and other cancers have described inhibited monocytes function (73-77), whereas Mariotta et al. (2002) suggested that NSCLC does not affect monocyte adherence and phagocytosis before chemotherapy in lung cancer patients compared to healthy controls (17). Other studies have demonstrated monocytes capable of both inhibiting and stimulating tumour growth at the same time (78).
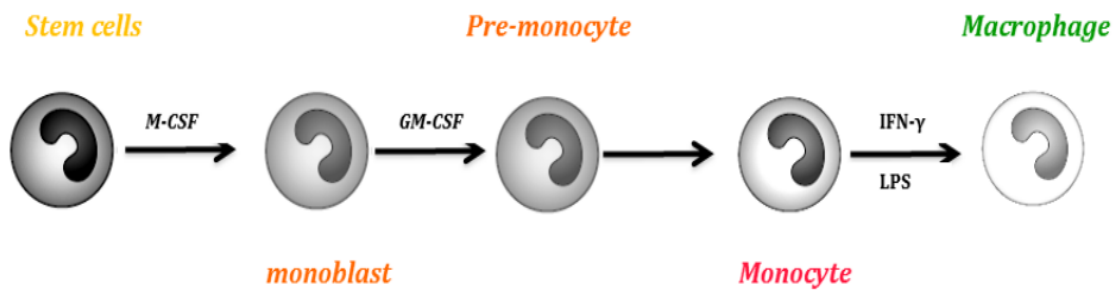
Figure 11: Monocyte and macrophage differentiation. Immature monocytes released from bone marrow migrate through the bloodstream under the influence of different cytokines and chemokines (e.g. M-CSF and GM-CSF) into tissues (lung, liver, spleen, peritoneal cavity and brain) where they differentiate into resident macrophages under the influence of IFN-γ and LPS.

Monocytes can be characterised into classical monocyte (CD14^{++}/CD16^{-}), intermediate monocyte (CD14^{+}/CD16^{+}) and non-classical monocyte (CD14^{+}/CD16^{++}) phenotypes, and all of these have been detected in circulating peripheral blood mononuclear cells (PBMC) (Fig. 12) (79, 80). Monocytes are known to differentiate into tissue macrophages. Classical monocytes (CD14^{++}/CD16^{-}) differentiate into M1 macrophages, while non-classical monocytes (CD14^{+}/CD16^{++}) differentiate into M2 macrophages (81). M1 cells function as antigen-presenting cells and have a vital role in immune activation and function (82). In contrast, M2 are known to be associated with poor antigen presentation and the production of factors that suppress T cell proliferation and activity (82). The major source of macrophage migration to the tumour site is from classical monocytes. In spite of this, the majority of macrophages within the tumour area have been identified as M2 macrophages (81). However, it has been reported that classical monocytes can differentiate into M2 macrophages (83).

Figure 12: Monocyte classification. Monocytes have been categorised based on their CD14 and CD16 expression into classical monocytes (CD14^{++}/CD16^{-}), intermediate monocytes (CD14^{++}/CD16^{+}) and non-classical monocytes (CD14^{+}/CD16^{++}).

Macrophages are mononuclear phagocyte cells that reside in different compartments within the body (lung, liver, spleen, peritoneal cavity and brain). They are crucial to the innate and adaptive immune system. Macrophages are released from bone marrow as immature monocytes and then migrate through the bloodstream into tissue sites where they can differentiate into resident macrophages (84). Thus, macrophages arise originally from haemopoietic progenitors (71), and then differentiate into subpopulations of tissue macrophages directly or via circulating monocytes (85). Resident macrophages are present in different organs under stressful conditions as well as in the absence of inflammation. Tissue macrophages can also be replicated and differentiated locally, depending on the stimulus and tissue environment (14). Macrophages are highly active cells and have been shown to express various receptors, cytokines and chemokines in normal and abnormal cells in different sites. They can perform endocytosis, phagocytosis, and secrete various products, including cytokines (TNF, IL-1, IL-6, IL-4, IL-13, IL-10), growth factors (transforming growth factor-beta (TGF-β), platelet derived growth factor (PDGF) and VEGF). They also demonstrate trophic and toxic functions, contribute to tissue remodelling and host defence in innate and adaptive immunity (14).

In the lung, macrophages termed AMs are localised in the air spaces and also exist in the lower airways in the presence or absence of infection (15) where they play a crucial part in immunity and inflammation (Fig. 13) (16). Macrophages in other sites of the human body are similar to AMs in the lungs, although their functions may differ according to the requirements of the tissue in which they reside. The main difference between AMs and peritoneal macrophages is their mode of metabolism as AMs use aerobic rather than anaerobic metabolism (28). AMs like other macrophage subtypes have diverse functions in the regulation of adaptive immunity, including the production of reactive oxygen and nitrogen species and antigen presentation (86). AMs and other macrophage subtypes regulate local

inflammatory reactions via the release of cytokines and provide primary defence by phagocytosis of foreign particles (87).
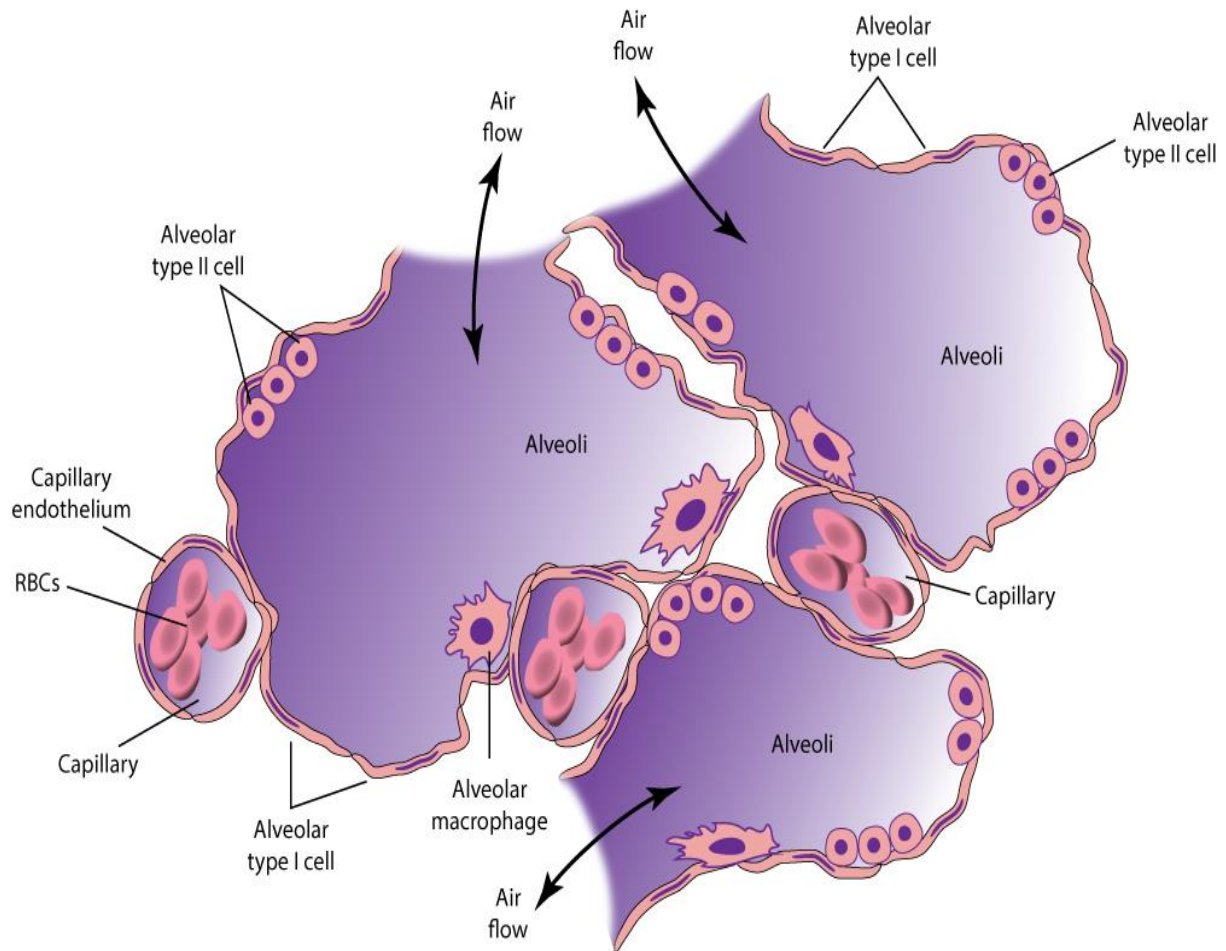
Figure 13: The alveolar structure and anatomical location of AMs. The main components of the alveolus are shown in this figure including AMs (88).

Cytokines are involved in numerous immune reactions, including tumouricidal activity (22). Upon stimulation, AMs secrete pro-inflammatory cytokines such as TNF-α, IL-1, IL-6 and IL-12 (24, 89) and anti-inflammatory cytokines such as IL-10, TGF-β and IL-13 (13, 90). Also AMs exert direct cytotoxic effects by phagocytosis or indirect anti-tumour effects via cytokine release and natural killer cell activation (23). AMs therefore play a critical role in lung immune regulation and the prevention of lung diseases, including lung cancer (91).

As mentioned before, the ultimate source of AM is the bone marrow, but under special circumstances the pulmonary interstitial cells is considered to be the immediate source. It has been demonstrated that most monocytes migrated to become AMs by passing into alveoli but a few of them differentiate in the interstitium (92, 93). The differentiation process of monocytes into AMs involves cytoplasmic enlargement, loss of myeloperoxidase and the development of lysosomes more characteristic of mature macrophages. Hence, the number of AMs might increase by enhanced migration from the interstitium and then division of cells (28, 92). AMs stay in the alveolus for 7 days, then the majority of the cells move to the terminal bronchiole and subsequently to the pharynx where AMs are eventually discarded (94). Respiratory movements stimulate AMs transport and this translocation of AMs is assumed to be important to antigen presentation and the induction of lung immunity (28).

1.8. Macrophages in lung cancer

The work of Coley William (1891) on sarcomas was the first to demonstrate that the immune system is involved in the regression of cancers (95). This work has led many scientists to start working on cancer immunology in order to find a better treatment for cancers. In regards to our study, the connection between lung cancer and macrophages especially TAMs has been widely reviewed (20, 96). However, less is known about AMs and monocytes compared to TAMs in lung cancer. Thus, this literature review will concentrate more on AM phenotype and function in lung cancer. Immature monocytes derived from bone marrow migrate through the bloodstream into tissues where they differentiate into resident macrophages (e.g. AMs) in the lungs through the influence of IFN-γ and lipopolysaccharide (LPS) (16). AMs are localised in the airspaces of the lungs (97) and exist in the lower airways in the presence or absence of infection (15), where they play a crucial part in immunity and inflammation of the lungs (16). The main role of AMs in the lung is to eliminate foreign substances (98).

Macrophages (AMs and TAMs) are known to be crucial cells in lung cancer as they are in close proximity to tumour cells compared to other stromal cells. Similar to TAMs, the enrichment of AMs (M2 phenotype) favours tumour growth and correlates with poor prognosis in lung cancer. AMs and TAMs are known to be responsible for releasing several growth factors, cytokines, chemokines, inflammatory mediators and other molecules (20). Many of these factors are well known and have been associated with tumour growth, poor prognosis and metastasis including VEGF, PDGF and IL-10. For instance, AMs and TAMs secrete high amounts of pro-angiogenic factors such as VEGF, which stimulate tumour vascularisation and metastasis. Another potential pathogenic activity of these cells is the suppression of anticancer immune responses (e.g. induce the secretion of IL-10) (99).

Complement receptors and toll-like receptors are important in the contribution of AMs to the initial defence in inflammation, infection and tumour via the production of cytokines and chemokines secretion (e.g. IFN-γ and IL-8), monocyte chemoattractant protein-1 (MCP-1) and growth factors. They also function diversely in the regulation of adaptive immunity, including via the production of ROS, NOS and metalloproteinases as well as through antigen presentation (86, 100).

AMs regulate local inflammatory reactions via the release of cytokines and provide a primary defence mechanism against foreign particles by phagocytosis (87). Cytokines are involved in numerous immune reactions, including tumouricidal activity (22). AMs secrete both pro-inflammatory cytokines such as TNF-α, IL-1, IL-6 and IL-12 (24, 89) and anti-inflammatory cytokines such as IL-10, TGF-β and IL-13 (13, 90). Upon stimulation, AMs may exert direct cytotoxic effects by phagocytosis, or anti-tumour effects via cytokine release and natural killer cell activation (23). Therefore, AMs appear to play a critical role in lung immunoregulation and potentially in the prevention of lung diseases, including lung cancer (91). Studies investigating the role of AMs in lung cancer have provided inconsistent results. Whilst some studies report increased cytotoxic activity and anti-tumour effects after AMs activation, others have reported decreased cytotoxic activity and pro-tumour effects (13, 22-27). A dual role for macrophages in lung cancer has therefore been suggested with the idea that AMs may both inhibit and/or promote tumour progression (13). The anti-tumour functions of AMs need further investigation in order to enable lung tumour to be treated with M1 macrophage-activating drugs. Similar to TAMs, AMs are attractive targets of lung cancer immunotherapy if M1 macrophage-activating drugs can be delivered to the lungs.

1.9. Macrophage polarisation and tumour progression

The role of macrophages (AMs, TAMs and monocytes) in the tumour environment has been widely reviewed (17, 20, 23, 27). TAMs have been suggested to be the most important macrophage subtype and immune cells in NSCLC, because the amount of TAMs in the tumour islets or stroma can be independently utilised to predict patient's survival time (101). There are two major phenotypes of macrophages that perform different functions: M1 and M2. The M1 macrophages inhibit cell proliferation, promote inflammation and tissue damage while M2 inhibit inflammation, promote cell proliferation and tissue remodelling and repair (102). The M1 macrophages are activated by IFN-γ with or without LPS and TNF-α (18-20, 103). M1 secret different pro-inflammatory cytokines such as IL-1, IL-12, TNF-α, and inducible nitric oxide synthase (iNOS) (Fig. 14) (20). A study has shown the presence of both M1 and M2 phenotypes within NSCLC tumour islets (18). In addition, the M1 macrophage subset appeared more frequently within tumour islets and was associated with extended survival time in patients with NSCLC (18). In contrast, the M2 phenotype has three well-defined forms: M2a which are induced by IL-4 or IL-13; M2b which are initiated by exposure to immune complexes and agonists of toll-like receptor (TLRs); and M2c which are induced by IL-10 and glucocorticoids (Fig. 14) (19). Macrophages have been shown to exhibit several phenotypes (e.g. M1, M2a, M2b, etc.) mainly depending on the environment in which they are found. There are many examples of macrophage-polarising events during tumour progression, including the secretion of tumour-derived mediators and hypoxic tissue damage, as well as influences from other immune cells and stromal components (18, 104-106). The exact characterisation of macrophage populations within M1 and M2 subtypes can perhaps be overgeneralised, as macrophages have been described as highly plastic cells that can demonstrate a variety of phenotypes (104). However, the markers of M1 and M2 phenotype can still be used to categorise the phenotype and function of macrophages (104). A

small number of macrophages express both M1 and M2 markers and this leads to the suggestion that a mixed phenotype occurs (106). A study previously verified that the M1 and M2 markers differentiate macrophage populations, although about 5% of the cells stained for both M1 and M2 markers using immunohistochemistry (IHC) (18).
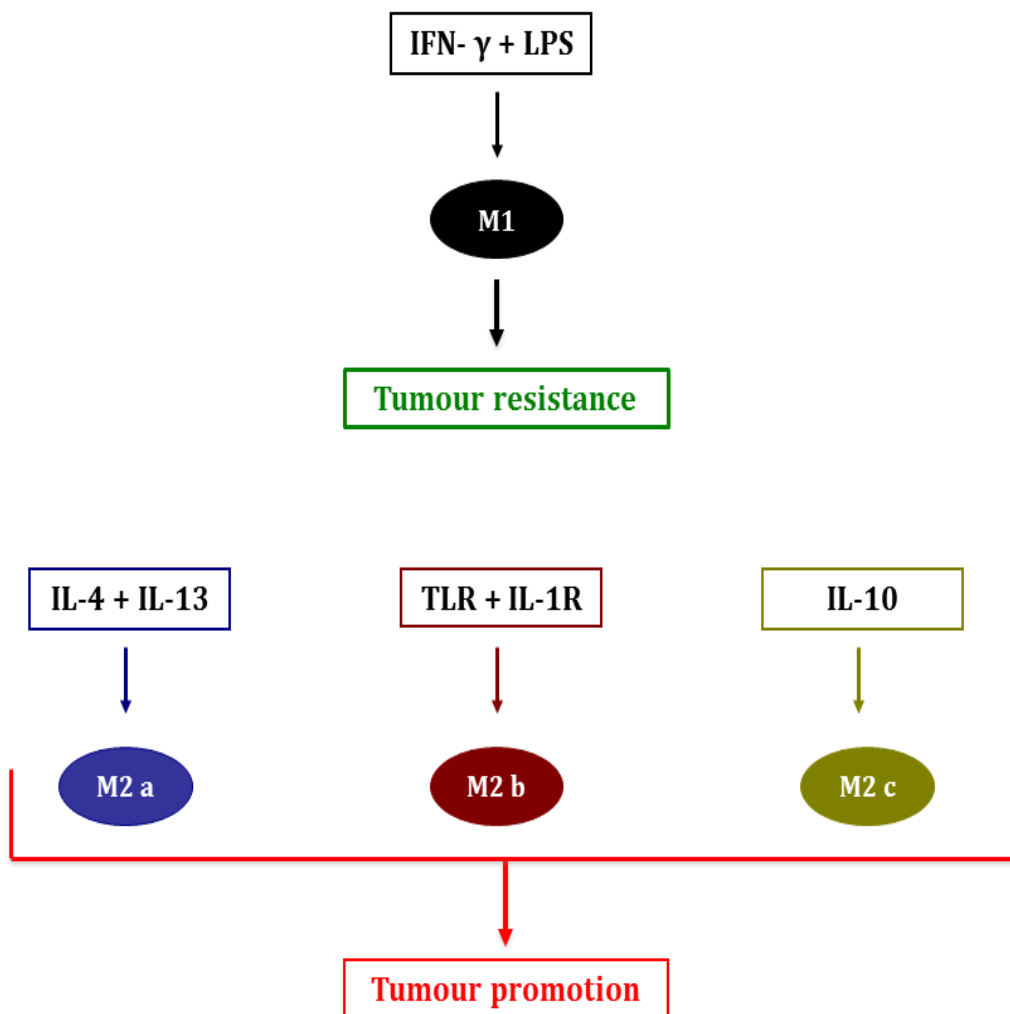
Figure 14: Macrophage subsets have distinctive inducers and multiple functions. Macrophages polarise into the M1 subset under the influence of IFN-γ and LPS and have anti-tumour functions via the secretion of effector molecules such as iNOS, IL-1 TNF and IL-6. In contrast, IL-4 and IL-13 stimulate M2a polarisation; M2b is induced by exposure to TLR and IL-1R, and IL-10 is described as an inducer of M2c. The three M2 subtypes are described as tumour promoters; they induce tumour growth through the inhibition of anti-tumour factors and/or over-expression of tumour progression factors such as IL-10, TGF-β and angiogenesis mediators.

The M2 macrophages have been associated with tumour initiation and progression and have also been described as an inhibitor of inflammatory responses and adaptive Th1 immunity (18, 103). The M2 macrophages produce anti-inflammatory cytokines such as IL-10 and stimulate the expression of the mannose receptor and arginase I, while simultaneously reducing iNOS and arginine (107). Other than their ability to reduce the amount of NO, which is significant for the elimination of tumour cells (108), M2 can inhibit antigen presentation (19) and T-cell proliferation (109). The cytokines that regulate M2 activation have been associated with NSCLC and other types of tumours (110). A recent study showed that early lung neoplasia *in vivo* is associated with increased numbers of M2 macrophages regardless of whether the model of carcinogenesis is genetically- or chemically-induced (107). Also *in vitro*, the M2 macrophages have been found to encourage the growth of various tumour cells (111) and to increase tumour cell survival (112). The M2 macrophages also play a vital role in promoting angiogenesis via VEGF, which is a prominent mediator of angiogenesis (18, 113).

1.10. The potential role of alveolar macrophages in tumour regression

1.10.1. The role of pro-inflammatory cytokines: TNF-α, IL-1 and lL-6

AMs derived from patients with lung cancer have been shown to function efficiently against tumour cell growth *in vitro* (Table 1) (22-25, 114). Increased TNF-α and IL-1 secretion from AMs of patients with lung cancer after stimulation with IFN-γ and granulocyte macrophage colony stimulating factor (GM-CSF) has been demonstrated when compared to AMs from patients with non-malignant disorders (24). IL-1 mediates cytotoxicity and suppression of tumour growth (115, 116) and TNF-α inhibits angiogenesis to prevent tumour growth. TNF-α can therefore act as an anti-tumour monokine and be responsible for spontaneous (without external activation) cytotoxic effects of AMs (117). Hence, AMs from patients with lung cancer may be able to secrete normal amounts of pro-inflammatory cytokines, suggesting that AMs function normally in patients with lung cancer. Despite these findings, decreased TNF-α secretion by AMs has also been reported in patients with lung cancer (13, 27, 116). However, Lentsch et al. (1996) showed that the reduction in TNF-α did not impair cytotoxic activity of AMs against lung cancer *in vivo* (116). Overall, the secretion of TNF-α by AM appears to have an important anti-tumour role, however, there may be other mechanisms that contribute to AMs anti-tumour effects in the absence of TNF-α.

Numerous studies have isolated AMs from BAL fluid to assess their function in the presence of known macrophage-activating agents such as IFN-γ and GM-CSF (25, 27, 89, 115, 118). IFN-γ stimulates IFN-γ inducible protein (IP-10), an anti-tumour molecule that impairs tumour angiogenesis, whereas GM-CSF promotes the proliferation of haematopoietic progenitor cells and influences the anti-tumour function of AMs (118). After IFN-γ stimulation, the cytotoxic effects of AMs in patients with lung cancer are enhanced even from a depressed baseline level (23, 115). Stimulation with GM-CSF enhanced expression of mRNA coding for TNF-α, IL-1 and IL-6 in AMs and monocytes from patients with lung

cancer in a time-dependent manner, and isolation of AMs from patients with lung cancer receiving GM-CSF therapy and cultured with LPS showed enhanced IL-6 secretion (89, 118). These findings suggest GM-CSF therapy may enhance tumouricidal activity of AMs in patients with lung cancer.

The ability of IL-6 to inhibit tumour cell growth has also been suggested (22). The elevation of IL-6 level has been detected in BAL cell culture and blood from patients with lung cancer compared to those with benign diseases (22). Upon LPS stimulation, IL-6 secretion was increased in AMs from patients with lung cancer (22). IL-6 functions synchronously with IL-1 and TNF-α in order to support anti-tumour immunity (118). A recent study investigated IL-6 levels in BAL fluid and serum from patients with lung cancer before and during radiotherapy (RT). The IL-6 level in BAL fluid was higher compared to controls and was further elevated during RT, potentially confirming the role of IL-6 in mediating an inflammatory response. However, the study did not specify the source of IL-6 secretion (119). However, other studies have demonstrated the ability of IL-6 to promote lung tumour growth and it has an association with a poor prognosis (120-122). A study has shown that tumour growth caused by tobacco smoke was mediated by IL-6 and TNF-α (120). Also the deficiency of IL-6 and TNF-α has led to decreased lung tumour cell proliferation (120). Similarly, another study has shown that IL-6 plays a vital role in promoting cancer stem cells derived from the NSCLC cell line H460 (121). Therefore, it was suggested that targeting IL-6 could potentially improve lung cancer therapeutic techniques (121). An interesting clinical study demonstrated that NSCLC patients with high plasma levels of IL-6 responded poorly to chemotherapy. Additionally, it was suggested that IL-6 level could be used as a prognostic marker for lung cancer survival among those patients who have received chemotherapy (123).

1.11. The potential role of AMs in tumour progression

1.11.1. The role of anti-inflammatory cytokines: TGF-β and IL-10

AMs in lung cancer have been shown to exert pro-tumour effects via their secretion of anti-inflammatory/immunosuppressive cytokines such as TGF-β and IL-10 (Table 1) (13, 25). TGF-β has been shown to enhance tumour cell proliferation *in vitro* and *in vivo*. (13). *In vitro* stimulation of AMs with LPS induced TGF-β secretion in patients with lung cancer (22). Also, increased TGF-β secretion has been reported in the serum of lung cancer patients compared to healthy controls (124). However, the mechanism underlying the increased production of TGF-β and its role in AMs regulation and lung cancer growth is unclear (124).

IL-10 is a potent tumour angiogenesis inhibitor released by AMs with or without LPS stimulation *in vitro*. Following LPS stimulation, Yanagawa et al. (1999) found no significant differences in IL-10 production by AMs from patients with lung cancer in comparison with control patients (13, 25). Conversely, IL-10 has been identified as a potential inhibitor of pro-inflammatory cytokines and other cytotoxic molecules that mediate the killing of tumour cells. Therefore, IL-10 has been found to inhibit the anti-tumour activities of AMs and may thus contribute to tumour progression (125).

1.11.2. Altered AMs function via inhibition of anti-tumour effects

AMs have also been shown to function inefficiently and to promote tumour growth in patients with lung cancer (23, 26, 27, 116, 125). Inhibition of pro-inflammatory cytokine secretion by AMs has been reported in the presence of elevated levels of serum IL-10 (116, 125). In murine peritoneal macrophages, LPS-induced TNF-α release was inhibited by IL-10 (126). The suppression of TNF-α function favours tumour proliferation and differentiation through the activation of IL-10. This is consistent with the suppression of AMs anti-tumour function in advanced-stage lung cancer (91).

The IL-10 secretion by AMs has also been found to inhibit the cytokine secretion of other T cell proliferation inducers, such as IL-2 (116). Although the anti-tumour effect of IL-2 is not completely understood, it has the capacity to mediate cytotoxicity and induce synthesis of IL-1 and TNF-α (127). In addition, IL-10 decreased Golgi apparatus (GA) and rough endoplasmic reticulum (RER) function in AMs from patients with lung cancer (116). The reduction of GA and RER negatively impact the synthesis and secretion of cytokines such as TNF-α, leading to dysfunction and down-regulation of AMs function. A reduction in TNF-α could also lead to a reduction in cytostatic activity of AMs and may promote tumour growth and proliferation (116). The cytostatic activity of AMs has been shown to be compromised in patients with lung cancer (23, 128-130). In some studies, the reduction in cytostatic activity is greater in AMs from tumour-bearing segments compared to non-tumour bearing segments (129), whereas in others the defect appears more generalised (23).

1.11.3. Altered cytotoxicity and cytokine release

Altered cytotoxic activity of AMs from patients with lung cancer has been demonstrated (13, 24, 26, 27) with both increased (24, 131) and decreased (13, 27) cytotoxic function described. Impaired cytotoxic ability of AMs from patients with lung cancer has been shown along with increased TNF-α and IL-1 production in the same patients (24). This revealed an obvious discrepancy in the correlation between cytokine release and cytotoxicity. Increased cytotoxic activity by AMs from lung cancer patients was discovered, however, with no reported alteration in cytokine release (131). These results suggest increased cytokine release or cytotoxicity may be a reaction to the presence of the tumour, rather than a primary mechanism preventing its occurrence. However, altered cytotoxic activity in AMs and TAMs has been shown to be mediated via decreased secretion of cytokines (IL-1, IL-6 and TNF-α) in patients with lung cancer (13, 27). Decreased TNF-α and IL-1 secretion has been demonstrated in AMs from patients with both NSCLC (squamous cell lung carcinoma and

large cell lung carcinoma subtypes) and small cell lung cancer, and reduced IL-6 secretion has been demonstrated from AMs derived from patients with large cell undifferentiated and small cell subtypes (27). TNF-α, IL-1 and IL-6 promote the induction of Th1 cells, which enable macrophage-mediated killing. Reduced Th1 mediated cytokines may consequently limit the cytotoxic potential of AMs or TAMs and enable tumour progression (13). Whilst IL-6 release can contribute to the anti-tumour function of AM, a pro-tumour function has also been proposed. Even with IFN-γ and LPS stimulation, IL-6 inhibited the development of tumouricidal function in AMs of patients with lung cancer (26). Therefore, overproduction or dysregulation of IL-6 by macrophages can contribute to the growth and metastasis of many carcinomas, including lung cancer (132).

1.11.4. Altered phagocytic capacity and receptor expression

Decreased antibody-mediated cytotoxicity in AMs from lung cancer patients has been reported. AMs normally take up antigens for processing and present them on major histocompatibility complex (MHC) class I and II molecules. This activates T cells and in turn stimulates phagocytosis (macrophage-mediated killing) and the release of pro-inflammatory cytokines (TNFα and IL-1) (87). A study has confirmed that AMs from patients with small cell and squamous cell lung carcinoma were impaired in their ability to uptake 40nm fluorescent polystyrene beads, in comparison with controls, while AMs from patients with small cell, squamous and large undifferentiated carcinoma showed decreased uptake of 1000nm beads (27). Impairment of uptake ability may highlight impairment in the phagocytic capability of AMs in lung cancer. The same study suggested differences in the phagocytic ability of AMs depending upon the histological subtype of lung cancer. Reduced functionality of AMs may thus promote tumour growth and differentiation.

Altered cell surface expression of MHC molecules on AMs has been found in patients with lung cancer. Decreased MHC class II expression on AMs from patients with small cell

carcinoma and decreased intracellular adhesion molecule (ICAM-1) and CD83 expression from patients with small, large and squamous cell lung carcinoma after IFN-γ stimulation has been demonstrated by flow cytometry (27). Conversely, McDonald et al. (1990) found no difference in the expression of ICAM-1 with or without IFN-γ stimulation (23). ICAM-1 plays an essential role in the early stages of T-cell activation. Reduced expression of ICAM-1 therefore impairs AMs-mediated cytotoxicity (87). In addition, reduced expression of mannose receptor by AMs in lung cancer patients has also been shown (27). The mannose receptor is a transmembrane glycoprotein that binds and internalises carbohydrate ligands such as mannose and fructose. Mannose receptor is expressed on AM and plays a role in host defence and immune regulation. Therefore, reduced receptor expression may impair anti-tumour function by AMs and favour tumour progression (133).

Alterations in the functional status of AMs vary with the stage of lung cancer (91, 129, 131). A decline in cytostatic and cytotoxic activity of AMs from patients with advanced stages of primary lung cancer has been observed (91, 129, 130), suggesting a growth-promoting effect of lung tumours on AMs function. In contrast, increased cytotoxicity in advanced stages of lung cancer has also been documented (131).

The underlying demographic and clinical characteristics of a patient may also influence AMs function. Such characteristics include age, smoking status, tumour histology, tumour stage and the presence of underlying comorbidities such as chronic obstructive pulmonary disease (COPD). BAL and whole blood cells from patients with small cell lung carcinoma and NSCLC cancer were compared in their secretion of IL-1, IL-6 and TNF-α. It was suggested that BAL and blood cells from patients with small cell lung carcinoma secreted significantly less cytokines (IL-1, IL-6 and TNF-α) than BAL and blood cells from patients with NSCLC (22). Although Pouniotis et al. (2006) noted differences in function between AMs from patients with different histological subtypes of lung cancer (27), the

majority of studies do not differentiate further than comparing between the two major categories of small cell lung carcinoma or NSCLC (13, 24, 25, 134).

1.12. Role of alveolar macrophages in angiogenesis

AMs have the ability to promote tumour progression by facilitating angiogenesis. Angiogenesis plays an important role in tumour growth, invasion and metastasis (132). It involves degradation of extracellular matrix and stromal invasion by endothelial cells (132). The proliferation, migration, and differentiation of endothelial cells into functional capillaries initiates the development of vasculature in the tumour (87). AMs are known to release growth factors, cytokines and inflammatory mediators in lung cancer. These factors and mediators include IL-8, VEGF, PDGF, basic fibroblast growth factor (bFGF) and MMPs, which are known to regulate angiogenesis (135).

Increased secretion of IL-8 by AMs has been reported in patients with lung cancer and increased gene expression of IL-8 in lung cancer cell lines after co-culture with TAMs has also been found (135). The IL-8 is a potent angiogenic factor that is released from AMs and has been identified as favouring tumour growth and metastasis (118). The IL-8 in serum and BAL fluid has been shown to be higher in patients with lung cancer than in non-cancer controls and the level of IL-8 in BAL fluid can be considered as a prognostic factor for decreased survival (119). Lung cancer cells from patients with NSCLC demonstrated increased IL-8 mRNA expression after interaction with tumour infiltrating macrophages *in vitro*, suggesting that tumour cells may be activated by macrophages and secrete angiogenic factors (such as IL-8) which then enable tumour progression (135). Tumour progression associated with reduced survival rates has also been found in patients with NSCLC whose tumour cell lines demonstrated increased IL-8 mRNA expression compared to those with reduced expression (135).

VEGF also plays an important role in angiogenesis (113). It has been reported that the transcription and protein production of VEGF is increased in multinuclear cells of pulmonary sarcoid granulomas (136). VEGF may have a chemotactic effect on TAMs and increased expression may guide migration to avascular areas, increasing blood vessel development in tumours (87). The expression of VEGF-C, a member of the VEGF family, has been shown in tumour cells and stromal macrophages of patients with NSCLC using the IHC technique. However, VEGF-C expression in tumour cells and stromal macrophages did not correlate with nodal metastasis or angiogenesis (137). The underlying mechanisms involved in VEGF expression in AMs and their functional significance in lung cancer remain incompletely determined (138).

Increased PDGF production by TAMs in tumour stroma has been reported (13, 134). Tumour stroma is specialised peritumoral and intratumoral connective tissue comprised of endothelial, mesenchymal, and inflammatory cells and sometimes described as a tumour microenvironment (13). It is suggested that elevated PDGF in the tumour stroma favours tumour progression and angiogenesis via the migration of endothelial and mesenchymal cells (13). This is supported by studies showing that PDGF stimulates cell migration in human lung carcinoma cells (139). Cell migration plays an important role in metastasis and can be promoted via the release of cytokines from AMs.

MMPs are matrix degrading enzymes that facilitate tumour growth and metastasis through the breakdown of extracellular matrix and in particular basement membranes (87). In patients with lung cancer, matrix metalloproteinase-12 (MMP-12) and matrix metalloproteinase-9 (MMP-9) have been shown to promote lung tumour growth (140, 141). MMP-12 is released by AMs and favours tumour progression by enhancing angiogenesis and the breakdown of elastin. Interestingly, an association between increased VEGF and MMP-12 gene expression and tumour vascularity has been demonstrated (140). MMPs are an

attractive target for therapeutic purposes because of their involvement in tumour progression. However, a recent trial has suggested that some MMPs might play a crucial role in host resistance against tumour progression. An increase in Lewis lung carcinoma pulmonary metastasis was shown in MMP12-deficient mice while normal MMP12 expression was associated with reduced tumour-associated microvessel density *in vivo* (142). Collectively, these results suggest an important role for MMP12 in inhibiting lung metastasis and indicate that specific MMP inhibitors could be designed to target tumour-promoting MMPs in order to inhibit tumour growth (142).

Increased MMP-9 levels and significant correlations between tumour stage and both BAL fluid and plasma MMP9 levels have been demonstrated in patients with NSCLC (143). It has also been suggested that serum MMP-9 levels (but not BAL fluid MMP-9 levels) can be useful in distinguishing between malignant and benign lung diseases. The same study also demonstrated that serum MMP-9 levels relate to both disease stage and general clinical status of patients with NSCLC (144). This study did not, however, specify which cells (macrophages or cancer cells) was the source of MMP-9. Further investigation is clearly required into the relationship between macrophage, MMPs and lung cancer.

Table 1: **Summary of pro- and anti-tumour roles of alveolar macrophages in lung cancer**

Primary lung cancer subtype	Type of macrophage	Anti-tumour role	Pro-tumour role	Clinical parameters	Reference
Small cell lung carcinoma	AMs		Decreased IL-6, TNFα and IL-1 production	Further reductions seen in phase IV	(22)
	AMs		Decreased IL-6, TNFα, IL-1, MHC class II surface expression	Inability to stimulate anti-tumour immunity	(27)
Non-small cell lung carcinoma (NSCLC)	AMs		IL-6 found to inhibit the development of tumouricidal activity	Correlate to metastatic potential of cancer cells	(26)
	TIM		Increased expression of IL-8 mRNA	Interaction with NSLC may promote invasiveness	(135)
	TAMs		Gene expression of IL-8 and MMP-9	GM/CSF induces a cellular expansion in the lung	(132)
	AMs	Increased AM count and IL-6 secretion with GM/CSF	Increased secretion of IL-8	Limit possible cytotoxicity and promote angiogenesis	(118)
	TAMs	Decreased TGF	Decreased IL-1, TNFα, IL-6 and increased PDGF		(13)
	TAMs	VEGF-C not correlated to angiogenesis	Expression of VEGF-C	Lower 5-year survival rate with high expression of VEGF in cancer cells	(137)
	AMs	Increased TNFα and IL-1			(24)
	AMs, Monocytes	Increased TNFα, IL-1, IL-6 mRNA expression with GS/CSF,	Impaired cytotoxic ability	GS/CSF therapy enhanced cytotoxic activity	(89)

Adenocarcinoma	TIM		High density (microvessel counts)	Short relapse-free survival of patients	(132)
	AMs	Increased IL-6 and IL-1β			(22)
Squamous cell lung carcinoma	AMs		Decreased TNFα, IL-1 and mannose receptor		(27)
Large cell lung carcinoma	AMs		Decreased TNFα, IL-1, IL-6		(27)

1.13. Altered alveolar macrophages function: the role of smoking and lung cancer

Smoking increases the risk of lung cancer. Many studies have looked at the impact of smoking on AM functionality (131, 138, 145-148). Some have shown suppressed anti-tumour activity of AMs from smokers with lung cancer compared to non-smokers with the same disease (91). Using LPS and IFN-γ stimulation, cytotoxicity levels were reduced in AMs from current smoking patients with lung cancer, compared to non-smokers and ex-smokers. Cigarette smoke contains approximately 4,000 components, 55 of which are described as carcinogenic. One of the most important nicotine derivatives is the nitrosamine 4 (methylnitrosamino)-1-(3-pyridyl)-1-butanone (NNK). NNK has been found to down-regulate cytokine production by AMs. NNK activation inhibits TNF and IL-12, while increasing IL-10 and PGD2 release. These results suggest that NNK favours the differentiation of AMs from M1 to M2 phenotype, which is known to induce tumour growth, angiogenesis and progression (146).

The impact of smoking on AM recognition molecules and phagocytic capacity in a non-cancer context was investigated in another study which found decreased phagocytic ability of AMs in both smokers and ex-smokers with COPD and healthy smokers when matched to non-smoking control participants. However, phagocytic ability was greater in COPD patients who had stopped smoking when compared to COPD patients who currently smoke. It has also been demonstrated that smoking impacts AMs recognition molecules and is associated with cyclic adenosine monophosphate (cAMP) increase (147).

A recent study showed that cigarette smoke is able to induce AMs polarisation towards M2 phenotype in patients with COPD by deactivating M1 macrophage. Researchers found that cigarette smoke was able to down-regulate M1-related genes such as CXCL9, CXCL10, CXCL11 and CCL5, while up-regulating M2-related genes such as MMP-2 and

MMP-7 (149). However, further investigation is required to determine the polarisation status of AMs within the tumour microenvironment of patients with lung cancer, the factors that favour AMs polarisation and whether alterations in polarisation modulate tumour growth and prognosis.

Down-regulation of IFN-γ signalling has been demonstrated in AMs from smokers. IFN-γ is an important cytokine, which can perform several functions important for the development of activated macrophages during inflammation. Dhillon et al. (2009) found that chronic exposure of the alveolar space to cigarette smoke could result in a loss of IFN-γR α-chain expression on AMs, followed by a down regulation of IFN-γ signalling. The function of IFN-γ in immune surveillance may thus be deficient in the lungs of smokers and could lead to both infection and the development of cancer (148). Many of the studies examining smoking and its effect on AMs have utilised different animal models of smoking. Although the translation from animal to human studies is still not clear, animal studies are able to provide greater focus on the interaction between cigarette smoking and AMs function. One study has shown that the release of MMP-12 and TNF-α by AMs was altered in mice exposed to cigarette smoke. MMP-12 secretion from mouse AMs was increased after cigarette smoke exposure, whereas TNF-α secretion showed an initial time-dependent increase and subsequent decrease over ten days (145). Cigarette smoke may thus progressively compromise AMs functionality, particularly in terms of TNF-α secretion. However, more research is required to investigate the role of cigarette smoking on pro-inflammatory and MMP secretion from AMs and its association with lung cancer.

1.14. Alveolar macrophages: roles of reactive nitrogen/oxygen species (ROS and NOS)

AMs release large amounts of toxic molecules such as ROS and NOS (150). Overproduction of ROS/NOS has been described as a potential factor leading to cancer through mechanisms such as inhibition of apoptosis, DNA damage and P53 mutation (3). The AMs taken from tumour-bearing lobes of patients with lung cancer were demonstrated in a study by Sharma et al. (1997) to produce significantly higher quantities of oxygen radicals compared with those from disease-free lobes (151).

The AMs are one of the main producers of cytokines and their production may be modified in response to alterations in NOS concentration. In studies which have investigated the role of NOS in human lung cancer (152-154), increasing NOS levels in BAL fluid were associated with squamous cell lung carcinoma compared to control subjects (153). Additionally, the generation of NOS was higher in cultured AMs from patients with lung cancer in comparison to controls (154). The NOS is able to regulate VEGF expression in mouse lung tumours as well as other systems, demonstrating NOS ability to modulate angiogenesis in lung tumours *in vivo*. Kisley et al. (2002) suggested that the absence of iNOS or inhibitors of its activity reduced mouse lung cancer development (155). The same results have also been achieved in studies of rodent cancer models (156). Most of the studies showing a clear role of macrophage-mediated NOS secretion in tumour inhibition have been in murine models and its role in human macrophages requires further investigation (157).

1.14.1. Therapeutic modulation and future directions

For many years, immunologists have considered that the presence of inflammatory cells such as macrophages is a sign of an effective host immune response against tumour growth (158). Contrary to this theory, various studies have now demonstrated that the recruitment to and

presence of macrophages in the tumour microenvironment can be associated with increased tumour growth and metastasis, poor prognosis and decreased patient survival (72, 159). A recent study showed that knocking down macrophages with clodronate-encapsulated liposomes reduced angiogenesis and tumour growth in mouse and in xenograft models of teratocarcinoma and rhabdomyosarcoma (160). These studies suggest that the mechanism reducing angiogenesis was mediated by the M2 macrophage subset, which has been shown to promote angiogenesis in these tumour models.

The M1 macrophages are able to kill and inhibit the growth of tumour cells when they are activated with LPS and IFN-γ. However, in tumour sites M1 macrophages are present in lower numbers and they are likely to polarise towards M2 phenotype under the influence of several factors such as IL-10 and the inhibition of NF-κB (96, 161). Recent evidence suggests that new therapeutic strategies should be targeting the 'switch' from M1 to M2 macrophage subsets in the early stages of tumour progression. Also re-adjusting M2 and skewing it to M1 subsets would be a possible therapeutic strategy to reduce already established tumours (20, 158). Recent studies have suggested that the use of CpG (C-phosphate-G) and anti-IL-10 receptor antibodies is able to switch M2 subsets back to M1 subsets with establishment of full anti-tumour activity (162). Another study revealed that the inhibition of STAT3 activity, which is known to mediate IL-10 function, resulted in restored pro-inflammatory M1 macrophage function (161). A DNA vaccine targeting legumain, which is a specific stress protein overexpressed by M2 macrophages, resulted in a robust immune response that decreased the number of legumain-expressing TAMs and increased survival rates in mouse models of metastatic breast, colon and non-small lung cancer (163). Interestingly, a recent study investigating the role of hypoxia and macrophage subsets showed that hypoxia-inducible factor 1-alpha (HIF-1α) knockout (HIF-1α$^{-/-}$) macrophages were still able to infiltrate hypoxic tumour regions and skew towards M2 phenotype with reduced cytotoxicity.

However, the HIF-1$\alpha^{-/-}$ macrophages were not able to display the same angiogenesis-promoting properties as wildtype (Wt) macrophages (164). Taken together, reducing or preventing M2 phenotype polarisation in tumour microenvironments may be a promising therapeutic strategy to reduce the pro-tumour effects of M2 macrophages.

1.15. Bronchoalveolar lavage (BAL) and flow cytometry

1.15.1. Bronchoalveolar lavage (BAL) as a research tool

Fibreoptic bronchoscopy was developed for clinical practice and it is commonly used for diagnostic and therapeutic purposes. Ikeda introduced the flexible fibreoptic bronchoscope in 1968 and from there a major development in this technique was made (165). The scope can be done using a flexible or rigid bronchoscope. A flexible scope is almost always used; however, in rare cases such as retrieving foreign objects a rigid bronchoscope might be used. Flexible bronchoscopy is the more common procedure because less discomfort is experienced for the patient compared to rigid bronchoscopy and it can also be performed easily and safely under moderate sedation (166, 167). This technique has some limitations that negatively impact its usage and outcomes such as the variation in the technical performance and application of bronchoscopy in clinical practice. Despite its limitations, bronchoscopy remains one of the most common clinical procedures for lung cancer diagnosis (166, 168).

Fibreoptic bronchoscopy with bronchoalveolar lavage (BAL) using manual hand held suction in order to remove non-adherent cells and lung lining fluid from the mucosal surface is widely used in the research environment (169). The BAL provides access to lower respiratory tract cells (macrophage, B- and T- cells) and their products, so it can be used to obtain immune cells and in particular to investigate their condition in a normal or stressful environment (166, 168). BAL is performed using 50 ml syringes prefilled with warmed normal saline. Gentle hand suction is then performed and the BAL retrieved volume is

usually between 100 and 150 ml. The BAL fluid is collected on ice and transferred to polypropylene containers in order to minimise macrophage adherence. BAL fluid gained from healthy non-smokers should consist of a majority of AMs (80–90%), some lymphocytes (5–15%), and very few neutrophils (3%) or eosinophils (1%) (39). Freshly taken BAL fluid has a milky or light brown to cloudy appearance. For research purposes, BAL fluid and cells are commonly processed for further investigation using different techniques such as flow cytometry (39, 170).

1.15.2. Flow cytometry

Flow cytometry is a device that illuminates cells (particles) as they flow individually in front of a light source and then collects and presents the signals from those particles (171). The common term that has been used to describe anything that can be detected by the instrument is "event". Flow cytometry has been widely used in laboratories for both research and diagnosis because it has the ability to process and detect various particles, including cells (128), cell lines (172), bacteria (173), sperm (174), latex beads (27) and DNA fragments (175). It also provides a large and diverse set of information about events as it can illuminate individual particles. The cell size, cytoplasmic complexity, DNA or RNA content, and a wide range of membrane-bound and intracellular proteins can be measured using flow cytometry (171). Flow cytometry is also increasingly being used in clinical applications because of the recent development of less-expensive, smaller, more user-friendly instruments (171). Several fluorescent dyes have been used to analyse particles by conjugating them to antibodies that bind either to the surface and/or intracellular compartments. A fluorescent dye absorbs light and then emits light of a different colour usually with longer wavelength. The light emitted from each event can be detected and stored for later analysis. Flow cytometry has been used to process and analyse BAL fluid samples from many conditions, including lung cancer and

other pulmonary disorders, and also to evaluate immune cell function in different diseases (27, 128, 149).

1.16. Summary and Implications

The role of macrophages in lung cancer appears paradoxical. Whilst macrophages are clearly implicated in inhibiting tumour growth with consequent tumour regression, they have also been demonstrated to have pro-tumour functions resulting in tumour onset and eventually tumour progression and metastasis. Differences between study outcomes may relate to the examination of different lung cancer histological subtypes, different tumour stages or examination of macrophages from different lung segments (i.e. tumour bearing or non-tumour bearing lung segments). Patient demographics such as smoking status, and the presence or absence of comorbidities such as COPD, may also contribute to differences. A number of pro- and/or anti-inflammatory cytokines have been described as possessing dual roles in lung cancer including TNF-α, IL-6, IL-8, IL-10, VEGF and PDGF. However, their direct effect on the function of macrophages in patients with lung cancer is not completely understood. Smoking has also been associated with altered macrophage functionality in lung cancer patients. Further studies are encouraged to examine macrophages (AMs, TAMs and monocytes) phenotype and function in lung cancer under a range of different conditions including diverse histological subtypes to answer the questions about the link between lung tumour environment and macrophages phenotype and function. Thus, our study aims to assess the complex connection between NSCLC and macrophage phenotype and function. Various surface and intracellular markers, cytokines, proteins and genes were utilised in this study in order to investigate this issue. Several techniques including flow cytometry, RT-PCR, quantities proteomics, CBA, Bio-Plex, MAGPIX-Luminex and IHC were also used in

this study to elucidate the relationship between lung cancer and macrophages function and phenotype.

1.17. Aims and hypotheses

Previous studies that examined the role of macrophages in lung cancer have provided inconsistent results. Some studies have shown alteration in macrophage phenotype and function in the presence of lung cancer while others show no effect. Macrophages (AMs, TAMs and monocytes) are part of the lung tumour microenvironment and have been suggested to play a major role in promoting and/or suppressing tumour growth and metastasis. The relationship between NSCLC and macrophage phenotype and function is controversial and still needs further intensive investigation. We hypothesise that macrophages in local and systemic environment (AMs, TAMs and monocytes) skew from the M1 to M2-activated phenotype in NSCLC. We also believe that NSCLC has the ability to alter some macrophage functions, Th1 and Th2 cytokine levels in serum and proteins expression in BAL fluid.

Here, we aim to assess this hypothesis by (I) characterising the M1 and M2 macrophage populations within the AM population using flow cytometry and PCR in patients with NSCLC compared to non-cancer controls; (II) evaluating the M1 and M2 monocyte populations (macrophage precursors) in patients with NSCLC compared to non-cancer controls using flow cytometry. Furthermore, Th1 and Th2 cytokine levels that contribute to the differentiation of these populations will be analysed in the serum of patients with NSCLC versus non-cancer controls; (III) using quantitative proteomics to investigate the up-regulation of novel proteins in BAL fluid from patients with primary lung adenocarcinoma to potentially identify new potential biomarkers expressed by alveolar macrophages; and (IV)

finally characterising the M1 and M2 macrophage populations within TAMs in different subtypes of NSCLC compared to non-tumour tissue.

In other words this study aims to identify if NSCLC has the ability to affect the phenotype and function of macrophage populations in the local and systemic environment using three different macrophage subtypes (AMs, TAMs and monocytes). It also investigates the presence of biomarkers expressed in the BAL fluid that may be associated with NSCLC. This study characterises the presence of specific macrophage subset markers from the lungs (AMs and TAMs), blood (monocytes) and serum of patients with NSCLC. In particular, we will determine their phenotypic similarity with the classically-activated M1 macrophage subset and the alternatively-activated M2 macrophage subset by examining the expression of specific cell surface and intracellular markers (HLA-DR, iNOS, CD163 and CD36) and several other markers e.g. CD71, CD11b, CD11c, CD44, IL-10, MMP-9, IL-6, IL-12, tumour necrosis factor (TNF) and interferon gamma (IFN-γ). It also aims to help in the identification of new potential biomarkers for NSCLC, which might assist in the development of more effective anti-tumour treatments.

1.18. Significance, Scope and Definitions

This research focused on macrophages phenotype and function in patients with NSCLC compared to non-cancer controls. Some of the surface expression markers, cytokines, chemokines, proteins and genes that are known to be associated with macrophage subtypes (AMs, TAMs and monocytes) were investigated in this study. A number of techniques were used in order to evaluate our hypothesis including flow cytometry, RT-PCR, quantitative proteomics, cytometric bead array (CBA), Bio-Plex assay and immunohistochemistry (IHC). The outcomes of this research will be beneficial in understanding the impact of NSCLC on macrophage phenotype and function.

Chapter 2 Materials and Methods

2.1. Sample collection

In this thesis different samples were collected and utilised to meet the aims of this research, including BAL fluid (AMs, protein and RNA), blood (monocytes, serum) and lung tissue (TAMs). BAL fluid and blood samples were collected through the Department of Respiratory and Sleep Medicine, Austin Health, Heidelberg, VIC, Australia. Also, tissues and additional serum samples were obtained from the Victorian Cancer Bio-Bank, Melbourne, Australia. This chapter will describe in detail all the samples, materials and methods that were used in this thesis.

2.2. Materials and methods for monocyte and serum Th1 and Th2 cytokine profile study

2.2.1. Monocyte study participants

Blood was obtained from patients undergoing diagnostic bronchoscopy for investigation of lung cancer or who were undergoing bronchoscopy for investigation of a non-cancer related symptom. Complete blood count (CBC) was completed for all blood samples using CELL-DYN Emerald (Abbott Diagnostics, USA) at the RMIT Hematology Department, Melbourne. Patients were recruited through the Department of Respiratory and Sleep Medicine, Austin Health, Heidelberg, VIC, Australia. Human Ethics approval was received from HREC Austin Health H2007/02814 and RMIT University Human Research Ethics Committee ASEHAPP 15-13 and the informed consent of all participants was obtained. Staging was applied in this study using the new TNM (tumour, node, metastases) staging system (seventh edition) for lung cancer (176).

2.2.2. Peripheral blood mononuclear cells (PBMC)

Venous blood was collected in heparinised tubes and PBMC were isolated by Ficoll-Paque density gradient centrifugation (GE Healthcare Bio-sciences, Uppsala, Sweden) (177). PBMC are a population of immune cells that remain at the less dense (mononuclear cell layer), upper interface of the Ficoll layer (Fig. 15). PBMC isolated populations consist of lymphocytes (T cells, B cells, and NK cells) (70-80%), monocytes (10-30%), and dendritic cells (1-2%). The blood was diluted (1:2) in sterile Phosphate buffered saline (PBS) and then 25 ml of the diluted cell suspension was layered over 15 ml of Ficoll-Paque in a 50 ml conical tube. The tube was then centrifuged at $400xg$ for 30 minutes without brake. The mononuclear cell layer (white blood cell ring fraction) was transferred into a new 50 ml tube using sterile Pasteur's pipette. The volume was then adjusted to 30 ml using sterile PBS and centrifuged at $300xg$ for 10 minutes. For removal of platelets, the cell pellet was resuspended in 30 ml of sterile PBS and centrifuged at $200xg$ for 10-15 minutes and the supernatant carefully removed completely. The pellet was resuspended in 10 ml PBS to be counted and freshly used or frozen down at -80°C in 90% fetal bovine serum (FBS) and 10% dimethyl sulfoxide (DMSO).
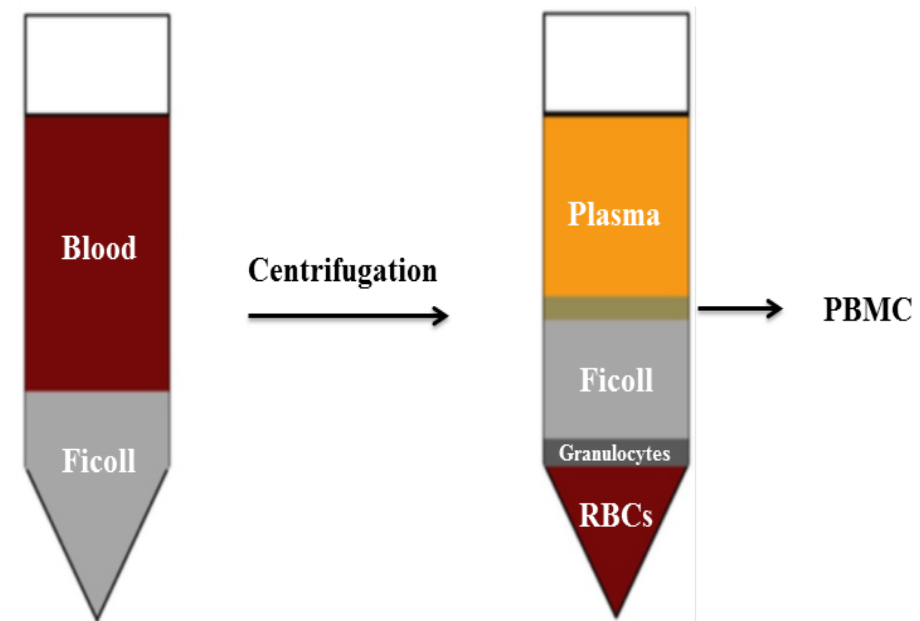
Figure 15: Ficoll-Paque density gradient centrifugation. Ficoll-Paque was used to isolate PBMC (mononuclear cell) from NSCLC patients and non-cancer controls. PBMC are the populations of immune cells (lymphocytes, monocyte and dendritic cells) that remain at the less dense, upper interface of the Ficoll layer.

2.2.3. Monocyte phenotype analysis by flow cytometry

Flow cytometry was used to assess monocyte expression of CD14, CD45 CD71, CD11b, CD44, CD16 and CD11c (BD Pharmingen ™, USA) as well as the M1 marker HLA-DR (BD Pharmingen ™, USA) and the M2 markers CD163 and CD36 (BD Pharmingen ™, USA) (Table 2).

The cells were fixed with 2% paraformaldehyde (PFA)/PBS at room temperature for 20 minutes. The cells were then centrifuged for 5 minutes at 604xg, washed in 0.5% (w/v) saponin/PBS and incubated at room temperature for another 15 minutes. The cells were stained with antibodies directly conjugated to fluorescent probes. All antibodies were diluted in 0.5% Bovine serum albumin (BSA)/PBS (w/v) based on cell numbers at the manufacturer's recommended concentrations and added to cells for 40 minutes in the dark on ice. After incubation, the cells were washed with PBS and then centrifuged for 5 minutes at 268xg. The pellet was then resuspended in FACS Fix buffer (1% BSA, 0.1% (w/v) sodium azide and 2% (w/v) paraformaldehyde (PFA) in 500µl of PBS) and analysed using flow cytometry (BD FACS Canto BD Biosciences, San Jose, CA, USA). Approximately 10^6 cells were stained with various combinations of antibodies. Purity of monocytes was assessed according to CD14^{++}, CD45$^+$ and CD16$^-$ expression by flow cytometry. At least 5,000 cells were collected and analysed (BD FACS Canto BD Biosciences, San Jose, CA, USA). All analysis was completed using the BD FACSDiva^{TM} analysis software (BD Biosciences, USA) within the RMIT Flow Cytometry Facility, Bundoora, Melbourne. All quadrants were set up according to matched isotype control antibodies and all results are shown as % surface expression (%SE) and/or mean fluorescence intensity (MFI).

2.2.4. Cytometric bead array (CBA)

The serum samples for the CBA assay were fractionated by leaving blood undisturbed for 15-30 minutes at room temperature. The clot was then removed by centrifuging at 2,000xg for 10 minutes. The blood samples were obtained from patients undergoing diagnostic bronchoscopy for investigation of lung cancer or who were undergoing bronchoscopy for investigation of a non-cancer related symptom. Patients were recruited through the Department of Respiratory and Sleep Medicine, Austin Health, Heidelberg, VIC, Australia. The Human Th1/Th2 11plex Ready-to-Use FlowCytomix Multiplex (eBiosciences, USA) was employed to detect the level (pg/ml) of Th1/ Th2 cytokines including IL-1β, IL-2, IL-4, IL-5, IL-8, IL-10, IL-12 (p70), TNF-α, tumour necrosis factor beta (TNF-β), and IFN-γ in serum samples of patients with primary lung cancer and non-cancer controls, according to the manufacturer's instructions (Human Th1/Th2 11plex RTU FlowCytomix Kit). Fluorescence was analysed using flow cytometry (FACS Canto, BD Biosciences, San Jose, CA, USA) and cytokine levels were determined using the BMS FlowCytomix Software within the RMIT Flow Cytometry Facility, Bundoora, Melbourne.

2.2.5. Cytokine and Chemokine Measurement by Bio-Plex multiplex system

Different groups of ready to use serum samples were purchased from the Victorian Cancer Bio-Bank (Victoria, Australia) to analyse the Th1 and Th2 cytokines profile using the Bio-Plex, MAGPIX-Luminex assay. The Bio-Plex assay kit from Bio-Rad was applied to detect the Th1/ Th2 cytokines including IL-1β, IL-4, IL-6, IL-8, IL-10, IL-12 (p70), IP-10, TNF-α, MCP-1 and VEGF in serum samples of patients with NSCLC (adenocarcinoma, squamous cell lung carcinoma and large cell lung carcinoma) and non-cancer controls. The method was performed by the same operator according to manufacturers' instructions. The kit supplied standards that were reconstituted and diluted at 7 serial concentrations following

manufacturer's instructions (standard curves). Standards included all recombinant cytokines tested and were considered as positive controls for the procedure. Bead fluorescence readings were analysed using the Bio-Plex MAGPIX multiplex reader (Bio-Rad, USA) and cytokine levels were determined using the Bio-Plex Manager Software (Bio-Rad, USA) within RMIT University, Bundoora, Melbourne.

2.2.6. Statistical analysis of monocyte and cytokine profiles studies

Experiments were performed in triplicate. The results are shown as mean values ± standard error (SEM) as error bars. The statistical analysis was performed using GraphPad Prism-6. One-way ANOVA multiple comparison test (as a post-test analysis) was performed with the Tukey test (multiple comparison test comparing every group with every other group).

Table 2: **Markers used to characterise the phenotype and function of monocytes in patients with NSCLC compared to non-cancer controls**

Cell types	Markers	Company	References
	CD14	BD Pharmingen ^{TM}, USA	(76, 178)
	CD11b	BD Pharmingen ^{TM}, USA	(179)
Monocyte / myeloid / macrophage markers	CD44	BD Pharmingen ^{TM}, USA	(180)
	CD16	BD Pharmingen ^{TM}, USA	(178, 181)
	CD11c	BD Pharmingen ^{TM}, USA	(182)
	CD71	BD Pharmingen ^{TM}, USA	(183)
M1	HLA-DR	BD Pharmingen ^{TM}, USA	(76, 179)
	CD163	BD Pharmingen ^{TM}, USA	(184)
M2	CD36	BD Pharmingen ^{TM}, USA	(184)

2.3. Materials and methods for alveolar macrophages and proteomics studies

2.3.1. BAL fluid participants

BAL fluid samples were obtained from patients undergoing diagnostic bronchoscopy for investigation of lung cancer through the Department of Respiratory and Sleep Medicine, Austin Health, Heidelberg, VIC, Australia. Human Ethics approval was received from HREC Austin Health H2007/02814 and RMIT University Human Research Ethics Committee ASEHAPP 15-13 and the informed consent of all participants was obtained. Staging was applied in this study using the new TNM (tumour, node, metastases) staging system (seventh edition) for lung cancer (176).

2.3.2. BAL fluid processing

BAL fluid was sampled at the time of diagnostic fibreoptic bronchoscopy using instilled aliquots of normal saline pre-warmed to 37°C. In the case of patients with lung cancer, the samples were taken from an adjacent uninvolved lobe. In the case of non-cancer controls, the sample was from the right middle lobe or lingula lobe. The BAL fluid samples were collected in sterile centrifuge tubes, immediately placed on ice and stored at 4°C until collection (185). The BAL fluid samples were stained using a Rapid Diff Kit (Australian Biostain) in order to differentiate WBC counts. Differential cell counts were ascertained by light microscopy. Cells were collected by centrifuging the BAL fluid at 500xg for 6 minutes at 4°C. The cells were then washed twice in 0.1% BSA/PBS (w/v) at 4°C. The cell suspension containing trypan blue 0.2% (w/v) (Sigma, USA) was counted using haemocytometer. After counting, cells were either analysed immediately or frozen and stored in liquid nitrogen for future analysis. For storage, AMs pellet was resuspended in RPMI-1640 medium (Greiner, Bio-one, USA) containing 10% fetal bovine serum (FBS) and 10% dimethyl sulfoxide (DMSO) at a

concentration of 1-5 x 10^6 cells/ml.

2.3.3. Differentiation of AMs phenotype using flow cytometry

Cell staining was carried out using antibodies directly conjugated to fluorescent probes. Flow cytometry was used to assess AMs expression of CD68 (macrophage marker) (Dako, Denmark), CD11b (macrophage-1 antigen), CD71 (transferrin receptor protein 1) and CD44 (cell-surface glycoprotein involved in cell–cell interactions, cell adhesion and migration) (BD Pharmingen ™, USA). The M1 conjugated marker HLA-DR (Human leukocyte antigen-D related) (BD Pharmingen™, USA) and the M2 conjugated marker CD163 (BD Pharmingen™, USA) were also investigated (Table 3). Crystal violet was used to overcome auto-fluorescence, and unstained and isotype controls were used to determine the quadrant positions. To overcome spectral overlapping between FITC (fluorescein isothiocyanate) and PE (phycoerythrin) fluorochrome emission spectra, compensation values were calculated and adjusted based on AMs FITC and PE fluorochromes. Each staining condition contained 10^6 cells/100μl.

2.3.3.1. Surface staining

AMs were washed with PBS and then centrifuged for 5 minutes at 268*xg*. All antibodies were diluted in 0.5% BSA/PBS (w/v) based on cell numbers at the manufacturer's recommended concentrations and added to cells for 40 minutes in the dark on ice. After incubation, cells were washed twice with cold PBS and then resuspended with 0.4% crystal violet in order to minimise AM autofluorescence. AMs were then centrifuged and resuspended in FACS Fix buffer (1% BSA, 0.1% (w/v) sodium azide and 2% (w/v) paraformaldehyde (PFA) in 500μl of PBS) and analysed using flow cytometry (BD FACS Canto BD Biosciences, San Jose, CA, USA).

2.3.3.2. Intracellular staining

AMs were fixed with 2% paraformaldehyde (PFA) /PBS at room temperature for 20 minutes. Cells were then centrifuged for 5 minutes at $604xg$, washed in 0.5% (w/v) saponin/PBS and incubated at room temperature for another 15 minutes. After incubation, AMs were centrifuged again for 5 minutes at $604xg$ and antibody staining was performed as outlined above for surface staining.

The cells were analysed based on CD68$^+$ expression and then further analysed for expression of defined M1 and M2 markers. At least 5,000 CD68$^+$ cells were analysed for each experimental condition. All experiments were performed in triplicate and quadrants were set up according to matched isotype control antibodies and all results are shown as percentage surface expression (%SE). Gates, dot plots, compensations and mean values were calculated and analysed using the BD FACSDiva^{TM} analysis software (BD Biosciences, USA).

Table 3: **Markers used to characterise the phenotype and function of alveolar macrophages (AMs) in patients with NSCLC compared to non-cancer controls**

Cell types	Markers	Company	References
Macrophage/ myeloid markers	CD68	Dako, Denmark	(27)
	CD11b	BD Pharmingen [TM], USA	(179)
	CD44	BD Pharmingen [TM], USA	(180)
	CD71	BD Pharmingen [TM], USA	(183)
M1	HLA-DR	BD Pharmingen [TM], USA	(76, 179)
M2	CD163	BD Pharmingen [TM], USA	(184)

2.3.4. RNA sample isolation

The RNA samples were isolated using a PARIS kit (Protein and RNA Isolation System) (Ambion, Life Technologies Australia, Mulgrave, VIC, Australia). The AMs were washed twice with PBS and cell disruption buffer added (at least 300μl) for $\geq 10^6$ cells. The lysate was then incubated on ice for 5-10 minutes to ensure complete cell disruption before continuing processing. Once the lysate was homogenised, the sample was immediately mixed with an equal volume of 2X lysis/binding solution at room temperature. Absolute ethanol (150μl) was added to the mixture containing the sample, disruption buffer and 2X lysis/ binding solution. The sample mixture was then applied to a filter cartridge assembled in a collection tube. The mixture was centrifuged at 604*xg* for 0.5-1 minute or until the lysate/ethanol mixture was passed through the filter. The wash solution I was applied to the filter cartridge and centrifuged at 604*xg* for 15-60 seconds. Wash solution 2/3 was then applied twice to the filter cartridge and drawn through the filter at 604*xg* for 1 minute. After discarding the wash solutions, the filter was centrifuged for 10-30 seconds at 9660*xg* to remove the last traces of wash solutions. The filter cartridge was then transferred into a new collection tube and 200μl preheated elution solution (95-100°C) applied to the filter. This eluate containing the RNA was then recovered by centrifugation for 30 seconds at 4293*xg*. The RNA quantity was measured using UV spectrophotometer (Cintras GBC scientific instrument, Australia). RNA samples were then stored at -80°C and kept on ice when in use.

2.3.5. Real-Time quantitative PCR Analysis

Primers were designed for the following genes (IL-6, IL-12, IL-10 and MMP9). The quantitative PCR was performed using (Bio-Rad, MyiQ^{TM} single color, Real-Time PCR detection system, USA). All the primers were designed using primer design software (Invitrogen, Life Technologies, USA) and were then purchased from Invitrogen (Invitrogen,

Life Technologies Australia, Mulgrave, VIC, Australia) (Table 4). A post-run melting curve program was employed in each assay to confirm the presence of a single, specific amplicon of the predicted size (amplicon is a segment of DNA that is amplified using PCR). The standard curve method was used to determine the relative concentration of each gene of interest with the average of triplicate amplifications normalised to a housekeeping gene, 60S ribosomal protein L32 (RPL32) [accession number NM_000994]. All samples were run in triplicate and the mean values were calculated. The relative expression of target genes was calculated in relation to the mean values of target gene expression in the control group using the delta Ct method.

Table 4: **The list of primers that were designed and performed using Bio-Rad, Real-Time PCR detection system**

Genes	Primer sequence
Human RPL32	F: GGC AGC CAT CTC CTT CTC GGC
	R: TGC CTC TGG GTT TCC GCC AGT
Human IL-6	F: GGA ACG CTC CTC TGC ATT GCC A
	R: ACA AGC ACT GGG GTG GGT CG
Human IL-12	F: GGC CTG AAC CAG ACG TGG CA
	R: GCC CGG GCT GGC CAA TAC AT
Human IL-10	F: GGA GGA GGT GAT GCC CCA AGC
	R: CGA TGA CAG CGC CGT AGC CTC
Human MMP-9	F: ACC GCC AAC TAC GAC CGG GA
	R: GAA GAC GCA CAG CTC CCC CG

F: forward primer sequence; R: reverse primer sequence

2.3.6. Statistical analysis of AM study results

Experiments were performed in triplicate. The results are shown as mean values ± standard error (SEM) as error bars. The statistical analysis was performed using GraphPad Prism-6. One-way ANOVA multiple comparison test (as a post-test analysis) was performed with the Tukey test (multiple comparison test comparing every group with every other group).

2.3.7. Protein sample isolation

The protein samples were isolated using the PARIS kit (Protein and RNA Isolation System) (Ambion, Life Technologies Australia, Mulgrave, VIC, Australia). The AMs pellet was washed twice with PBS and cell disruption buffer added (at least 300µl) for $\geq 10^6$ cells. The lysate was incubated on ice for 5-10 minutes to ensure complete cell disruption before continuing processing of the sample. Protein samples were then stored at -80°C and kept on ice when in use.

2.3.8. Protein sample preparation

The protein samples (150µl) were mixed and washed twice with 750µl of ice cold acetone (Merck Millipore, Darmstadt, Germany) and then incubated overnight at -20°C. They were then centrifuged at 13,148*xg* for 10 minutes at 4°C and the supernatant discarded. The pellets were carefully layered with ice cold acetone (750µl) and then centrifuged at 17,968*xg* for 10 minutes at 4°C and the supernatant discarded. The resultant pellets were dissolved in 100µl of 8 M urea (Merck Millipore, Darmstadt, Germany) and 50 mM TEAB (triethyl ammonium bicarbonate) (Sigma-Aldrich, St. Louis, MO, USA) with alternate sonication and vortexing. Protein concentration estimation was carried out using the micro BCA assay kit (Thermo Scientific, Rockford, IL, USA) and then micro-plate reader at 562nm (Biochrom ASYS UVM 340 micro-plate reader, UK). The concentration was adjusted to 100µg/100µL using 8 M urea, 50 mM TEAB buffer. Reduction was carried out using TCEP (Tris2-carboxyethyl

phosphine) (Thermo Scientific, Rockford, IL, USA) to a final concentration of 10 mM and incubated at 37°C for 30 minutes. Alkylation was carried out with iodoacetamide (Sigma-Aldrich, St. Louis, MO, USA) to a final concentration of 55 mM and incubated for 45 minutes in the dark. The urea was diluted to a 1 M final concentration using 25 mM TEAB, prior to digestion. Digestion was then carried out using sequencing grade modified trypsin (Promega, Madison, WI, USA) based on a ratio of 1:40 (1μg trypsin: 40μg protein) overnight at 37°C.

The peptide mixture samples were collected after overnight incubation and acidified using formic acid to a final concentration of 1% (v/v). Solid phase extraction clean-up of samples (to remove any traces of primary amine-containing molecules that could react with formaldehyde) was carried out using Oasis HLB cartridges based on the manufacturer's instruction (Waters, Milford, MA, USA). The eluted samples were partially dried using CentriVap Centrifugal Vacuum Concentrators (Labconco, Kansas City, MO, USA) for 20 minutes followed by overnight freeze drying (Virtis Benchtop SLC Freeze Dryer, SP Scientific, Warminster, PA, USA).

2.3.9. 2-plex dimethylation labelling

Dimethyl labelling was carried out as described previously (186). Peptide samples were first resuspended in 400μl of 100 mM TEAB. To 100 μl of the buffer, 4μl of 4% (v/v) CH_2O and CD_2O were added to the samples to be labelled with light and heavy dimethyl, respectively. This was followed by the addition of 4μl of 0.6 M $NaBH_3CN$ to both the light and intermediate label. The samples were incubated in a fume hood for one hour at room temperature (15-22°C) while mixing using a bench top test tube mixer. The labelling reaction was quenched by adding 16μl of 1% (v/v) ammonia solution then the samples were briefly mixed and centrifuged in a fume hood. For further reaction quenching, 8μl of formic acid was added to the samples on ice to acidify the samples. The differentially labelled samples were

then mixed at a 1:1 ratio and analysed using liquid chromatography–mass spectrometry (LC-MS/MS).

2.3.10. LC-MS/MS and data analysis

The dimethyl-labelled samples were analysed on a LTQ Orbitrap Elite (Thermo Scientific, Rockford, IL, USA) instrument coupled to an Ultimate 3000 RSLC nanosystem (Dionex) (Thermo Scientific, Rockford, IL, USA). A nanoLC system was equipped with an Acclaim Pepmap nano-trap column (Dionex − C_{18}, 100 Å, 75 μm×2 cm) and an Acclaim Pepmap analytical column (Dionex C_{18}, 2μm, 100 Å, 75 μm×15 cm) running in 3-80% CH_3CN containing 0.1% formic acid gradient over 25 minutes. The LTQ Orbitrap Elite mass spectrometer was operated in the data-dependent mode, whereby spectra were acquired first in positive mode at 240,000 resolution followed by high energy collisional dissociation at 15,000 resolution. Ten of the most intense peptide ions with charge states ≥2 were isolated and fragmented using normalised collision energy of 35 and activation time of 0.1 ms (high energy collisional dissociation).

The Orbitrap MS data were analysed using Proteome Discoverer (Thermo Scientific version 1.4, Rockford, IL, USA) with the Mascot search engine (Matrix Science version 2.4, Boston, MA, USA) against the Uniprot database maintained at the Bio21 Institute, University of Melbourne, Australia (currently containing 26,617,536 sequences). Search parameters were precursor mass tolerance of 10 ppm and fragment mass tolerance of 0.2 Da. Carbamidomethyl of cysteine was set as fixed modification and dimethyl labelling (light and medium at +28.0313 and +32.0564, respectively) at the peptide *N*-terminus and lysine set as variable modifications. Trypsin with a maximum of 0 missed cleavage was used as the cleavage enzyme. A false discovery rate threshold of 1% was applied and identification of two or more unique peptides and two or more peptides were required for positive

identification and quantification, respectively. A two-fold differential expression was chosen as being significant.

2.4. Materials and methods for tumour-associated macrophage (TAM) study

2.4.1. Lung specimen collection and sectioning

All tissue samples were purchased from Victorian Cancer Bio-Bank (Victoria, Australia). All lung specimens were fixed with 4% formaldehyde, followed by dehydration through graded alcohols, paraffin embedding and preparation of 4-μm sections. For H&E staining, sections were rehydrated, stained with haematoxylin for 2 minutes and rinsed in running tap water for 2 minutes. The sections were then blued in Scott's tap water for 1 minute, rinsed with tap water for 2 minutes, stained with eosin for 2 minutes, dehydrated in alcohols cleared in xylene and coverslipped using DePeX mounting media.

2.4.2. Immunohistochemical staining

Lung sections were heated at 60°C for 1 hour, hydrated and rinsed in tap water for 2 minutes. The sections were then boiled in 10 mM citrate buffer, pH=6 for 10 minutes for antigen retrieval followed by cooling at room temperature for 20 minutes. The sections were then incubated with peroxidase incubator 0.3% H_2O_2 for 15 minutes at room temperature and then protein blocker (2% goat serum, 1% BSA, 0.1% cold fish gelatin, 0.1% Triton X-100, 0.05% Tween 20 and 0.05% sodium azide) to block nonspecific staining for 30 minutes at room temperature. Primary antibodies to CD68 (monoclonoal mouse anti-human CD68 Clone KP1, ready-to-use) (Dako, Carpinteria, CA, USA), NCL-CD163 (1:100; Novocastra^{TM} liquid mouse monoclonal antibody CD163 clone 10D6) (Leica Biosystems, UK) and iNOS (inducible nitric oxide synthase) (1:200; rabbit polyclonal anti-human iNOS, Abcam, UK)

were incubated for 1 hour at room temperature and then washed three times using washing buffer for 5 minutes. The CD68 sections were incubated with EnVision™+ FLEX+ mouse linker for 15 minutes and then washed three times using washing buffer for 5 minutes. All sections were then incubated with secondary antibody Dako EnVision™+ Dual Link system-HRP) (Dako, Glostrup, Denmark). The sections were incubated at room temperature for 30 minutes and washed with washing buffer three times for 5 minutes. The sections were then incubated with DAB solution (Dako, Glostrup, Denmark) for 1-3 minutes and washed in the washing buffer three times for 5 minutes. The sections counterstained with haematoxylin while being observed under a microscope, dehydrated, cleared and coverslipped using DePeX mounting media.

2.4.3. Quantitative analysis of immunohistochemical staining

All slides were scanned at an absolute magnification of 20x using the Aperio Scanscope XT pathology digital imaging systems at Austin Health, Heidelberg, VIC, Australia (Aperio Technologies, USA). The background illumination levels were calibrated using a prescan procedure. The acquired digital images representing whole tissue sections were evaluated for image quality. All acquired images were labeled, placed in dedicated project folders, and stored in a designated external hard drive. The slides were viewed and analysed using ImageScope analysis software (version 12; Aperio Technologies, USA). The colocalisation algorithm (version 11; Aperio Technologies, USA) were applied to quantify IHC staining. The algorithm calculated the percentage area of positive staining based on the deconvolution method to separate the stains and classify each pixel according to the number of stains present. The threshold for each stain was specified and the algorithm reports the percentage of area for which each stain combination is detected: 1, 2, 3, 1+2, 1+3, 2+3, 1+2+3 or none.

2.4.4. Statistical analysis of TAM study

The results are shown as % of positive area ± standard error (SEM) as error bars. The statistical analysis was performed using GraphPad Prism-6. One-way ANOVA multiple comparison test (as a post-test analysis) was performed with the Tukey test (multiple comparison test comparing every group with every other group).

Chapter 3 Blood Monocyte Phenotype and Th1/Th2 Cytokine Profiles in NSCLC

3.1. Introduction

Monocytes are a type of white blood cell (leukocyte). They can be classified into classical monocyte (pro-inflammatory), intermediate monocyte and non-classical monocyte (anti-inflammatory) phenotypes, all of which have been detected in circulating PBMC (79, 80). Monocytes are a macrophage precursor and are known to differentiate into macrophages after entering the tissue spaces. Classical monocytes ($CD14^{++}/CD16^{-}$) have been shown to differentiate into M1 macrophages, while non-classical monocytes ($CD14^{+}/CD16^{++}$) differentiate into M2 macrophages (81).

Classical monocytes are used in this study as they are the main source of tissue macrophages and the majority of the macrophages within the tumour area have been identified as M2 macrophages (81). However, a recent study has reported that classical monocytes can differentiate into M2 macrophages (83). There is controversy regarding monocyte differentiation and their effect in the tumour microenvironment. Therefore, further understanding of the immunology of lung cancer may enable the development of immune-modulatory strategies beyond those in current use, such as monoclonal antibodies targeted to specific cellular receptors.

In this study, two different techniques (CBA and Bio-Plex, MAGPIX-Luminex) were used to study the Th1 and Th2 cytokine level in the serum of patients with NSCLC compared to non-cancer controls. Both techniques provide quantitative measurement of large numbers of analytes using an automated 96-well plate format. However, recent studies have questioned the sensitivity and reproducibility of the CBA assay and suggest the Luminex-

based kit with magnetic beads to be a better technique (187-189). Therefore, the Bio-Plex, MAGPIX-Luminex was used here to analyse Th1 and Th2 cytokine levels. Also the serum samples for Bio-Plex assay were obtained from the Victorian Cancer Bio-Bank to include all NSCLC subtypes.

Here, fresh un-stimulated classical monocytes were used to ascertain the phenotype and function changes in patients with NSCLC compared to non-cancer controls. Also, Th1/Th2 cytokine profiles were assessed to determine the possible impact of NSCLC compared to non-cancer controls. This part of the study is trying to give a better understanding of the effect of NSCLC on the macrophage precursor (monocytes) phenotype and function outside the lung (systemically) compared to non-cancer controls, as well as to identify if the presence of NSCLC would alter the cytokine profiles (Th1 and Th2) in serum samples compared to non-cancer controls.

3.2. Results

The demographic details of all NSCLC and non-cancer control subjects are shown in Table 5. Blood samples were collected at Austin Health (Heidelberg, VIC, Australia) to gain PBMC (flow cytometry) and serum samples (used in CBA assay).

Complete blood count (CBC) was investigated in all patients to verify if the patients had significant underlying medical conditions e.g. infection, which could result in monocyte phenotype alteration. The total mean number of WBC (white blood cells) in NSCLC patients was significantly higher than in non-cancer controls. The mean values of all WBC types (except basophil cells) and RBCs were tended to be higher in patients with NSCLC compared to non-cancer controls. However, there were no significant differences in the mean values of all WBC types and RBCs in NSCLC compared to non-cancer controls. Also the mean values of all WBC types and RBCs were within the normal range in both groups (Table 6).

In flow cytometry results, there were no statistically significant differences in M1 marker (HLA-DR), M2 markers (CD163 and CD36) or CD11c and CD44 in patients with NSCLC (undifferentiated NSCLC, adenocarcinoma and squamous cell lung carcinoma) compared to non-cancer controls. Both %SE (% surface expression) and MFI (mean fluorescence intensity) expression of surface markers showed similar values. The expression of CD11b and CD71 was also shown to be similar between patient groups (undifferentiated NSCLC, adenocarcinoma and squamous cell lung carcinoma) and non-cancer controls.

Table 5: **Demographic details of NSCLC and non-cancer control subjects**

	n	Age (years) Mean ± SD	Gender	Smoking status	Stages	Subtypes
			M/F	N/Ex/S	I/II/III/IV	N/A/S
Control	20	60.45 ± 19.31	10/10	7/11/2		
Cancer	30	67.1 ± 10.68	17/13	3/16/11	8/3/7/12	9/11/10

n: number; SD: standard deviation; M: male; F: female; N: non-smoker; Ex: ex-smoker; S: smoker; N: undifferentiated NSCLC; A: adenocarcinoma; S: squamous cell lung carcinoma. Demographic details of the participants and staging details of lung cancer patients. This Table shows the total number of patient samples, age, gender, smoking status and lung tumour subtypes and stages. Full samples detail (e.g. GOLD stages) are displayed in Appendix A - Tables 16 and 17.

Table 6: **Complete blood count (CBC) details of NSCLC and non-cancer control patients**

Groups	Total number	WBC	NE	LY	MO	EO	BA	RBC
Normal Value (x10^9/L)		4 - 11	2 - 7.5	1.5 - 4	0.2 - 0.80	0.04 - 0.40	0.02 - 0.10	3.80 - 6.50
Control	20	4.35 ± 1.82	2.11 ± 1.07	1.31 ± 0.47	0.23 ± 0.14	0.13 ± 0.06	0.38 ± 0.50	4.85 ± 0.91
Cancer	30	6.76 ± 3.90	3.4095 ± 3.46	1.68 ± 1.31	0.34 ± 0.22	0.20 ± 0.17	0.29 ± 0.20	5.04 ± 1.08

CBC analysis was performed on whole blood collected from patients with primary NSCLC and non-cancer controls using Beckman Coulter (AcT 5 blood differentiation) (Fullerton, CA, USA). WBC: white blood cell; NE: neutrophil; LY: lymphocyte; MO: monocyte; EO: eosinophil; BA: basophil; RBC: red blood cell.

3.2.1. No difference in HLA-DR, CD163 and CD36 expression in patients with NSCLC compared to non-cancer controls

The impact of NSCLC on the classical monocytes expression of HLA-DR (M1 phenotypes), CD163 and CD36 (M2 phenotypes) was investigated in patients with NSCLC compared to non-cancer controls using flow cytometry. Classical monocytes were gated based on forward scatter (FSC) and side scatter (SSC) profiles within patient groups and based on the expression of CD14, CD45 and CD16 markers. Results show that there were no significant differences in %SE (P=0.155) and MFI (P=0.1048) of HLA-DR (M1 marker) expression in patients with NSCLC (undifferentiated NSCLC, adenocarcinoma and squamous cell lung carcinoma) compared to non-cancer controls (Figs. 16 and 17). In addition, flow cytometry analysis showed there were no significant differences in the %SE (P=0.505) and MFI (P=0.4582) of CD163 (M2 marker) in NSCLC patients (undifferentiated NSCLC, adenocarcinoma and squamous cell lung carcinoma) compared to non-cancer controls. We also showed that there were no significant differences in the %SE (P=0.160) and MFI (P=0.4018) of CD36 (M2 marker) staining between the NSCLC patient group and non-cancer controls (Figs. 16 and 17). The expression of HLA-DR, CD163 and CD36 were also examined between early and advanced lung cancer criteria and results showed no difference in patients with more advanced stages compared to early lung cancer.
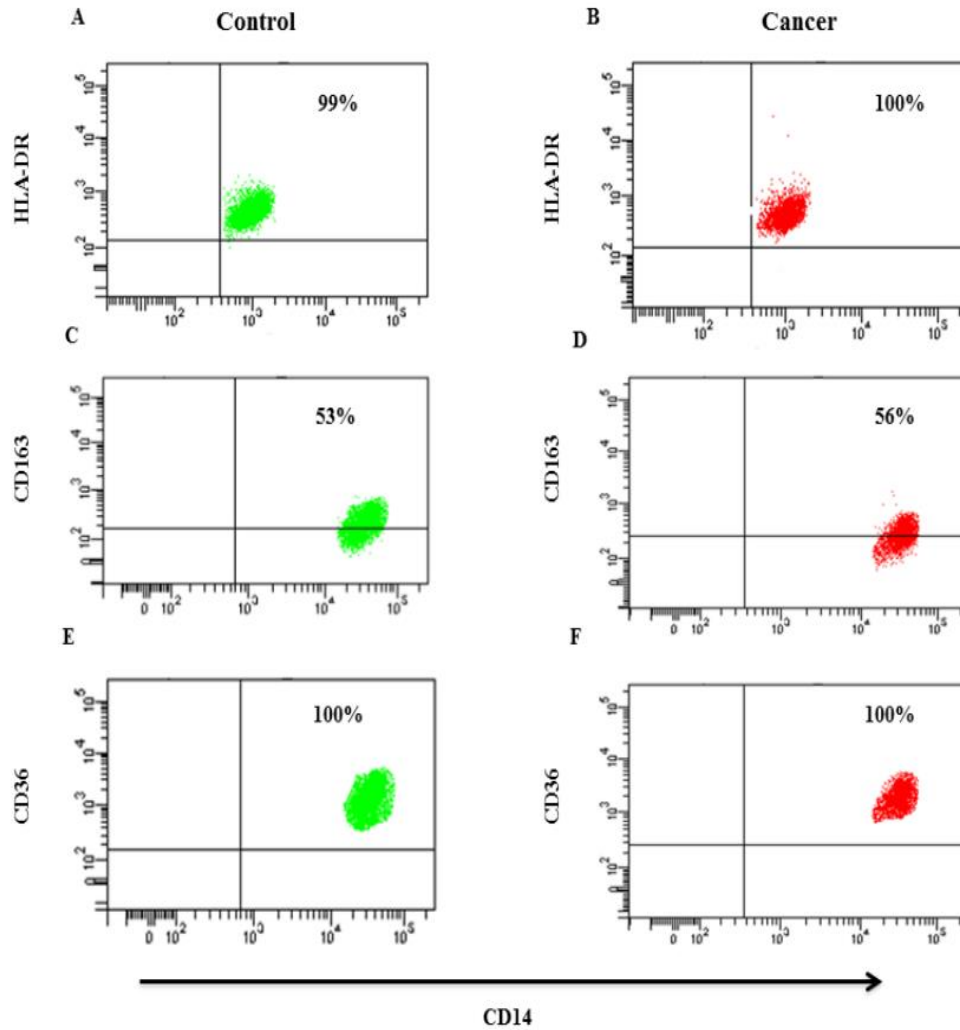
Figure 16: HLA-DR, CD163 and CD36 surface expression on (CD14^{++}/CD16^{-}) blood monocytes in patients with primary NSCLC compared to non-cancer controls. (A-F) Representative flow cytometry dot plots from PBMC stained against CD14 and then co-stained with HLA-DR, CD163 and CD36 on patients with NSCLC (red colour) and non-cancer controls (green colour). All data was collected on a BD FACS Canto (BD Biosciences, San Jose, CA, USA) within the RMIT Flow Cytometry Facility (Bundoora, Melbourne).
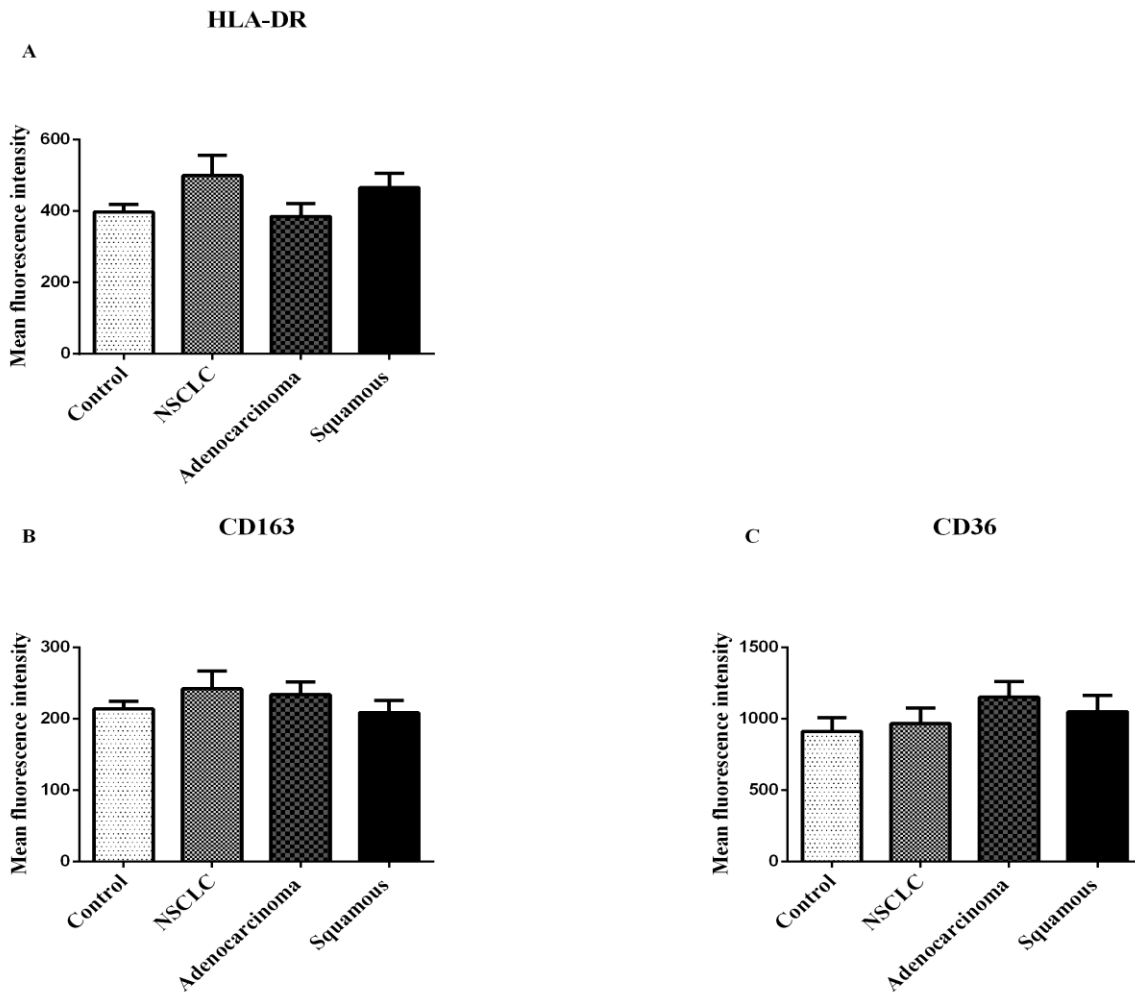
Figure 17: HLA-DR, CD163 and CD36 expression on (CD14^{++}/CD16^{-}) blood monocytes in patients with NSCLC compared to non-cancer controls. Summary graphs show the mean values of MFI ± SEM of (A) HLA-DR, (B) CD163 and (C) CD36 markers from patients with NSCLC (n=9 undifferentiated NSCLC, 11 adenocarcinoma and 10 squamous cell lung carcinoma) versus non-cancer controls (n=20). One-way ANOVA multiple comparison test (as a post-test analysis) was performed.

3.2.2. No difference in CD11b, CD71, CD11c and CD44 expression

The potential impact of NSCLC on the classical monocytes expression of CD11b, CD71 and CD44 was investigated in patients with NSCLC compared to non-cancer controls using flow cytometry. The %SE and MFI of CD11b, CD71, CD11c and CD44 were similar between patient groups (undifferentiated NSCLC, adenocarcinoma and squamous cell lung carcinoma) and non-cancer controls (Figs. 18, 19 and 20). The %SE and MFI of the myeloid marker CD11b was not different between cancer and non-cancer control subjects: %SE (P=0.58), MFI (P=0.5396). Also, CD71 results indicated that there were no significant differences in the %SE (P=0.97) and MFI (P=0.0558) of the transferrin receptor marker in patients with NSCLC compared to non-cancer controls. There was no significant difference in the %SE (P=0.93) or MFI (P=0.4313) of the CD11c in patients with NSCLC compared to non-cancer controls. In addition, CD44 results revealed that there were no significant differences in the %SE (P=0.50) or MFI (P=0.7495) of the CD44 marker in NSCLC patients compared to non-cancer controls.
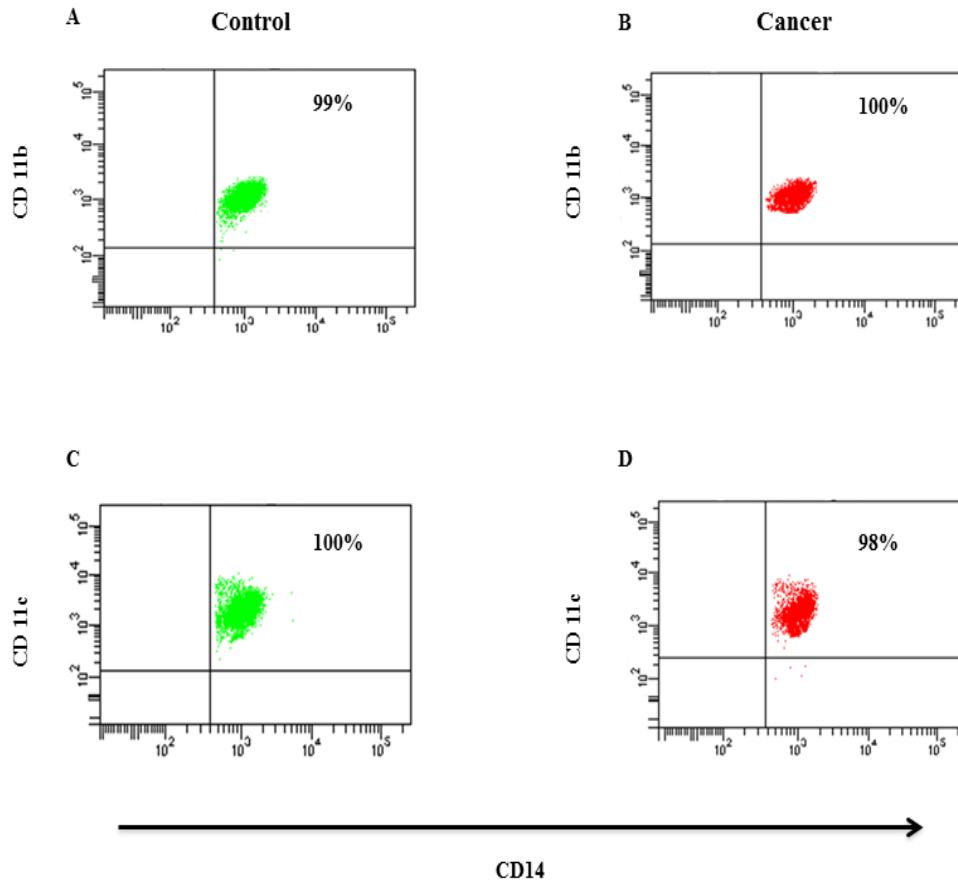
Figure 18: CD11b and CD11c surface expression in PBMC by flow cytometry. (A-D) Representative flow cytometry dot plots example from PBMC stained against CD14 and then co-stained with CD11b and CD11c on patients with NSCLC (red colour) and non-cancer controls (green colour). All data was collected on a BD FACS Canto (BD Biosciences, San Jose, CA, USA)within the RMIT Flow Cytometry Facility (Bundoora, Melbourne).
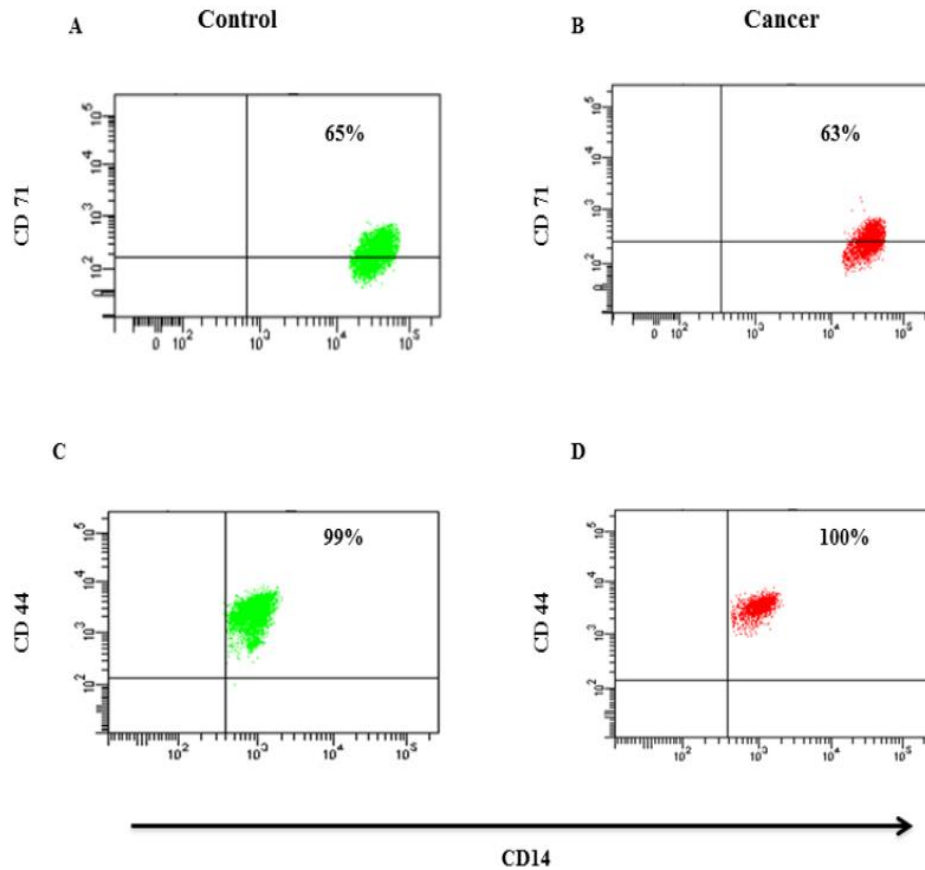
Figure 19: CD71 and CD44 surface expression in PBMC by flow cytometry. (A-D) Representative flow cytometry dot plots example from PBMC stained against CD14 and then co-stained with CD71 and CD44 on patients with NSCLC (red colour) and non-cancer controls (green colour). All data was collected on a BD FACS Canto (BD Biosciences, San Jose, CA, USA)within the RMIT Flow Cytometry Facility (Bundoora, Melbourne).
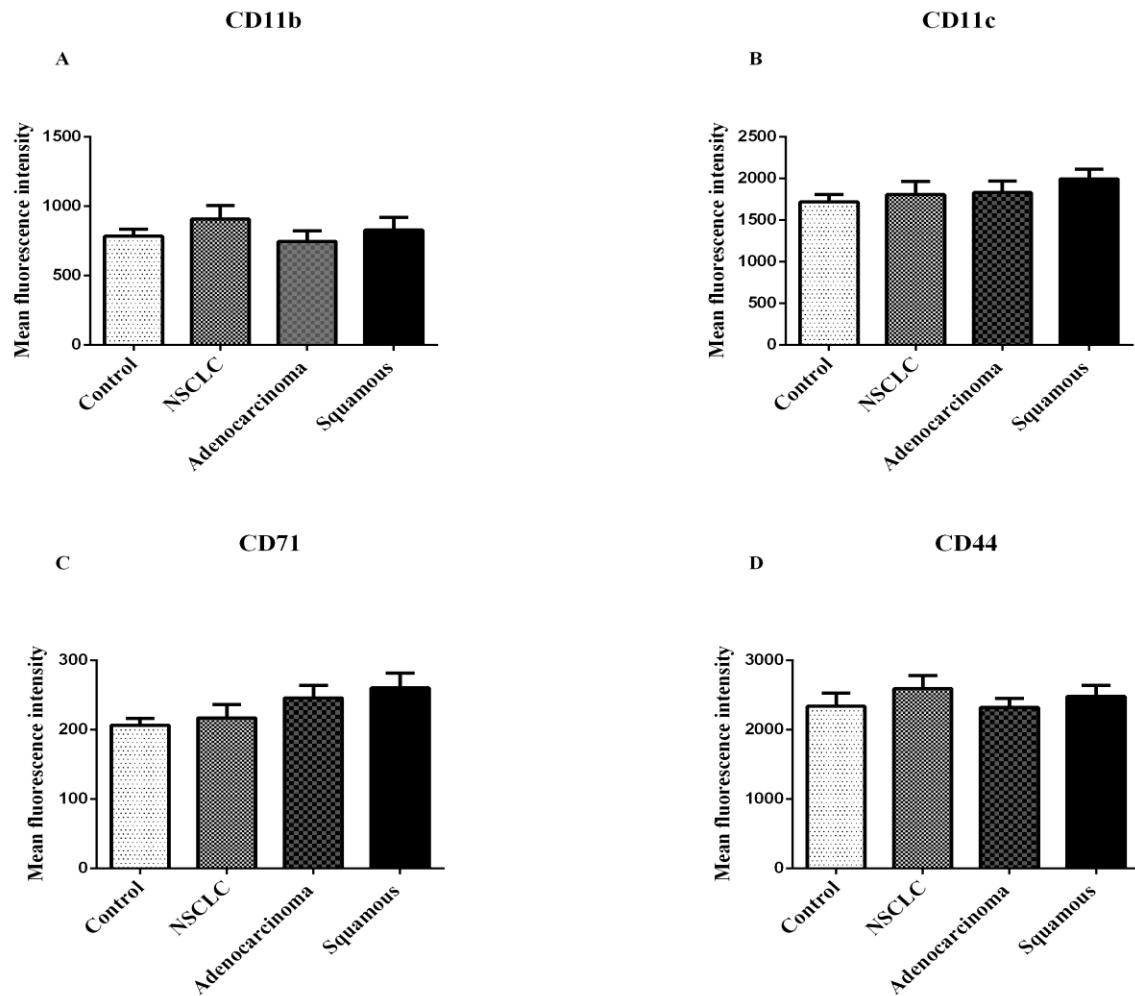
Figure 20: CD11b, CD11c, CD71 and CD44 expression on $(CD14^{++}/CD16^{-})$ blood monocytes in patients with NSCLC compared to non-cancer controls. Summary graphs show the mean values of MFI ± SEM of (A) CD11b, (B) CD11c, (D) CD71 and (D) CD44 markers from patients with NSCLC (n=9 undifferentiated NSCLC, 11 adenocarcinoma and 10 squamous cell lung carcinoma) versus non-cancer controls (n=20). One-way ANOVA multiple comparison test (as a post-test analysis) was performed.

3.2.3. No significant difference in Th1/Th2 cytokines serum levels in patients with NSCLC compared to non-cancer controls using CBA assay

The possible influence of NSCLC on the Th1/Th2 cytokines serum levels was investigated in patients with NSCLC compared to non-cancer controls using cytometric bead array (CBA) analysis. Cytokine analysis revealed no significant difference in Th1/Th2 cytokine serum levels in patients with NSCLC (undifferentiated NSCLC, adenocarcinoma and squamous cell lung carcinoma) compared to non-cancer controls (Figs. 21 and 22). Large cell lung carcinoma subtype was not included as only one sample was collected during two years of samples collection. This is predictable as large cell lung carcinoma is known to be a less common lung cancer in comparison to other NSCLC subtypes (47). Cytokines were analysed in patients with NSCLC and non-cancer controls by the CBA analysis.

Cytokines that were detectable in patient serum samples included Th1 cytokines TNF-α, TNF-β, IFN-γ, IL-2, IL-12 (p70), and IL-1β, and Th2 cytokines IL-4 and IL-5 showed no significant differences between patients with NSCLC compared to non-cancer controls. The quality and reproducibility of Th1 and Th2 cytokine results using the CBA assay was not sufficient as some cytokines such as IL-12 (p70), IL-8, IL-4 and IL-5 were barely identified. This proves the previous outcomes regarding the quality and reproducibility of the CBA assay technique (187-189). Therefore, this part of the study was repeated with a different group of serum samples using the most recommended technique the Bio-Plex, MAGPIX-Luminex assay (188).
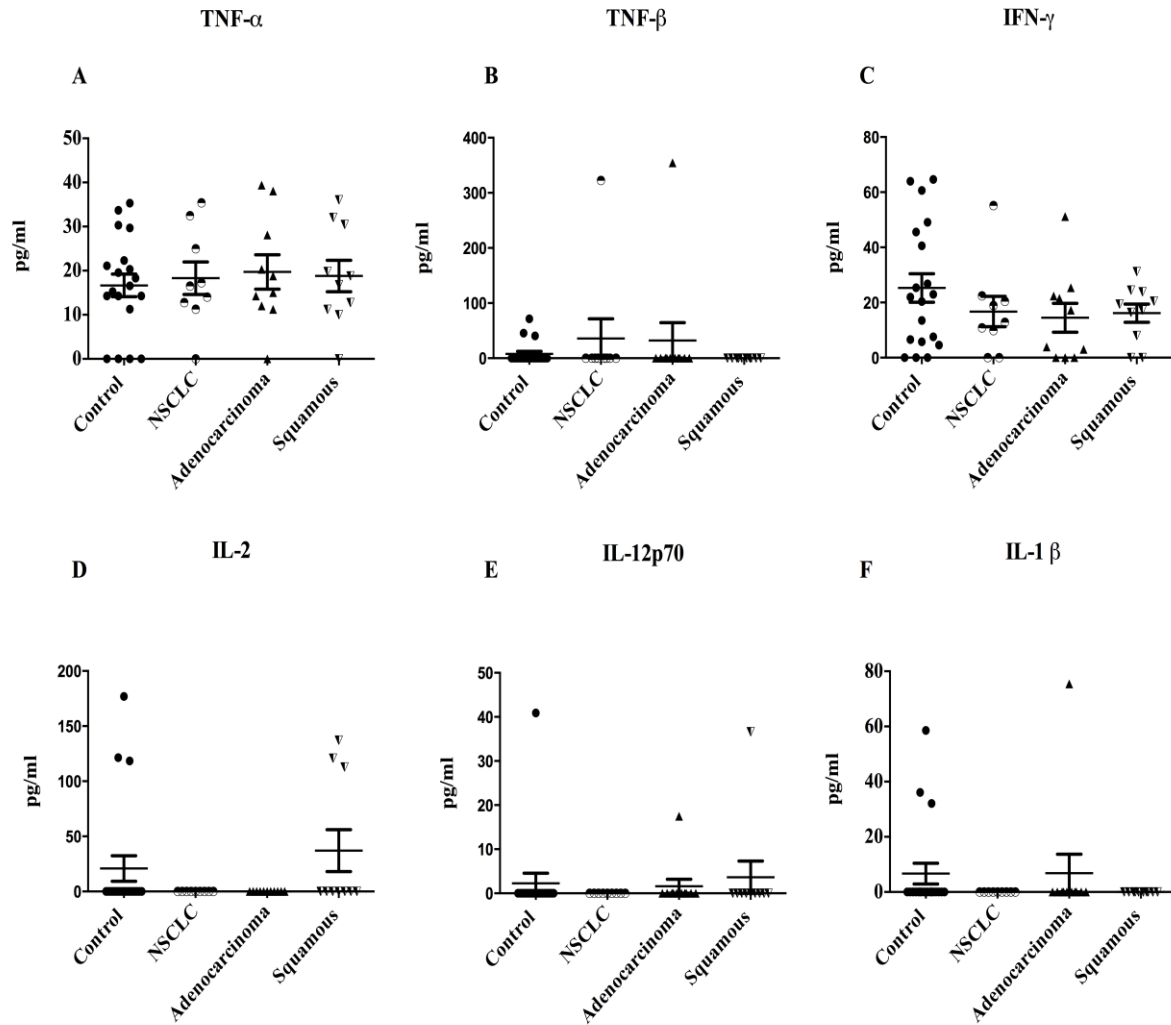
Figure 21: Th1 cytokine secretion profiles in serum of patients with NSCLC (undifferentiated NSCLC, adenocarcinoma and squamous cell lung carcinoma) compared to controls. Serum was analysed for (A) TNF-α, (B) TNF-β, (C) IFN-γ, (D) IL-2, (E) IL-12 (p70) and (F) IL-1β using the CBA assay. Data was analysed using the FCAP Array™ v3.0.1 Software (BD Biosciences, USA) and results are expressed as mean (pg/ml) ± SEM, (n=20 controls, 9 undifferentiated NSCLC, 11 adenocarcinoma and 10 squamous cell lung carcinoma). One-way ANOVA multiple comparison test (as a post-test analysis) was performed.

IL-8   IL-10   IL-5

A   **B**   **C**
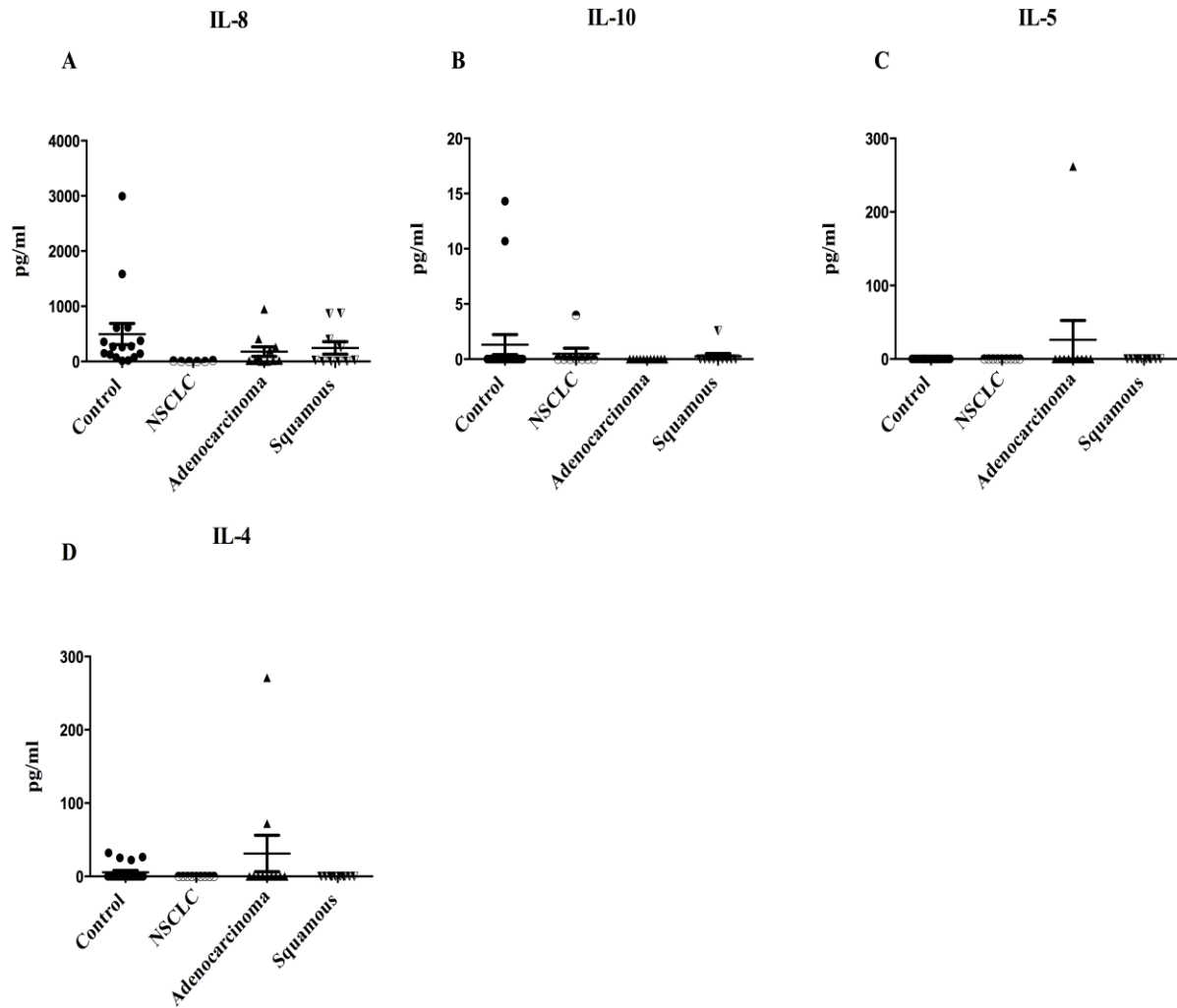
D   IL-4

Figure 22: Th2 cytokine secretion profiles in serum of patients with NSCLC (undifferentiated NSCLC, lung adenocarcinoma and squamous cell lung carcinoma) compared to controls. Serum was analysed for (A) IL-8, (B) IL-10, (C) IL-5 and (D) IL-4 using the CBA assay. Data was analysed using the FCAP Array™ v3.0.1 Software (BD Biosciences, USA) and results are expressed as mean (pg/ml) ± SEM, (n=20 controls, 9 undifferentiated NSCLC, 11 adenocarcinoma and 10 squamous cell lung carcinoma). One-way ANOVA multiple comparison test (as a post-test analysis) was performed.

3.2.4. Th1/Th2 cytokines level in serum of patients with NSCLC compared to non-cancer controls using Bio-Plex assay

In this part of the study all serum samples were purchased from the Victorian Cancer Bio-Bank (Victoria, Australia) to include all NSCLC subtypes (see Table 7). Unlike the CBA assay, 10 serum samples of patients with large cell lung carcinoma were added to be analysed using the Bio-Plex, MAGPIX-Luminex assay. Large cell lung carcinoma samples were ordered directly from the Bio-Bank as it is a less common subtype and there were not enough patients with this type of tumour during sample collection.

The potential impact of NSCLC on the Th1/Th2 cytokines levels in serum was investigated in patients with NSCLC compared to non-cancer controls using Bio-Plex, MAGPIX-Luminex assay. Similar to CBA analysis, Th1/Th2 cytokine serum analysis using the Bio-Plex, MAGPIX-Luminex assay indicated no significant difference in patients with adenocarcinoma and squamous cell lung carcinoma compared to non-cancer controls. However, patients with large cell lung carcinoma showed significant increase in the level of IL-1β, IL-4, IL-6 and IL-8 in serum using the Bio-Plex, MAGPIX-Luminex assay (Figs. 23 and 24). IL-1β level in serum was found to be significantly increased in patients with large cell lung carcinoma compared to non-cancer controls ($P{\leq}0.01$) and to patients with squamous cell lung carcinoma ($P{\leq}0.05$). Also the IL-4 and IL-8 level in serum was significantly increased in patients with large cell lung carcinoma compared to non-cancer controls ($P{\leq}0.01$) and to patients with adenocarcinoma ($P{\leq}0.05$) as well as squamous cell lung carcinoma (IL-4= $P{\leq}0.01$ and IL-8= $P{\leq}0.05$). Finally, large cell lung carcinoma was found to promote the level of IL-6 compared to non-cancer controls ($P{\leq}0.01$) and adenocarcinoma patients ($P{\leq}0.05$).

Table 7: **Demographic details of lung cancer and non-cancer control subjects for serum samples using Bio-Plex assay**

	n	Age (years) Mean ± SD	Gender	Subtypes	Smoking status	Subtypes
			M/F	I/II/III/IV	N/Ex/S	A/S/L
Control	10	43.5 ± 17.69	0/10		4/4/2	
Cancer	30	66.83 ± 11.30	23/7	2/15/11/2	7/11/12	10/10/10

n: number; SD: standard deviation; M: male; F: female; A: adenocarcinoma; S: squamous cell lung carcinoma; L: large cell lung carcinoma. Serum samples were obtained from patients with and without NSCLC. Samples were obtained from the Victorian Cancer Bio-Bank, Melbourne, Australia.
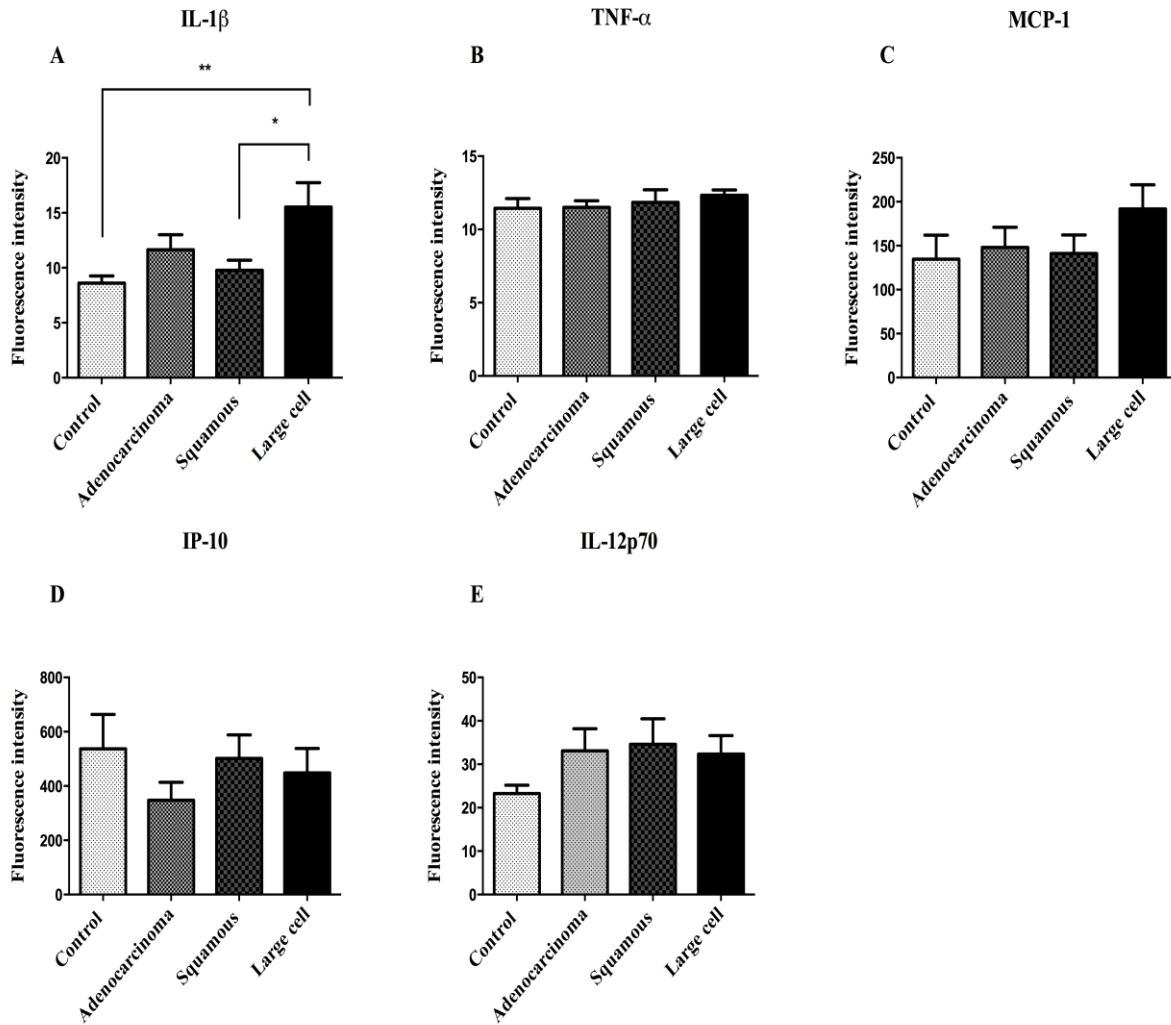
Figure 23: Th1 cytokine secretion profiles in serum of patients with NSCLC (lung adenocarcinoma, squamous cell lung carcinoma, large cell lung carcinoma) compared to non-cancer controls. Serum was analysed for (A) IL-1β, (B) TNF-α, (C) MCP-1, (D) IP-10 and (E) IL-12 (p70) by Bio-Plex assay using the MAGPIX-Luminex instrument. Data was analysed using the Bio-Plex Manager Software (Bio-Rad) and results are expressed as median fluorescence intensity (FI) ± SEM, (n=10 controls, 10 adenocarcinoma, 10 squamous cell lung carcinoma and 10 large cell lung carcinoma). One-way ANOVA multiple comparison test (as a post-test analysis) was performed with the Tukey test (multiple comparison test comparing every group with every other group). *$P{\leq}0.05$ and **$P{\leq}0.01$ indicates statistical significance.
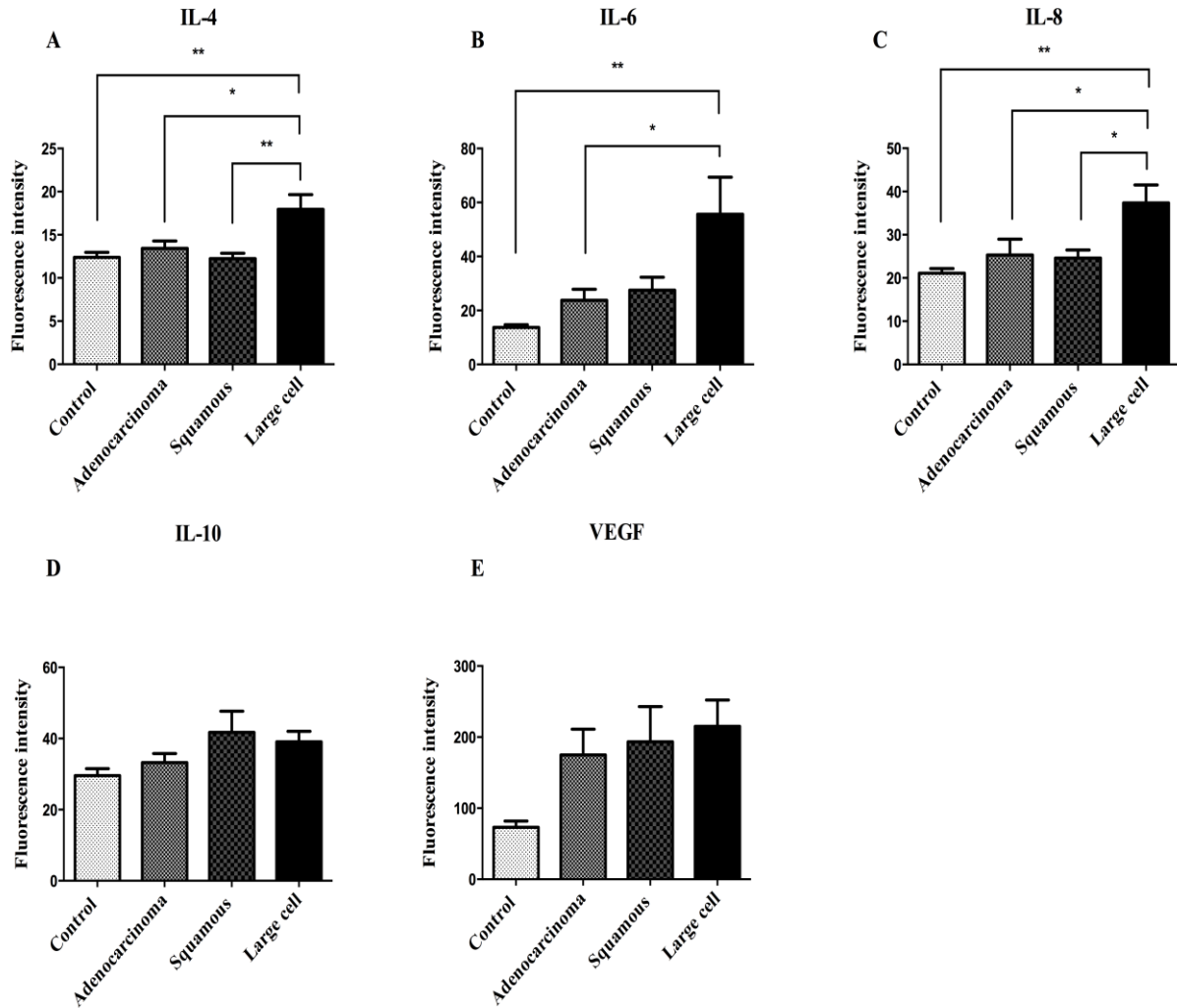
Figure 24: Th2 cytokine secretion profiles in serum of patients with NSCLC (adenocarcinoma, squamous cell lung carcinoma, large cell lung carcinoma) compared to non-cancer controls. Serum was analysed for (A) IL-4, (B) IL-6, (C) IL-8, (D) IL-10 and (E) VEGF by Bio-Plex assay using the MAGPIX-Luminex instrument. Data was analysed using the Bio-Plex Manager Software (Bio-Rad) and results are expressed as median fluorescence intensity (FI) ± SEM, (n=10 controls, 10 adenocarcinoma, 10 squamous cell lung carcinoma and 10 large cell lung carcinoma). One-way ANOVA multiple comparison test (as a post-test analysis) was performed with the Tukey test (multiple comparison test comparing every group with every other group). *$P \leq 0.05$ and **$P \leq 0.01$ indicates statistical significance.

2.3. Discussion

The concept that the immune system has a protective role in tumour development is well established (12). Recent work has demonstrated that the immune system can not only prevent tumour formation but potentially also function to promote tumour initiation and progression (72). In particular, immune cells such as blood monocytes can function differently depending on the cancer types (78). While some studies indicated that monocyte function in cancer patients is within the normal range (17, 190), another study has shown impairment in monocyte function (77).

In this study we demonstrated that the phenotype of freshly isolated blood classical monocytes from patients with NSCLC is not altered and does not show clear skewing from an anti-tumour (M1) to a pro-tumour (M2) phenotype. There were no significant differences in expression of M1 marker (HLA-DR), M2 markers (CD163 and CD36), CD11c, CD44, CD11b and CD71 in patients with NSCLC compared to non-cancer controls. In addition, there were no significant differences in the secretion of Th1/Th2 cytokines measured in the serum of NSCLC patients compared to non-cancer controls.

The M1 phenotype was assessed here using HLA-DR as a marker. The HLA-DR molecule plays a vital role in the immune response by regulating the interaction between antigen-presenting cells including monocytes (191, 192). It has been described as an M1 marker in the monocyte-macrophage system (179). Some studies have reported reduced HLA-DR expression on blood monocytes in human cancers such as prostate and ovarian cancer (76, 193, 194). As well as examining M1 phenotype, M2 phenotype markers (CD163 and CD36) were used to investigate skewing from M1 to M2 markers on classical monocytes in blood from patients with NSCLC. CD163 is a scavenger receptor that plays a major role in the anti-inflammatory response and has been identified as M2 marker (184, 195). CD36 is also expressed on monocytes and is involved mainly in phagocytosis (184, 196). Sugai et al.

(2004) studied the alteration of monocyte characteristics by examining the intracellular expression of IL-10 and IL-12 cytokines (197). They found that patients with advanced gastric cancer had different monocyte phenotypic characteristics compared to those with early stage cancer and non-cancer control subjects (197). In our study, there were no significant differences in expression of CD163 and CD36 between non-cancer controls and NSCLC patients. Additionally, there was no apparent influence of tumour stage upon expression of these markers, although it is acknowledged that the numbers are small. These results when viewed in the context of previous studies raise questions regarding the impact of experimental design such as culturing and the use of molecules like LPS on monocyte polarisation and function.

CD11b and CD11c are myeloid cell markers that are expressed on monocytes and macrophages (198). CD11b plays a major role in many functions of myeloid cells including adhesion, migration, chemotaxis and phagocytosis (198-200). In this study we therefore investigated the effect of NSCLC on monocyte expression of CD11b and CD11c. There were no significant differences in expression of CD11b and CD11c in NSCLC patients compared to non-cancer controls. These results are consistent with those of Mariotta et al. (2002) who suggested NSCLC does not affect monocyte adherence and phagocytosis in patients with lung cancer when compared to healthy controls (17).

Another marker that was examined was transferrin receptor (CD71). CD71 is known to be associated with rapidly proliferating cells such as cancer cells and plays a major role in cell growth and DNA synthesis, proliferation and cell survival (201, 202). Increased CD71 expression has been demonstrated in cancer patients, including those with lung cancer, in lung tissue and BAL fluid but not in serum (202, 203). Dowlati et al. (1997) investigated soluble CD71 in the serum of NSCLC patients. They verified no difference in the level of secreted CD71 in NSCLC patients compared to the control group (202). Similar to this

outcome we demonstrated that there was no significant difference in surface expression of CD71 on classical monocytes in NSCLC patients compared to non-cancer controls.

CD44 expression was also investigated in this study as it has been suggested to be a potential marker of tumour onset in lung cancer. Elevated CD44 expression has been observed in the serum of patients with gastric and renal cancer (204, 205). However, another study showed that NSCLC does not influence CD44 level in the serum of NSCLC patients compared to benign lung diseases (190). Similarly, this study revealed no significant difference in surface expression of CD44 on classical monocytes in NSCLC patients compared to non-cancer controls.

The presence of cytokines is essential for initiation of immune responses (22, 206). Th1 cells have been found to play a major role in anti-tumour immunity and stimulation of cell-mediated responses. Pro-inflammatory cytokines such as TNF-α and IFN-γ are known to stimulate Th1 cells. In contrast, Th2 cells are known to act as the helper cells that influence B-cell development and produce anti-inflammatory cytokines such as IL-4 and IL-10 (207, 208). Analysis of Th1 and Th2 cytokines in the serum revealed no differences in NSCLC patients overall compared to non-cancer controls. Similarly, Gursel et al. (1995) also observed no differences in TNF-α concentration between pleural effusion and serum in patients with cancer (209). Although many studies have not looked at specific cytokine profiles in lung cancer, it has been shown that freshly prepared monocytes do not show any differences in pro-inflammatory and anti-inflammatory cytokine responses except IL-12 (p70) in endometrial cancer patients when compared to controls (77). In our study, IL-1β, IL-4, IL-6 and IL-8 cytokine levels were found to be up-regulated in the serum of large cell lung carcinoma patients. IL-6 levels in serum was found to be significantly increased in patients with large cell lung carcinoma compared to non-cancer controls and to patients with adenocarcinoma. Different studies have demonstrated the ability of IL-6 to promote lung

tumour growth and it has an association with a poor prognosis. Also, the IL-6 level in serum was investigated in patients with lung cancer before and during radiotherapy (RT). They found that IL-6 levels were higher compared to controls and were further elevated during RT (119-122). In addition, IL-1β and IL-8 both are known to promote tumour progression through regulating tumour growth and invasion (210, 211). IL-1β promotes matrix metalloproteinase secretion and angiogenic factors in the tumour microenvironment (212). The elevation of IL-1β gene expression in normal lung tissue was also shown to be related to increased risk of developing lung cancer (212). In this study, IL-1β level in serum was significantly increased in patients with large cell lung carcinoma compared to non-cancer controls and to patients with squamous cell lung carcinoma. Moreover, increased IL-8 expression was shown to be associated with poor lung cancer patient survival (135). Elevated circulating IL-8 level has been shown to be associated with lung cancer models (213). Similarly, our results indicated that the IL-4 and IL-8 level in serum was highly increased in patients with large cell lung carcinoma compared to non-cancer controls and to patients with adenocarcinoma as well as squamous cell lung carcinoma. Taken together, IL-1β, IL-4, IL-6 and IL-8 levels have been found to be elevated in most patients suffering from different common cancers (214, 215). Our results indicate that large cell lung carcinoma is associated with a systemic alteration in cytokines (IL-1β, IL-4, IL-6 and IL-8) and these cytokines have been shown to promote tumour growth and metastasis. However, all non-cancer controls were female and 76.6% of NSCLC patients were male so this may influence the accuracy of this outcome. Gender difference was described to have the ability to influence the Th1/Th2 production pathways in health and some disease states (216). For example, sex steroids have been shown to influence the regulation of TH cell network balance and to alter the response type of Th1 and/or Th2 (217). Although the majority of NSCLC serum samples were collected from male patients in this study, only large cell lung carcinoma was shown to

influence Th1/Th2 cytokine expression and not the other NSCLC subtypes compared to non-cancer controls, which might exclude the effect of gender difference in this case.

Although the final results of CBA and Bio-Plex, MAGPIX-Luminex were similar regarding adenocarcinoma and squamous cell lung carcinoma, the sensitivity, reproducibility and quality of CBA results was not ideal compared to Bio-Plex, MAGPIX-Luminex. As the majority of tested cytokines such as IL-2, IL-4, IL-5 and IL-8 were hardly identified using the CBA assay unlike their expression using the Bio-Plex, MAGPIX-Luminex technique. These results are similar to the recent studies that have questioned the sensitivity and reproducibility of the CBA assay and suggest the Luminex-based kit with magnetic beads to be a better technique (187-189).

In this study, there are some limitations including an inability to compare results of monocyte and Th1/Th2 cytokine profile (using CBA assay) from subtypes within the NSCLC grouping as all patients' samples were undifferentiated NSCLC, lung adenocarcinoma and squamous cell lung carcinoma and not large cell lung carcinoma. However, the large cell lung carcinoma samples were included to study Th1/Th2 cytokine level using the Bio-Plex assay. In future studies, examining monocyte phenotype and function in non-cancer controls versus lung cancer should be done on all monocytes subsets by using freshly isolated un-stimulated monocytes as well as cytokine treated monocytes at the same time to observe any variation that may occur. Other lung cancer subtypes should be considered to inspect if they have any potential role in altering monocyte functions and phenotypes. Also the samples of control and cancer should be properly balanced to exclude the influence of gender differences.

In conclusion, the studies described in this chapter showed that monocyte phenotype and function were not impaired in the presence of NSCLC subtypes (undifferentiated NSCLC, adenocarcinoma and squamous cell lung carcinoma) compared to non-cancer controls. It also indicated that there was no alteration in Th1/Th2 cytokine level in the serum

of patients with adenocarcinoma and squamous cell lung carcinoma compared to non-cancer controls. However, patients with large cell lung carcinoma showed significant difference in the level of IL-1β, IL-4, IL-6 and IL-8 compared to non-cancer controls. Serum biomarkers are a practical and non-invasive method of diagnosing disease, and predicting prognosis and possibly treatment response. Thus, the elevated cytokines IL-1, IL-4, IL-6 and IL-8 might be utilised in the future as a potential diagnostic and/or prognostic biomarker in the serum of patients with large cell lung carcinoma.

Chapter 4 Alveolar Macrophage Phenotype and Function is Altered in NSCLC

4.1. Introduction

The human lungs are highly vascularised and expose to numerous toxic substances from the external environment possibly resulting in lung injury. However, the respiratory tract has various defence mechanisms, including mucus, cilia and phagocytosis that are mainly operated by alveolar macrophages (AMs) (2, 3). The lungs are altered due to environmental challenges, infection, smoking and tumour, so AMs as well are known to be adjusted in response to these challenges (218, 219). AMs are mononuclear phagocytic cells, which migrate as circulating monocytes from the circulation to the lungs, where they differentiate into AMs (16). AMs play an important role in immunity and inflammation of the lungs through various mechanisms such as phagocytosis and pro-inflammatory action (19). Two phenotypes of macrophage have been described: M1 and M2 macrophage subsets.

The M1 macrophage is activated by interferon-γ with or without LPS and TNF-α (19). The M1 macrophage is able to control local inflammatory reactions via the release of cytokines (e.g. TNF-α, IL-1 and IL-12) and provides a primary defence mechanism by phagocytosis. The existence of M1 macrophage has also been related to the increased expression of pro-inflammatory cytokines (e.g. IL-12 and IL-1) in NSCLC (89). These pro-inflammatory cytokines (IL-12 and IL-1) have been identified to play an essential role in tumour regression (220). In addition, the M1 macrophage has been associated with a positive prognosis and extended survival time in patients with NSCLC (18). In contrast, the M2 macrophage is known to secrete anti-inflammatory cytokines such as IL-10, MMPs, TGF-β and IL-13 (14, 19). These cytokines are known to be associated with tumour cell

proliferation, progression and metastasis (19, 96). The M2 macrophages have the ability to stimulate the expression of the mannose receptor while reducing the iNOS expression (19). M2 can also inhibit antigen presentation and T-cell proliferation (13, 19). In addition, increased expression of cytokines such as IL-10 and IL-13 that regulate M2 activation have been shown to be associated with NSCLC (20).

A dual role of macrophages in cancer has been suggested with the idea that they may both inhibit and promote tumour progression (12, 24). The macrophage subsets have been well characterised in many cancers, however AMs phenotype and function in lung cancer still needs further investigation. Therefore this study will investigate their role by examining the influence of NSCLC on AMs phenotype by characterising the M1 and M2 subsets using well defined markers (HLA-DR and CD163). Also, a number of main functions of AMs are assessed in patients with NSCLC compared to non-cancer controls using CD11b, CD71 and CD44 markers. The expressions of IL-6, IL-12, IL-10 and MMP-9 cytokines are also measured to examine the impact of NSCLC on the level of these cytokines as they are related to macrophages phenotype and function.

4.2. Results

The demographic details of all NSCLC and non-cancer control subjects are shown in Table 8. BAL fluid samples were collected at Austin Health (Heidelberg, VIC, Australia), AMs isolated and further processed for flow cytometry and RT-PCR investigations. AMs were analysed using flow cytometry, where FSC and SSC linear scale were selected in order to identify the AM (CD68$^+$) populations (Fig. 25). CD68 marker was used as the principal surface marker to identify the AMs populations within BAL fluid (Fig. 26). Over 65% of the gated cells within BAL fluids were CD68 positive. Dot plots showed fairly consistent FSC/SSC and CD68$^+$ profiles within BAL fluid cells whereby AMs could be clearly identified.

% surface expression (%SE) of CD68, CD163 (M2 marker), CD71 and CD44 on AMs were highly expressed in patients with NSCLC compared to non-cancer control subjects. In addition, there were no significant differences in the %SE of M1 marker (HLA-DR) ($p=0.9131$) and myeloid markers CD11b ($P=0.8884$) in patients with NSCLC compared to non-cancer controls (Figs. 27, 28 and 29). In addition, different cytokines (IL-6, IL-12, IL-10 and MMP-9) were measured as they are correlated to macrophages phenotype and function. The expression of IL-6 on AMs ($P=0.4835$) was not statistically significant in NSCLC patients compared to non-cancer controls. IL-12 expression on AMs as well was not statistically significant ($P=0.3080$) in NSCLC patients compared to non-cancer controls. The mRNA expression of IL-10 ($P=0.0327$) was found to be significantly increased in adenocarcinoma but not in squamous cell lung carcinoma and large cell lung carcinoma. Finally, mRNA expression of MMP-9 level was highly increased in all NSCLC subtypes patients compared to non-cancer controls (Fig. 30).

Table 8: **Demographic details of NSCLC patients and non-cancer control subjects**

	n	Age (years) Mean ± SD	Gender	Smoking status	Stages	Subtypes
			M/F	N/Ex/S	I/II/III/IV	A/S/L
Control	16	49.5±18.6	9/7	7/4/5		
Cancer	13	62.8±10.1	7/6	1/6/6	2/2/2/7	8/3/2

n: number; SD: standard deviation; M: male; F: female; N: non-smoker; Ex: ex-smoker; S: smoker; A: adenocarcinoma; S: squamous cell lung cancer; L: large cell lung carcinoma. Demographic details of the participants and staging details of lung cancer patients. This table shows the total number of patient samples, age, gender, smoking status and lung tumour stages and subtypes. Full samples detail (e.g. GOLD stages) are displayed in Appendix A - Tables 16 and 17.
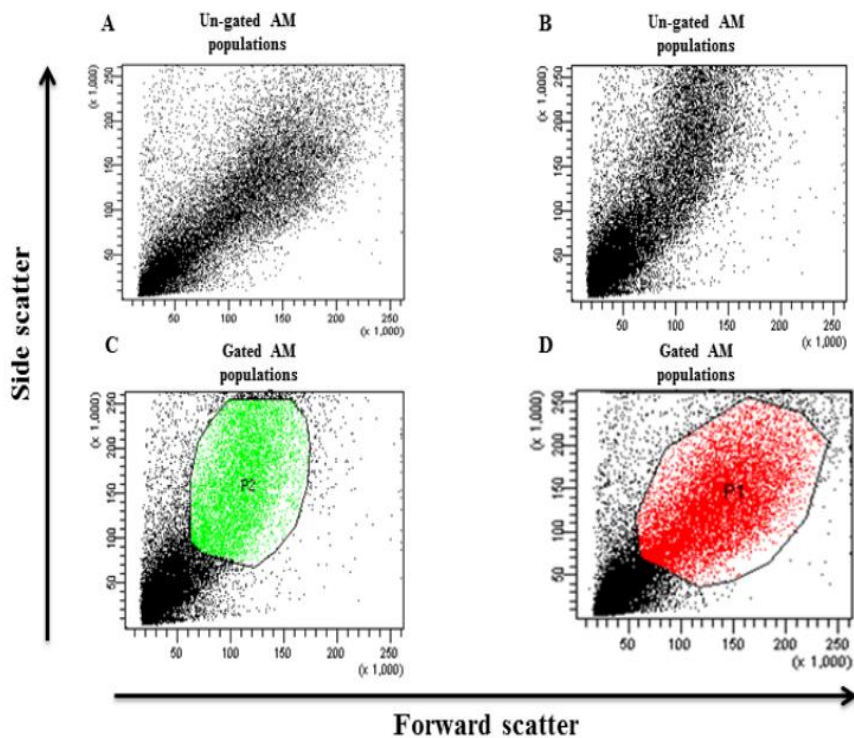
Figure 25: FSC and SSC profiles from freshly isolated AMs from BAL fluid using flow cytometry. The figure shows representative examples of AMs that have been collected from BAL fluid and analysed using flow cytometry: (A and B) FSC/SSC profiles of freshly isolated AMs prior to gating, (C and D) gating profiles of FSC/SSC plots of freshly isolated AMs from non-cancer controls (green colour) and cancer samples (red colour) based on CD68$^+$ expression. All data was collected on a BD FACS Canto (BD Biosciences, San Jose, CA, USA) within the RMIT Flow Cytometry Facility (Bundoora, Melbourne) and analysed using FACSDiva analysis software (BD Biosciences, USA).
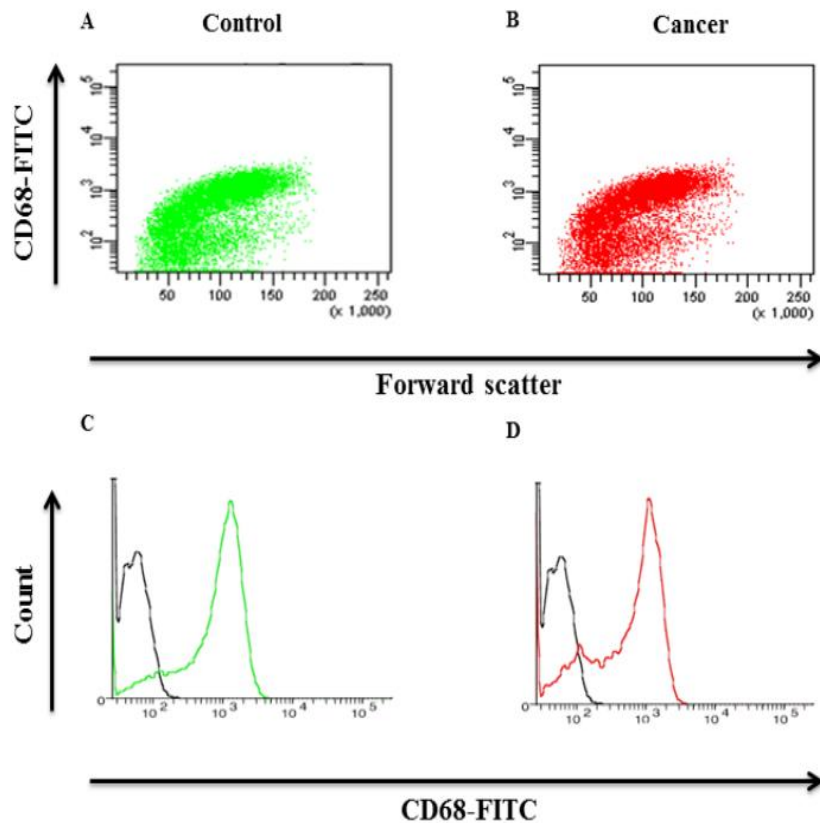
Figure 26: CD68^{+} expression on freshly isolated AMs obtained from BAL fluid using flow cytometry. Expression of CD68^{+} against FSC profiles from freshly isolated AMs from (A) non-cancer controls and (B) cancer subjects. (C and D) Histograms display the unstained AMs (black line) and CD68^{+} expression of non-cancer controls (green line) and NSCLC AMs (red line). All data was collected on a BD FACS Canto (BD Biosciences, San Jose, CA, USA) within the RMIT Flow Cytometry Facility (Bundoora, Melbourne) and analysed using FACSDiva analysis software (BD Biosciences, USA).

4.2.1. Analysis of functional receptors CD11b, CD71 and CD44 on AMs from patients with NSCLC and non-cancer controls by flow cytometry

The potential impact of NSCLC on the AMs expression of CD11b, CD71 and CD44 was investigated in patients with NSCLC compared to non-cancer controls using flow cytometry. Freshly isolated AMs were gated based on $CD68^+$ marker expression. There was no significant difference (P=0.8884) in the CD11b expression between NSCLC and non-cancer controls. Transferrin receptor CD71 was also measured and used as an indicator of monocyte-macrophage differentiation in BAL fluid. CD71 expression was found to be significantly increased in NSCLC patients compared to non-cancer control participants (Fig. 27). In addition, CD44 was also analysed on AMs of NSCLC patients and non-cancer controls. CD44 expression increased in NSCLC patients versus non-cancer controls (Fig. 27).
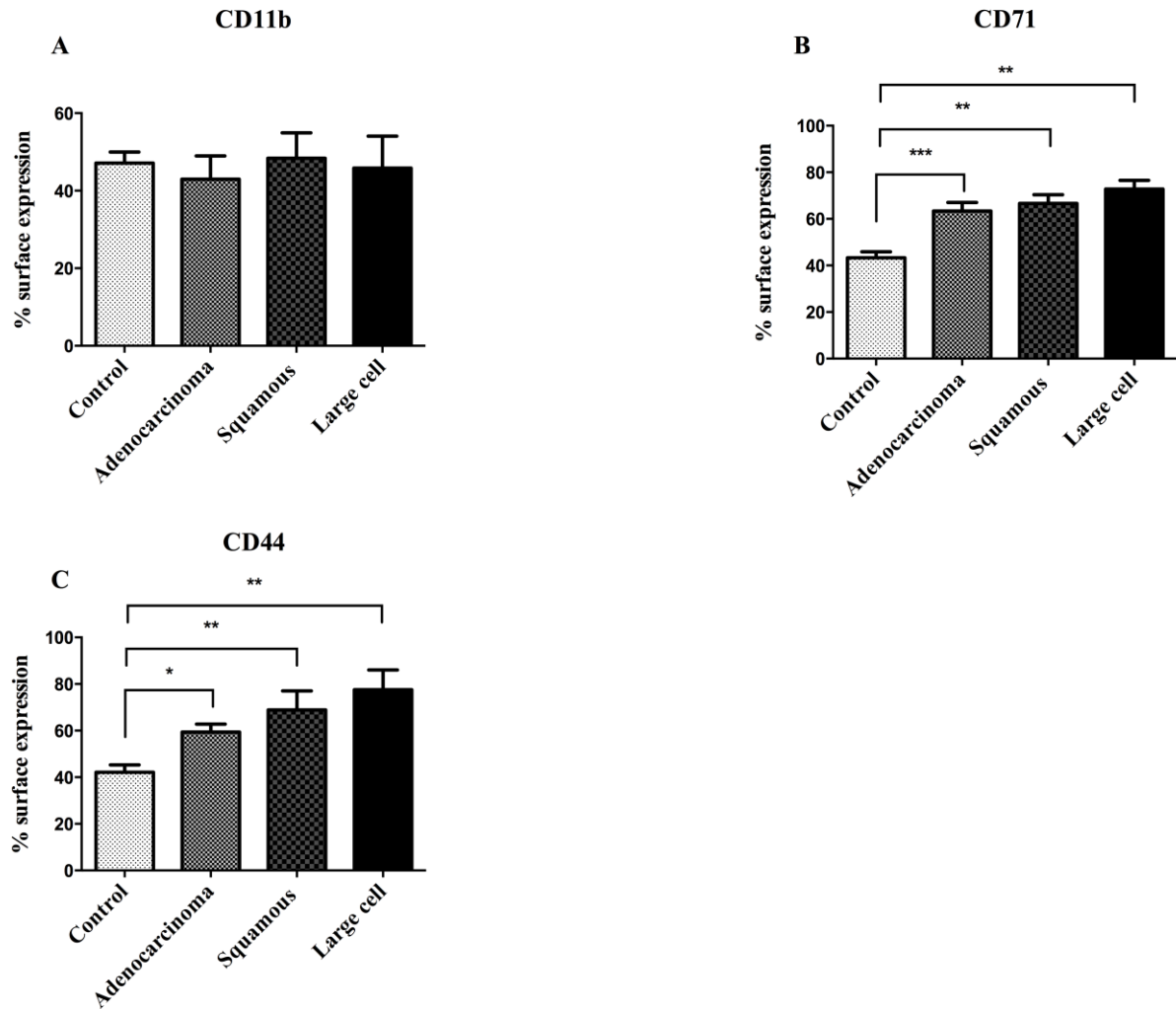
Figure 27: CD11b, CD71 and CD44 marker expression in AMs by flow cytometry. Representative graphs show %SE ± SEM of (A) CD11b, (B) CD71 and (C) CD44 in AMs from control and NSCLC patients. Results expressed as mean values of %SE ± SEM, (n= 16 control, 8 adenocarcinoma, 3 squamous cell lung carcinoma and 2 large cell lung carcinoma). One-way ANOVA multiple comparison test (as a post-test analysis) was performed with the Tukey test (multiple comparison test comparing every group with every other group). *$P \leq 0.05$, **$P \leq 0.01$ and ***$P \leq 0.001$ indicates statistical significance.

4.2.2. Analysis of M1 marker (HLA-DR) and M2 marker (CD163) surface expression on AMs from patients with NSCLC and non-cancer controls by flow cytometry

The potential impact of NSCLC on the AMs expression of HLA-DR (M1) and CD163 (M2) was examined in patients with NSCLC compared to non-cancer controls using flow cytometry. HLA-DR and CD163 markers were used to differentiate between M1 and M2 macrophage subsets by flow cytometry. Around 45% of AMs that were CD68$^+$ positive expressed HLA-DR marker, while CD163 was expressed by 25% of AMs. There was no significant difference in the expression of HLA-DR on AMs (P=0.9131) from NSCLC patients compared to non-cancer controls (Fig. 28). However, patients with NSCLC showed higher expression of CD163 on AMs in comparison to non-cancer controls (Figs. 28 and 29).
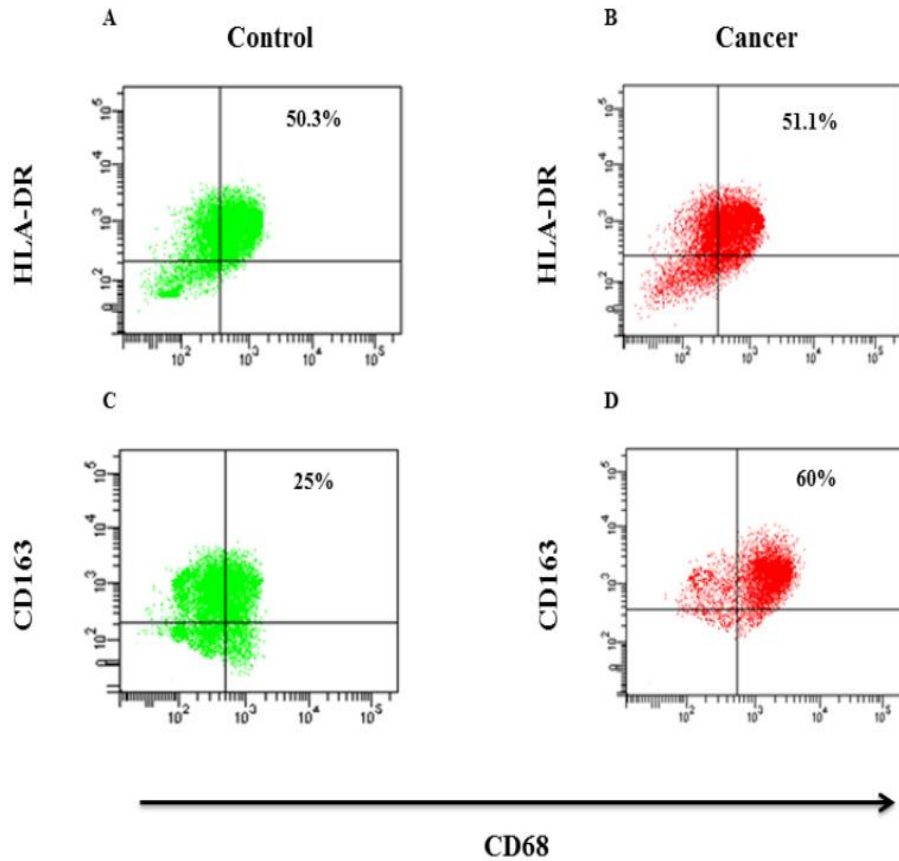
Figure 28: M1 and M2 marker expression on AMs (CD68) by flow cytometry. Representative dot plots (A and C) CD68^{+} AMs stained against HLA-DR and CD163 of non-cancer controls and (B and D) of NSCLC. All data was collected on a BD FACS Canto (BD Biosciences, San Jose, CA, USA) and analysed using FACSDiva software within the RMIT Flow Cytometry Facility (Bundoora, Melbourne).
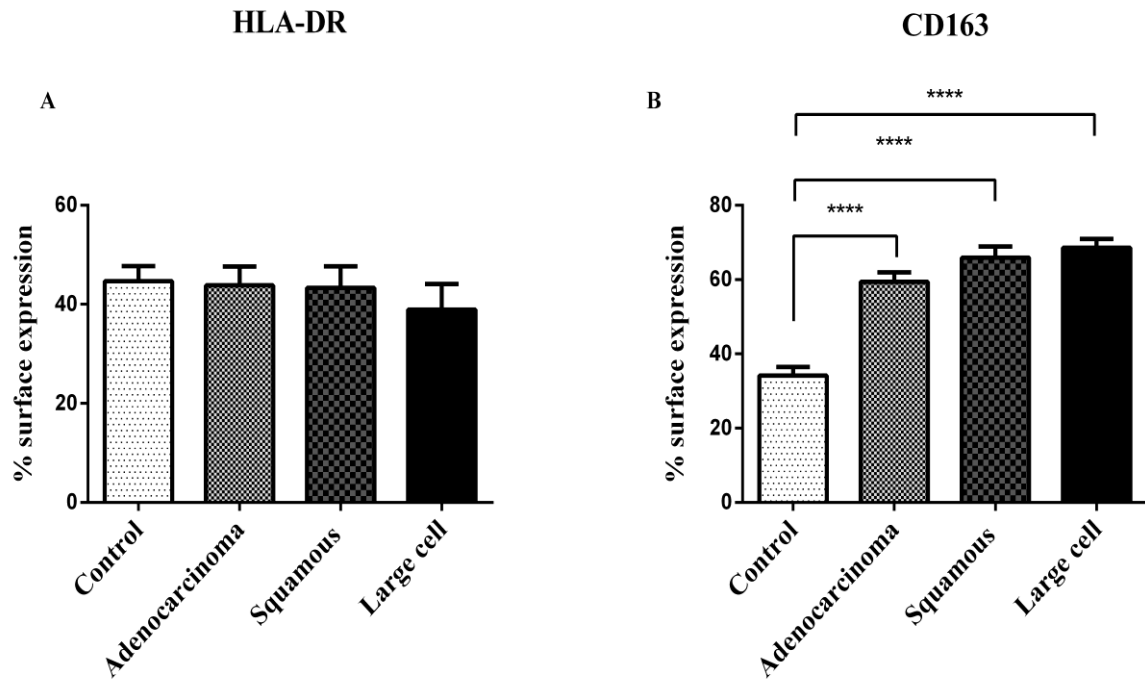
HLA-DR

CD163

Figure 29: HLA-DR (M1) and CD163 (M2) surface expression on AMs from patients with NSCLC and non-cancer controls by flow cytometry. The graphs show %SE ± SEM of (A) HLA-DR and (B) CD163 on AMs from non-cancer control and (adenocarcinoma (n=8), squamous cell (n=3) and large cell (n=2) primary lung cancer patients. Results expressed as mean values of %SE ± SEM. One-way ANOVA multiple comparison test (as a post-test analysis) was performed with the Tukey test (multiple comparison test comparing every group with every other group). ****$P \leq 0.0001$ indicates statistical significance difference

4.2.3. IL-6, IL-12, IL-10 and MMP-9 mRNA expression level in NSCLC compared to non-cancer controls

The mRNA expression of IL-6, IL-12, IL-10 and MMP-9 was measured on AMs to investigate the impact of NSCLC their levels as they are related to macrophage phenotype and function. The expression of IL-6 (P=0.4835) and IL-12 (P=0.3080) was similar in NSCLC patients compared to non-cancer controls. However, the expression of IL-10 was found to be highly increased in adenocarcinoma patients compared to non-cancer controls. However, the IL-10 expression was not altered in other NSCLC subtypes (squamous cell lung carcinoma and large cell lung carcinoma) compared to non-cancer controls. Lastly, the mRNA expression level of MMP-9 was found to be increased in all NSCLC subtypes compared to non-cancer controls (Fig. 30).
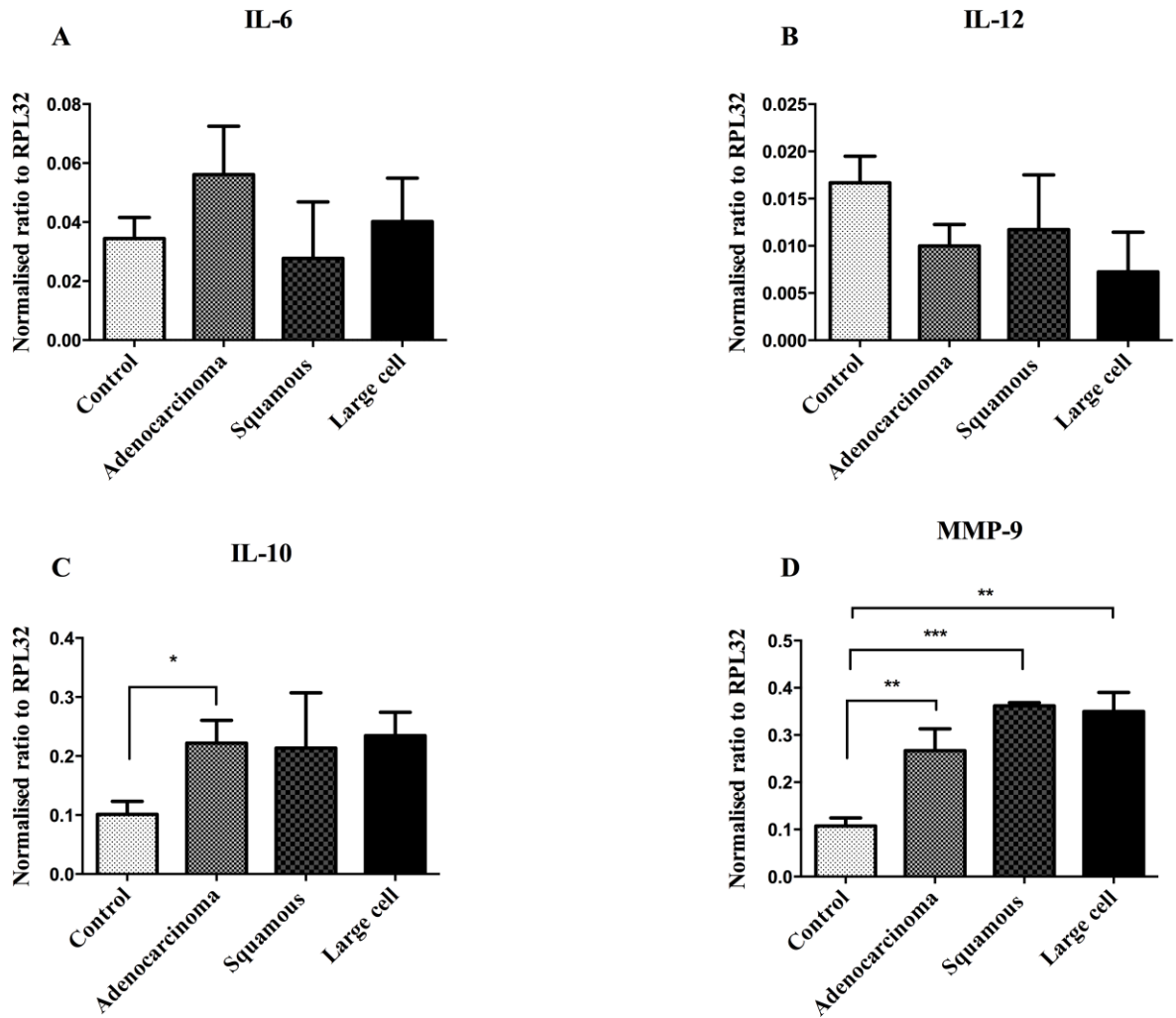
Figure 30: mRNA expression of IL-6, IL-12, IL-10 and MMP-9 on AMs in patients with NSCLC compared to non-cancer controls. Results show mRNA expression ± SEM, (n= 16 control, 8 adenocarcinoma, 3 squamous cell lung carcinoma and 2 large cell lung carcinoma). One-way ANOVA multiple comparison test (as a post-test analysis) was performed with the Tukey test (multiple comparison test comparing every group with every other group). *$P{\leq}0.05$, **$P{\leq}0.01$ and ***$P{\leq}0.001$ indicates statistical significance.

4.3. Discussion

Macrophages have been shown to exhibit several phenotypes, mainly depending on their environment (18, 104-106). Characterisation of macrophage phenotypes (M1 and M2) is likely to be an overgeneralisation, as macrophages have been described as a highly plastic cell that can display several phenotypes (104). The macrophage's ability to display different phenotypes and functions has led to their broad classification as either M1 macrophages or M2 macrophages.

HLA-DR and CD163 markers were used to distinguish between M1 and M2 phenotypes using flow cytometry. There was no significant difference in the surface expression of HLA-DR in all NSCLC subtypes patients compared to non-cancer controls. This result confirms our previous study that looked at HLA-DR expression on AMs from NSCLC patients compared to controls (27). However, AMs from all NSCLC subtypes patients showed high expression of CD163 compared to non-cancer controls. Similarly, a recent study demonstrated higher CD163 expression associated with lung cancer compared to non-malignant controls (221). Expression of CD163 on macrophages is associated with tumours and inflammation (18, 221). Our results verify the previous observations of the co-existence of macrophages in different activation states and unique or mixed phenotypes (106, 222).

Not all CD68^{+} cells were CD11b positive and this because both neutrophils and dendritic cells are detectable in BAL fluid and they can, similarly to macrophages, express high levels of CD11b (223, 224). Also, CD11b is known to be expressed on newly migrant macrophages more than resident macrophages (223). Thus, using this marker to examine cells within BAL fluid is fairly complicated, as it is hard to differentiate between macrophages and dendritic cells (224). Here, AMs from patients with all NSCLC subtypes expressed similar CD11b level compared to non-cancer control subjects.

The transferrin receptor (CD71) was measured as an indicator of macrophage differentiation in BAL fluid. In this study, 70% of AMs expressed CD71 and was found to be highly expressed on AMs from all NSCLC subtypes patients compared to non-cancer control participants. Increased CD71 expression has been shown in many malignant tumours including lung cancer, gastric cancer and breast cancer using different methods (201, 202, 225). In particular, a study has shown elevated expression of CD71 in COPD patients on AMs using flow cytometry (147). Similar to our results, it has been shown that the expression of CD71 correlates with tumour differentiation. Dowlati et al. (1997) showed that cell-associated CD71 levels are significantly higher in the BAL fluid of NSCLC patients compared to patients with small cell carcinoma and COPD (202). No correlation existed, however, between BAL fluid cells associated CD71 and tumour size, nodal status, the presence of metastases and serum transferrin receptor (202). Another study also displayed high expression of cellular CD71 in adenocarcinoma of the lung (226).

CD44 is a membrane glycoprotein with multiple functions including cell proliferation, differentiation, migration, and angiogenesis (227). It has been shown to be expressed on the surface of several human cells including AMs (228). CD44 has also been demonstrated to interact with osteopontin (OPN) and regulate its cellular functions leading to tumour progression (229). Here, CD44 surface expression was increased in all NSCLC subtypes patients compared to non-cancer controls. Similarly, other studies that examined the expression of CD44 on NSCLC patients demonstrated results (230, 231). Taken together, all these results are consistent with the prior suggestion regarding the association of CD44 with the proliferation, migration, angiogenesis (229).

AMs derived from patients with lung cancer have been shown *in vitro* to function efficiently against tumour cell growth (22-25, 114). They are able to control local inflammatory reactions via the release of cytokines such as IL-12 and IL-6 (87). These

cytokines are involved in numerous immune reactions, including tumouricidal activity (22). However, AMs secrete both pro-inflammatory cytokines and anti-inflammatory cytokines (13, 24, 89, 90). The M1 macrophages have been related to the increased expression of pro-inflammatory cytokines (e.g. IL-6 and IL-12) within NSCLC tumours and play a role in tumour regression (18). The ability of IL-6 to inhibit tumour cell growth has been suggested (22). Although IL-6 release can contribute to the anti-tumour function of AMs, a pro-tumour function has also been proposed (121). Even with IFN-γ and LPS stimulation, IL-6 inhibited the development of tumouricidal function in AMs of patients with lung cancer (26). Reduced IL-6 secretion was demonstrated in AMs that were derived from patients with large cell undifferentiated and small cell subtype tumours (13, 27). However, significantly elevated IL-6 levels have been detected in BAL fluid cell cultures from patients with lung cancer compared to those with benign disease (22). A study demonstrated that IL-6 levels in BAL fluid of lung cancer were higher compared to controls and were further elevated during radiotherapy, potentially confirming the role of IL-6 in mediating an inflammatory response (119). However, our results indicated the mRNA expression of IL-6 in all NSCLC subtypes patients compared to non-cancer controls was not statistically significant. This might be because of the lower number of NSCLC samples and the fact that tumour samples were from different stages, subtypes and early-diagnosed patients who have had no therapy as yet. IL-12 expression was also examined in this study and we found that there was no significant difference between non-cancer controls and NSCLC patients. Similar results have been shown in TAMs (tumour associated macrophages) from patients with NSCLC using RT-PCR (232).

AMs have been shown to promote tumour growth in patients with lung cancer (26, 27, 116, 125). Inhibition of pro-inflammatory cytokine secretion has been reported in the presence of elevated levels of serum IL-10 (116, 125). IL-10 is a potent angiogenesis

inhibitor and in AMs culture is released with or without LPS stimulation. Interestingly, following LPS stimulation, Yanagawa et al. (1999) found no significant differences in IL-10 production by AMs from patients with lung cancer compared to non-cancer controls (13, 25). However, increased IL-10 expression from TAMs has been confirmed in patients with NSCLC using RT-PCR technique (232). Here, mRNA expression of IL-10 was examined and found to be increased in patients with adenocarcinoma compared to non-cancer controls. However, the mRNA level was found not to be affected in the patients with squamous cell lung carcinoma and large cell lung carcinoma compared to non-cancer controls. This might be because of the fact that the majority of the analysed cancer samples (61%) were from patients with adenocarcinoma. In addition, as 70% of the samples that were processed were from NSCLC patients with late stage disease, these findings suggest that AMs in patients with advanced lung cancer express high levels of IL-10, which can inhibit pro-inflammatory functions and other cytotoxic molecules that mediate the killing of tumour cells. Taken together, IL-10 may be able to inhibit the anti-tumour activities of AMs and may contribute to tumour progression (125).

MMPs are matrix degrading enzymes that facilitate tumour growth through metastasis and the breakdown of basement membranes (87). In patients with lung cancer, macrophage MMP-12 and MMP-9 have been shown to promote lung tumour growth (140, 141). MMPs are an attractive target for therapeutic purposes because of their involvement in tumour progression. However, a recent trial has suggested that some MMPs might play a crucial role in host resistance against tumour progression (142). Collectively, these studies suggested an important role for MMP-9 in lung metastasis and indicated that MMP inhibitors could be designed to target tumour-promoting MMPs in order to inhibit tumour growth (142). Elevated MMP-9 levels have been demonstrated in BAL fluid and plasma samples of NSCLC patients (143). It has also been suggested that serum MMP-9 level (but not BAL

fluid MMP-9 level) might be useful to distinguish between malignant and benign lung diseases. The same study also demonstrated that serum MMP-9 levels relate to both disease stage and general clinical status of patients with NSCLC (144). Rui Wang et al. (2011) demonstrated using RT-PCR that macrophage expression of MMP-9 was higher in NSCLC patients compared to controls and associated with tumour progression (232). Similarly, our results indicated that the expression of MMP-9 was increased in all NSCLC subtypes patients compared to non-cancer controls (143).

The quality of BAL fluid samples was always a concern throughout the study, in particular the quality of sample, the amount of blood present within the samples and overall quantity of AM recovered from the processing method. Also, most of the collected samples were from patients with advanced stage disease, so we could not confidently address the question of whether NSCLC influences AM function and polarisation changes with tumour progression. The number of collected samples was from a relatively small pool of subjects (61% of the NSCLC samples were adenocarcinoma) and needs to be confirmed with a larger and more diverse cohort of patients with NSCLC. Despite our relatively comprehensive methodology, further techniques would be worth adding to future studies such as enzyme-linked immunosorbent assay (ELISA) and Western blot in order to strengthen some of the study outcomes. For example, ELISA could be used to investigate the up-regulated markers and cytokines in other body fluids e.g. serum. Based on the experience that we gained from this work, we believe that further improvements in BAL fluid sample preparation protocols would be highly desirable and necessary.

In conclusion, AM phenotype was found to be altered in patients with NSCLC compared to non-cancer controls. The M2 macrophage marker (CD163) significantly increased in NSCLC patients compared to non-cancer controls. The elevation of M2 macrophage is expected to be associated with angiogenesis and poor prognosis. In addition,

the CD71 and CD44 expression was found to be increased in NSCLC patients compared to non-cancer controls. The IL-10 and MMP-9 levels were also recognised to be increased in NSCLC patients compared to non-cancer controls. These results show that AM phenotype and function is altered in the presence of NSCLC compared to non-cancer controls. These results indicate the potential importance of targeting M2 macrophage and their pro-tumour activity to eventually skew them back to the M1 phenotype to promote a more potent anti-tumour activity. The elevated expression of CD163, CD71, CD44, IL-10 and MMP-9 may be utilised in the future as a potential diagnostic and/or prognostic biomarker in the BAL fluid of patients with NSCLC.

Chapter 5 Quantitative Proteomics of Bronchoalveolar Lavage Fluid in Primary Lung Adenocarcinoma

5.1. Introduction

Adenocarcinoma is the most frequently reported subtype of lung cancer in many countries (233, 234). Advances in the knowledge of the molecular pathways that are related to malignancy have opened up new methods for lung cancer treatment, particularly for adenocarcinoma, where molecular characterisation has led to the use of agents with high levels of antitumor activity. For example, epidermal growth factor receptor (EGFR) tyrosine kinase inhibitors are being used to treat patients with metastatic lung adenocarcinoma and an active mutation in EGFR (41, 42). As lung adenocarcinoma has been described histologically to be the most variable and heterogeneous subtype of lung cancer (233), urgent further research is needed in this area to understand its onset and progression.

Recently, quantitative proteomics has been utilised as a new technique to investigate the complex mix of proteins present in the tissue of patients with cancer compared to non-cancer controls (235). Extensive efforts have been directed towards examining protein dynamics, which eventually determine cell behaviour (236). Cellular proteins mostly function as components of protein complexes rather than as single polypeptides. Therefore, characterising the structure and dynamics of multi-protein complexes is crucial to understand and possibly manipulate the tumour microenvironment via various therapies (237). These investigations are aimed at understanding the proteins and protein interactions that may lead to treatments that can favour improved patient outcomes as well as developing valuable cancer biomarkers (236).

Proteomic studies of human body fluids, such as BAL fluid, are important in understanding both tumour pathways and identifying potential tumour biomarkers, which may ultimately lead to new treatments for lung cancer. The investigation of the BAL fluid proteome has already delivered vital information concerning alterations in protein expression and secretion in a range of pulmonary disorders including lung cancer (235, 238, 239). Alterations in protein expression have been shown in sarcoidosis, cystic fibrosis, hypersensitivity pneumonitis, COPD, as well as lung cancer (238-242). BAL fluid has been sampled during bronchoscopy of patients with a range of pulmonary disorders and has provided a sample of physiological fluid from the pulmonary compartment (243, 244). BAL fluid has been commonly used to obtain inflammatory cells (alveolar macrophages, neutrophils and monocytes) and other soluble components that are present in alveoli (244). Proteins that are found in BAL fluid are secreted from epithelial and inflammatory cells as well as being derived from the bloodstream (244). An advantage of using BAL fluid samples in proteomic analysis is the low protein concentration in the fluid. This advantage increases the chances of detecting more lung cancer biomarkers due to the absence of highly abundant and non-specific proteins in BAL fluid samples that potentially mask lung-derived molecules in other physiological fluids such as serum (238, 244). Thus, the proteomic analysis of BAL fluid can be utilised to investigate important pathophysiological functions that relate to a particular pulmonary disease, such as lung cancer (238). However, not all proteins that are present in BAL fluid can be identified using mass spectrometry, given that the dynamic range of BAL fluid protein abundance is estimated to be around 10^{10}, while the resolving power of mass spectrometry is limited to 10^2-10^4 (245).

In this part of the study, adenocarcinoma was chosen for investigation, as it is the most frequent primary lung cancer in many countries. The study aim was to identify biological processes, cellular components and molecular functions in BAL fluid samples

from patients with adenocarcinoma of the lung compared to non-cancer control subjects using quantitative proteomics. We also categorised the up-regulated proteins and their biological processes, cellular components and molecular functions in patients with adenocarcinoma of the lung. Identification of up- or down-regulated proteins in patients with primary lung adenocarcinoma may provide increased knowledge regarding the tumour microenvironment, cancer pathways and potential biomarkers.

5.2. Results

5.2.1. Lung adenocarcinoma alters BAL fluid protein expression

In this study, quantitative proteomics was used to identify biological processes, cellular components and molecular functions in BAL fluid samples from patients with adenocarcinoma of the lung compared to non-cancer control subjects. Also to categorise the up-regulated proteins and their biological processes, cellular components and molecular functions in patients with adenocarcinoma of the lung.

The demographic details of all adenocarcinoma and non-cancer controls subjects are shown in Table 9. BAL fluid samples were collected at Austin Health (Heidelberg, VIC, Australia) to isolate protein samples (analysed using proteomics). The number of proteins that were consistently identified in all samples was approximately 1,100. The main biological processes that were associated with BAL fluid proteins were metabolic processes (~19%), response to stimulus (~12%) and transport (~9%). Additionally, the main cellular components or compartments found to be linked to BAL fluid proteins were the cytoplasm (~23%), cell membrane (~14%), cytosol (~9%), nucleus (~8%), extracellular (~8%) and organelle lumen (~8%), respectively. For molecular functions, protein binding (~28%), catalytic activity (~22%), nucleotide binding (~11%), metal ion binding (~9%) and RNA binding (~5%) were found to be the leading molecular functions that BAL fluid proteins displayed (Fig. 31).

In this study, 1,100 proteins were identified (Appendix A, Table 18), of which 33 were found to be up-regulated consistently in all lung adenocarcinoma samples compared to non-cancer controls (Table 10). Eighteen percent of the up-regulated proteins were expressed at levels 3- to 5-fold higher in BAL fluid from patients with lung adenocarcinoma compared to non-cancer controls. The remaining up-regulated proteins (81%) were found to have a higher fold change, with a 5- to 11-fold increase in BAL fluid from patients with

adenocarcinoma compared to non-cancer controls. The top five up-regulated proteins were galectin-1, ADP/ATP translocase 2, 78 kDa glucose-regulated protein, cystatin-B and carbonic anhydrase II, respectively (Table 10). Other well recognised proteins were also identified to be up-regulated in the BAL fluid of lung adenocarcinoma compared to non-cancer controls such as S100-A8, annexin A1, annexin A2, thymidine phosphorylase (TP), transglutaminase 2 (TG2), Alpha-actinin-4. The biological processes, cellular components and molecular functions of all 33 up-regulated proteins were also shown in this study (Table 11).

Table 9: **Demographic details of lung adenocarcinoma and non-cancer control subjects**

	n	Age (years) Mean ± SD	Gender	Smoking status	Stages
			M/F	N/Ex/S	I/II/III/IV
Control	8	60 ± 8.71	3/5	3/2/3	
Cancer	8	68.1 ± 7.56	5/3	1/2/5	2/2/1/3

n: number; SD: standard deviation; M: male; F: Female; N: non-smoker; Ex: Ex-smoker; S: smoker. Demographic details of the participants and staging details of lung adenocarcinoma patients. This table shows the total number of patient samples, age, gender, smoking status and stages. Full sample details are displayed in appendix A - Tables 16 and 17.

A: Biological processes

- 18.59% Metabolic process
- 12.56% Regulation of biological process
- 12.42% Responose to stimulus
- 9.44% Transport
- 9.17% Cell organization and biogenesis
- 7.47% Cell communication
- 5.32% Development
- 4.07% Cell death
- 3.78% Defence response
- 3.34% Cell differentiation
- 2.85% Cellular component movement
- 2.63% No annotation available
- 2.34% Cell proliferation
- 1.83% Cellular homeostasis
- 1.68% Coagulation
- 1.15% Reproduction
- 0.68% Cell division
- 0.66% Cell growth

B: Cellular components

- 22.56% Cytoplasm
- 14.44% Membrane
- 8.65% Cytosol
- 8.35% Nucleus
- 8.16% Extracellular
- 7.87% Organelle lumen
- 6.52% Mitochondrion
- 3.96% Cytoskeleton
- 3.85% Endoplasmic reticulum
- 3.07% No annotation available
- 2.96% Vacuole
- 2.69% Golgi
- 2.13% Endosome
- 1.46% Cell surface
- 1.40% Ribosome
- 0.75% Chromosome
- 0.65% Proteasome
- 0.51% Spliceosomal complex

C: Molecular functions

- 28.43% Protein binding
- 22.06% Catalytic activity
- 10.72% Nucleotide binding
- 9.07% Metal ion binding
- 5.36% RNA binding
- 4.66% Transporter activity
- 4.53% No annotation available
- 4.10% Structural molecule activity
- 2.75% Enzyme regulator activity
- 2.44% DNA binding
- 1.79% Signal tranducer activity
- 1.70% Receptor activity
- 1.39% Antioxidant activity
- 0.78% Motor activity
- 0.17% Translation regulator activity
- 0.04% Transcription regulator activity

Figure 31: Distribution and classification of all proteins that were identified in BAL fluid samples. The Pie charts display the profiles of (A) biological process, (B) cellular component and (C) molecular function of all proteins that were identified in all BAL fluid samples (n=16) of lung adenocarinoma and non-cancer controls. The data of these graphs are shown in the Appendix A (Tables 13, 14 and 15). The Orbitrap MS data were analysed using Proteome Discoverer (Thermo Scientific version 1.4, Rockford, IL, USA) with the Mascot search engine (Matrix Science version 2.4, Boston, MA, USA) against the Uniprot database maintained at the Bio21 Institute, University of Melbourne, Australia (currently containing 26,617,536 sequences).

Table 10: **List of up-regulated proteins in BAL fluid from patients with lung adenocarcinoma compared to non-cancer controls using**

quantitative proteomic analysis

No.	Protein name[a]	Protein description[a]	MW [KDa][a]	# Peptide count	# Unique peptide	Fold change (A vs. N)[b]
1	ACTN4_HUMAN	Alpha-actinin-4	104.8	19	8	3.095
2	ADT2_HUMAN	ADP/ATP translocase 2	32.8	9	2	10.611
3	ANXA1_HUMAN	Annexin A1	38.7	12	12	6.283
4	ANXA2_HUMAN	Annexin A2	38.6	17	17	5.799
5	B4DIT7_HUMAN	Transglutaminase 2 (TG2)	68.6	11	11	7.073
6	B4DJV2_HUMAN	Citrate synthase	50.4	5	4	5.681
7	B4DQJ8_HUMAN	6-phosphogluconate dehydrogenase, decarboxylating	51.8	6	6	4.774
8	B4DW52_HUMAN	cDNA FLJ55253, highly similar to Actin, cytoplasmic 1	38.6	13	7	4.949
9	B4E1F5_HUMAN	cDNA FLJ57475, highly similar to Pulmonary surfactant-associated protein B	38.5	5	5	8.734
10	B7Z7A9_HUMAN	Phosphoglycerate kinase B	41.4	9	9	7.414
11	C9JGI3_HUMAN	Thymidine phosphorylase (TP)	46.1	9	9	4.928
12	CAH2_HUMAN	Carbonic anhydrase-II (CA II)	29.2	9	9	9.888
13	CATA_HUMAN	Catalase	59.7	16	16	8.358
14	CLIC1_HUMAN	Chloride intracellular channel protein 1	26.9	5	5	6.092
15	CX7A2_HUMAN	Cytochrome c oxidase subunit 7A2, mitochondrial	9.4	2	2	7.147
16	CYTB_HUMAN	Cystatin-B	11.1	3	3	10.051
17	EFHD2_HUMAN	Swiprosin-1	26.7	5	5	6.037
18	ENOA_HUMAN	Alpha-enolase	47.1	14	11	6.060
19	F8W0P2_HUMAN	HLA class II histocompatibility antigen, DR alpha chain	26.9	6	5	6.313
20	GRP78_HUMAN	78 kDa glucose-regulated protein	72.3	15	13	10.385
21	H4_HUMAN	Histone H4	11.4	3	3	8.292
22	LEG1_HUMAN	Galectin-1	14.7	4	4	11.386
23	LKHA4_HUMAN	Leukotriene A-4 hydrolase	69.2	22	22	6.851

24	MYH9_HUMAN	Myosin-9	226.4	20	20	4.034
25	O60744_HUMAN	Thioredoxin delta 3	9.3	2	2	8.664
26	PLSL_HUMAN	Plastin-2	70.2	21	21	5.640
27	PROF1_HUMAN	Profilin-1	15.0	6	6	8.870
28	Q53FJ5_HUMAN	Prosaposin	58.1	9	9	9.982
29	Q5TCU6_HUMAN	Talin 1	257.9	23	23	7.410
30	Q6DC98_HUMAN	LMNB1 protein	38.1	6	5	7.298
31	S10A8_HUMAN	Protein S100-A8	10.8	4	4	8.512
32	SAMH1_HUMAN	SAM domain and HD domain-containing protein 1	72.2	10	10	4.769
33	TAGL2_HUMAN	Transgelin-2	22.4	9	9	9.572

MW: Molecular weight; #peptide count: sum of peptide count; #unique peptides: sum of unique peptides; A: lung adenocarcinoma; N: non-cancer controls; HLA: human leukocyte antigen; DR: D related; SAM: sterile alpha motif; HD: homodimer. [a] Refers to the accession number of proteins, protein name and molecular weight from the Uniprot database.[b] Refers to the fold difference in expression in patients with cancer versus controls. The Orbitrap MS data were analysed using Proteome Discoverer (Thermo Scientific version 1.4, Rockford, IL, USA) with the Mascot search engine (Matrix Science version 2.4, Boston, MA, USA) against the Uniprot database maintained at the Bio21 institute, University of Melbourne, Australia (currently containing 26,617,536 sequences). Search parameters were precursor mass tolerance of 10 ppm and fragment mass tolerance of 0.2 Da. Carbamidomethyl of cysteine was set as fixed modification and dimethyl labelling (light and medium at +28.0313 and +32.0564, respectively) at the peptide *N*-terminus and lysine set as variable modifications. Trypsin with a maximum of 0 missed cleavage was used as the cleavage enzyme. A false discovery rate threshold of 1% was applied and identification of two or more unique peptides and two or more peptides were required for positive identification and quantification, respectively. A two-fold differential expression was chosen as being significant. The number of the samples that were processed is 8 controls and 8 adenocarcinomas.

Table 11: **The molecular functions, cellular components and biological processes of up-regulated proteins identified in the BAL fluid from patients with adenocarcinoma compared to non-cancer controls by proteomic analysis**

	Protein name	Protein description	Molecular function	Cellular component	Biological process
1	ACTN4_HUMAN	Alpha-actinin-4			
2	ADT2_HUMAN	ADP/ATP translocase 2			
3	ANXA1_HUMAN	Annexin A1			
4	ANXA2_HUMAN	Annexin A2			
5	B4DIT7_HUMAN	Transglutaminase 2 (TG2)			
6	B4DJV2_HUMAN	Citrate synthase			
7	B4DQJ8_HUMAN	6-phosphogluconate dehydrogenase, decarboxylating			
8	B4DW52_HUMAN	cDNA FLJ55253, highly similar to Actin, cytoplasmic 1			
9	B4E1F5_HUMAN	cDNA FLJ57475, highly similar to Pulmonary surfactant-associated protein B			
10	B7Z7A9_HUMAN	Phosphoglycerate kinase B			
11	C9JGI3_HUMAN	Thymidine phosphorylase (TP)			
12	CAH2_HUMAN	Carbonic anhydrase II (CA II)			
13	CATA_HUMAN	Catalase			
14	CLIC1_HUMAN	Chloride intracellular channel protein 1			
15	CX7A2_HUMAN	Cytochrome c oxidase subunit 7A2, mitochondrial			
16	CYTB_HUMAN	Cystatin-B			
17	EFHD2_HUMAN	Swiprosin-1			
18	ENOA_HUMAN	Alpha-enolase			
19	F8W0P2_HUMAN	HLA class II histocompatibility antigen, DR alpha chain			
20	GRP78_HUMAN	78 kDa glucose-regulated protein			

21	H4_HUMAN	Histone H4			
22	LEG1_HUMAN	Galectin-1			
23	LKHA4_HUMAN	Leukotriene A-4 hydrolase			
24	MYH9_HUMAN	Myosin-9			
25	O60744_HUMAN	Thioredoxin delta 3			
26	PLSL_HUMAN	Plastin-2			
27	PROF1_HUMAN	Profilin-1			
28	Q53FJ5_HUMAN	Prosaposin			
29	Q5TCU6_HUMAN	Talin 1			
30	Q6DC98_HUMAN	LMNB1 protein			
31	S10A8_HUMAN	Protein S100-A8			
32	SAMH1_HUMAN	SAM domain and HD domain-containing protein 1			
33	TAGL2_HUMAN	Transgelin-2			

HLA: human leukocyte antigen; DR: D related; SAM: sterile alpha motif; HD: homodimer. **Colours definition**: (I) Molecular function: protein binding, metal ion binding, catalytic activity, nucleotide binding, structural molecule activity, enzyme regulator activity, RNA binding, DNA binding, transporter activity, motor activity, signal transducer activity, antioxidant activity; (II) Cellular component: cytoskeleton, extracellular, nucleus, cytoplasm, mitochondrion, organelle lumen, membrane, endosome, cell surface, cytosol, vacuole, endoplasmic reticulum, Golgi, chromosome; (III) Biological process: response to stimulus, transport, coagulation, regulation of biological process, cell death, cell organisation and biogenesis, cellular component movement, metabolic process, cell communication, defence response, cell differentiation, development, cell proliferation, reproduction development, cellular homeostasis, reproduction, cell division, cell growth. The Orbitrap MS data were analysed using Proteome Discoverer (Thermo Scientific version 1.4, Rockford, IL, USA) with the Mascot search engine (Matrix Science version 2.4, Boston, MA, USA) against the Uniprot database maintained at the Bio21 Institute, University of Melbourne, Australia (currently containing 26,617,536 sequences).

5.3. Discussion

Lung cancer is one of the most common cancers with a poor prognosis and high mortality rate (6, 53). Adenocarcinoma, squamous cell lung carcinoma and large cell carcinoma are classified as one group (NSCLC) of lung cancers because they show a very similar behaviour in response to treatment. However, a new pathologic typing of lung cancer was established in 2011 by the IASLC, ATS and ERS (246). The alteration of lung cancer classification regarding treatment was significant because it has been recognised that different lung cancer subtypes respond differently to treatment. For example, metastatic lung adenocarcinoma that express EGFR or KRAS (Kirsten rat sarcoma viral oncogene homolog) can be treated with biological agents that are not as yet helpful for other subtypes, e.g. squamous cell lung carcinoma (41, 42). Lung adenocarcinoma is the most common diagnosed subtype of lung cancer and shows high variability and heterogeneity in its histological features (233, 234, 247). Therefore, it is essential and necessary to use new techniques to improve our knowledge about the complexity of the lung adenocarcinoma molecular environment. Quantitative proteomics is a new technique that has recently been utilised to investigate the protein dynamics in lung cancer and other pulmonary disorders (235). To date, most of the published literature has focused on plasma samples, cell lines associated with squamous cell lung carcinoma but not lung adenocarcinoma (235). In this study, BAL fluid was used as the source of proteins to be studied. We focused on displaying biological processes, cellular components and molecular functions of all identified proteins as well as examining the impact of lung adenocarcinoma on protein expression comparing cancer samples to non-cancer controls using quantitative proteomics.

Traditional biochemical methods investigate only one or a few proteins, while proteomics has the ability to identify thousands of proteins and provide comprehensive BAL fluid proteome information (248, 249). Being able to access all of this information can be

significant in understanding the molecular mechanisms underlying lung adenocarcinoma. In this study, 1,100 distinct proteins were identified and their biological processes, cellular components and molecular functions were discussed. Previous studies identified a similar number of up-regulated proteins in BAL fluid samples of normal and asthmatic subjects (245, 248). Biological processes, cellular components and molecular functions have been examined previously in normal, allergic asthma, lung cancer cell lines and pulmonary squamous cell lung carcinoma (245, 248, 250, 251). In this study, different biological processes associated with BAL fluid proteins such as metabolism, response to stimuli, transport, cell proliferation, cell growth and cell differentiation. Also, numerous cellular components were found to be associated to BAL fluid proteins such as cytoplasm, membrane, cytosol, nucleus, extracellular, organelle lumen and cell surface. The molecular functions that were recognised in BAL fluid proteins include protein binding, catalytic activity, nucleotide binding, metal ion binding, DNA binding and RNA binding.

Up-regulated proteins that were associated with lung adenocarcinoma samples are shown in Table 10. All 33 proteins were found to be consistently up-regulated in all lung adenocarcinoma patient samples compared to non-cancer controls. These proteins were considered significant as they had a minimum of two-fold change and ≥2 of unique peptides and peptide counts. A number of over-expressed proteins have been shown previously to be related to lung cancer progression including S100-A8, annexin A1, annexin A2, thymidine phosphorylase (TP) and transglutaminase 2 (TG2) (252-255). In our laboratory, a number of those over-expressed proteins were previously identified to be up-regulated in peripheral cholangiocarcinoma, including Alpha-actinin-4 and 78 kDa glucose-regulated protein (256).

S100-A8 is an important protein and recent studies have focused on its critical role in tumour growth, progression and invasion. It was also proposed to be both a potential therapeutic target and as an indicator for tumour progression in different tumours including

lung adenocarcinoma (252, 257). In this study, the expression of S100-A8 was significantly increased in lung adenocarcinoma samples compared to non-cancer controls. S100-A8 is a low molecular weight member of the S100 protein family which is characterised by the presence of two calcium ion Ca^{2+} binding EF-hand motifs (258). It naturally presents at high concentrations in the cytoplasm of monocytes and neutrophils and has been shown to play an essential role in lung tumour growth, progression and invasion (252, 258). In previous studies, the up-regulation of S100-A8 has been shown in the tissue of lung adenocarcinoma subjects and in BAL fluid of patients with acute respiratory distress syndrome (252, 259). S100-A8 has been established as a pro-inflammatory mediator in chronic and acute inflammation (260). It has also been correlated to tumour progression in other cancer types including kidney and breast cancer (261, 262). Another study has also confirmed the role of S100-A8 protein in promoting cell migration and invasion by the activation of p38 MAPK (p38 mitogen-activated protein kinases) and nuclear factor-κB (NF-κB) in gastric cancer cells (257).

Other proteins shown to be up-regulated in the BAL fluid of lung adenocarcinoma subjects have been shown to be associated with tumour growth and treatment resistance such as annexin A1 and A2 (253). These proteins belong to the annexin superfamily of calphobindin and play vital physiological roles in cytoskeletal movement, regulating cell growth and forming ion channels (263). Annexin A1 and A2 have been shown to participate in tumour drug resistance in lung adenocarcinoma *in vivo* and *in vitro* (253). Our results revealed that annexin A1 and A2 proteins to be over-expressed in lung adenocarcinoma patients compared to non-cancer controls. Similarly, a number of studies have indicated that high annexin expression is important for lung cancer (e.g. NSCLC) progression and suggested annexin to be a potential prognostic and diagnostic factor and therapeutic target for new lung cancer drug development (253, 264-266). In fact, circulating antibodies to annexin

A1 and another protein named DEAD box protein 53 (DDX53) have been used as biomarkers for early lung cancer diagnosis (265).

Another protein up-regulated in adenocarcinoma is thymidine phosphorylase (TP), also known as platelet-derived endothelial cell growth factor (PD-ECGF). Overexpression of TP has been shown in lung cancer, including lung adenocarcinoma (254, 267). It has been reported that high TP expression is associated with tumour growth, invasiveness, increased microvessel density, metastasis and poor prognosis in lung cancer (254, 267, 268). TP has also been suggested by many studies as a potential biomarker for poor prognosis and a novel target for treatment of lung adenocarcinoma and other cancers (267, 269, 270). Interestingly, TP is one of the major catabolic enzymes of 5-fluorouracil (5-FU) cancer chemotherapy and its level in NSCLC tissue correlates to the effectiveness of 5-FU treatment (271).

The other protein that was found to be elevated in patients with adenocarcinoma is Transglutaminase 2 (TG2). It has been linked to invasion and metastasis in different cancer types including breast, ovarian cancer and lung cancer (255, 272, 273). It is a multi-functional protein that plays an essential role in drug resistance in NSCLC (274, 275). A previous study has verified that increased TG2 expression is associated with increased invasion and migration in NSCLC cells *in vitro* and suggested TG2 to be a promising prognostic marker (255). Our study confirmed the association of elevated expression of TG2 protein in the BAL fluid of patients with lung adenocarcinoma compared to non-cancer controls.

Other overexpressed proteins such as chloride intracellular channel protein 1, transgelin-2, catalase, carbonic anhydrase II, galectin-1, and Lamin-B1 have been shown to be promising new lung cancer biomarkers (239, 275-278). CA II protein has been suggested to be a potential biomarker for early diagnosis for colorectal cancer and as a significant prognostic factor in gastrointestinal stromal tumour (279, 280). CA II has potential roles in both proliferation via changes in pH and the association with Na/H transporter and also

adaptation to acidified pH as is seen in tumour microenvironments. Another CA family member (CA IX) has been associated with adenocarcinoma progression and poor prognosis (281).

This study not only identified proteins that are associated with lung cancer progression, but also proteins that have been suggested to play anti-cancer roles and can thus be used as an indication of good tumour prognosis or as potential biomarkers for tumour aggressiveness such as profilin-1, prosaposin (282-284). Identifying proteins with pro-tumour functions as well as anti-tumour functions may validate the previous proposal that some of the inflammatory cells, such as macrophages which are found in BAL fluid samples may play a dual role in the tumour microenvironment (13).

Our study does have a number of limitations, which include small sample size number because of the low quality and quantity of BAL fluid samples. Therefore the number of samples needs to be expanded to confirm these results. Individual proteins that have been shown to be up-regulated in proteomics studies need to be validated using other techniques such as ELISA and/or Western blot to ascertain tissue distribution and specificity. Despite the broad coverage of proteomics technique, proteomics still has a tendency to detect proteins with higher abundance and larger molecular weight. Unfortunately, even the depletion of high abundance proteins in the BAL fluid has been shown previously to be associated with protein sample loss (285). Thus, further improvements in BAL fluid sample preparation protocols and proteomic technology are highly desirable.

In conclusion, biological processes, cellular components and molecular functions in BAL fluid samples from patients with and without adenocarcinoma were identified using quantitative proteomics. 33 different proteins were identified to be up-regulated in patients with adenocarcinoma compared to non-cancer controls. Identification of these up-regulated proteins may provide further knowledge regarding the tumour microenvironment, cancer

pathways and potential biomarkers. Finally, using proteomics to study BAL fluid samples in lung cancer is a promising technique that can be utilised to discover new biomarkers, treatment targets and prognostic and diagnostic indicators.

Chapter 6 Characterisation of M1 and M2 Tumour-Associated Macrophages (TAMs) in Patients with NSCLC

6.1. Introduction

The progression of lung cancer is a complex and multistep process where several mechanisms such as transformation, hypoxia, invasion, migration and metastasis are known to be the main hallmarks (286, 287). Improving our understanding of these mechanisms is a fundamental approach to control the aggressiveness of lung cancer and eventually overcome the obstacles to successful lung cancer treatment. Macrophages within the tumour microenvironment termed tumour associated macrophages (TAMs) are known to be crucial cells in lung cancer as they are in close proximity to tumour cells compared to other stromal cells (286). They are known to be responsible for releasing several growth factors, cytokines, chemokines, inflammatory mediators and other molecules (20). Many of these factors are well known and have been associated with tumour growth, poor prognosis and metastasis including VEGF, PDGF and IL-10 (20). In addition, the presence of high numbers of TAMs has been connected with the invasion, angiogenesis, hypoxia and early occurrence of metastasis in different tumour types including lung cancer (287-290).

TAMs are a type of cell that belong to the monocyte-macrophage lineage and like other macrophages have been described as a heterogeneous population (290). The activation of TAMs in response to cytokines, pro- (e.g. IFN-γ, TNF and IL-12) or anti-inflammatory (e.g. IL-4 and IL-10) molecules and microbial agents such as LPS (lipopolysaccharide) are well known (19, 20, 287). There are two main phenotypes of macrophages: M1 and M2. The M1 phenotype is activated by IFN-γ, LPS and TNF-α (18-20, 103). The M1 macrophage phenotype has been connected to the expression of IL-1, IL-12, TNF-α, and inducible nitric

oxide synthase (iNOS) and also has been correlated with extended survival time in patients with NSCLC (18, 20). On the other hand, the M2 macrophages have been correlated with tumour initiation and progression and have also been described as inhibitor of inflammation (18, 103). The M2 macrophages produce anti-inflammatory cytokines such as IL-10 and reduce the expression of iNOS, inhibit antigen presentation and T cell proliferation (19, 107, 109). The M2 macrophages have been found to encourage the growth of various tumour cells *in vitro* (111) and to increase tumour cell survival (112). They also play a vital role in promoting angiogenesis via VEGF, which is a prominent mediator of angiogenesis (18, 113).

In this study, lung tissues from patients with NSCLC were used to determine the possible phenotypic changes in TAM phenotype and this was compared to non-tumour tissue from the same patient. TAM phenotype was determined using immunohistochemistry (IHC). The TAM phenotype was determined using CD68 (macrophage marker), iNOS (M1) and CD163 (M2) antibodies, respectively. This study aims to provide a better understanding of the effect of NSCLC on TAM phenotype and is an important aspect of macrophage investigation since TAMs are the macrophages most likely to come in direct contact with lung tumour cells.

6.2. Results

6.2.1. Expression of CD68, iNOS (M1 marker) and CD163 (M2 marker) in NSCLC tumour tissue compared to non-tumour tissue

In this study, immunohistochemistry (IHC) were used to determine the possible phenotypic changes in TAM phenotype of NSCLC compared to non-tumour tissue from the same patient. The TAM phenotype was determined using CD68 (macrophage marker), iNOS (M1) and CD163 (M2) antibodies, respectively.

The demographic details of tissue samples are presented in Table 12. CD68 staining was used to evaluate TAMs in the NSCLC lung tissue compared to non-cancer tissue. The presence of TAMs (CD68 positive staining) was significantly higher in all NSCLC subtypes (adenocarcinoma $P \leq 0.0001$, squamous cell lung carcinoma $P \leq 0.0001$ and large cell lung carcinoma $P \leq 0.0001$) compared to non-tumour tissue. This result was expected as previous studies suggested that more TAMs are recruited to the tumour area and are associated with pulmonary disorders such as lung cancer (232, 291). All NSCLC subtypes (adenocarcinoma $P \leq 0.0001$, squamous cell lung carcinoma $P \leq 0.0001$ and large cell lung carcinoma $P \leq 0.0001$) were found to have significantly higher CD68 and CD163-positive cells when compared to non-tumour tissues (Figs. 32, 33 and 34). The % area of positive staining for CD163 was greatly increased in all NSCLC tissues (adenocarcinoma $P \leq 0.0001$, squamous cell lung carcinoma $P \leq 0.0001$ and large cell lung carcinoma $P \leq 0.0001$) compared to non-tumour tissues (Fig. 35).

For iNOS-stained M1 TAMs, staining was found to be decreased in the tissues of patients with adenocarcinoma $P \leq 0.01$ and squamous cell lung carcinoma $P \leq 0.05$ but not in large cell lung carcinoma compared to non-tumour tissue (Figs. 32, 33 and 34). Surprisingly, the result of the multiple comparison tests demonstrated that the % area of positive staining

for iNOS was significantly decreased in adenocarcinoma $P \leq 0.01$ and squamous cell lung carcinoma $P \leq 0.01$ compared to large cell lung carcinoma (Fig. 35).

Table 12: **Demographic details of lung cancer subjects for TAM tissue samples using immunohistochemistry staining (IHC)**

	n	Age (years) Mean ± SD	Gender	Stages	Smoking status	Subtypes
			M/F	I/II/III/IV	N/Ex/S	A/S/L
Tissue samples	32	66.78 ± 11.51	20/12	2/18/11/1	9/11/12	11/10/11

n: number; SD: standard deviation; M: male; F: female; N: non-smoker; Ex: ex-smoker; S: smoker; A: adenocarcinoma; S: squamous cell lung carcinoma; L: large cell lung carcinoma. TAMs of tumour and non-cancer tissue samples were obtained from the same patients with NSCLC. Samples were purchased from the Victorian Cancer Bio-Bank, Melbourne, Australia.
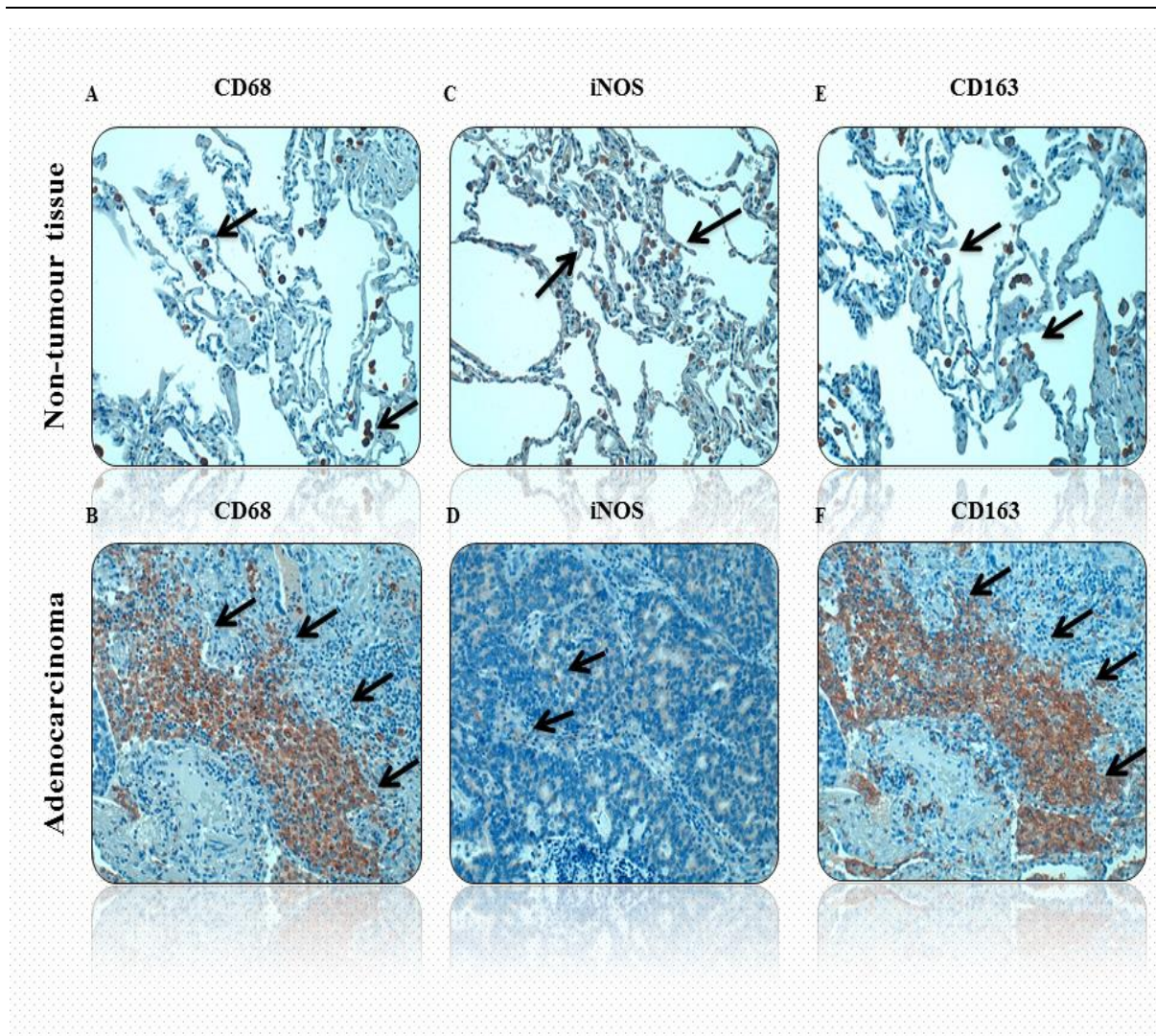
Figure 32: Expression of CD68, iNOS and CD163 in tumour (adenocarcinoma) and non-tumour tissue by immunohistochemistry. (A and B) CD68 (macrophage marker), (C and D) iNOS (M1 macrophage marker) and (E and F) CD163 (M2 macrophage marker) were used to stain tumour (adenocarcinoma) and non-tumour tissue. Black arrows indicate the expression of CD68/iNOS/CD163, x20. The slides were viewed and analysed using ImageScope analysis software. The colocalisation algorithm was applied to quantify IHC staining. The algorithm calculated the percentage area of positive staining based on the deconvolution method to separate the stains and classify each pixel according to the number of stains present. The slides were observed and all photos were taken using Leica DMD108 (Leica Microsystems, Germany). Please refer to pages 78-79.
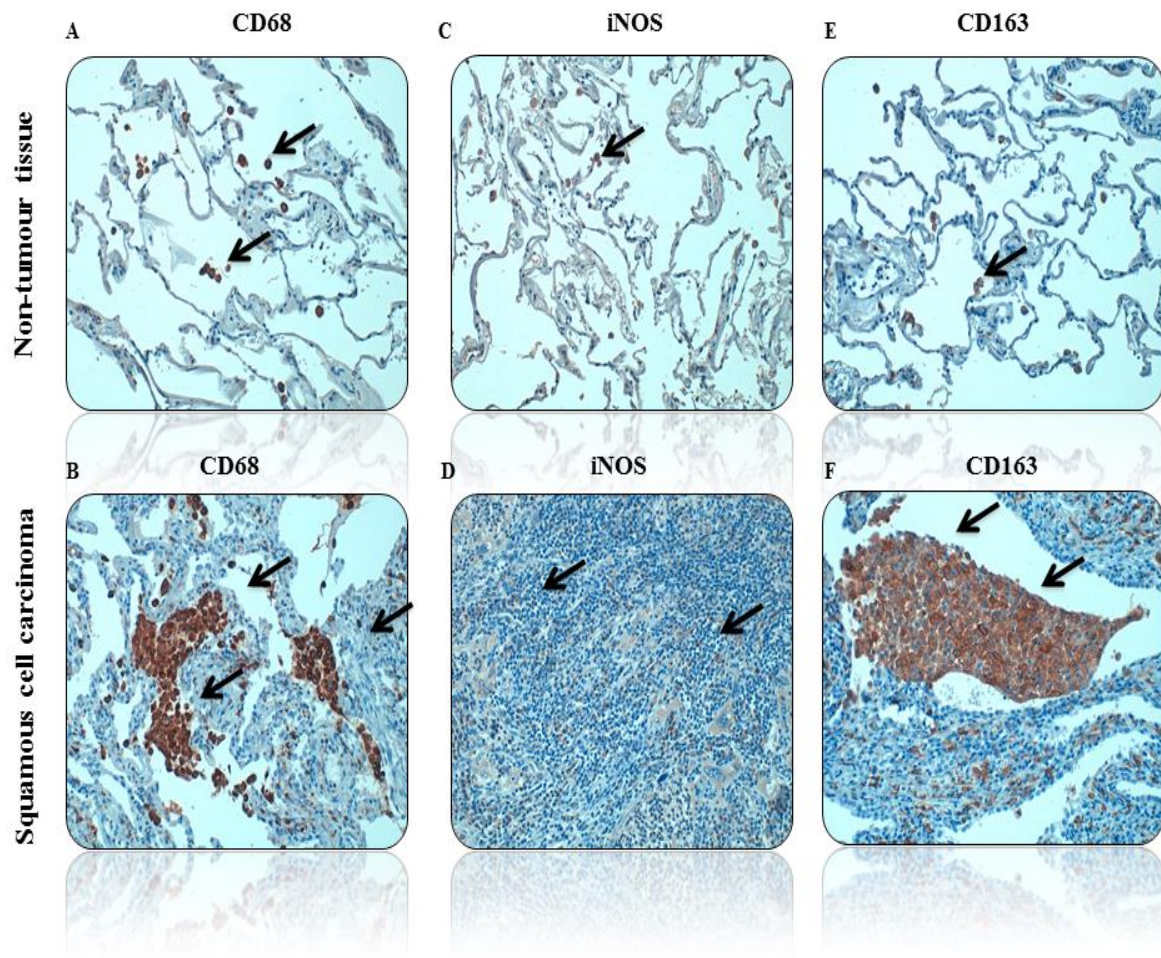
Figure 33: Expression of CD68, iNOS and CD163 in tumour (squamous cell lung carcinoma) and non-tumour tissue by immunohistochemistry. (A and B) CD68 (macrophage marker), (C and D) iNOS (M1 macrophage marker) and (E and F) CD163 (M2 macrophage marker) were used to stain tumour (squamous cell lung carcinoma) and non-tumour tissue. Black arrows indicate the expression of CD68/iNOS/CD163, x20. The slides were viewed and analysed using ImageScope analysis software. The colocalisation algorithm was applied to quantify IHC staining. The algorithm calculated the percentage area of positive staining based on the deconvolution method to separate the stains and classify each pixel according to the number of stains present. The slides were observed and all photos were taken using Leica DMD108 (Leica Microsystems, Germany). Please refer to pages 78-79.
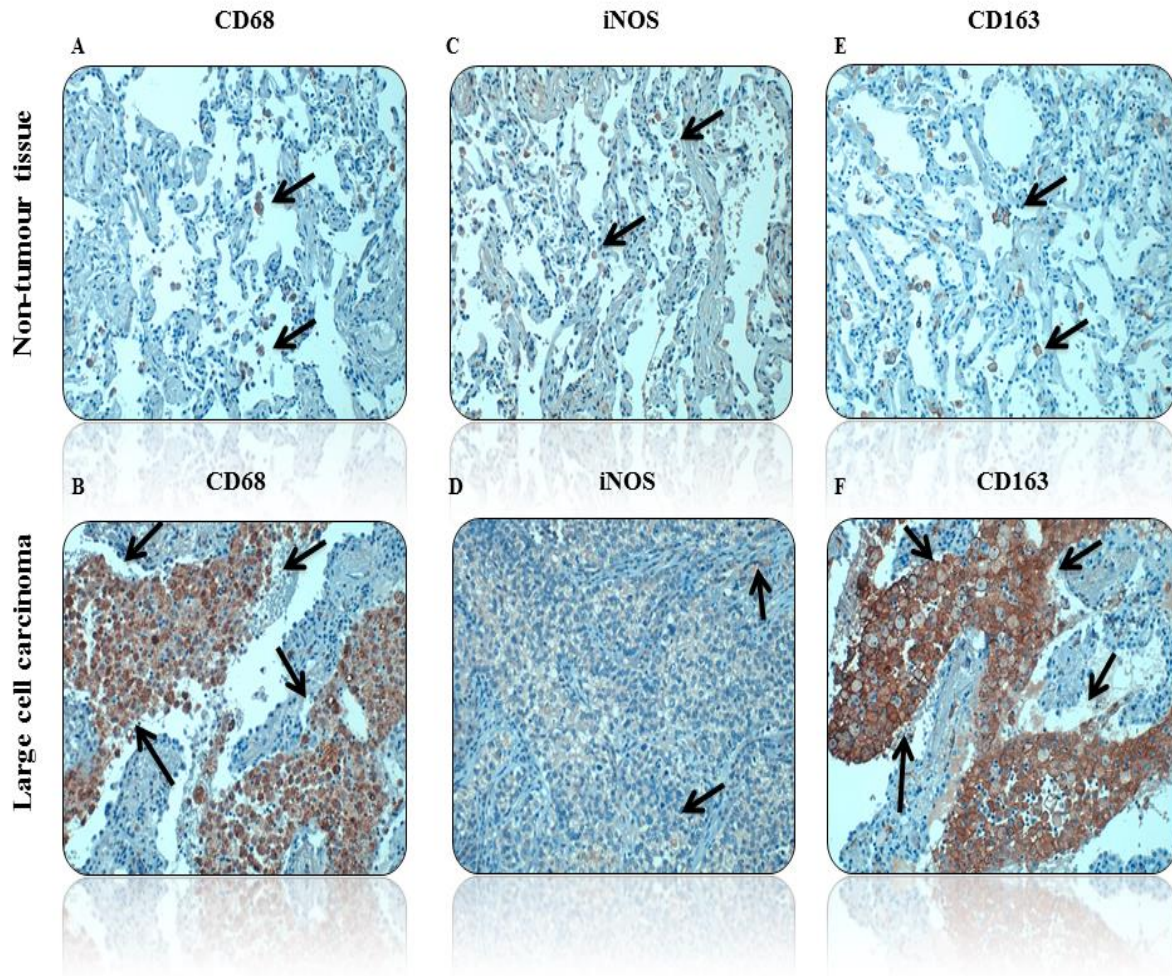
Figure 34: Expression of CD68, iNOS and CD163 in tumour (large cell lung carcinoma) and non-tumour tissue by immunohistochemistry. (A and B) CD68 (macrophage marker), (C and D) iNOS (M1 macrophage marker) and (E and F) CD163 (M2 macrophage marker) were used to stain tumour (large cell lung carcinoma) and non-tumour tissue. Black arrows indicate the expression of CD68/iNOS/CD163, x20. The slides were viewed and analysed using ImageScope analysis software. The colocalisation algorithm was applied to quantify IHC staining. The algorithm calculated the percentage area of positive staining based on the deconvolution method to separate the stains and classify each pixel according to the number of stains present. The slides were observed and all photos were taken using Leica DMD108 (Leica Microsystems, Germany). Please refer to pages 78-79.
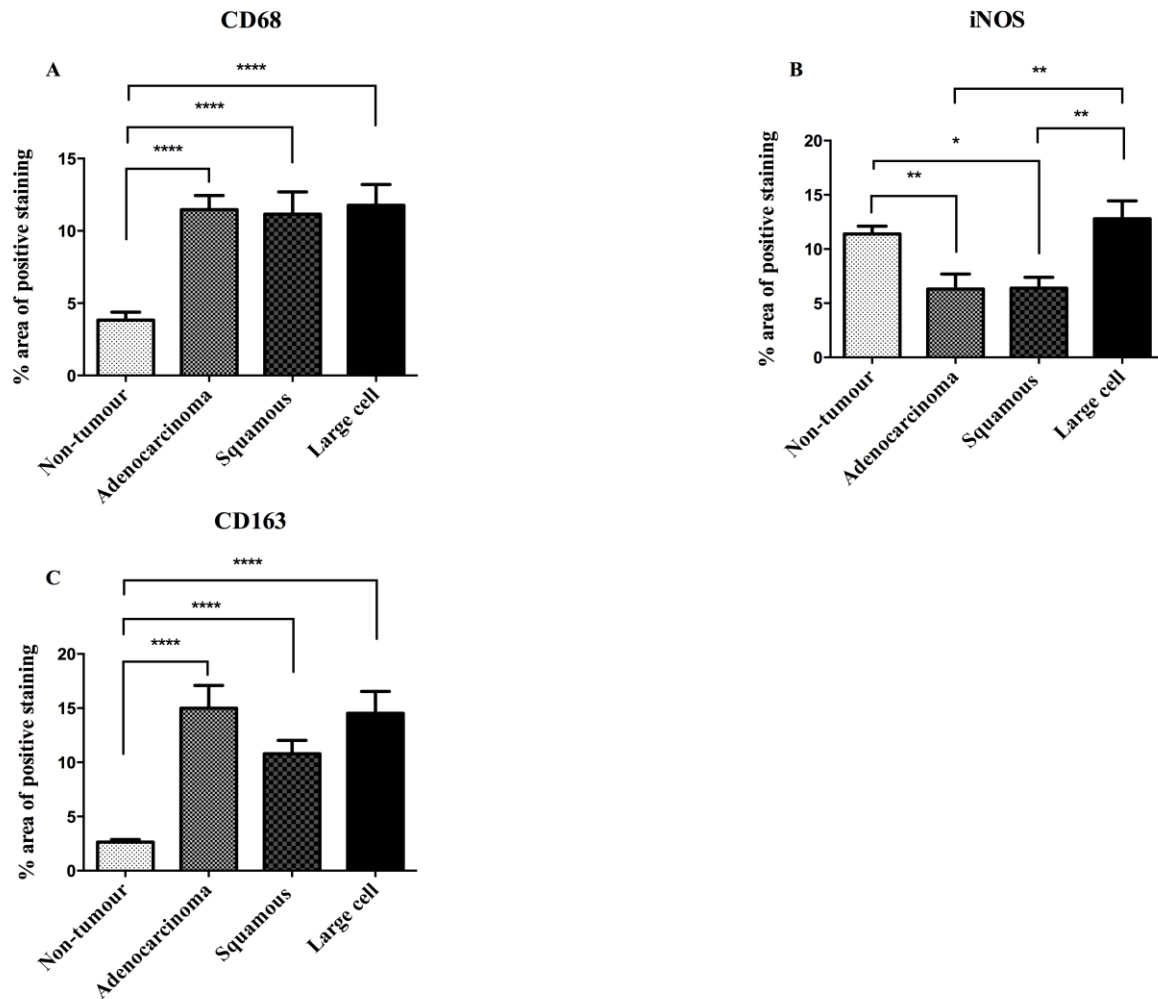
Figure 35: Percentage area of positive staining of CD68, iNOS and CD163 in lung tissue of different NSCLC subtypes (adenocarcinoma, squamous cell lung carcinoma and large cell lung carcinoma) compared to non-tumour tissue. The graphs show % area of positive staining ± SEM of (A) CD68, (B) iNOS and (C) CD163 on TAMs from non-tumour and tumour tissues from the same patient. Results expressed as % area of positive staining ± SEM, (n= 30 non-tumour tissues, 10 adenocarcinoma, 10 squamous cell lung carcinoma and 10 large cell lung carcinoma). Slides were viewed and analysed using the ImageScope analysis software and co-localisation algorithm were applied to quantify IHC staining. One-way ANOVA multiple comparison test (as a post-test analysis) was performed with the Tukey test (multiple comparison test comparing every group with every other group). $*P \leq 0.05$, $**P \leq 0.01$, $***P \leq 0.001$ and $****P \leq 0.0001$ indicates statistical significance.

6.3. Discussion

TAMs have been suggested to represent M2 macrophage-like phenotype in lung cancer and other tumour types, however it has become clear that TAMs consist of multiple distinct populations with different features (20, 290). Factors that contribute to altering TAMs towards a M2 phenotype include the location of TAMs within the tumour microenvironment, tumour stage and type of cancer. Nevertheless, it is still not fully defined whether the diversity within the TAM population is due to the maturation of unique monocytic precursors or rom the various factors within the local tumour microenvironment (290). In addition, further clarification regarding TAM phenotype within NSCLC subtypes is needed. Here, lung tissues from patients with NSCLC (adenocarcinoma, squamous cell lung carcinoma and large cell lung carcinoma) were used to investigate M1 and M2 marker expression in TAM populations within tumour and non-tumour tissue using immunohistochemistry.

Various studies have demonstrated increased TAM infiltration in NSCLC using CD68 macrophage marker (62, 159, 232, 291, 292). Some of these studies indicated the clinical importance of detecting increased macrophage number and was suggested as a powerful predictor of survival in NSCLC (18, 291, 293). In our study, all NSCLC subtypes were found to have significantly more CD68-positive cells when compared to non-tumour tissues. Similarly, other studies have shown the extensive TAM infiltration with lung tumour tissue and linked it with poor prognosis (87, 287). Taken together, these results suggest that TAMs contribute to tumour growth and lung cancer progression rather than supporting an effective host anti-tumour response. Interestingly, other studies have not supported this correlation between TAMs and good and/or poor prognosis in human lung cancer, as they reported no correlation with prognosis (294, 295). Differences between study results may relate to the examination of different lung cancer histological subtypes, different tumour stages or examination of macrophages from different lung segments. Other factors may also

contribute to differences such as patient demographics (e.g. smoking status and gender) and the presence or absence of comorbidities such as COPD.

TAMs that express iNOS have been found to be associated with extended survival in patients with NSCLC (18, 296). Ohri et al. (2009) used phenotypic markers including iNOS and CD163 to study the association of TAM subsets with prognosis (18). They looked at NSCLC patients with extended survival versus NSCLC patients with poor survival and established that M1 macrophages (CD68$^+$ and iNOS$^+$) within tumour islets was greatly increased in patients with extended survival compared to poor survival group (18). Also, the ratio of M1 macrophages in tumour islets and stroma was significantly increased compared to M2 (CD68$^+$ and CD163$^+$) macrophages in patients with extended survival but not the reduced survival cohort (18). All these results tend to validate the association of M1 TAMs with better lung cancer prognosis. In our study, M1 TAMs were identified using CD68 and iNOS marker in tumour compared to non-tumour tissue in NSCLC patients. Our results indicate that the presence of NSCLC correlated with significantly decreased expression of iNOS in patients with adenocarcinoma and squamous cell lung carcinoma compared to non-tumour tissues but this was not the case in large cell lung carcinoma. Similarly, decreased expression of iNOS in TAMs has been demonstrated in previous studies (108, 297). A previous study showed reduced iNOS expression in TAMs that were directly isolated from the tumour in tumour-bearing mice (108). Reduced iNOS expression has also been associated with defective NF-kB signalling, which eventually may lead to incorrect regulation of immune response (297). Overall these results suggest iNOS as an important mediator that might be targeted in future studies to alter the TAM phenotype and to be able eventually to manipulate these cells to improve tumour suppressing function. Also, the differences between the NSCLC subtypes expression of iNOS might be a possible explanation to recent queries that different lung cancer subtypes present different behaviour and respond differently to treatment (298).

TAMs that express M2 marker CD163 can stimulate tumour growth by producing cytokines to induce proliferation of tumour cells directly or indirectly through increasing endothelial cell proliferation and angiogenesis (20). In addition, the percentage of TAMs within a tumour microenvironment has been linked with tumour metastasis (299). Our results showed that the expression of CD163 was significantly increased in all NSCLC subtypes (adenocarcinoma, squamous cell lung carcinoma and large cell lung carcinoma) compared to non-tumour tissues. A study that investigated TAMs in advanced NSCLC found that more than 95% of CD68^{+} TAMs were located in the tumour stroma and were positively co-stained with CD163 (300). Also, the CD68^{+} and CD163^{+} TAMs count was found to be significantly increased in patients with progressive disease (300). Furthermore, other studies have shown that the expression of the M2 marker in TAMs was significantly correlated to poor prognosis, p-TNM staging and lymph node metastasis in patients with adenocarcinoma (292, 299).

Despite the relatively comprehensive and high sensitivity and specificity methodology, further techniques would be worth adding to future studies such as Western blot, immunofluorescence (IF) in order to strengthen the study outcomes. For example, immunofluorescence (IF) method would be used to generate high-resolution image, quantitate the fluorescence signal and perform multiple staining. Other lung cancer subtypes should be considered to inspect if they have any potential role in altering TAM functions and phenotypes. Also, the number of tissue samples needs to be expanded to confirm these results in a larger cohort.

In conclusion, the results of this study indicate that all NSCLC subtypes (adenocarcinoma, squamous cell lung carcinoma and large cell lung carcinoma) express significantly more CD68 and CD163 compared to non-tumour tissues. Also, the expression of iNOS in patients with adenocarcinoma and squamous cell lung carcinoma was significantly decreased compared to non-tumour tissues but not to that in the large cell lung carcinoma.

Also, all these results of TAMs indicate the importance of aiming to target M2 TAMs and their pro-tumour activity to eventually skew them back to the M1 TAMs phenotype and thus stimulate their anti-tumour activity. This could be potentially done by targeting M2 TAMs recruitment, polarisation and pro-tumour functions.

Chapter 7 General Discussion & Conclusion

This thesis hypothesised that macrophages in local and systemic environment (AMs, monocytes and TAMs) alter from M1 to M2-activated phenotype. It has been suggested in the literature that NSCLC might have the ability to alter macrophage phenotypes and functions and thus eventually lead to tumour onset, progression and metastasis. The aim of this study was to assess this theory by identifying if patients diagnosed with NSCLC have altered macrophage phenotypes and functions in the local (AMs and TAMs) and/or systemic environment (monocytes and serum). This study also looked at identifying potential biomarkers that could be associated with NSCLC. Different biological samples (BAL fluid, serum, PBMC, RNA, lung tissue and protein) were collected from NSCLC and non-cancer controls to assess evidence supporting our hypothesis. Serum samples for Bio-Plex, MAGPIX-Luminex were obtained from the Victorian Cancer Bio-Bank to include all NSCLC subtypes, especially large cell lung carcinoma as it is not a common subtype (accounts for 10-15% of lung cancers). A number of methods were also utilised including flow cytometry, RT-PCR, CBA, Bio-Plex, MAGPIX-Luminex assay, IHC and proteomics.

The study results suggest that NSCLC have the ability to alter some macrophage (AMs and TAMs) functions and play a role in changing the AM and TAM phenotype. The expression of CD163, a M2 macrophage marker was increased on AMs and TAMs from patients with NSCLC compared to non-cancer controls. The expression of CD71 and CD44 was also increased on AMs from NSCLC patients compared to non-cancer controls. The mRNA level of MMP-9 and IL-10 was shown to be higher in NSCLC compared to non-cancer controls. Also, a number of specific proteins such as S100-A8, annexin A1 and annexin A2 in BAL fluid of NSCLC patients were found to be up-regulated in

adenocarcinoma compared to non-cancer controls. Although this study showed alteration in macrophage populations such as AMs and TAMs, it did not show any alteration in peripheral classical monocyte phenotype in patients with NSCLC compared to non-cancer controls. This has been associated with unchanged Th1 and Th2 cytokine levels in the serum of NSCLC (except large cell lung carcinoma) patients compared to non-cancer controls. Therefore, these results suggest that there is no systemic impairment in Th1/Th2 cytokine expression and monocyte phenotype and function in patients with NSCLC versus non-cancer controls. However, only patients with large cell lung carcinoma showed increased serum levels of IL-1β, IL-4, IL-6 and IL-8. This result suggests that the impact of NSCLC on macrophage phenotypes and functions might change based on tumour subtypes. Another example of the influence of tumour subtypes is the recognised difference in the expression of iNOS on TAMs between NSCLC subtypes (adenocarcinoma, squamous cell lung carcinoma and large cell lung carcinoma). These results suggest that different lung cancer subtypes present a unique behaviour and pathway within the tumour microenvironment.

Taken together, the results of this study suggest for the first time that NSCLC might have the ability to alter macrophage phenotype and function within the local tumour microenvironment (AMs and TAMs) but not in the systemic environment (classical monocytes and serum) except for the patients with large cell lung carcinoma. This might be because of the direct interaction between macrophages (AMs and TAMs) and tumour cells within the tumour microenvironment. This contact potentially makes the AMs and TAMs more vulnerable to the influence of tumour cells through various growth factors, cytokines, chemokines, cell-surface receptors and other molecules in the local environment unlike in the systemic environment (monocytes).

In addition, the up-regulation of specific proteins in BAL fluid of lung adenocarcinoma patients may be useful as potential biomarkers for lung adenocarcinoma. Using proteomic

techniques to study BAL fluid samples in lung cancer patients and other pulmonary disorders is a promising technique that may be utilised to identify new biomarkers, treatment targets and prognostic and diagnostic indicators. Further investigations are required to ascertain if the skewing of M1 to M2 phenotype in primary lung cancer can lead to the upregulation of new biomarkers that can be used for diagnostic and/or therapeutic benefits.

Despite the findings described in this study, it does present with some limitations including an inability to compare results from subtypes within NSCLC groups, as the majority of the NSCLC samples were adenocarcinoma. Therefore, we could not confidently address the question of whether alteration in AM phenotype and function was NSCLC subtype dependent (e.g. squamous cell lung carcinoma and large cell lung carcinoma). The small sample size of AM tested may explain the different results seen in IL-6 expression between serum and mRNA samples. Although, IL-6 level was increased in the serum of large cell lung carcinoma patients compared to non-cancer controls, the IL-6 mRNA expression was not affected in the presence of large cell lung carcinoma. Therefore, the number of AM samples needs to be expanded to confirm if large cell lung carcinoma would have the same impact on IL-6 mRNA expression. For the proteomics study, we suggest that the sample size number needs to be expanded to confirm these results. Also, individual proteins that have been shown to be up-regulated in the proteomics studies should be validated using other techniques such as ELISA and/or Western blot. In future studies, examining macrophage phenotype and function in non-cancer controls versus lung cancer should be done by using fresh un-stimulated AMs and monocytes as well as cytokine treated AMs and monocytes at the same time to observe any variation that may occur. Future studies should also be performed to clarify if the alteration in macrophage phenotypes (skewing to M2-activated phenotype) and functions is a cause and/or an effect. The illumination of the complex relationship between NSCLC and macrophage would be highly beneficial in improving our

understanding regarding this association. Also, the quality of BAL fluid samples need to be kept in mind as some samples were processed below the optimum quality and quantity of BAL cells. Therefore, further improvements in BAL fluid collection protocols are needed. In addition, proteomics has a tendency to detect proteins with higher abundance and larger molecular weight. Unfortunately, even the depletion of high abundance proteins in BAL fluid has been shown previously to be associated with protein sample loss. Thus, further improvements in BAL fluid sample preparation protocols and proteomic technology are highly desirable. Despite the comprehensive nature of our methodology, further techniques would be worth adding to future studies such as ELISA and Western blot in order to strengthen some of the study outcomes. For example, the up-regulated proteins (e.g. CD163, S100-A8, annexin A1, annexin A2, thymidine phosphorylase and transglutaminase 2) that were identified in our study are desired to be confirmed using Western blot technique.

Finally, the outcome of this work suggests that the presence of NSCLC is associated with a certain alteration in macrophages phenotype and function. Therefore, these results suggest that targeting M2 macrophages to reduce their numbers or function, as well as to skew the M2 macrophages back to a M1 phenotype, may be beneficial to the outcomes of primary lung cancer patients. Lastly, this study revealed a number of specific proteins (e.g. CD163, S100-A8, annexin A1, annexin A2, thymidine phosphorylase and transglutaminase 2) and cytokines (IL-1β, IL-4, IL-6, IL-8, IL-10 and MMP-9) that were identified to be associated with NSCLC patients may be used as novel prognostic and/or diagnostic biomarkers in patients with NSCLC.

Chapter 8 References

1.   Geiser M, Kreyling WG. Deposition and biokinetics of inhaled nanoparticles. Part Fibre Toxicol. 2010;7:2.

2.   Scherbart AM. Mechanisms and Consequences of Particle Uptake in Alveolar Macrophages: Heinrich-Heine university; 2010.

3.   Azad N, Rojanasakul Y, Vallyathan V. Inflammation and lung cancer: roles of reactive oxygen/nitrogen species. J Toxicol Environ Health B Crit Rev. 2008;11(1):1-15.

4.   AIHW. Cancer survival and prevalence in Australia: period estimates from 1982 to 2010. Asia Pac J Clin Oncol. 2013;9(1):29-39.

5.   AIHW. Lung cancer in Australia: An overview

 2011. Available from: http://www.aihw.gov.au/publication-detail/?id=10737420419.

6.   Parkin DM, Bray F, Ferlay J, et al. Global cancer statistics, 2002. CA Cancer J Clin. 2005;55(2):74-108.

7.   Breath S. Lung cancer alliance issues inaugural report on lung cancer: Spirit and Breath; 2006. Available from: http://www.lungcanceralliance.org/.

8.   Henley SJ, Richards TB, Underwood JM, et al. Lung cancer incidence trends among men and women--United States, 2005-2009. MMWR Morb Mortal Wkly Rep. 2014;63(1):1-5.

9.   Esendagli G, Bruderek K, Goldmann T, et al. Malignant and non-malignant lung tissue areas are differentially populated by natural killer cells and regulatory T cells in non-small cell lung cancer. Lung Cancer. 2008;59(1):32-40.

10.   Street SE, Cretney E, Smyth MJ. Perforin and interferon-gamma activities independently control tumor initiation, growth, and metastasis. Blood. 2001;97(1):192-7.

11.   Girardi M, Oppenheim DE, Steele CR, et al. Regulation of cutaneous malignancy by gammadelta T cells. Science. 2001;294(5542):605-9.

12.   Dunn GP, Bruce AT, Ikeda H, et al. Cancer immunoediting: from immunosurveillance to tumor escape. Nat Immunol. 2002;3(11):991-8.

13. Kataki A, Scheid P, Piet M, et al. Tumor infiltrating lymphocytes and macrophages have a potential dual role in lung cancer by supporting both host-defense and tumor progression. J Lab Clin Med. 2002;140(5):320-8.

14. Gordon S, Martinez FO. Alternative activation of macrophages: mechanism and functions. Immunity. 2010;32(5):593-604.

15. Féréol S, Fodil R, Pelle G, et al. Cell mechanics of alveolar epithelial cells (AECs) and macrophages (AMs). Respir Physiol Neurobiol. 2008;163(1-3):3-16.

16. Flaherty DM, Monick MM, Hinde SL. Human alveolar macrophages are deficient in PTEN. The role of endogenous oxidants. J Biol Chem. 2006;281(8):5058-64.

17. Mariotta S, Aquilini M, Ricci A, et al. Changes in monocyte phagocyting activity after multi-agent chemotherapy in non-small cell lung cancer. Eur Rev Med Pharmacol Sci. 2002;6(4):67-73.

18. Ohri CM, Shikotra A, Green RH, et al. Macrophages within NSCLC tumour islets are predominantly of a cytotoxic M1 phenotype associated with extended survival. Eur Respir J. 2009;33(1):118-26.

19. Mantovani A, Sica A, Sozzani S, et al. The chemokine system in diverse forms of macrophage activation and polarization. Trends Immunol. 2004;25(12):677-86.

20. Mantovani A, Sozzani S, Locati M, et al. Macrophage polarization: tumor-associated macrophages as a paradigm for polarized M2 mononuclear phagocytes. Trends Immunol. 2002;23(11):549-55.

21. Sica A, Bronte V. Altered macrophage differentiation and immune dysfunction in tumor development. J Clin Invest. 2007;117(5):1155-66.

22. Matanic D, Beg-Zec Z, Stojanovic D, et al. Cytokines in patients with lung cancer. Scand J Immunol. 2003;57(2):173-8.

23. McDonald CF, Atkins RC. Defective cytostatic activity of pulmonary alveolar macrophages in primary lung cancer. Chest. 1990;98(4):881-5.

24. Siziopikou KP, Harris JE, Casey L, et al. Impaired tumoricidal function of alveolar macrophages from patients with non-small cell lung cancer. Cancer. 1991;68(5):1035-44.

25.   Yanagawa H, Takeuchi E, Suzuki Y, et al. Production of interleukin-10 by alveolar macrophages from lung cancer patients. Respir Med. 1999;93(9):666-71.

26.   Ahn MC, Siziopikou KP, Plate JM, et al. Modulation of tumoricidal function in alveolar macrophages from lung cancer patients by interleukin-6. Cancer Immunol Immunother. 1997;45(1):37-44.

27.   Pouniotis DS, Plebanski M, Apostolopoulos V, et al. Alveolar macrophage function is altered in patients with lung cancer. Clin Exp Immunol. 2006;143(2):363-72.

28.   Corrin B, Nicholson AG. Chapter 1 - The structure of the normal lungs. Pathology of the Lungs (Third Edition). Edinburgh: Churchill Livingstone; 2011. p. 1-37.

29.   Emmendoerffer A, Hecht M, Boeker T, et al. Role of inflammation in chemical-induced lung cancer. Toxicol Lett. 2000;112-113:185-91.

30.   Ayers MM, Jeffery PK. Proliferation and differentiation in mammalian airway epithelium. Eur Respir J. 1988;1(1):58-80.

31.   Richardson J, Bouchard T, Ferguson CC. Uptake and transport of exogenous proteins by respiratory epithelium. Lab Invest. 1976;35(4):307-14.

32.   Crapo JD, Barry BE, Gehr P, et al. Cell number and cell characteristics of the normal human lung. Am Rev Respir Dis. 1982;125(6):740-5.

33.   Low FN. The pulmonary alveolar epithelium of laboratory mammals and man. Anat Rec. 1953;117(2):241-63.

34.   Haber PS, Colebatch HJ, Ng CK, et al. Alveolar size as a determinant of pulmonary distensibility in mammalian lungs. J Appl Physiol. 1983;54(3):837-45.

35.   La Vecchia C, Bosetti C, Lucchini F, et al. Cancer mortality in Europe, 2000-2004, and an overview of trends since 1975. Ann Oncol. 2010;21(6):1323-60.

36.   Gibbons DL, Byers LA, Kurie JM. Smoking, p53 mutation, and lung cancer. Mol Cancer Res . 2014;12(1):3-13.

37.   Pfeifer GP, Denissenko MF, Olivier M, et al. Tobacco smoke carcinogens, DNA damage and p53 mutations in smoking-associated cancers. Oncogene. 2002;21(48):7435-51.

38.   Ryberg D, Hewer A, Phillips DH, et al. Different susceptibility to smoking-induced DNA damage among male and female lung cancer patients. Cancer Res. 1994;54(22):5801-3.

39.   Meyer KC, Raghu G. Bronchoalveolar lavage for the evaluation of interstitial lung disease: is it clinically useful? Eur Respir J. 2011;38(4):761-9.

40.   Beadsmoore CJ, Screaton NJ. Classification, staging and prognosis of lung cancer. Eur J Radiol. 2003;45(1):8-17.

41.   Siegelin MD, Borczuk AC. Epidermal growth factor receptor mutations in lung adenocarcinoma. Lab Invest. 2014;94(2):129-37.

42.   Munfus-McCray D, Harada S, Adams C, et al. EGFR and KRAS mutations in metastatic lung adenocarcinomas. Hum Pathol. 2011;42(10):1447-53.

43.   Katoh S, Matsubara Y, Taniguchi H, et al. Characterization of CD44 expressed on alveolar macrophages in patients with diffuse panbronchiolitis. Clin Exp Immunol. 2001;126(3):545-50.

44.   Bombi JA, Martinez A, Ramirez J, et al. Ultrastructural and molecular heterogeneity in non-small cell lung carcinomas: study of 110 cases and review of the literature. Ultrastruct Pathol. 2002;26(4):211-8.

45.   Roggli VL, Vollmer RT, Greenberg SD, et al. Lung cancer heterogeneity: a blinded and randomized study of 100 consecutive cases. Hum Pathol. 1985;16(6):569-79.

46.   Begin P, Sahai S, Wang NS. Giant cell formation in small cell carcinoma of the lung. Cancer. 1983;52(10):1875-9.

47.   Corrin B, Nicholson AG. Chapter 12 - Tumours. In: Nicholson BCG, editor. Pathology of the Lungs (Third Edition). Edinburgh: Churchill Livingstone; 2011. p. 531-705.

48.   Keehn R, Auerbach O, Nambu S, et al. Reproducibility of major diagnoses in a binational study of lung cancer in uranium miners and atomic bomb survivors. Am J Clin Pathol. 1994;101(4):478-82.

49.   Sindrilaru A, Peters T, Wieschalka S, et al. An unrestrained proinflammatory M1 macrophage population induced by iron impairs wound healing in humans and mice. J Clin Invest. 2011;121(3):985-97.

50. Valaitis J, Warren S, Gamble D. Increasing incidence of adenocarcinoma of the lung. Cancer. 1981;47(5):1042-6.

51. Zheng T, Holford TR, Boyle P, et al. Time trend and the age-period-cohort effect on the incidence of histologic types of lung cancer in Connecticut, 1960-1989. Cancer. 1994;74(5):1556-67.

52. Janssen-Heijnen MLG, Coebergh J-WW. Trends in incidence and prognosis of the histological subtypes of lung cancer in North America, Australia, New Zealand and Europe. Lung Cancer. 2001;31(2–3):123-37.

53. Lortet-Tieulent J, Soerjomataram I, Ferlay J, et al. International trends in lung cancer incidence by histological subtype: Adenocarcinoma stabilizing in men but still increasing in women. Lung Cancer. 2014;84(1):13-22.

54. Bourke W, Milstein D, Giura R, et al. Lung cancer in young adults. Chest. 1992;102(6):1723-9.

55. Yano T, Haro A, Shikada Y, et al. Non-small cell lung cancer in never smokers as a representative 'non-smoking-associated lung cancer': epidemiology and clinical features. Int J Clin Oncol. 2011;16(4):287-93.

56. Steinhauer JR, Moran CA, Suster S. 'Secretory endometrioid-like' adenocarcinoma of the lung. Histopathology. 2005;47(2):219-20.

57. Inamura K, Satoh Y, Okumura S, et al. Pulmonary adenocarcinomas with enteric differentiation: histologic and immunohistochemical characteristics compared with metastatic colorectal cancers and usual pulmonary adenocarcinomas. Am J Surg Pathol. 2005;29(5):660-5.

58. Downey RS, Sewell CW, Mansour KA. Large cell carcinoma of the lung: a highly aggressive tumor with dismal prognosis. Ann Thorac Surg. 1989;47(6):806-8.

59. Sturgis CD, Nassar DL, D'Antonio JA, et al. Cytologic features useful for distinguishing small cell from non-small cell carcinoma in bronchial brush and wash specimens. Am J Clin Pathol. 2000;114(2):197-202.

60. Marchevsky AM, Gal AA, Shah S, et al. Morphometry confirms the presence of considerable nuclear size overlap between "small cells" and "large cells" in high-grade pulmonary neuroendocrine neoplasms. Am J Clin Pathol. 2001;116(4):466-72.

61.   Bhatia A, Kumar Y. Cancer-Immune Equilibrium: Questions Unanswered. Cancer Microenviron. 2011;4(2):209-17.

62.   Takanami I, Takeuchi K, Kodaira S. Tumor-associated macrophage infiltration in pulmonary adenocarcinoma: association with angiogenesis and poor prognosis. Oncology. 1999;57(2):138-42.

63.   Lissbrant IF, Stattin P, Wikstrom P, et al. Tumor associated macrophages in human prostate cancer: relation to clinicopathological variables and survival. Int J Oncol. 2000;17(3):445-51.

64.   Kerr KM, Johnson SK, King G, et al. Partial regression in primary carcinoma of the lung: does it occur? Histopathology. 1998;33(1):55-63.

65.   Siveen KS, Kuttan G. Role of macrophages in tumour progression. Immunology Letters. 2009;123(2):97-102.

66.   Micke P, tman A. Tumour-stroma interaction: cancer-associated fibroblasts as novel targets in anti-cancer therapy? Lung Cancer. 2004;45(Supplement 2):S163-S75.

67.   Pietras K, Ostman A. Hallmarks of cancer: interactions with the tumor stroma. Exp Cell Res . 2010;316(8):1324-31.

68.   Bhowmick NA, Moses HL. Tumor-stroma interactions. Curr Opin Genet Dev. 2005;15(1):97-101.

69.   Koyama H, Kobayashi N, Harada M, et al. Significance of tumor-associated stroma in promotion of intratumoral lymphangiogenesis: pivotal role of a hyaluronan-rich tumor microenvironment. Am J Pathol. 2008;172(1):179-93.

70.   Ahmed F, Steele JC, Herbert JM, et al. Tumor stroma as a target in cancer. Curr Cancer Drug Targets. 2008;8(6):447-53.

71.   Geissmann F, Manz MG, Jung S, et al. Development of monocytes, macrophages, and dendritic cells. Science. 2010;327(5966):656-61.

72.   Qian BZ, Pollard JW. Macrophage diversity enhances tumor progression and metastasis. Cell. 2010;141(1):39-51.

73.   Nakata Y, Yamashita J, Kishi T, et al. Decreased monocyte-mediated cytostasis of human cancer cell in patients with lung cancer. Cancer Immunol Immunother. 1985;20(1):43-6.

74.   Snyderman R, Meadows L, Holder W, et al. Abnormal monocyte chemotaxis in patients with breast cancer: evidence for a tumor-mediated effect. J Natl Cancer Inst. 1978;60(4):737-40.

75.   Unger SW, Bernhard MI, Pace RC, et al. Monocyte dysfunction in human cancer. Cancer. 1983;51(4):669-74.

76.   Vuk-Pavlovic S, Bulur PA, Lin Y, et al. Immunosuppressive CD14+HLA-DRlow/-monocytes in prostate cancer. Prostate. 2010;70(4):443-55.

77.   Brooks N, Stojanovska L, Grant P, et al. Characterization of blood monocyte phenotype in patients with endometrial cancer. Int J Gynecol Cancer. 2012;22(9):1500-8.

78.   Mytar B, Baj-Krzyworzeka M, Majka M, et al. Human monocytes both enhance and inhibit the growth of human pancreatic cancer in SCID mice. Anticancer Res. 2008;28(1A):187-92.

79.   Satoh N, Shimatsu A, Himeno A, et al. Unbalanced M1/M2 phenotype of peripheral blood monocytes in obese diabetic patients: effect of pioglitazone. Diabetes Care. 2010;33(1):e7.

80.   Garrett S, Dietzmann-Maurer K, Song L, et al. Polarization of primary human monocytes by IFN-gamma induces chromatin changes and recruits RNA Pol II to the TNF-alpha promoter. J Immunol. 2008;180(8):5257-66.

81.   Lee HW, Choi HJ, Ha SJ, et al. Recruitment of monocytes/macrophages in different tumor microenvironments. Biochim Biophys Acta. 2013;1835(2):170-9.

82.   Nagorsen D, Deola S, Smith K, et al. Polarized monocyte response to cytokine stimulation. Genome Biol. 2005;6(2):R15.

83.   Movahedi K, Laoui D, Gysemans C, et al. Different tumor microenvironments contain functionally distinct subsets of macrophages derived from Ly6C(high) monocytes. Cancer Res. 2010;70(14):5728-39.

84.   Graham E, Michael. Tumor macrophage redox and effector mechanisms associated with hypoxia. Free Radic Biol Med. 2006;41(11):1621-8.

85.   Steinman RM, Idoyaga J. Features of the dendritic cell lineage. Immunol Rev. 2010;234(1):5-17.

86.   Wu HM, Jin M, Marsh CB. Toward functional proteomics of alveolar macrophages. Am J Physiol Lung Cell Mol Physiol. 2005;288(4):L585-95.

87.   Bingle L, Brown N, Lewis C. The role of tumour- associated macrophages in tumour progression: implications for new anticancer therapies. J Pathol. 2002;196(3):254-65.

88.   Luiz Carlos Junqueira JC. Basic Histology text & atlas. 11th ed: McGraw-Hill; 2005. 502 p.

89.   Thomassen MJ, Ahmad M, Barna BP, et al. Induction of cytokine messenger RNA and secretion in alveolar macrophages and blood monocytes from patients with lung cancer receiving granulocyte-macrophage colony-stimulating factor therapy. Cancer Res. 1991;51(3):857-62.

90.   Watson ML, White AM, Campbell EM, et al. Anti-inflammatory actions of interleukin-13: suppression of tumor necrosis factor-alpha and antigen-induced leukocyte accumulation in the guinea pig lung. Am J Respir Cell Mol Biol. 1999;20(5):1007-12.

91.   Kuda T, Yasumoto K, Yano T, et al. Role of antitumor activity of alveolar macrophages in lung cancer patients. Cancer Res. 1987;47(8):2199-202.

92.   Adamson IY, Bowden DH. Role of monocytes and interstitial cells in the generation of alveolar macrophages II. Kinetic studies after carbon loading. Lab Invest. 1980;42(5):518-24.

93.   Bowden DH, Adamson IY. Alveolar macrophage response to carbon in monocyte-depleted mice. Am Rev Respir Dis. 1982;126(4):708-11.

94.   Corry D, Kulkarni P, Lipscomb MF. The migration of bronchoalveolar macrophages into hilar lymph nodes. Am J Pathol. 1984;115(3):321-8.

95.   Coley WB. II. Contribution to the Knowledge of Sarcoma. Ann Surg. 1891;14(3):199-220.

96.   Mantovani A, Sica A. Macrophages, innate immunity and cancer: balance, tolerance, and diversity. Curr Opin Immunol. 2010;22(2):231-7.

97.   Fathi M, Johansson A, Lundborg M, et al. Functional and morphological differences between human alveolar and interstitial macrophages. Exp Mol Pathol. 2001;70(2):77-82.

98.   Taniguchi H, Shimada Y, Sawachi K, et al. Lipopolysaccharide-activated alveolar macrophages having cytotoxicity toward lung tumor cells through cell-to-cell binding-dependent mechanism. Anticancer Res. 2010;30(8):3159-65.

99.   Ostuni R, Kratochvill F, Murray PJ, et al. Macrophages and cancer: from mechanisms to therapeutic implications. Trends Immunol. 2015;36(4):229-39.

100.   Majewska M, Szczepanik M. [The role of Toll-like receptors (TLR) in innate and adaptive immune responses and their function in immune response regulation]. Postepy Hig Med Dosw (Online). 2006;60:52-63.

101.   Dai F, Liu L, Che G, et al. The number and microlocalization of tumor-associated immune cells are associated with patient's survival time in non-small cell lung cancer. BMC Cancer. 2010;10:220.

102.   Mills CD. M1 and M2 Macrophages: Oracles of Health and Disease. Crit Rev Immunol. 2012;32(6):463-88.

103.   Lopez-Gonzalez JS, Avila-Moreno F, Prado-Garcia H, et al. Lung carcinomas decrease the number of monocytes/macrophages (CD14+ cells) that produce TNF-alpha. Clin Immunol. 2007;122(3):323-9.

104.   Edin S, Wikberg ML, Dahlin AM, et al. The distribution of macrophages with a M1 or M2 phenotype in relation to prognosis and the molecular characteristics of colorectal cancer. PLoS One. 2012;7(10):e47045.

105.   Edin S, Wikberg ML, Oldenborg PA, et al. Macrophages: Good guys in colorectal cancer. Oncoimmunology. 2013;2(2):e23038.

106.   Sica A, Mantovani A. Macrophage plasticity and polarization: in vivo veritas. J Clin Invest. 2012;122(3):787-95.

107.   Redente EF, Dwyer-Nield LD, Merrick DT, et al. Tumor progression stage and anatomical site regulate tumor-associated macrophage and bone marrow-derived monocyte polarization. Am J Pathol. 2010;176(6):2972-85.

108.   Dinapoli MR, Calderon CL, Lopez DM. The altered tumoricidal capacity of macrophages isolated from tumor-bearing mice is related to reduce expression of the inducible nitric oxide synthase gene. J Exp Med. 1996;183(4):1323-9.

109.   Zea AH, Rodriguez PC, Atkins MB, et al. Arginase-producing myeloid suppressor cells in renal cell carcinoma patients: a mechanism of tumor evasion. Cancer Res. 2005;65(8):3044-8.

110.   Huang M, Wang J, Lee P, et al. Human non-small cell lung cancer cells express a type 2 cytokine pattern. Cancer Res. 1995;55(17):3847-53.

111.   Chang CI, Liao JC, Kuo L. Macrophage arginase promotes tumor cell growth and suppresses nitric oxide-mediated tumor cytotoxicity. Cancer Res. 2001;61(3):1100-6.

112.   Biswas SK, Sica A, Lewis CE. Plasticity of macrophage function during tumor progression: regulation by distinct molecular mechanisms. J Immunol. 2008;180(4):2011-7.

113.   Gorrin-Rivas MJ, Arii S, Mori A, et al. Implications of human macrophage metalloelastase and vascular endothelial growth factor gene expression in angiogenesis of hepatocellular carcinoma. Ann Surg. 2000;231(1):67-73.

114.   Siziopikou KP, Ahn MC, Casey L, et al. Augmentation of impaired tumoricidal function in alveolar macrophages from lung cancer patients by cocultivation with allogeneic, but not autologous lymphocytes. Cancer Immunol Immunother. 1997;45(1):29-36.

115.   Eifuku R, Yoshimatsu T, Yoshino I, et al. Heterogeneous response patterns of alveolar macrophages from patients with lung cancer by stimulation with interferon-gamma. Jpn J Clin Oncol. 2000;30(7):295-300.

116.   Lentsch AB, Edwards MJ, Sims DE, et al. Interleukin-10 inhibits interleukin-2-induced tumor necrosis factor production but does not reduce toxicity in C3H/HeN mice. J Leukoc Biol. 1996;60(1):51-7.

117.   Dumont S, Mabondzo A, Hartmann D, et al. Study of the dependence of human monocytes and macrophages antitumoral properties upon TNF-alpha expression or release. Anticancer Res. 1990;10(4):949-54.

118.   Gatti E, Scagliotti GV, Ferrari G, et al. Blood cell redistribution in the lung after administration of recombinant human granulocyte-macrophage colony-stimulating factor. Eur Respir J. 1995;8(9):1566-71.

119.   Crohns M, Saarelainen S, Laine S, et al. Cytokines in bronchoalveolar lavage fluid and serum of lung cancer patients during radiotherapy - Association of interleukin-8 and VEGF with survival. Cytokine. 2010;50(1):30-6.

120.   Takahashi H, Ogata H, Nishigaki R, et al. Tobacco smoke promotes lung tumorigenesis by triggering IKKbeta- and JNK1-dependent inflammation. Cancer Cell. 2010;17(1):89-97.

121.   Yi H, Cho HJ, Cho SM, et al. Blockade of interleukin-6 receptor suppresses the proliferation of H460 lung cancer stem cells. Int J Oncol. 2012;41(1):310-6.

122.   De Vita F, Orditura M, Auriemma A, et al. Serum levels of interleukin-6 as a prognostic factor in advanced non-small cell lung cancer. Oncol Rep. 1998;5(3):649-52.

123.   Chang CH, Hsiao CF, Yeh YM, et al. Circulating interleukin-6 level is a prognostic marker for survival in advanced nonsmall cell lung cancer patients treated with chemotherapy. Int J Cancer. 2013;132(9):1977-85.

124.   Barthelemy-Brichant N, David JL, Bosquee L, et al. Increased TGFbeta1 plasma level in patients with lung cancer: potential mechanisms. Eur J Clin Invest. 2002;32(3):193-8.

125.   Nabioullin R, Sone S, Mizuno K, et al. Interleukin-10 is a potent inhibitor of tumor cytotoxicity by human monocytes and alveolar macrophages. J Leukoc Biol. 1994;55(4):437-42.

126.   Bogdan C, Vodovotz Y, Nathan C. Macrophage deactivation by interleukin 10. J Exp Med. 1991;174(6):1549-55.

127.   Marcinkiewicz J, Grabowska A, Bryniarski K, et al. Enhancement of CD4+ T-cell-dependent interleukin-2 production in vitro by murine alveolar macrophages: the role of leukotriene B4. Immunology. 1997;91(3):369-74.

128.   McDonald CF, Hutchinson P, Atkins RC. Delineation of pulmonary alveolar macrophage subpopulations by flow cytometry in normal subjects and in patients with lung cancer. Clin Exp Immunol. 1993;91(1):126-30.

129.   Nakahashi H, Yasumoto K, Nagashima A, et al. Antitumor activity of macrophages in lung cancer patients with special reference to location of macrophages. Cancer Res. 1984;44(12 Pt 1):5906-9.

130.   Takeo S, Yasumoto K, Nagashima A, et al. Role of tumor-associated macrophages in lung cancer. Cancer Res. 1986;46(6):3179-82.

131.   Kan-Mitchell J, Hengst JC, Kempf RA, et al. Cytotoxic activity of human pulmonary alveolar macrophages. Cancer Res. 1985;45(1):453-8.

132.   Chen XL, Huang SS, Liu K, et al. Modulatory action of endogenous and exogenous nitric oxide on survival of alveolar macrophages from normal and bleomycin-treated rats. Sheng Li Xue Bao. 2005;57(5):619-26.

133.   Lane KB, Egan B, Vick S, et al. Characterization of a rat alveolar macrophage cell line that expresses a functional mannose receptor. J Leukoc Biol. 1998;64(3):345-50.

134.   Vignaud JM, Marie B, Klein N, et al. The role of platelet-derived growth factor production by tumor-associated macrophages in tumor stroma formation in lung cancer. Cancer Res. 1994;54(20):5455-63.

135.   Chen JJ, Yao PL, Yuan A, et al. Up-regulation of tumor interleukin-8 expression by infiltrating macrophages: its correlation with tumor angiogenesis and patient survival in non-small cell lung cancer. Clin Cancer Res. 2003;9(2):729-37.

136.   Tolnay E, Kuhnen C, Voss B, et al. Expression and localization of vascular endothelial growth factor and its receptor flt in pulmonary sarcoidosis. Virchows Arch. 1998;432(1):61-5.

137.   Ogawa E, Takenaka K, Yanagihara K, et al. Clinical significance of VEGF-C status in tumour cells and stromal macrophages in non-small cell lung cancer patients. Br J Cancer. 2004;91(3):498-503.

138.   Nagai K, Betsuyaku T, Ito Y, et al. Decrease of vascular endothelial growth factor in macrophages from long-term smokers. Eur Respir J. 2005;25(4):626-33.

139.   Sasaki M, Ito T, Kashima M, et al. Erythromycin and clarithromycin modulation of growth factor-induced expression of heparanase mRNA on human lung cancer cells in vitro. Mediators Inflamm. 2001;10(5):259-67.

140.   Gorrin-Rivas MJ, Arii S, Furutani M, et al. Mouse macrophage metalloelastase gene transfer into a murine melanoma suppresses primary tumor growth by halting angiogenesis. Clin Cancer Res. 2000;6(5):1647-54.

141.   Nenan S, Boichot E, Lagente V, et al. Macrophage elastase (MMP-12): a pro-inflammatory mediator? Mem Inst Oswaldo Cruz. 2005;100 Suppl 1:167-72.

142.   Houghton AM, Grisolano JL, Baumann ML, et al. Macrophage elastase (matrix metalloproteinase-12) suppresses growth of lung metastases. Cancer Res. 2006;66(12):6149-55.

143.   Bugdayci G, Kaplan T, Sezer S, et al. Matrix metalloproteinase-9 in broncho-alveolar lavage fluid of patients with non-small cell lung cancer. Exp Oncol. 2006;28(2):169-71.

144.   Koc M, Ediger D, Budak F, et al. Matrix metalloproteinase-9 (MMP-9) elevated in serum but not in bronchial lavage fluid in patients with lung cancer. Tumori. 2006;92(2):149-54.

145.   da Hora K, Valenca SS, Porto LC. Immunohistochemical study of tumor necrosis factor-alpha, matrix metalloproteinase-12, and tissue inhibitor of metalloproteinase-2 on alveolar macrophages of BALB/c mice exposed to short-term cigarette smoke. Exp Lung Res. 2005;31(8):759-70.

146.   Proulx LI, Castonguay A, Bissonnette EY. Cytokine production by alveolar macrophages is down regulated by the alpha-methylhydroxylation pathway of 4-(methylnitrosamino)-1-(3-pyridyl)-1-butanone (NNK). Carcinogenesis. 2004;25(6):997-1003.

147.   Hodge S, Hodge G, Ahern J, et al. Smoking alters alveolar macrophage recognition and phagocytic ability: implications in chronic obstructive pulmonary disease. Am J Respir Cell Mol Biol. 2007;37(6):748-55.

148.   Dhillon NK, Murphy WJ, Filla MB, et al. Down modulation of IFN-[gamma] signaling in alveolar macrophages isolated from smokers. Toxicol Appl Pharmacol. 2009;237(1):22-8.

149.   Shaykhiev R, Krause A, Salit J, et al. Smoking-dependent reprogramming of alveolar macrophage polarization: implication for pathogenesis of chronic obstructive pulmonary disease. J Immunol. 2009;183(4):2867-83.

150.   Folkerts G, Kloek J, Muijsers RB, et al. Reactive nitrogen and oxygen species in airway inflammation. Eur J Pharmacol. 2001;429(1-3):251-62.

151.   Sharma RN, Behera D, Khanduja KL. Increased reactive oxygen species production by alveolar macrophages from malignant lobe of lung cancer patients. J Clin Biochem Nutr. 1997;22(3):183-91.

152.   Ambs S, Bennett WP, Merriam WG, et al. Vascular endothelial growth factor and nitric oxide synthase expression in human lung cancer and the relation to p53. Br J Cancer. 1998;78(2):233-9.

153.   Arias-Diaz J, Vara E, Torres-Melero J, et al. Nitrite/nitrate and cytokine levels in bronchoalveolar lavage fluid of lung cancer patients. Cancer. 1994;74(5):1546-51.

154.   Liu CY, Wang CH, Chen TC, et al. Increased level of exhaled nitric oxide and up-regulation of inducible nitric oxide synthase in patients with primary lung cancer. Br J Cancer. 1998;78(4):534-41.

155.   Kisley LR, Barrett BS, Bauer AK, et al. Genetic ablation of inducible nitric oxide synthase decreases mouse lung tumorigenesis. Cancer Res. 2002;62(23):6850-6.

156.   Rao CV, Indranie C, Simi B, et al. Chemopreventive properties of a selective inducible nitric oxide synthase inhibitor in colon carcinogenesis, administered alone or in combination with celecoxib, a selective cyclooxygenase-2 inhibitor. Cancer Res. 2002;62(1):165-70.

157.   Klimp AH, de Vries EG, Scherphof GL, et al. A potential role of macrophage activation in the treatment of cancer. Crit Rev Oncol Hematol. 2002;44(2):143-61.

158.   Sica A, Larghi P, Mancino A, et al. Macrophage polarization in tumour progression. Semin Cancer Biol. 2008;18(5):349-55.

159.   Zeni E, Mazzetti L, Miotto D, et al. Macrophage expression of interleukin-10 is a prognostic factor in nonsmall cell lung cancer. Eur Respir J. 2007;30(4):627-32.

160.   Zeisberger SM, Odermatt B, Marty C, et al. Clodronate-liposome-mediated depletion of tumour-associated macrophages: a new and highly effective antiangiogenic therapy approach. Br J Cancer. 2006;95(3):272-81.

161.   Sica A. Role of tumour-associated macrophages in cancer-related inflammation. Exp Oncol. 2010;32(3):153-8.

162.   Tang X, Mo C, Wang Y, et al. Anti-tumour strategies aiming to target tumour-associated macrophages. Immunology. 2013;138(2):93-104.

163.   Luo Y, Zhou H, Krueger J, et al. Targeting tumor-associated macrophages as a novel strategy against breast cancer. J Clin Invest. 2006;116(8):2132-41.

164.   Werno C, Menrad H, Weigert A, et al. Knockout of HIF-1alpha in tumor-associated macrophages enhances M2 polarization and attenuates their pro-angiogenic responses. Carcinogenesis. 2010;31(10):1863-72.

165.   Ikeda S, Yanai N, Ishikawa S. Flexible bronchofiberscope. Keio J Med. 1968;17(1):1-16.

166.   Rennard SI, Spurzem JR. Bronchoalveolar lavage in the diagnosis of lung cancer. Chest. 1992;102(2):331-2.

167.   Somu N, Vijayasekaran D, Subramanyam L, et al. Flexible fiberoptic bronchoscopy. Indian J Pediatr. 1996;63(2):171-80.

168.   Pirozynski M. Bronchoalveolar lavage in the diagnosis of peripheral, primary lung cancer. Chest. 1992;102(2):372-4.

169.   Collins AM, Rylance J, Wootton DG, et al. Bronchoalveolar lavage (BAL) for research; obtaining adequate sample yield. J Vis Exp. 2014(85).

170.   Meyer KC. The role of bronchoalveolar lavage in interstitial lung disease. Clin Chest Med. 2004;25(4):637-49, v.

171.   Arbini AA. Methods in Molecular Biology: Flow Cytometry Protocols, Second Edition: Teresa S. Hawley, Robert G. Hawley (Eds.), Humana Press, 17 March 2004, 434 pp. Leukemia research. 2005;29(1):109-10.

172.   Daigneault M, Preston JA, Marriott HM, et al. The identification of markers of macrophage differentiation in PMA-stimulated THP-1 cells and monocyte-derived macrophages. PLoS One. 2010;5(1):e8668.

173.   Fuhrmann S, Streitz M, Kern F. How flow cytometry is changing the study of TB immunology and clinical diagnosis. Cytometry A. 2008;73(11):1100-6.

174.   Ricci G, Presani G, Guaschino S, et al. Leukocyte detection in human semen using flow cytometry. Hum Reprod. 2000;15(6):1329-37.

175.   Ferris MM, Yan X, Habbersett RC, et al. Performance assessment of DNA fragment sizing by high-sensitivity flow cytometry and pulsed-field gel electrophoresis. J Clin Microbiol. 2004;42(5):1965-76.

176.   UyBico SJ, Wu CC, Suh RD, et al. Lung cancer staging essentials: the new TNM staging system and potential imaging pitfalls. Radiographics. 2010;30(5):1163-81.

177.   Boyum A. Isolation of mononuclear cells and granulocytes from human blood. Isolation of monuclear cells by one centrifugation, and of granulocytes by combining centrifugation and sedimentation at 1 g. Scand J Clin Lab Invest Suppl. 1968;97:77-89.

178. Zawada AM, Rogacev KS, Schirmer SH, et al. Monocyte heterogeneity in human cardiovascular disease. Immunobiology. 2012;217(12):1273-84.

179. Lechner MG, Megiel C, Russell SM, et al. Functional characterization of human Cd33+ and Cd11b+ myeloid-derived suppressor cell subsets induced from peripheral blood mononuclear cells co-cultured with a diverse set of human tumor cell lines. J Transl Med. 2011;9:90.

180. Mytar B, Siedlar M, Woloszyn M, et al. Cross-talk between human monocytes and cancer cells during reactive oxygen intermediates generation: the essential role of hyaluronan. Int J Cancer. 2001;94(5):727-32.

181. Sanchez-Torres C, Garcia-Romo GS, Cornejo-Cortes MA, et al. CD16+ and CD16- human blood monocyte subsets differentiate in vitro to dendritic cells with different abilities to stimulate CD4+ T cells. Int Immunol. 2001;13(12):1571-81.

182. Gower RM, Wu H, Foster GA, et al. CD11c/CD18 expression is upregulated on blood monocytes during hypertriglyceridemia and enhances adhesion to vascular cell adhesion molecule-1. Arterioscler Thromb Vasc Biol. 2011;31(1):160-6.

183. Wahlstrom J, Berlin M, Skold CM, et al. Phenotypic analysis of lymphocytes and monocytes/macrophages in peripheral blood and bronchoalveolar lavage fluid from patients with pulmonary sarcoidosis. Thorax. 1999;54(4):339-46.

184. Moniuszko M, Kowal K, Rusak M, et al. Monocyte CD163 and CD36 expression in human whole blood and isolated mononuclear cell samples: influence of different anticoagulants. Clin Vaccine Immunol. 2006;13(6):704-7.

185. Meyer KC, Raghu G, Baughman RP, et al. An official American Thoracic Society clinical practice guideline: the clinical utility of bronchoalveolar lavage cellular analysis in interstitial lung disease. Am J Respir Crit Care Med. 2012;185(9):1004-14.

186. Boersema PJ, Raijmakers R, Lemeer S, et al. Multiplex peptide stable isotope dimethyl labeling for quantitative proteomics. Nat Protoc. 2009;4(4):484-94.

187. Moncunill G, Aponte JJ, Nhabomba AJ, et al. Performance of multiplex commercial kits to quantify cytokine and chemokine responses in culture supernatants from Plasmodium falciparum stimulations. PLoS One. 2013;8(1):e52587.

188. Richens JL, Urbanowicz RA, Metcalf R, et al. Quantitative validation and comparison of multiplex cytokine kits. J Biomol Screen. 2010;15(5):562-8.

189. Tighe P, Negm O, Todd I, et al. Utility, reliability and reproducibility of immunoassay multiplex kits. Methods. 2013;61(1):23-9.

190. Takigawa N, Segawa Y, Mandai K, et al. Serum CD44 levels in patients with non-small cell lung cancer and their relationship with clinicopathological features. Lung Cancer. 1997;18(2):147-57.

191. Imamura Y, Yokoyama T, Takesue Y, et al. The TH1/TH2 ratio in patients with diminished expression of HLA-DR on monocytes. Int Congr Ser 2003;1255(0):225-9.

192. Hiraki A, Kaneshige T, Kiura K, et al. Loss of HLA haplotype in lung cancer cell lines: implications for immunosurveillance of altered HLA class I/II phenotypes in lung cancer. Clin Cancer Res. 1999;5(4):933-6.

193. Soares-Schanoski A, Jurado T, Cordoba R, et al. Impaired antigen presentation and potent phagocytic activity identifying tumor-tolerant human monocytes. Biochem Biophys Res Commun. 2012;423(2):331-7.

194. Loercher AE, Nash MA, Kavanagh JJ, et al. Identification of an IL-10-producing HLA-DR-negative monocyte subset in the malignant ascites of patients with ovarian carcinoma that inhibits cytokine protein expression and proliferation of autologous T cells. J Immunol. 1999;163(11):6251-60.

195. Lovren F, Pan Y, Quan A, et al. Adiponectin primes human monocytes into alternative anti-inflammatory M2 macrophages. Am J Physiol Heart Circ Physiol. 2010;299(3):H656-63.

196. Huh HY, Pearce SF, Yesner LM, et al. Regulated expression of CD36 during monocyte-to-macrophage differentiation: potential role of CD36 in foam cell formation. Blood. 1996;87(5):2020-8.

197. Sugai H, Kono K, Takahashi A, et al. Characteristic alteration of monocytes with increased intracellular IL-10 and IL-12 in patients with advanced-stage gastric cancer. J Surg Res. 2004;116(2):277-87.

198. Ahn GO, Tseng D, Liao CH, et al. Inhibition of Mac-1 (CD11b/CD18) enhances tumor response to radiation by reducing myeloid cell recruitment. Proc Natl Acad Sci U S A. 2010;107(18):8363-8.

199.   Cifarelli V, Libman IM, Deluca A, et al. Increased Expression of Monocyte CD11b (Mac-1) in Overweight Recent-Onset Type 1 Diabetic Children. Rev Diabet Stud. 2007;4(2):112-7.

200.   Srivastava MK, Zhu L, Harris-White M, et al. Myeloid suppressor cell depletion augments antitumor activity in lung cancer. PLoS One. 2012;7(7):e40677.

201.   Habashy HO, Powe DG, Staka CM, et al. Transferrin receptor (CD71) is a marker of poor prognosis in breast cancer and can predict response to tamoxifen. Breast Cancer Res Treat. 2010;119(2):283-93.

202.   Dowlati A, Loo M, Bury T, et al. Soluble and cell-associated transferrin receptor in lung cancer. Br J Cancer. 1997;75(12):1802-6.

203.   Whitney JF, Clark JM, Griffin TW, et al. Transferrin receptor expression in nonsmall cell lung cancer. Histopathologic and clinical correlates. Cancer. 1995;76(1):20-5.

204.   Guo YJ, Liu G, Wang X, et al. Potential use of soluble CD44 in serum as indicator of tumor burden and metastasis in patients with gastric or colon cancer. Cancer Res. 1994;54(2):422-6.

205.   Kan M, Kanayama H, Naruo S, et al. Serological evaluation of soluble CD44 in renal cancer. Jpn J Cancer Res. 1996;87(11):1191-4.

206.   Belardelli F, Ferrantini M. Cytokines as a link between innate and adaptive antitumor immunity. Trends Immunol. 2002;23(4):201-8.

207.   Romagnani S. Biology of human TH1 and TH2 cells. J Clin Immunol. 1995;15(3):121-9.

208.   Romagnani S. Th1 and Th2 in human diseases. Clin Immunol Immunopathol. 1996;80(3 Pt 1):225-35.

209.   Gursel G, Gokcora N, Elbeg S, et al. Tumor necrosis factor-alpha (TNF-alpha) in pleural fluids. Tuber Lung Dis. 1995;76(4):370-1.

210.   Juarez E, Nunez C, Sada E, et al. Differential expression of Toll-like receptors on human alveolar macrophages and autologous peripheral monocytes. Respir Res. 2010;11:2.

211.   Waugh DJ, Wilson C. The interleukin-8 pathway in cancer. Clin Cancer Res. 2008;14(21):6735-41.

212.   Apte RN, Dotan S, Elkabets M, et al. The involvement of IL-1 in tumorigenesis, tumor invasiveness, metastasis and tumor-host interactions. Cancer Metastasis Rev. 2006;25(3):387-408.

213.   Millar HJ, Nemeth JA, McCabe FL, et al. Circulating human interleukin-8 as an indicator of cancer progression in a nude rat orthotopic human non-small cell lung carcinoma model. Cancer Epidemiol Biomarkers Prev. 2008;17(8):2180-7.

214.   Culig Z. Cytokine disbalance in common human cancers. Biochim Biophys Acta. 2011;1813(2):308-14.

215.   Albulescu R, Codrici E, Popescu ID, et al. Cytokine Patterns in Brain Tumour Progression. Mediators Inflamm. 2013;2013:7.

216.   Pellegrini P, Contasta I, Del Beato T, et al. Gender-specific cytokine pathways, targets, and biomarkers for the switch from health to adenoma and colorectal cancer. Clin Dev Immunol. 2011:819724.

217.   Schuurs AH, Verheul HA. Effects of gender and sex steroids on the immune response. J Steroid Biochem. 1990;35(2):157-72.

218.   Hussell T, Bell TJ. Alveolar macrophages: plasticity in a tissue-specific context. Nat Rev Immunol. 2014;14(2):81-93.

219.   Edwards JP, Zhang X, Frauwirth KA, et al. Biochemical and functional characterization of three activated macrophage populations. J Leukoc Biol. 2006;80(6):1298-307.

220.   Chyczewska E, Mroz RM. Cytokines in lung cancer. Rocz Akad Med Bialymst. 1997;42 Suppl 1:8-22.

221.   Chen L, Li Q, Zhou XD, et al. Increased pro-angiogenic factors, infiltrating neutrophils and CD163 macrophages in bronchoalveolar lavage fluid from lung cancer patients. Int Immunopharmacol. 2014;20(1):74-80.

222.   Biswas SK, Mantovani A. Macrophage plasticity and interaction with lymphocyte subsets: cancer as a paradigm. Nat Immunol. 2010;11(10):889-96.

223.   Lloyd CM, Phillips AR, Cooper GJ, et al. Three-colour fluorescence immunohistochemistry reveals the diversity of cells staining for macrophage markers in murine spleen and liver. J Immunol Methods. 2008;334(1-2):70-81.

224.   Bratke K, Lommatzsch M, Julius P, et al. Dendritic cell subsets in human bronchoalveolar lavage fluid after segmental allergen challenge. Thorax. 2007;62(2):168-75.

225.   Gatter KC, Brown G, Trowbridge IS, et al. Transferrin receptors in human tissues: their distribution and possible clinical relevance. J Clin Pathol. 1983;36(5):539-45.

226.   Kondo K, Noguchi M, Mukai K, et al. Transferrin receptor expression in adenocarcinoma of the lung as a histopathologic indicator of prognosis. Chest. 1990;97(6):1367-71.

227.   Naor D, Nedvetzki S, Golan I, et al. CD44 in cancer. Crit Rev Clin Lab Sci. 2002;39(6):527-79.

228.   Matsubara Y, Katoh S, Taniguchii H, et al. Expression of CD44 variants in lung cancer and its relationship to hyaluronan binding. J Int Med Res. 2000;28(2):78-90.

229.   Jaggupilli A, Elkord E. Significance of CD44 and CD24 as cancer stem cell markers: an enduring ambiguity. Clin Dev Immunol. 2012;2012:708036.

230.   Penno MB, August JT, Baylin SB, et al. Expression of CD44 in human lung tumors. Cancer Res. 1994;54(5):1381-7.

231.   Leung EL, Fiscus RR, Tung JW, et al. Non-small cell lung cancer cells expressing CD44 are enriched for stem cell-like properties. PLoS One. 2010;5(11):e14062.

232.   Wang R, Zhang J, Chen S, et al. Tumor-associated macrophages provide a suitable microenvironment for non-small lung cancer invasion and progression. Lung Cancer. 2011;74(2):188-96.

233.   Kerr KM. Pulmonary adenocarcinomas: classification and reporting. Histopathology. 2009;54(1):12-27.

234.   Devesa SS, Bray F, Vizcaino AP, et al. International lung cancer trends by histologic type: male:female differences diminishing and adenocarcinoma rates rising. Int J Cancer. 2005;117(2):294-9.

235.   Zhou X, Xue L, Hao L, et al. Proteomics-based identification of tumor relevant proteins in lung adenocarcinoma. Biomed Pharmacother. 2013;67(7):621-7.

236.   Cecconi D, Zamò A. Proteomics of human cancer tissues and cells. TrAC Trends in Analytical Chemistry. 2011;30(2):346-59.

237.   Ahmad Y, Lamond AI. A perspective on proteomics in cell biology. Trends Cell Biol. 2014;24(4):257-64.

238.   Okamoto T, Miyazaki Y, Shirahama R, et al. Proteome analysis of bronchoalveolar lavage fluid in chronic hypersensitivity pneumonitis. Allergol Int. 2012;61(1):83-92.

239.   Pastor MD, Nogal A, Molina-Pinelo S, et al. Identification of proteomic signatures associated with lung cancer and COPD. J Proteomics. 2013;89:227-37.

240.   Ohlmeier S, Vuolanto M, Toljamo T, et al. Proteomics of human lung tissue identifies surfactant protein A as a marker of chronic obstructive pulmonary disease. J Proteome Res. 2008;7(12):5125-32.

241.   Wattiez R, Hermans C, Cruyt C, et al. Human bronchoalveolar lavage fluid protein two-dimensional database: study of interstitial lung diseases. Electrophoresis. 2000;21(13):2703-12.

242.   Bai Y, Galetskiy D, Damoc E, et al. High resolution mass spectrometric alveolar proteomics: identification of surfactant protein SP-A and SP-D modifications in proteinosis and cystic fibrosis patients. Proteomics. 2004;4(8):2300-9.

243.   Dooms C, Muylle I, Yserbyt J, et al. Endobronchial ultrasound in the management of nonsmall cell lung cancer. Eur Respir Rev. 2013;22(128):169-77.

244.   Noel-Georis I, Bernard A, Falmagne P, et al. Database of bronchoalveolar lavage fluid proteins. J Chromatogr B Analyt Technol Biomed Life Sci. 2002;771(1-2):221-36.

245.   Nguyen EV, Gharib SA, Schnapp LM, et al. Shotgun MS proteomic analysis of bronchoalveolar lavage fluid in normal subjects. Proteomics Clin Appl. 2014;8(9-10):737-47.

246.   Travis WD, Brambilla E, Riely GJ. New pathologic classification of lung cancer: relevance for clinical practice and clinical trials. J Clin Oncol. 2013;31(8):992-1001.

247.   Charloux A, Quoix E, Wolkove N, et al. The increasing incidence of lung adenocarcinoma: reality or artefact? A review of the epidemiology of lung adenocarcinoma. Int J Epidemiol. 1997;26(1):14-23.

248.   Wu J, Kobayashi M, Sousa EA, et al. Differential proteomic analysis of bronchoalveolar lavage fluid in asthmatics following segmental antigen challenge. Mol Cell Proteomics. 2005;4(9):1251-64.

249.   Waldburg N, Kahne T, Reisenauer A, et al. Clinical proteomics in lung diseases. Pathol Res Pract. 2004;200(2):147-54.

250. Planque C, Kulasingam V, Smith CR, et al. Identification of five candidate lung cancer biomarkers by proteomics analysis of conditioned media of four lung cancer cell lines. Mol Cell Proteomics. 2009;8(12):2746-58.

251. Lihong H, Linlin G, Yiping G, et al. Proteomics Approaches for Identification of Tumor Relevant Protein Targets in Pulmonary Squamous Cell Carcinoma by 2D-DIGE-MS. PLoS One. 2014;9(4):e95121.

252. Su YJ, Xu F, Yu JP, et al. Up-regulation of the expression of S100A8 and S100A9 in lung adenocarcinoma and its correlation with inflammation and other clinical features. Chin Med J (Engl). 2010;123(16):2215-20.

253. Wang C, Xiao Q, Li YW, et al. Regulatory mechanisms of annexin-induced chemotherapy resistance in Cisplatin resistant lung adenocarcinoma. Asian Pac J Cancer Prev. 2014;15(7):3191-4.

254. Brockenbrough JS, Morihara JK, Hawes SE, et al. Thymidine kinase 1 and thymidine phosphorylase expression in non-small-cell lung carcinoma in relation to angiogenesis and proliferation. J Histochem Cytochem. 2009;57(11):1087-97.

255. Choi CM, Jang SJ, Park SY, et al. Transglutaminase 2 as an independent prognostic marker for survival of patients with non-adenocarcinoma subtype of non-small cell lung cancer. Mol Cancer. 2011;10:119.

256. Darby IA, Vuillier-Devillers K, Pinault E, et al. Proteomic analysis of differentially expressed proteins in peripheral cholangiocarcinoma. Cancer Microenviron. 2010;4(1):73-91.

257. Kwon CH, Moon HJ, Park HJ, et al. S100A8 and S100A9 promotes invasion and migration through p38 mitogen-activated protein kinase-dependent NF-kappaB activation in gastric cancer cells. Mol Cells. 2013;35(3):226-34.

258. Fritz G, Botelho HM, Morozova-Roche LA, et al. Natural and amyloid self-assembly of S100 proteins: structural basis of functional diversity. Febs j. 2010;277(22):4578-90.

259. Lorenz E, Muhlebach MS, Tessier PA, et al. Different expression ratio of S100A8/A9 and S100A12 in acute and chronic lung diseases. Respir Med. 2008;102(4):567-73.

260. Gebhardt C, Nemeth J, Angel P, et al. S100A8 and S100A9 in inflammation and cancer. Biochem Pharmacol. 2006;72(11):1622-31.

261. Mirza Z, Schulten HJ, Farsi HM, et al. Impact of S100A8 expression on kidney cancer progression and molecular docking studies for kidney cancer therapeutics. Anticancer Res. 2014;34(4):1873-84.

262. McKiernan E, McDermott EW, Evoy D, et al. The role of S100 genes in breast cancer progression. Tumour Biol. 2011;32(3):441-50.

263. Mussunoor S, Murray GI. The role of annexins in tumour development and progression. J Pathol. 2008;216(2):131-40.

264. Jia JW, Li KL, Wu JX, et al. Clinical significance of annexin II expression in human non-small cell lung cancer. Tumour Biol. 2013;34(3):1767-71.

265. Wang W, Guan S, Sun S, et al. Detection of circulating antibodies to linear peptide antigens derived from ANXA1 and DDX53 in lung cancer. Tumour Biol. 2014;35(5):4901-5.

266. Biaoxue R, Xiling J, Shuanying Y, et al. Upregulation of Hsp90-beta and annexin A1 correlates with poor survival and lymphatic metastasis in lung cancer patients. J Exp Clin Cancer Res. 2012;31:70.

267. Sato J, Sata M, Nakamura H, et al. Role of thymidine phosphorylase on invasiveness and metastasis in lung adenocarcinoma. Int J Cancer. 2003;106(6):863-70.

268. Tertil M, Skrzypek K, Florczyk U, et al. Regulation and Novel Action of Thymidine Phosphorylase in Non-Small Cell Lung Cancer: Crosstalk with Nrf2 and HO-1. PLoS One. 2014;9(5):e97070.

269. Kojima H, Shijubo N, Abe S. Thymidine phosphorylase and vascular endothelial growth factor in patients with Stage I lung adenocarcinoma. Cancer. 2002;94(4):1083-93.

270. Han JY, Hong EK, Lee SY, et al. Thymidine phosphorylase expression in tumour cells and tumour response to capecitabine plus docetaxel chemotherapy in non-small cell lung cancer. J Clin Pathol. 2005;58(6):650-4.

271. Chujo M, Miura T, Kawano Y, et al. Thymidine phosphorylase levels and dihydropyrimidine dehydrogenase levels in non-small cell lung cancer tissues. Oncol Rep. 2006;16(4):777-80.

272. Hwang JY, Mangala LS, Fok JY, et al. Clinical and biological significance of tissue transglutaminase in ovarian carcinoma. Cancer Res. 2008;68(14):5849-58.

273.   Mangala LS, Fok JY, Zorrilla-Calancha IR, et al. Tissue transglutaminase expression promotes cell attachment, invasion and survival in breast cancer cells. Oncogene. 2007;26(17):2459-70.

274.   Jeong JH, Cho BC, Shim HS, et al. Transglutaminase 2 expression predicts progression free survival in non-small cell lung cancer patients treated with epidermal growth factor receptor tyrosine kinase inhibitor. J Korean Med Sci. 2013;28(7):1005-14.

275.   Park KS, Kim HK, Lee JH, et al. Transglutaminase 2 as a cisplatin resistance marker in non-small cell lung cancer. J Cancer Res Clin Oncol. 2010;136(4):493-502.

276.   Carlini MJ, Roitman P, Nuñez M, et al. Clinical relevance of galectin-1 expression in non-small cell lung cancer patients. Lung Cancer. 2014;84(1):73-8.

277.   Rho JH, Roehrl MH, Wang JY. Tissue proteomics reveals differential and compartment-specific expression of the homologs transgelin and transgelin-2 in lung adenocarcinoma and its stroma. J Proteome Res. 2009;8(12):5610-8.

278.   Sun S, Xu MZ, Poon RT, et al. Circulating Lamin B1 (LMNB1) biomarker detects early stages of liver cancer in patients. J Proteome Res. 2010;9(1):70-8.

279.   Zhou R, Huang W, Yao Y, et al. CA II, a potential biomarker by proteomic analysis, exerts significant inhibitory effect on the growth of colorectal cancer cells. Int J Oncol. 2013;43(2):611-21.

280.   Liu LC, Xu WT, Wu X, et al. Overexpression of carbonic anhydrase II and Ki-67 proteins in prognosis of gastrointestinal stromal tumors. World J Gastroenterol. 2013;19(16):2473-80.

281.   Kon-no H, Ishii G, Nagai K, et al. Carbonic anhydrase IX expression is associated with tumor progression and a poor prognosis of lung adenocarcinoma. Lung Cancer. 2006;54(3):409-18.

282.   Kang SY, Halvorsen OJ, Gravdal K, et al. Prosaposin inhibits tumor metastasis via paracrine and endocrine stimulation of stromal p53 and Tsp-1. Proc Natl Acad Sci U S A. 2009;106(29):12115-20.

283.   Ding Z, Joy M, Bhargava R, et al. Profilin-1 downregulation has contrasting effects on early vs late steps of breast cancer metastasis. Oncogene. 2014;33(16):2065-74.

284.   Zoidakis J, Makridakis M, Zerefos PG, et al. Profilin 1 is a potential biomarker for bladder cancer aggressiveness. Mol Cell Proteomics. 2012;11(4):M111.009449.

285. Govender P, Dunn MJ, Donnelly SC. Proteomics and the lung: Analysis of bronchoalveolar lavage fluid. Proteomics Clin Appl. 2009;3(9):1044-51.

286. Shih J-Y, Yuan A, Chen JJ-W, et al. Tumor-associated macrophage: its role in cancer invasion and metastasis. J Cancer Mol. 2006;2(3):101-6.

287. Lewis CE, Pollard JW. Distinct role of macrophages in different tumor microenvironments. Cancer Res. 2006;66(2):605-12.

288. Dirkx AE, Oude Egbrink MG, Wagstaff J, et al. Monocyte/macrophage infiltration in tumors: modulators of angiogenesis. J Leukoc Biol. 2006;80(6):1183-96.

289. Lamagna C, Aurrand-Lions M, Imhof BA. Dual role of macrophages in tumor growth and angiogenesis. J Leukoc Biol. 2006;80(4):705-13.

290. Quatromoni JG, Eruslanov E. Tumor-associated macrophages: function, phenotype, and link to prognosis in human lung cancer. Am J Transl Res. 2012;4(4):376-89.

291. Welsh TJ, Green RH, Richardson D, et al. Macrophage and mast-cell invasion of tumor cell islets confers a marked survival advantage in non-small-cell lung cancer. J Clin Oncol. 2005;23(35):8959-67.

292. Ohtaki Y, Ishii G, Nagai K, et al. Stromal macrophage expressing CD204 is associated with tumor aggressiveness in lung adenocarcinoma. J Thorac Oncol. 2010;5(10):1507-15.

293. Ohri CM, Shikotra A, Green RH, et al. The Tissue Microlocalisation and Cellular Expression of CD163, VEGF, HLA-DR, iNOS, and MRP 8/14 Is Correlated to Clinical Outcome in NSCLC. PLoS ONE. 2011;6(7):e21874.

294. Toomey D, Smyth G, Condron C, et al. Infiltrating immune cells, but not tumour cells, express FasL in non-small cell lung cancer: No association with prognosis identified in 3-year follow-up. Int J Cancer. 2003;103(3):408-12.

295. Tataroglu C, Kargi A, Ozkal S, et al. Association of macrophages, mast cells and eosinophil leukocytes with angiogenesis and tumor stage in non-small cell lung carcinomas (NSCLC). Lung Cancer. 2004;43(1):47-54.

296. Ma J, Liu L, Che G, et al. The M1 form of tumor-associated macrophages in non-small cell lung cancer is positively associated with survival time. BMC Cancer. 2010;10:112.

297.   Biswas SK, Gangi L, Paul S, et al. A distinct and unique transcriptional program expressed by tumor-associated macrophages (defective NF-kappaB and enhanced IRF-3/STAT1 activation). Blood. 2006;107(5):2112-22.

298.   Scagliotti GV, Parikh P, von Pawel J, et al. Phase III study comparing cisplatin plus gemcitabine with cisplatin plus pemetrexed in chemotherapy-naive patients with advanced-stage non-small-cell lung cancer. J Clin Oncol. 2008;26(21):3543-51.

299.   Zhang B, Yao G, Zhang Y, et al. M2-Polarized tumor-associated macrophages are associated with poor prognoses resulting from accelerated lymphangiogenesis in lung adenocarcinoma. Clinics. 2011;66(11):1879-86.

300.   Chung FT, Lee KY, Wang CW, et al. Tumor-associated macrophages correlate with response to epidermal growth factor receptor-tyrosine kinase inhibitors in advanced non-small cell lung cancer. Int J Cancer. 2012;131(3):E227-35.

Chapter 9 Appendices

Appendix A: Additional tables

Table 13: **A list of the molecular functions that were found using proteomics technique**

No.	Molecular functions	Percentage
1	Protein binding	28.42%
2	Catalytic activity	22.06%
3	Nucleotide binding	10.72%
4	Metal ion binding	9.07%
5	RNA binding	5.36%
6	Transporter activity	4.66%
7	No annotation available	4.53%
8	Structural molecule activity	4.10%
9	Enzyme regulator activity	2.75%
10	DNA binding	2.44%
11	Signal tranducer activity	1.79%
12	Receptor activity	1.70%
13	Anti-oxidant activity	1.39%
14	Motor activity	0.78%
15	Translation regulator activity	0.17%
16	Transcription regulator activity	0.04%

Table 14: **A list of the cellular components that were found using proteomics technique**

No.	Cellular components	Percentage
1	Cytoplasm	22.55%
2	Membrane	14.44%
3	Cytosol	8.65%
4	Nucleus	8.35%
5	Extracellular	8.16%
6	Organelle lumen	7.87%
7	Mitochondrion	6.52%
8	Cytoskeleton	3.96%
9	Endoplasmic reticulum	3.85%
10	No annotation available	3.07%
11	Vacuole	2.96%
12	Golgi	2.69%
13	Endosome	2.13%
14	Cell surface	1.46%
15	Ribosome	1.40%
16	Chromosome	0.75%
17	Proteasome	0.65%
18	Spliceosomal complex	0.51%

Table 15: **A list of the biological processes that were found using proteomics technique**

No.	Biological process	Percentage
1	Metabolic process	18.59%
2	Regulation of biological process	12.56%
3	Responose to stimulus	12.42%
4	Transport	9.44%
5	Cell organization and biogenesis	9.17%
6	Cell communication	7.47%
7	Development	5.32%
8	Cell death	4.07%
9	Defence response	3.78%
10	Cell differentiation	3.34%
11	Cellular component movement	2.85%
12	No annotation available	2.63%
13	Cell proliferation	2.34%
14	Cellular homeostasis	1.83%
15	Coagulation	1.68%
16	Reproduction	1.15%
17	Cell division	0.68%
18	Cell growth	0.66%

Table 16: **A list of all BAL fluid and blood processed samples with the diagnosis and stages**

Subject ID	Small cell carcinoma	Non-small cell carcinoma	Squamous cell	Adenocarcinoma	Large cell	Infection	Negative	Control	Stage	GOLD
1	0	0	0	0	0	0	1	1		0
2	0	0	0	0	0	0	1	0	3B	4
3	0	1	0	0	0	0	1	0	1A	2
4	0	0	1	0	0	0	0	0	2B	0
5	0	0	0	0	0	0	1	1		0
6	0	1	0	0	0	0	1	0	3A	0
7	0	0	0	0	0	0	1	1		2
8	0	0	0	0	0	0	1	1		Not tested
9	0	0	0	0	0	0	1	1		2
10	0	0	0	0	0	0	1	1		0
11	0	0	0	1	0	0	0	0		0
12	0	0	0	0	0	0	1	1		0
13	0	0	1	0	0	0	0	0	3B	Not tested
14	0	0	0	0	0	0	1	0	1B	0

15	0	0	0	0	0	0	1	1		0
16	0	0	0	0	0	0	1	1		1
17	0	0	0	0	0	0	1	1		1
18	0	0	0	0	0	0	1	1		2
19	0	0	0	1	0	0	0	Metastasis from Renal Carcinoma		Not tested
20	0	0	0	0	0	0	1	1		1
21	0	0	0	0	0	0	1	1		Not tested
22	0	0	0	0	0	0	1	0	1A	0
23	0	0	0	0	0	0	1	1		Not tested
24	0	0	0	0	0	0	1	1		0
25	0	0	0	0	1	0	0	0	4	Not tested
26	0	0	1	0	0	0	0	0	4	0
27	0	0	0	0	0	1	0	0		1
28	0	0	1	0	0	0	0	0		Not tested
29	0	1	0	0	0	1	1	0	1A	2
30	0	0	0	0	0	0	1	1		0
31	0	0	0	1	0	0	0	0	4	2

32	0	0	0	0	0	0	1	1		Not tested
33	0	0	0	0	0	0	1	1		Not tested
34	0	0	0	0	0	0	1	1		0
35	0	0	0	0	0	0	1	1		3
36	0	0	0	0	0	0	1	1		Not tested
37	0	0	0	0	0	0	1	1		Not tested
38	0	0	0	0	0	0	1	1		0
39	0	1	0	0	0	0	0	0	4	3
40	0	0	0	0	0	0	1	1		0
41	0	0	0	1	0	0	1	0	2A	0
42	0	1	0	1	0	0	0	Breast Ca Metastisis		1
43	0	0	0	0	0	0	1	0	3B	0
44	0	1	1	0	0	0	0	0	4	0
45	0	1	0	1	0	0	0	0	4	Not tested
46	0	1	0	1	0	0	0	0	2A	0
47	0	0	0	0	0	0	1	1		2
48	0	0	0	0	0	0	1	1		3
49	0	0	1	0	0	0	0	0	3A	2

50	0	0	0	0	0	0	0			2
51	0	0	0	0	0	0	1			2
52	0	0	0	0	0	0	0			3
53	0	0	0	1	0	0	0	0	1A	4
54	0	0	0	0	0	0	1	1		Not tested
55	0	0	0	1	0	0	0	0	4	3
56	0	0	1	0	0	0	0	0	3A	2
57	0	1	1	0	0	0	0	0	1A	2
58	0	0	0	0	0	0	1	0		0
59	0	0	0	1	0	0	0	0	4	3
60	0	0	1	0	0	0	0	0	4	Not tested
61	0	1	0	1	0	0	0	0	4	0
62	0	1	0	1	0	0	0	0	4	2
63	0	0	0	0	0	0	1			0
64	0	0	0	1	0	0	0	0	4	4
65	0	0	1	0	0	0	0	0	3A	2
66	0	0	0	0	0	1	0	1		2
67	0	0	1	0	0	0	0	0	4	1
68	0	0	1	0	0	0	0	0	3A	0

69	0	0	0	0	0	0	1	1		Not tested
70	0	1	0	1	0	0	0	0	1B	1
71	0	1	1	0	0	0	0	0	2A	0
72	0	0	1	0	0	0	0	0	4	2
73	0	1	0	1	0	0	0	0	4	0

Table 17: **A list of all BAL fluid and blood processed samples with age, smoking, cough, haemoptysis and malignancy data**

Subject ID	Age	Smoker	Ex-smoker	Never smoked	Cigarettes per day	Smoking years	Pack-years	Cough	Haemoptysis	Malignancy
1	18	1	0	0	7	2	0.7	1	0	0
2	67	0	1	0			50	0	0	1
3	81	0	1	0			75	0	0	1
4	70	0	1	0			40	0	0	1
5	44	0	0	1			0	0	1	0
6	65	1	0	0	15	30	22.5	0	0	1
7	75	0	1	0	40	50	100	0	1	0
8	77	0	0	1	0	0	0	0	0	1
9	71	0	1	0	50	55	137.5	0	0	1
10	80	0	0	1	0	0	0	1	0	0
11	73	1	0	0	2		10	0	0	1
12	48	0	1	0			25	0	1	0
13	73	0	0	1	0	0	0	0	0	1
14	75	1	0	0	30	63	94.5	0	0	1

15	38	0	0	1	0	0	0	0	0	1
16	64	0	0	1	0	0	0	0	1	1
17	66	0	1	0	0		56	0	1	1
18	60	1	0	0	10		63	0	0	1
19	67	0	0	1	0	0	0	1	0	1
20	69	0	1	0			20	0	0	1
21	60	0	1	0			38	0	1	0
22	73	0	1	0	10	50	25	0	0	1
23	40	0	0	1	0	0	0	1	0	0
24	63	1	0	0	6	24	7.2	0	0	1
25	55	0	1	0			15	0	0	1
26	63	0	1	0			50	0	1	1
27	81	0	1	0			60	0	0	1
28	54	0	1	0			35	0	0	1
29	72	0	1	0	0	0	44	0	0	1
30	39	0	1	0			5	1	0	0
31	74	1	0	0	12	60	36	0	0	1
32	26	0	0	1	0	0	0	1	1	0
33	55	0	0	1	0	0	0	0	0	1

34	41	1	0	0	5		10	0	1	0
35	64	0	1	0			66	1	0	1
36	47	1	0	0	5	20	4	1	0	0
37	42	0	0	1	0	0	0	0	1	0
38	20	1	0	0	2		2	1	0	0
39	66	0	1	0	40	35	70	0	0	1
40	51	0	0	1	0	0	0	1	0	0
41	66	0	1	0			66	0	0	1
42	62	0	1	0	5	22	5	0	0	1
43	58	0	0	1	0	0	0	0	0	1
44	50	1	0	0			15	0	0	1
45	63	0	1	0				0	0	1
46	66	0	1	0			100	0	0	1
47	78	0	1	0			40	0	0	1
48	84	0	1	0				0	0	1
49	74	1	0	0			108	0	0	1
50	57	1	0	0			13	0	0	1
51	66	1	0	0	10		40	0	0	1
52	67	0	1	0			55	0	0	1

53	61	1	0	0	15	41	30.75	0	0	1
54	72	0	1	0	5	20	4	0	0	1
55	75	0	1	0			15	0	0	1
56	81	0	1	0			82.5	0	0	1
57	79	0	1	0			55	0	0	1
58	70	0	1	0			50	0	0	1
59	57	1	0	0			41.25	0	0	1
60	42	0	1	0			20	0	0	1
61	67	0	0	1	0	0	0	0	0	1
62	80	1	0	0			55	0	0	1
63	82	0	1	0			26	0	0	1
64	63	1	0	0			45	0	0	1
65	54	0	1	0			80	0	0	1
66	74	0	1	0			110	0	0	1
67	82	0	1	0			18	0	0	1
68	69	0	1	0	12	30	18	0	0	1
69	68	0	1	0			53	0	0	1
70	77	1	0	0			140	0	0	1
71	72	0	1	0			5	0	0	1

72	76	1	0	0			60	0	0	1
73	75	0	0	1	0	0	0	0	0	1

Table 18: **A list of all identified proteins in BAL fluid samples**

No.	Protein name	Description	MW [kDa]	Σ# Peptides	Σ# Unique Peptides
1	1433B_HUMAN	RecName: Full=14-3-3 protein beta/alpha; AltName: Full=Protein 1054; AltName: Full=Protein kinase C inhibitor protein 1; Short=KCIP-1; Contains: RecName: Full=14-3-3 protein beta/alpha, N-terminally processed; - OS=Homo sapiens (Human).	28.1	8	6
2	1433E_HUMAN	RecName: Full=14-3-3 protein epsilon; Short=14-3-3E; - OS=Homo sapiens (Human).	29.2	6	4
3	1433F_HUMAN	RecName: Full=14-3-3 protein eta; AltName: Full=Protein AS1; - OS=Homo sapiens (Human).	28.2	4	2
4	1433T_HUMAN	RecName: Full=14-3-3 protein theta; AltName: Full=14-3-3 protein T-cell; AltName: Full=14-3-3 protein tau; AltName: Full=Protein HS1; - OS=Homo sapiens (Human).	27.7	4	2
5	1433Z_HUMAN	RecName: Full=14-3-3 protein zeta/delta; AltName: Full=Protein kinase C inhibitor protein 1; Short=KCIP-1; - OS=Homo sapiens (Human).	27.7	7	5
6	3HIDH_HUMAN	RecName: Full=3-hydroxyisobutyrate dehydrogenase, mitochondrial; Short=HIBADH; EC=1.1.1.31; Flags: Precursor; - OS=Homo sapiens (Human).	35.3	3	3
7	6PGL_HUMAN	RecName: Full=6-phosphogluconolactonase; Short=6PGL; EC=3.1.1.31; - OS=Homo sapiens (Human).	27.5	2	2
8	A0PJ62_HUMAN	SubName: Full=RPL14 protein; Flags: Fragment; - OS=Homo sapiens (Human).	14.6	1	1
9	A1A5C5_HUMAN	SubName: Full=RRBP1 protein; - OS=Homo sapiens (Human).	84.3	4	4
10	A1AT_HUMAN	RecName: Full=Alpha-1-antitrypsin; AltName: Full=Alpha-1 protease inhibitor; AltName: Full=Alpha-1-antiproteinase; AltName: Full=Serpin A1; Contains: RecName: Full=Short peptide from AAT; Short=SPAAT; Flags: Precursor; - OS=Homo sapiens (Human).	46.7	4	4
11	A1JUI8_HUMAN	SubName: Full=Chaperonin subunit 6A; Flags: Fragment; - OS=Homo sapiens (Human).	53.6	5	4
12	A1L0W4_HUMAN	SubName: Full=CDC37 protein; SubName: Full=MBD5 protein; Flags: Fragment; - OS=Homo	12.2	1	1

		sapiens (Human).			
13	A1L172_HUMAN	SubName: Full=Acyl-CoA thioesterase 1; - OS=Homo sapiens (Human).	46.3	7	7
14	A2A2D0_HUMAN	RecName: Full=Stathmin; Flags: Fragment; - OS=Homo sapiens (Human).	9.9	2	2
15	A2A2F9_HUMAN	SubName: Full=Chromosome 20 open reading frame 3; Flags: Fragment; - OS=Homo sapiens (Human).	45.3	5	5
16	A2ACR1_HUMAN	RecName: Full=Proteasome subunit beta type; EC=3.4.25.1; - OS=Homo sapiens (Human).	20.9	2	2
17	A2BEY0_HUMAN	SubName: Full=Valyl-tRNA synthetase; Flags: Fragment; - OS=Homo sapiens (Human).	131.7	1	1
18	A2VCQ4_HUMAN	SubName: Full=PRKCSH protein; Flags: Fragment; - OS=Homo sapiens (Human).	20.3	3	2
19	A4D1R6_HUMAN	SubName: Full=Similar to 60S ribosomal protein L17 (L23) (Amino acid starvation-induced protein) (ASI); - OS=Homo sapiens (Human).	11.9	1	1
20	A4FRB6_HUMAN	SubName: Full=MHC class II antigen; Flags: Fragment; - OS=Homo sapiens (Human).	21.7	2	2
21	A4FU71_HUMAN	SubName: Full=C3orf60 protein; SubName: Full=Chromosome 3 open reading frame 60, isoform CRA_c; - OS=Homo sapiens (Human).	13.8	1	1
22	A4QPB0_HUMAN	SubName: Full=IQ motif containing GTPase activating protein 1; - OS=Homo sapiens (Human).	189.2	16	16
23	A4UCS8_HUMAN	RecName: Full=Enolase; EC=4.2.1.11; Flags: Fragment; - OS=Homo sapiens (Human).	17.8	4	1
24	A5YM50_HUMAN	SubName: Full=RAB11B protein; - OS=Homo sapiens (Human).	24.5	5	5
25	A6H8Y6_HUMAN	SubName: Full=EML4 protein; - OS=Homo sapiens (Human).	102.4	4	4
26	A6NKB8_HUMAN	SubName: Full=Aminopeptidase B; - OS=Homo sapiens (Human).	68.1	2	2
27	A6NMU3_HUMAN	SubName: Full=Signal transducing adapter molecule 1; Flags: Fragment; - OS=Homo sapiens (Human).	19.2	1	1
28	A7UMH1_HUMAN	SubName: Full=MHC class II antigen; Flags: Fragment; - OS=Homo sapiens (Human).	10.8	4	0
29	A7UP02_HUMAN	SubName: Full=MHC class II antigen; Flags: Fragment; - OS=Homo sapiens (Human).	11.0	3	0
30	A7Y9J9_HUMAN	SubName: Full=Mucin 5AC, oligomeric mucus/gel-forming; - OS=Homo sapiens (Human).	648.4	7	3
31	A8K0T9_HUMAN	SubName: Full=cDNA FLJ75422, highly similar to Homo sapiens capping protein (actin filament) muscle Z-line, alpha 1, mRNA; - OS=Homo sapiens (Human).	32.9	5	4

32	A8K2Q6_HUMAN	RecName: Full=Peptidyl-prolyl cis-trans isomerase; EC=5.2.1.8; - OS=Homo sapiens (Human).	22.7	1	1
33	A8K335_HUMAN	SubName: Full=cDNA FLJ76254, highly similar to Homo sapiens gamma-glutamyl hydrolase (GGH), mRNA; - OS=Homo sapiens (Human).	36.0	2	2
34	A8K3W4_HUMAN	SubName: Full=cDNA FLJ75163, highly similar to Homo sapiens heterogeneous nuclear ribonucleoprotein U-like 1 (HNRPUL1), transcript variant 4, mRNA; - OS=Homo sapiens (Human).	84.8	2	2
35	A8K486_HUMAN	RecName: Full=Peptidyl-prolyl cis-trans isomerase; EC=5.2.1.8; - OS=Homo sapiens (Human).	18.0	5	5
36	A8K4G3_HUMAN	SubName: Full=Tyrosine-protein kinase HCK; SubName: Full=cDNA FLJ78472, highly similar to Human hemopoietic cell protein-tyrosine kinase (HCK) gene; - OS=Homo sapiens (Human).	57.4	2	2
37	A8K4W2_HUMAN	SubName: Full=cDNA FLJ78635, highly similar to Homo sapiens ATP synthase, H+ transporting, mitochondrial F0 complex, subunit b, isoform 1 (ATP5F1), transcript variant 1, mRNA; - OS=Homo sapiens (Human).	28.9	3	3
38	A8K4W5_HUMAN	SubName: Full=cDNA FLJ76813, highly similar to Homo sapiens acetyl-Coenzyme A acetyltransferase 2 (acetoacetyl Coenzyme A thiolase), mRNA; - OS=Homo sapiens (Human).	41.4	3	3
39	A8K590_HUMAN	SubName: Full=cDNA FLJ77456, highly similar to Homo sapiens interleukin enhancer binding factor 3, 90kDa (ILF3), transcript variant 2, mRNA; - OS=Homo sapiens (Human).	76.0	2	2
40	A8K5W7_HUMAN	RecName: Full=Isoleucine--tRNA ligase A; EC=6.1.1.5; AltName: Full=Isoleucyl-tRNA synthetase A; - OS=Homo sapiens (Human).	105.9	5	5
41	A8K646_HUMAN	SubName: Full=cDNA FLJ75699, highly similar to Homo sapiens osteoclast stimulating factor 1 (OSTF1), mRNA; - OS=Homo sapiens (Human).	23.7	2	2
42	A8K766_HUMAN	SubName: Full=cDNA FLJ77343, highly similar to Homo sapiens electron-transfer-flavoprotein, beta polypeptide(ETFB), mRNA; - OS=Homo sapiens (Human).	27.9	2	2
43	A8K7J3_HUMAN	SubName: Full=cDNA FLJ75535, highly similar to Homo sapiens early endosome antigen 1, 162kD (EEA1), mRNA; Flags: Fragment; - OS=Homo sapiens (Human).	92.6	1	1
44	A8K7W1_HUMAN	SubName: Full=cDNA FLJ75779, highly similar to Homo sapiens docking protein 2, 56kDa (DOK2), transcript variant 1, mRNA; - OS=Homo sapiens (Human).	45.4	2	2

45	A8K8F6_HUMAN	SubName: Full=cDNA FLJ78417, highly similar to Homo sapiens low density lipoprotein receptor-related protein associated protein 1 (LRPAP1), mRNA; - OS=Homo sapiens (Human).	41.4	1	1
46	A8K8J9_HUMAN	SubName: Full=Dynactin 2 (P50), isoform CRA_b; SubName: Full=cDNA FLJ31120 fis, clone IMR322000730, highly similar to Dynactin subunit 2; SubName: Full=cDNA FLJ77785; - OS=Homo sapiens (Human).	34.5	3	3
47	A8K9B9_HUMAN	SubName: Full=cDNA FLJ77391, highly similar to Homo sapiens EH-domain containing 4 (EHD4), mRNA; - OS=Homo sapiens (Human).	61.1	1	1
48	A8K9J7_HUMAN	RecName: Full=Histone H2B; - OS=Homo sapiens (Human).	14.0	3	1
49	A8K9K4_HUMAN	SubName: Full=cDNA FLJ75504, highly similar to Homo sapiens glucosidase I, mRNA; - OS=Homo sapiens (Human).	62.2	2	2
50	A8KA41_HUMAN	SubName: Full=cDNA FLJ75060, highly similar to Homo sapiens 2'-5'-oligoadenylate synthetase 2, 69/71kDa, mRNA; - OS=Homo sapiens (Human).	78.8	2	2
51	A8KA83_HUMAN	SubName: Full=cDNA FLJ78586, highly similar to Homo sapiens VAMP (vesicle-associated membrane protein)-associated protein A, 33kDa (VAPA), mRNA; SubName: Full=cDNA, FLJ96653, Homo sapiens VAMP (vesicle-associated membrane protein)-associated protein A, 33kDa (VAPA), mRNA; - OS=Homo sapiens (Human).	27.3	2	2
52	A8KAK1_HUMAN	SubName: Full=cDNA FLJ77398, highly similar to Homo sapiens UDP-glucose ceramide glucosyltransferase-like 1, transcript variant 2, mRNA; - OS=Homo sapiens (Human).	174.9	2	2
53	A8MTY9_HUMAN	SubName: Full=Down syndrome critical region protein 3; - OS=Homo sapiens (Human).	27.9	1	1
54	A8MXL6_HUMAN	SubName: Full=Protein SEC13 homolog; - OS=Homo sapiens (Human).	31.6	1	1
55	ABRAL_HUMAN	RecName: Full=Costars family protein ABRACL; AltName: Full=ABRA C-terminal-like protein; - OS=Homo sapiens (Human).	9.1	1	1
56	ACBP_HUMAN	RecName: Full=Acyl-CoA-binding protein; Short=ACBP; AltName: Full=Diazepam-binding inhibitor; Short=DBI; AltName: Full=Endozepine; Short=EP; - OS=Homo sapiens (Human).	10.0	2	2
57	ACOT9_HUMAN	RecName: Full=Acyl-coenzyme A thioesterase 9, mitochondrial; Short=Acyl-CoA thioesterase 9;	49.9	2	2

		EC=3.1.2.-; AltName: Full=Acyl-CoA thioester hydrolase 9; Flags: Precursor; - OS=Homo sapiens (Human).			
58	ACOX1_HUMAN	RecName: Full=Peroxisomal acyl-coenzyme A oxidase 1; Short=AOX; EC=1.3.3.6; AltName: Full=Palmitoyl-CoA oxidase; AltName: Full=Straight-chain acyl-CoA oxidase; Short=SCOX; - OS=Homo sapiens (Human).	74.4	7	7
59	ACTN4_HUMAN	RecName: Full=Alpha-actinin-4; AltName: Full=F-actin cross-linking protein; AltName: Full=Non-muscle alpha-actinin 4; - OS=Homo sapiens (Human).	104.8	19	8
60	ADT2_HUMAN	RecName: Full=ADP/ATP translocase 2; AltName: Full=ADP,ATP carrier protein 2; AltName: Full=ADP,ATP carrier protein, fibroblast isoform; AltName: Full=Adenine nucleotide translocator 2; Short=ANT 2; AltName: Full=Solute carrier family 25 member 5; - OS=Homo sapiens (Human).	32.8	9	2
61	ADT3_HUMAN	RecName: Full=ADP/ATP translocase 3; AltName: Full=ADP,ATP carrier protein 3; AltName: Full=ADP,ATP carrier protein, isoform T2; Short=ANT 2; AltName: Full=Adenine nucleotide translocator 3; Short=ANT 3; AltName: Full=Solute carrier family 25 member 6; - OS=Homo sapiens (Human).	32.8	9	2
62	ADX_HUMAN	RecName: Full=Adrenodoxin, mitochondrial; AltName: Full=Adrenal ferredoxin; AltName: Full=Ferredoxin-1; AltName: Full=Hepatoredoxin; Flags: Precursor; - OS=Homo sapiens (Human).	19.4	1	1
63	AHNK_HUMAN	RecName: Full=Neuroblast differentiation-associated protein AHNAK; AltName: Full=Desmoyokin; - OS=Homo sapiens (Human).	628.7	49	46
64	AHSP_HUMAN	RecName: Full=Alpha-hemoglobin-stabilizing protein; AltName: Full=Erythroid differentiation-related factor; AltName: Full=Erythroid-associated factor; - OS=Homo sapiens (Human).	11.8	2	2
65	AIFM1_HUMAN	RecName: Full=Apoptosis-inducing factor 1, mitochondrial; EC=1.-.-.-; AltName: Full=Programmed cell death protein 8; Flags: Precursor; - OS=Homo sapiens (Human).	66.9	4	4
66	AK1A1_HUMAN	RecName: Full=Alcohol dehydrogenase [NADP(+)]; EC=1.1.1.2; AltName: Full=Aldehyde reductase; AltName: Full=Aldo-keto reductase family 1 member A1; - OS=Homo sapiens (Human).	36.5	5	4
67	AL5AP_HUMAN	RecName: Full=Arachidonate 5-lipoxygenase-activating protein; AltName: Full=FLAP; AltName:	18.1	3	3

		Full=MK-886-binding protein; - OS=Homo sapiens (Human).			
68	ALDH2_HUMAN	RecName: Full=Aldehyde dehydrogenase, mitochondrial; EC=1.2.1.3; AltName: Full=ALDH class 2; AltName: Full=ALDH-E2; AltName: Full=ALDHI; Flags: Precursor; - OS=Homo sapiens (Human).	56.3	20	18
69	ALDR_HUMAN	RecName: Full=Aldose reductase; Short=AR; EC=1.1.1.21; AltName: Full=Aldehyde reductase; AltName: Full=Aldo-keto reductase family 1 member B1; - OS=Homo sapiens (Human).	35.8	2	1
70	AMPL_HUMAN	RecName: Full=Cytosol aminopeptidase; EC=3.4.11.1; AltName: Full=Leucine aminopeptidase 3; Short=LAP-3; AltName: Full=Leucyl aminopeptidase; AltName: Full=Peptidase S; AltName: Full=Proline aminopeptidase; EC=3.4.11.5; AltName: Full=Prolyl aminopeptidase; - OS=Homo sapiens (Human).	56.1	9	9
71	ANK1_HUMAN	RecName: Full=Ankyrin-1; Short=ANK-1; AltName: Full=Ankyrin-R; AltName: Full=Erythrocyte ankyrin; - OS=Homo sapiens (Human).	206.1	9	9
72	ANXA1_HUMAN	RecName: Full=Annexin A1; AltName: Full=Annexin I; AltName: Full=Annexin-1; AltName: Full=Calpactin II; AltName: Full=Calpactin-2; AltName: Full=Chromobindin-9; AltName: Full=Lipocortin I; AltName: Full=Phospholipase A2 inhibitory protein; AltName: Full=p35; - OS=Homo sapiens (Human).	38.7	12	12
73	ANXA2_HUMAN	RecName: Full=Annexin A2; AltName: Full=Annexin II; AltName: Full=Annexin-2; AltName: Full=Calpactin I heavy chain; AltName: Full=Calpactin-1 heavy chain; AltName: Full=Chromobindin-8; AltName: Full=Lipocortin II; AltName: Full=Placental anticoagulant protein IV; Short=PAP-IV; AltName: Full=Protein I; AltName: Full=p36; - OS=Homo sapiens (Human).	38.6	17	17
74	ANXA5_HUMAN	RecName: Full=Annexin A5; AltName: Full=Anchorin CII; AltName: Full=Annexin V; AltName: Full=Annexin-5; AltName: Full=Calphobindin I; Short=CBP-I; AltName: Full=Endonexin II; AltName: Full=Lipocortin V; AltName: Full=Placental anticoagulant protein 4; Short=PP4; AltName: Full=Placental anticoagulant protein I; Short=PAP-I; AltName: Full=Thromboplastin inhibitor; AltName: Full=Vascular anticoagulant-alpha; Short=VAC-alpha; - OS=Homo sapiens (Human).	35.9	11	10
75	AP2A1_HUMAN	RecName: Full=AP-2 complex subunit alpha-1; AltName: Full=100 kDa coated vesicle protein A;	107.5	3	3

		AltName: Full=Adapter-related protein complex 2 alpha-1 subunit; AltName: Full=Adaptor protein complex AP-2 subunit alpha-1; AltName: Full=Alpha-adaptin A; AltName: Full=Alpha1-adaptin; AltName: Full=Clathrin assembly protein complex 2 alpha-A large chain; AltName: Full=Plasma membrane adaptor HA2/AP2 adaptin alpha A subunit; - OS=Homo sapiens (Human).			
76	APOA1_HUMAN	RecName: Full=Apolipoprotein A-I; Short=Apo-AI; Short=ApoA-I; AltName: Full=Apolipoprotein A1; Contains: RecName: Full=Truncated apolipoprotein A-I; AltName: Full=Apolipoprotein A-I(1-242); Flags: Precursor; - OS=Homo sapiens (Human).	30.8	6	6
77	APOA2_HUMAN	RecName: Full=Apolipoprotein A-II; Short=Apo-AII; Short=ApoA-II; AltName: Full=Apolipoprotein A2; Contains: RecName: Full=Truncated apolipoprotein A-II; AltName: Full=Apolipoprotein A-II(1-76); Flags: Precursor; - OS=Homo sapiens (Human).	11.2	1	1
78	APOD_HUMAN	RecName: Full=Apolipoprotein D; Short=Apo-D; Short=ApoD; Flags: Precursor; - OS=Homo sapiens (Human).	21.3	1	1
79	ARC1B_HUMAN	RecName: Full=Actin-related protein 2/3 complex subunit 1B; AltName: Full=Arp2/3 complex 41 kDa subunit; AltName: Full=p41-ARC; - OS=Homo sapiens (Human).	40.9	4	4
80	ARF6_HUMAN	RecName: Full=ADP-ribosylation factor 6; - OS=Homo sapiens (Human).	20.1	2	2
81	ARP2_HUMAN	RecName: Full=Actin-related protein 2; AltName: Full=Actin-like protein 2; - OS=Homo sapiens (Human).	44.7	3	3
82	ARP3_HUMAN	RecName: Full=Actin-related protein 3; AltName: Full=Actin-like protein 3; - OS=Homo sapiens (Human).	47.3	9	9
83	ARP5L_HUMAN	RecName: Full=Actin-related protein 2/3 complex subunit 5-like protein; AltName: Full=Arp2/3 complex 16 kDa subunit 2; Short=ARC16-2; - OS=Homo sapiens (Human).	16.9	1	1
84	ARPC2_HUMAN	RecName: Full=Actin-related protein 2/3 complex subunit 2; AltName: Full=Arp2/3 complex 34 kDa subunit; Short=p34-ARC; - OS=Homo sapiens (Human).	34.3	4	4
85	ARPC4_HUMAN	RecName: Full=Actin-related protein 2/3 complex subunit 4; AltName: Full=Arp2/3 complex 20 kDa subunit; Short=p20-ARC; - OS=Homo sapiens (Human).	19.7	3	3

86	ARPC5_HUMAN	RecName: Full=Actin-related protein 2/3 complex subunit 5; AltName: Full=Arp2/3 complex 16 kDa subunit; Short=p16-ARC; - OS=Homo sapiens (Human).	16.3	1	1
87	ASC_HUMAN	RecName: Full=Apoptosis-associated speck-like protein containing a CARD; Short=hASC; AltName: Full=Caspase recruitment domain-containing protein 5; AltName: Full=PYD and CARD domain-containing protein; AltName: Full=Target of methylation-induced silencing 1; - OS=Homo sapiens (Human).	21.6	3	3
88	AT2A2_HUMAN	RecName: Full=Sarcoplasmic/endoplasmic reticulum calcium ATPase 2; Short=SERCA2; Short=SR Ca(2+)-ATPase 2; EC=3.6.3.8; AltName: Full=Calcium pump 2; AltName: Full=Calcium-transporting ATPase sarcoplasmic reticulum type, slow twitch skeletal muscle isoform; AltName: Full=Endoplasmic reticulum class 1/2 Ca(2+) ATPase; - OS=Homo sapiens (Human).	114.7	5	5
89	ATG3_HUMAN	RecName: Full=Ubiquitin-like-conjugating enzyme ATG3; EC=6.3.2.-; AltName: Full=Autophagy-related protein 3; Short=APG3-like; Short=hApg3; AltName: Full=Protein PC3-96; - OS=Homo sapiens (Human).	35.8	2	2
90	ATP5H_HUMAN	RecName: Full=ATP synthase subunit d, mitochondrial; Short=ATPase subunit d; - OS=Homo sapiens (Human).	18.5	5	5
91	ATP5I_HUMAN	RecName: Full=ATP synthase subunit e, mitochondrial; Short=ATPase subunit e; - OS=Homo sapiens (Human).	7.9	1	1
92	ATPA_HUMAN	RecName: Full=ATP synthase subunit alpha, mitochondrial; Flags: Precursor; - OS=Homo sapiens (Human).	59.7	12	12
93	ATPD_HUMAN	RecName: Full=ATP synthase subunit delta, mitochondrial; AltName: Full=F-ATPase delta subunit; Flags: Precursor; - OS=Homo sapiens (Human).	17.5	1	1
94	ATPO_HUMAN	RecName: Full=ATP synthase subunit O, mitochondrial; AltName: Full=Oligomycin sensitivity conferral protein; Short=OSCP; Flags: Precursor; - OS=Homo sapiens (Human).	23.3	6	6
95	ATRAP_HUMAN	RecName: Full=Type-1 angiotensin II receptor-associated protein; AltName: Full=AT1 receptor-associated protein; - OS=Homo sapiens (Human).	17.4	1	1

96	B0I1T1_HUMAN	SubName: Full=MYO1F variant protein; - OS=Homo sapiens (Human).	124.7	4	4
97	B0QY04_HUMAN	SubName: Full=Neutrophil cytosol factor 4; SubName: Full=Neutrophil cytosolic factor 4, 40kDa; Flags: Fragment; - OS=Homo sapiens (Human).	18.9	3	3
98	B0QY68_HUMAN	SubName: Full=SUN domain-containing protein 2; SubName: Full=Unc-84 homolog B (C. elegans); Flags: Fragment; - OS=Homo sapiens (Human).	11.1	1	1
99	B0QYR9_HUMAN	SubName: Full=ADP-ribosylation factor-binding protein GGA1; SubName: Full=Golgi associated, gamma adaptin ear containing, ARF binding protein 1; Flags: Fragment; - OS=Homo sapiens (Human).	3.3	1	1
100	B0QZK4_HUMAN	SubName: Full=Heterochromatin protein 1, binding protein 3; SubName: Full=Heterochromatin protein 1-binding protein 3; Flags: Fragment; - OS=Homo sapiens (Human).	28.5	1	1
101	B0UZC1_HUMAN	SubName: Full=Proteasome (Prosome, macropain) subunit, beta type, 8 (Large multifunctional peptidase 7); SubName: Full=Proteasome subunit beta type-8; - OS=Homo sapiens (Human).	27.8	1	1
102	B0V109_HUMAN	SubName: Full=Flotillin 1; SubName: Full=Flotillin-1; Flags: Fragment; - OS=Homo sapiens (Human).	39.8	2	2
103	B1AHA8_HUMAN	SubName: Full=Heme oxygenase (Decycling) 1; SubName: Full=Heme oxygenase 1; Flags: Fragment; - OS=Homo sapiens (Human).	21.6	4	4
104	B1AHC7_HUMAN	SubName: Full=X-ray repair complementing defective repair in Chinese hamster cells 6 (Ku autoantigen, 70kDa); SubName: Full=X-ray repair cross-complementing protein 6; - OS=Homo sapiens (Human).	64.0	2	2
105	B1AHM1_HUMAN	SubName: Full=DEAD (Asp-Glu-Ala-Asp) box polypeptide 17; - OS=Homo sapiens (Human).	72.5	4	2
106	B1AJY5_HUMAN	SubName: Full=26S proteasome non-ATPase regulatory subunit 10; SubName: Full=Proteasome (Prosome, macropain) 26S subunit, non-ATPase, 10; - OS=Homo sapiens (Human).	20.2	1	1
107	B1AK13_HUMAN	SubName: Full=3-hydroxymethyl-3-methylglutaryl-Coenzyme A lyase; SubName: Full=3-hydroxymethyl-3-methylglutaryl-Coenzyme A lyase (Hydroxymethylglutaricaciduria), isoform CRA_b; SubName: Full=Hydroxymethylglutaryl-CoA lyase, mitochondrial; SubName: Full=cDNA	31.7	2	2

		FLJ16378 fis, clone TKIDN2016399, highly similar to Hydroxymethylglutaryl-CoA lyase, mitochondrial (EC 4.1.3.4); - OS=Homo sapiens (Human).			
108	B1AK87_HUMAN	SubName: Full=Capping protein (Actin filament) muscle Z-line, beta; SubName: Full=Capping protein (Actin filament) muscle Z-line, beta, isoform CRA_a; SubName: Full=F-actin-capping protein subunit beta; - OS=Homo sapiens (Human).	29.3	3	3
109	B1ALA7_HUMAN	SubName: Full=Phosphoribosyl pyrophosphate synthetase 1; SubName: Full=Ribose-phosphate pyrophosphokinase 1; - OS=Homo sapiens (Human).	18.4	2	2
110	B1AMI8_HUMAN	SubName: Full=Torsin A interacting protein 1; Flags: Fragment; - OS=Homo sapiens (Human).	33.6	2	2
111	B1APM4_HUMAN	SubName: Full=Sterol O-acyltransferase (Acyl-Coenzyme A: cholesterol acyltransferase) 1; SubName: Full=Sterol O-acyltransferase 1; Flags: Fragment; - OS=Homo sapiens (Human).	29.9	1	1
112	B1AVS1_HUMAN	SubName: Full=Metaxin 1; Flags: Fragment; - OS=Homo sapiens (Human).	35.1	1	1
113	B1B5Q3_HUMAN	SubName: Full=N-acylsphingosine amidohydrolase 1; Flags: Fragment; - OS=Homo sapiens (Human).	24.7	5	1
114	B2M1S7_HUMAN	SubName: Full=Beta-globin Showa Yakushiji variant; Flags: Fragment; - OS=Homo sapiens (Human).	4.5	3	1
115	B2MG_HUMAN	RecName: Full=Beta-2-microglobulin; Contains: RecName: Full=Beta-2-microglobulin form pI 5.3; Flags: Precursor; - OS=Homo sapiens (Human).	13.7	2	2
116	B2R4A2_HUMAN	SubName: Full=cDNA, FLJ92016, highly similar to Homo sapiens ubiquinol-cytochrome c reductase binding protein (UQCRB), mRNA; - OS=Homo sapiens (Human).	13.5	1	1
117	B2R4J7_HUMAN	SubName: Full=cDNA, FLJ92117, highly similar to Homo sapiens chemokine (C-X-C motif) ligand 9 (CXCL9), mRNA; - OS=Homo sapiens (Human).	13.9	1	1
118	B2R4M6_HUMAN	SubName: Full=cDNA, FLJ92148, highly similar to Homo sapiens S100 calcium binding protein A9 (calgranulin B) (S100A9), mRNA; - OS=Homo sapiens (Human).	13.2	4	4
119	B2R4V4_HUMAN	SubName: Full=cDNA, FLJ92232, highly similar to Homo sapiens barrier to autointegration factor 1 (BANF1), mRNA; - OS=Homo sapiens (Human).	10.0	1	1
120	B2R5B6_HUMAN	RecName: Full=Histone H2A; - OS=Homo sapiens (Human).	14.1	3	1
121	B2R5M8_HUMAN	RecName: Full=Isocitrate dehydrogenase [NADP]; EC=1.1.1.42; - OS=Homo sapiens (Human).	46.6	10	9

122	B2R6C0_HUMAN	SubName: Full=cDNA, FLJ92881, highly similar to Homo sapiens glycerol-3-phosphate dehydrogenase 1 (soluble) (GPD1), mRNA; - OS=Homo sapiens (Human).	37.6	5	5
123	B2R6K1_HUMAN	SubName: Full=cDNA, FLJ92992, highly similar to Homo sapiens methylmalonyl Coenzyme A mutase (MUT), nuclear gene encoding mitochondrial protein, mRNA; - OS=Homo sapiens (Human).	83.0	1	1
124	B2R6X6_HUMAN	RecName: Full=Peptidyl-prolyl cis-trans isomerase; EC=5.2.1.8; - OS=Homo sapiens (Human).	22.0	1	1
125	B2R774_HUMAN	SubName: Full=cDNA, FLJ93313, highly similar to Homo sapiens lectin, mannose-binding, 1 (LMAN1), mRNA; - OS=Homo sapiens (Human).	57.5	1	1
126	B2R7M1_HUMAN	SubName: Full=cDNA, FLJ93507, highly similar to Homo sapiens ATPase, H+ transporting, lysosomal 38kDa, V0 subunit d isoform 1 (ATP6V0D1), mRNA; - OS=Homo sapiens (Human).	40.3	7	7
127	B2R7Z6_HUMAN	SubName: Full=cDNA, FLJ93674; - OS=Homo sapiens (Human).	52.5	11	11
128	B2R8A2_HUMAN	SubName: Full=cDNA, FLJ93804, highly similar to Homo sapiens gp25L2 protein (HSGP25L2G), mRNA; - OS=Homo sapiens (Human).	25.1	1	1
129	B2R8N0_HUMAN	SubName: Full=cDNA, FLJ93975, highly similar to Homo sapiens epoxide hydrolase 1, microsomal (xenobiotic) (EPHX1), mRNA; - OS=Homo sapiens (Human).	52.9	4	4
130	B2R923_HUMAN	SubName: Full=cDNA, FLJ94174; - OS=Homo sapiens (Human).	37.3	2	2
131	B2R959_HUMAN	SubName: Full=cDNA, FLJ94229, highly similar to Homo sapiens heterogeneous nuclear ribonucleoprotein L (HNRPL),mRNA; - OS=Homo sapiens (Human).	60.2	1	1
132	B2R983_HUMAN	SubName: Full=cDNA, FLJ94267, highly similar to Homo sapiens glutathione S-transferase omega 1 (GSTO1), mRNA; - OS=Homo sapiens (Human).	27.5	7	7
133	B2R9S4_HUMAN	SubName: Full=cDNA, FLJ94534, highly similar to Homo sapiens capping protein (actin filament), gelsolin-like(CAPG), mRNA; - OS=Homo sapiens (Human).	38.5	9	9
134	B2RAL6_HUMAN	SubName: Full=cDNA, FLJ94991, highly similar to Homo sapiens integrin, alpha L (antigen CD11A (p180), lymphocyte function-associated antigen 1; alpha polypeptide) (ITGAL), mRNA; - OS=Homo sapiens (Human).	128.8	1	1
135	B2RAQ8_HUMAN	SubName: Full=cDNA, FLJ95058, highly similar to Homo sapiens carnitine palmitoyltransferase 1A	88.3	1	1

		(liver) (CPT1A),nuclear gene encoding mitochondrial protein, mRNA; - OS=Homo sapiens (Human).			
136	B2RAW0_HUMAN	SubName: Full=cDNA, FLJ95154, highly similar to Homo sapiens disabled homolog 2, mitogen-responsive phosphoprotein (Drosophila) (DAB2), mRNA; - OS=Homo sapiens (Human).	82.4	3	3
137	B2RB06_HUMAN	SubName: Full=cDNA, FLJ95242, highly similar to Homo sapiens L-3-hydroxyacyl-Coenzyme A dehydrogenase, short chain (HADHSC), mRNA; - OS=Homo sapiens (Human).	34.2	4	4
138	B2RB23_HUMAN	SubName: Full=cDNA, FLJ95265, highly similar to Homo sapiens acetyl-Coenzyme A acyltransferase 2 (mitochondrial 3-oxoacyl-Coenzyme A thiolase) (ACAA2), nuclear gene encoding mitochondrial protein, mRNA; - OS=Homo sapiens (Human).	42.0	9	9
139	B2RBG3_HUMAN	SubName: Full=cDNA, FLJ95493, highly similar to Homo sapiens fucosidase, alpha-L- 1, tissue (FUCA1), mRNA; - OS=Homo sapiens (Human).	53.2	1	1
140	B2RDI5_HUMAN	SubName: Full=cDNA, FLJ96627, highly similar to Homo sapiens calpain 1, (mu/I) large subunit (CAPN1), mRNA; - OS=Homo sapiens (Human).	81.8	3	3
141	B2RDM2_HUMAN	SubName: Full=HCG1811539, isoform CRA_b; SubName: Full=Thioredoxin domain-containing protein 5; SubName: Full=cDNA, FLJ96678, Homo sapiens thioredoxin domain containing 5 (TXNDC5), mRNA; - OS=Homo sapiens (Human).	36.2	2	2
142	B2RE38_HUMAN	SubName: Full=cDNA, FLJ96906, highly similar to Homo sapiens solute carrier family 17 (anion/sugar transporter), member 5 (SLC17A5), mRNA; - OS=Homo sapiens (Human).	54.6	1	1
143	B2RE46_HUMAN	SubName: Full=cDNA, FLJ96923, highly similar to Homo sapiens ribophorin II (RPN2), mRNA; - OS=Homo sapiens (Human).	69.3	7	7
144	B2REB8_HUMAN	SubName: Full=Protein SET; SubName: Full=SET nuclear oncogene; - OS=Homo sapiens (Human).	31.0	2	2
145	B2ZP79_HUMAN	SubName: Full=BH3 interacting domain death agonist, isoform CRA_b; SubName: Full=BID isoform ES(1b); - OS=Homo sapiens (Human).	11.3	1	1
146	B3AT_HUMAN	RecName: Full=Band 3 anion transport protein; AltName: Full=Anion exchange protein 1; Short=AE 1; Short=Anion exchanger 1; AltName: Full=Solute carrier family 4 member 1; AltName: CD_antigen=CD233; - OS=Homo sapiens (Human).	101.7	14	14

147	B3KM80_HUMAN	SubName: Full=Nucleolin, isoform CRA_c; SubName: Full=cDNA FLJ10452 fis, clone NT2RP1000966, highly similar to NUCLEOLIN; - OS=Homo sapiens (Human).	58.5	10	10
148	B3KM97_HUMAN	SubName: Full=cDNA FLJ10554 fis, clone NT2RP2002385, highly similar to Synaptic glycoprotein SC2; - OS=Homo sapiens (Human).	36.0	1	1
149	B3KMR6_HUMAN	SubName: Full=cDNA FLJ12440 fis, clone NT2RM1000131, highly similar to Homo sapiens transmembrane protein 63A (TMEM63A), mRNA; - OS=Homo sapiens (Human).	92.0	1	1
150	B3KMV5_HUMAN	SubName: Full=cDNA FLJ12728 fis, clone NT2RP2000040, highly similar to Protein FAM62A; - OS=Homo sapiens (Human).	122.8	15	15
151	B3KN06_HUMAN	SubName: Full=cDNA FLJ13143 fis, clone NT2RP3003230, highly similar to Coronin-1C; - OS=Homo sapiens (Human).	53.2	8	8
152	B3KNM6_HUMAN	SubName: Full=cDNA FLJ14968 fis, clone THYRO1000288, highly similar to CAAX prenyl protease 1 homolog (EC 3.4.24.84); - OS=Homo sapiens (Human).	27.1	1	1
153	B3KPA6_HUMAN	SubName: Full=Acyl-Coenzyme A dehydrogenase, very long chain, isoform CRA_e; SubName: Full=cDNA FLJ31521 fis, clone NT2RI2000255, highly similar to Very-long-chain specific acyl-CoAdehydrogenase, mitochondrial (EC 1.3.99.-); - OS=Homo sapiens (Human).	62.5	15	15
154	B3KPH8_HUMAN	RecName: Full=Lon protease homolog; EC=3.4.21.-; - OS=Homo sapiens (Human).	85.5	2	2
155	B3KPP1_HUMAN	SubName: Full=cDNA FLJ32014 fis, clone NTONG1000047, highly similar to Lymphocyte-specific protein 1; - OS=Homo sapiens (Human).	30.2	1	1
156	B3KPS3_HUMAN	SubName: Full=cDNA FLJ32131 fis, clone PEBLM2000267, highly similar to Tubulin alpha-ubiquitous chain; - OS=Homo sapiens (Human).	46.2	11	2
157	B3KPZ7_HUMAN	SubName: Full=cDNA FLJ32517 fis, clone SMINT1000117, highly similar to Pyruvate dehydrogenase (lipoamide)-phosphatase 1 (EC 3.1.3.43); - OS=Homo sapiens (Human).	60.8	1	1
158	B3KQK0_HUMAN	SubName: Full=cDNA FLJ90599 fis, clone PLACE1001340, highly similar to Mitochondrial proteins importreceptor; - OS=Homo sapiens (Human).	26.5	1	1
159	B3KQQ3_HUMAN	SubName: Full=cDNA PSEC0016 fis, clone NT2RM1001076, highly similar to Procollagen-lysine,2-	84.6	2	2

		oxoglutarate 5-dioxygenase 3 (EC 1.14.11.4); - OS=Homo sapiens (Human).			
160	B3KQT9_HUMAN	SubName: Full=cDNA PSEC0175 fis, clone OVARC1000169, highly similar to Protein disulfide-isomerase A3 (EC 5.3.4.1); - OS=Homo sapiens (Human).	54.1	13	11
161	B3KQV6_HUMAN	SubName: Full=cDNA FLJ33169 fis, clone ADRGL2000384, highly similar to Serine/threonine-protein phosphatase 2A 65 kDa regulatory subunit A alpha isoform; - OS=Homo sapiens (Human).	45.6	3	3
162	B3KR50_HUMAN	SubName: Full=cDNA FLJ33691 fis, clone BRAWH2002976, highly similar to GROWTH FACTOR RECEPTOR-BOUND PROTEIN 2; - OS=Homo sapiens (Human).	25.2	4	4
163	B3KRW2_HUMAN	SubName: Full=cDNA FLJ34977 fis, clone NTONG2005822, highly similar to Homo sapiens RAB11 family interacting protein 1 (class I) (RAB11FIP1), transcript variant 1, mRNA; - OS=Homo sapiens (Human).	45.4	1	1
164	B3KRY3_HUMAN	SubName: Full=cDNA FLJ35079 fis, clone PLACE6005283, highly similar to Lysosome-associated membrane glycoprotein 1; - OS=Homo sapiens (Human).	42.6	3	3
165	B3KS31_HUMAN	SubName: Full=Tubulin beta-6 chain; SubName: Full=Tubulin, beta 6, isoform CRA_a; SubName: Full=cDNA FLJ35358 fis, clone PUAEN2000497, highly similar to Tubulin beta-6 chain; - OS=Homo sapiens (Human).	41.9	4	1
166	B3KS50_HUMAN	SubName: Full=cDNA FLJ35494 fis, clone SMINT2008720, highly similar to Interferon-induced protein with tetratricopeptide repeats 1; - OS=Homo sapiens (Human).	51.7	1	1
167	B3KT32_HUMAN	SubName: Full=cDNA FLJ37546 fis, clone BRCAN2027364, highly similar to Homo sapiens formin-like 2 (FMNL2), transcript variant 2, mRNA; - OS=Homo sapiens (Human).	41.7	1	1
168	B3KT45_HUMAN	SubName: Full=cDNA FLJ37607 fis, clone BRCOC2010980, highly similar to Thioredoxin-like protein 1; - OS=Homo sapiens (Human).	18.9	1	1
169	B3KT93_HUMAN	SubName: Full=cDNA FLJ37875 fis, clone BRSSN2018771, highly similar to Poly(A)-binding protein 1; - OS=Homo sapiens (Human).	70.6	3	3
170	B3KUH7_HUMAN	SubName: Full=cDNA FLJ39919 fis, clone SPLEN2020154, highly similar to Coronin-7; - OS=Homo sapiens (Human).	66.4	3	3

171	B3KUK2_HUMAN	RecName: Full=Superoxide dismutase; EC=1.15.1.1; - OS=Homo sapiens (Human).	19.7	5	5
172	B3KUR3_HUMAN	RecName: Full=2,3-bisphosphoglycerate-dependent phosphoglycerate mutase B; Short=BPG-dependent PGAM B; Short=PGAM B; Short=Phosphoglyceromutase B; Short=dPGM B; EC=5.4.2.1; - OS=Homo sapiens (Human).	28.0	2	2
173	B3KUZ8_HUMAN	RecName: Full=Aspartate aminotransferase; EC=2.6.1.1; - OS=Homo sapiens (Human).	41.3	3	3
174	B3KVN0_HUMAN	SubName: Full=cDNA FLJ16785 fis, clone NT2RI2015342, highly similar to Solute carrier family 2, facilitated glucose transporter member 1; - OS=Homo sapiens (Human).	45.8	2	2
175	B3KVX6_HUMAN	SubName: Full=cDNA FLJ41699 fis, clone HCHON2004776, highly similar to Homo sapiens cytoskeleton-associated protein 4 (CKAP4), mRNA; - OS=Homo sapiens (Human).	58.1	1	1
176	B3KW21_HUMAN	SubName: Full=cDNA FLJ41945 fis, clone PLACE6019676, highly similar to Coatomer subunit gamma; - OS=Homo sapiens (Human).	67.8	3	3
177	B3KW79_HUMAN	SubName: Full=cDNA FLJ42481 fis, clone BRACE2032090, highly similar to Probable serine carboxypeptidase CPVL (EC 3.4.16.-); - OS=Homo sapiens (Human).	54.1	3	3
178	B3KWA1_HUMAN	SubName: Full=Iduronate 2-sulfatase; SubName: Full=Iduronate 2-sulfatase (Hunter syndrome), isoform CRA_e; SubName: Full=cDNA FLJ42669 fis, clone BRAMY2022168, highly similar to IDURONATE 2-SULFATASE (EC 3.1.6.13); - OS=Homo sapiens (Human).	38.6	1	1
179	B3KWD9_HUMAN	SubName: Full=cDNA FLJ42834 fis, clone BRCAN2019002, highly similar to GTP:AMP phosphotransferase mitochondrial (EC 2.7.4.10); - OS=Homo sapiens (Human).	18.2	3	3
180	B3KX15_HUMAN	SubName: Full=cDNA FLJ44468 fis, clone UTERU2026025, moderately similar to SPLICING FACTOR, ARGININE/SERINE-RICH 2; - OS=Homo sapiens (Human).	13.8	1	1
181	B3KXF2_HUMAN	SubName: Full=cDNA FLJ45314 fis, clone BRHIP3005142, highly similar to Proteasome-associated protein ECM29 homolog; - OS=Homo sapiens (Human).	145.3	1	1
182	B3KY04_HUMAN	SubName: Full=cDNA FLJ46506 fis, clone THYMU3030752, highly similar to BTB/POZ domain-containing protein KCTD12; - OS=Homo sapiens (Human).	35.7	3	3
183	B3VL17_HUMAN	SubName: Full=Beta globin; Flags: Fragment; - OS=Homo sapiens (Human).	11.5	10	2

184	B3VTQ2_HUMAN	SubName: Full=MHC class II antigen; Flags: Fragment; - OS=Homo sapiens (Human).	10.9	4	0
185	B4DDF8_HUMAN	SubName: Full=cDNA FLJ51786, highly similar to Retinal dehydrogenase 1 (EC 1.2.1.36); - OS=Homo sapiens (Human).	46.0	9	7
186	B4DDG1_HUMAN	SubName: Full=Ubiquitin-conjugating enzyme E2 L3; SubName: Full=cDNA FLJ59174, highly similar to Ubiquitin-conjugating enzyme E2 L3 (EC 6.3.2.19); - OS=Homo sapiens (Human).	14.1	2	2
187	B4DDM5_HUMAN	SubName: Full=cDNA FLJ53298, highly similar to Peroxisomal multifunctional enzyme type 2; - OS=Homo sapiens (Human).	77.4	9	9
188	B4DDV4_HUMAN	SubName: Full=cDNA FLJ52530, highly similar to Tumor protein D54; - OS=Homo sapiens (Human).	17.2	2	2
189	B4DE02_HUMAN	RecName: Full=Annexin; - OS=Homo sapiens (Human).	34.4	6	5
190	B4DE36_HUMAN	RecName: Full=Glucose-6-phosphate isomerase; EC=5.3.1.9; - OS=Homo sapiens (Human).	60.1	6	6
191	B4DE67_HUMAN	SubName: Full=cDNA FLJ57259, highly similar to Lysosomal acid lipase/cholesteryl esterhydrolase (EC 3.1.1.13); - OS=Homo sapiens (Human).	23.5	1	1
192	B4DEA3_HUMAN	SubName: Full=cDNA FLJ56531, highly similar to UV excision repair protein RAD23 homolog B; - OS=Homo sapiens (Human).	42.3	3	3
193	B4DEB9_HUMAN	SubName: Full=cDNA FLJ61099, highly similar to ADP-ribosylation factor 1; - OS=Homo sapiens (Human).	19.6	4	2
194	B4DEK4_HUMAN	SubName: Full=Sorting nexin-2; SubName: Full=cDNA FLJ51799, highly similar to Sorting nexin-2; - OS=Homo sapiens (Human).	46.1	4	4
195	B4DEQ0_HUMAN	SubName: Full=cDNA FLJ59482, highly similar to Electron transfer flavoprotein-ubiquinone oxidoreductase, mitochondrial (EC 1.5.5.1); - OS=Homo sapiens (Human).	61.3	1	1
196	B4DF22_HUMAN	SubName: Full=cDNA FLJ55615, highly similar to SWI/SNF-related matrix-associatedactin-dependent regulator of chromatin subfamily C member 2; - OS=Homo sapiens (Human).	112.1	1	1
197	B4DF70_HUMAN	SubName: Full=cDNA FLJ60461, highly similar to Peroxiredoxin-2 (EC 1.11.1.15); - OS=Homo sapiens (Human).	20.1	6	5

198	B4DF97_HUMAN	SubName: Full=cDNA FLJ59673, highly similar to Homo sapiens growth and transformation-dependent protein (E2IG5), mRNA; - OS=Homo sapiens (Human).	15.9	1	1
199	B4DFH3_HUMAN	SubName: Full=Inorganic pyrophosphatase 2, mitochondrial; SubName: Full=cDNA FLJ59863, highly similar to Inorganic pyrophosphatase 2, mitochondrial (EC 3.6.1.1); - OS=Homo sapiens (Human).	23.0	2	1
200	B4DFL1_HUMAN	RecName: Full=Dihydrolipoyl dehydrogenase; EC=1.8.1.4; - OS=Homo sapiens (Human).	48.9	6	6
201	B4DFL2_HUMAN	RecName: Full=Isocitrate dehydrogenase [NADP]; EC=1.1.1.42; - OS=Homo sapiens (Human).	45.2	7	6
202	B4DFM0_HUMAN	SubName: Full=Phenylalanine-tRNA synthetase-like, beta subunit, isoform CRA_c; SubName: Full=cDNA FLJ57266, highly similar to Phenylalanyl-tRNA synthetase beta chain (EC 6.1.1.20); - OS=Homo sapiens (Human).	54.8	1	1
203	B4DFP1_HUMAN	SubName: Full=cDNA FLJ51818, highly similar to Phosphoglucomutase-1 (EC 5.4.2.2); - OS=Homo sapiens (Human).	58.7	2	2
204	B4DG62_HUMAN	SubName: Full=cDNA FLJ56506, highly similar to Hexokinase-1 (EC 2.7.1.1); - OS=Homo sapiens (Human).	102.2	9	9
205	B4DGK8_HUMAN	SubName: Full=cDNA FLJ57723, moderately similar to Protein-tyrosine phosphatase mitochondrial 1, mitochondrial (EC 3.1.3.48); - OS=Homo sapiens (Human).	15.8	1	1
206	B4DGN5_HUMAN	RecName: Full=Glutamate dehydrogenase; - OS=Homo sapiens (Human).	46.5	5	5
207	B4DGN8_HUMAN	SubName: Full=cDNA FLJ53377, highly similar to Procollagen-lysine, 2-oxoglutarate 5-dioxygenase 1 (EC 1.14.11.4); - OS=Homo sapiens (Human).	79.3	1	1
208	B4DHC4_HUMAN	SubName: Full=cDNA FLJ51843, highly similar to 14-3-3 protein gamma; - OS=Homo sapiens (Human).	25.6	5	3
209	B4DHP6_HUMAN	SubName: Full=Non-specific lipid-transfer protein; SubName: Full=cDNA FLJ53991, highly similar to Nonspecific lipid-transfer protein (EC 2.3.1.176); - OS=Homo sapiens (Human).	50.3	7	7
210	B4DI38_HUMAN	RecName: Full=Adenylyl cyclase-associated protein; - OS=Homo sapiens (Human).	49.0	11	8
211	B4DIC4_HUMAN	SubName: Full=cDNA FLJ52195, highly similar to LIM and SH3 domain protein 1; - OS=Homo	14.6	1	1

		sapiens (Human).			
212	B4DIH0_HUMAN	SubName: Full=cDNA FLJ58381, highly similar to COMM domain-containing protein 9; - OS=Homo sapiens (Human).	13.5	1	1
213	B4DIT7_HUMAN	SubName: Full=Protein-glutamine gamma-glutamyltransferase 2; SubName: Full=cDNA FLJ58187, highly similar to Protein-glutamine gamma-glutamyltransferase 2(EC 2.3.2.13); - OS=Homo sapiens (Human).	68.6	11	11
214	B4DJ24_HUMAN	SubName: Full=cDNA FLJ58575, highly similar to Dolichyl-diphosphooligosaccharide--protein glycosyltransferase subunit STT3A (EC 2.4.1.119); - OS=Homo sapiens (Human).	69.6	1	1
215	B4DJ81_HUMAN	SubName: Full=NADH-ubiquinone oxidoreductase 75 kDa subunit, mitochondrial; SubName: Full=cDNA FLJ60586, highly similar to NADH-ubiquinone oxidoreductase 75 kDa subunit, mitochondrial (EC 1.6.5.3); - OS=Homo sapiens (Human).	66.9	1	1
216	B4DJD7_HUMAN	SubName: Full=cDNA FLJ52505, highly similar to Homo sapiens lectin, galactoside-binding, soluble 9, transcript variant short, mRNA; - OS=Homo sapiens (Human).	29.9	2	2
217	B4DJI2_HUMAN	SubName: Full=cDNA FLJ53342, highly similar to Granulins; - OS=Homo sapiens (Human).	56.8	4	4
218	B4DJV2_HUMAN	RecName: Full=Citrate synthase; - OS=Homo sapiens (Human).	50.4	5	4
219	B4DKS8_HUMAN	SubName: Full=cDNA FLJ57121, highly similar to Heterogeneous nuclear ribonucleoprotein F; - OS=Homo sapiens (Human).	37.2	2	1
220	B4DL14_HUMAN	RecName: Full=ATP synthase gamma chain; - OS=Homo sapiens (Human).	27.5	3	3
221	B4DL49_HUMAN	SubName: Full=cDNA FLJ58073, moderately similar to Cathepsin B (EC 3.4.22.1); - OS=Homo sapiens (Human).	30.7	6	6
222	B4DLI2_HUMAN	SubName: Full=cDNA FLJ55714, highly similar to Dolichyl-diphosphooligosaccharide--protein glycosyltransferase 48 kDa subunit (EC 2.4.1.119); - OS=Homo sapiens (Human).	48.9	4	4
223	B4DLL8_HUMAN	SubName: Full=cDNA FLJ59335, highly similar to Transmembrane glycoprotein NMB; - OS=Homo sapiens (Human).	50.5	2	2
224	B4DLW8_HUMAN	SubName: Full=Probable ATP-dependent RNA helicase DDX5; SubName: Full=cDNA FLJ59339,	60.5	3	1

		highly similar to Probable ATP-dependent RNA helicase DDX5 (EC 3.6.1.-); - OS=Homo sapiens (Human).			
225	B4DLX4_HUMAN	SubName: Full=cDNA FLJ54021, highly similar to Dipeptidyl-peptidase 3 (EC 3.4.14.4); - OS=Homo sapiens (Human).	79.2	1	1
226	B4DM33_HUMAN	SubName: Full=cDNA FLJ52068, highly similar to Microtubule-associated protein RP/EB family member 1; - OS=Homo sapiens (Human).	26.6	1	1
227	B4DMA2_HUMAN	RecName: Full=Chaperone protein HtpG B; AltName: Full=Heat shock protein HtpG B; AltName: Full=High temperature protein G B; - OS=Homo sapiens (Human).	79.1	13	6
228	B4DMQ7_HUMAN	SubName: Full=Tumor protein p53 inducible protein 3, isoform CRA_c; SubName: Full=cDNA FLJ61719, highly similar to quinone oxidoreductase (EC 1.-.-.-); - OS=Homo sapiens (Human).	26.8	1	1
229	B4DMT4_HUMAN	SubName: Full=cDNA FLJ52695, highly similar to Alpha-centractin; - OS=Homo sapiens (Human).	34.5	1	1
230	B4DN40_HUMAN	SubName: Full=cDNA FLJ54368, highly similar to Phosphoglucomutase-2 (EC 5.4.2.2); - OS=Homo sapiens (Human).	50.7	1	1
231	B4DN45_HUMAN	RecName: Full=S-adenosylmethionine synthase; EC=2.5.1.6; - OS=Homo sapiens (Human).	32.9	1	1
232	B4DNR3_HUMAN	SubName: Full=cDNA FLJ52710, highly similar to Abhydrolase domain-containing protein 14B; - OS=Homo sapiens (Human).	19.8	1	1
233	B4DNS2_HUMAN	SubName: Full=cDNA FLJ51602, highly similar to Interferon-induced guanylate-binding protein 1; - OS=Homo sapiens (Human).	41.2	2	1
234	B4DNS3_HUMAN	SubName: Full=cDNA FLJ50593, moderately similar to Pulmonary surfactant-associated protein A1; - OS=Homo sapiens (Human).	20.1	3	3
235	B4DP50_HUMAN	RecName: Full=Proline--tRNA ligase A; EC=6.1.1.15; AltName: Full=Prolyl-tRNA synthetase A; - OS=Homo sapiens (Human).	54.1	1	1
236	B4DPJ2_HUMAN	RecName: Full=Annexin; - OS=Homo sapiens (Human).	45.6	4	4
237	B4DPN0_HUMAN	SubName: Full=cDNA FLJ51265, moderately similar to Beta-2-glycoprotein 1 (Beta-2-glycoprotein I); - OS=Homo sapiens (Human).	30.3	4	4

238	B4DQ03_HUMAN	SubName: Full=cDNA FLJ57859, highly similar to Ras-related GTP-binding protein C; - OS=Homo sapiens (Human).	31.7	1	1
239	B4DQH4_HUMAN	SubName: Full=T-complex protein 1 subunit theta; SubName: Full=cDNA FLJ59382, highly similar to T-complex protein 1 subunit theta; - OS=Homo sapiens (Human).	51.6	2	2
240	B4DQJ8_HUMAN	RecName: Full=6-phosphogluconate dehydrogenase, decarboxylating; EC=1.1.1.44; - OS=Homo sapiens (Human).	51.8	6	6
241	B4DQT8_HUMAN	SubName: Full=cDNA FLJ61158, highly similar to ADP-ribosylation factor-like protein 8B; - OS=Homo sapiens (Human).	20.6	2	2
242	B4DR31_HUMAN	SubName: Full=Dihydropyrimidinase-related protein 2; SubName: Full=cDNA FLJ53166, highly similar to Dihydropyrimidinase-related protein 2; - OS=Homo sapiens (Human).	58.1	10	10
243	B4DR68_HUMAN	RecName: Full=Chaperone protein HtpG C; AltName: Full=Heat shock protein HtpG C; AltName: Full=High temperature protein G C; - OS=Homo sapiens (Human).	74.2	3	2
244	B4DRD7_HUMAN	SubName: Full=cDNA FLJ54752, highly similar to Poly(rC)-binding protein 2; - OS=Homo sapiens (Human).	29.7	5	4
245	B4DRF4_HUMAN	SubName: Full=3-hydroxyacyl-CoA dehydratase 3; SubName: Full=cDNA FLJ54138, highly similar to Homo sapiens butyrate-induced transcript 1 (HSPC121), mRNA; - OS=Homo sapiens (Human).	36.4	1	1
246	B4DRK5_HUMAN	SubName: Full=cDNA FLJ59584, highly similar to Mitochondrial-processing peptidase alpha subunit, mitochondrial (EC 3.4.24.64); - OS=Homo sapiens (Human).	28.2	1	1
247	B4DS27_HUMAN	SubName: Full=cDNA FLJ51288, highly similar to Kinesin heavy chain; - OS=Homo sapiens (Human).	49.9	1	1
248	B4DS43_HUMAN	SubName: Full=cDNA FLJ51063, highly similar to Dihydrolipoyllysine-residue acetyltransferasecomponent of pyruvate dehydrogenase complex, mitochondrial (EC 2.3.1.12); - OS=Homo sapiens (Human).	44.6	2	2
249	B4DSA8_HUMAN	SubName: Full=cDNA FLJ51067, highly similar to DNA damage-binding protein 1; - OS=Homo sapiens (Human).	111.9	1	1

250	B4DSD8_HUMAN	RecName: Full=Phosphorylase; EC=2.4.1.1; - OS=Homo sapiens (Human).	85.7	2	1
251	B4DSE2_HUMAN	SubName: Full=cDNA FLJ57277, highly similar to Tripeptidyl-peptidase 1 (EC 3.4.14.9); - OS=Homo sapiens (Human).	41.6	6	6
252	B4DSF0_HUMAN	SubName: Full=cDNA FLJ56734, moderately similar to Sepiapterin reductase (EC 1.1.1.153); - OS=Homo sapiens (Human).	13.0	1	1
253	B4DSR6_HUMAN	SubName: Full=cDNA FLJ52684, highly similar to Dynein heavy chain, cytosolic; - OS=Homo sapiens (Human).	28.4	1	1
254	B4DSU9_HUMAN	SubName: Full=cDNA FLJ58421, highly similar to Cleavage and polyadenylation specificity factor 6; - OS=Homo sapiens (Human).	33.6	2	2
255	B4DSZ1_HUMAN	SubName: Full=cDNA FLJ54877, highly similar to Syntaxin-12; - OS=Homo sapiens (Human).	26.6	2	2
256	B4DT77_HUMAN	RecName: Full=Annexin; - OS=Homo sapiens (Human).	37.8	1	1
257	B4DTB1_HUMAN	SubName: Full=cDNA FLJ52936, weakly similar to Tropomyosin alpha-4 chain; - OS=Homo sapiens (Human).	17.6	3	1
258	B4DTT0_HUMAN	SubName: Full=cDNA FLJ51090, highly similar to N-acetylglucosamine-6-sulfatase (EC 3.1.6.14); - OS=Homo sapiens (Human).	53.4	6	6
259	B4DUB7_HUMAN	RecName: Full=Phosphorylase; EC=2.4.1.1; - OS=Homo sapiens (Human).	92.9	3	2
260	B4DUH1_HUMAN	SubName: Full=cDNA FLJ51323, highly similar to Short-chain specific acyl-CoA dehydrogenase, mitochondrial (EC 1.3.99.2); - OS=Homo sapiens (Human).	43.6	1	1
261	B4DUJ3_HUMAN	SubName: Full=cDNA FLJ52895, highly similar to Carbonic anhydrase 3 (EC 4.2.1.1); - OS=Homo sapiens (Human).	26.8	2	2
262	B4DUL5_HUMAN	SubName: Full=cDNA FLJ51625, highly similar to Ubiquinol-cytochrome-c reductase complex coreprotein I, mitochondrial (EC 1.10.2.2); - OS=Homo sapiens (Human).	40.3	5	5
263	B4DUP0_HUMAN	SubName: Full=cDNA FLJ59433, highly similar to Elongation factor 1-gamma; - OS=Homo sapiens (Human).	24.1	1	1
264	B4DV28_HUMAN	SubName: Full=cDNA FLJ54170, highly similar to Cytosolic nonspecific dipeptidase; - OS=Homo	51.5	5	5

		sapiens (Human).			
265	B4DVD8_HUMAN	SubName: Full=Caspase-1 subunit p10; SubName: Full=cDNA FLJ59442, highly similar to Caspase-1 (EC 3.4.22.36); - OS=Homo sapiens (Human).	33.0	3	3
266	B4DVE1_HUMAN	SubName: Full=cDNA FLJ53478, highly similar to Galectin-3-binding protein; - OS=Homo sapiens (Human).	64.1	4	4
267	B4DVS2_HUMAN	SubName: Full=cDNA FLJ57617; - OS=Homo sapiens (Human).	88.8	1	1
268	B4DVT4_HUMAN	SubName: Full=cDNA FLJ53761, highly similar to Macrosialin; - OS=Homo sapiens (Human).	34.6	1	1
269	B4DVZ4_HUMAN	RecName: Full=Sulfurtransferase; - OS=Homo sapiens (Human).	27.7	1	1
270	B4DW52_HUMAN	SubName: Full=cDNA FLJ55253, highly similar to Actin, cytoplasmic 1; - OS=Homo sapiens (Human).	38.6	13	7
271	B4DW94_HUMAN	SubName: Full=Ras-related protein Rap-1b; SubName: Full=cDNA FLJ50714, moderately similar to Ras-related protein Rap-1b; - OS=Homo sapiens (Human).	15.3	5	5
272	B4DWD1_HUMAN	SubName: Full=cDNA FLJ60919, highly similar to Cytochrome b-245 heavy chain; - OS=Homo sapiens (Human).	35.1	3	3
273	B4DWM8_HUMAN	SubName: Full=cDNA FLJ56259, highly similar to Vacuolar ATP synthase subunit S1 (EC 3.6.3.14); - OS=Homo sapiens (Human).	32.9	1	1
274	B4DWN0_HUMAN	SubName: Full=cDNA FLJ51351, highly similar to GTPase, IMAP family member 4; - OS=Homo sapiens (Human).	29.9	1	1
275	B4DWN1_HUMAN	SubName: Full=cDNA FLJ52285, highly similar to Vesicular integral-membrane protein VIP36; - OS=Homo sapiens (Human).	32.6	3	3
276	B4DWS6_HUMAN	SubName: Full=cDNA FLJ61181, highly similar to Homo sapiens hydroxysteroid (17-beta) dehydrogenase 12 (HSD17B12), mRNA; - OS=Homo sapiens (Human).	33.5	2	2
277	B4DWU0_HUMAN	SubName: Full=cDNA FLJ56791, highly similar to Keratin, type I cytoskeletal 16; - OS=Homo sapiens (Human).	15.7	3	1
278	B4DWV5_HUMAN	RecName: Full=Protein GrpE A; AltName: Full=HSP-70 cofactor A; - OS=Homo sapiens (Human).	21.9	1	1

279	B4DWX6_HUMAN	SubName: Full=cDNA FLJ53936, highly similar to Medium-chain specific acyl-CoA dehydrogenase, mitochondrial (EC 1.3.99.3); - OS=Homo sapiens (Human).	42.5	4	4
280	B4DXC4_HUMAN	SubName: Full=cDNA FLJ58636, moderately similar to Atlastin; - OS=Homo sapiens (Human).	58.7	3	3
281	B4DXN0_HUMAN	SubName: Full=cDNA FLJ53371, highly similar to Major vault protein; - OS=Homo sapiens (Human).	92.7	5	5
282	B4DY09_HUMAN	SubName: Full=cDNA FLJ51660, highly similar to Interleukin enhancer-binding factor 2; - OS=Homo sapiens (Human).	38.9	1	1
283	B4DY46_HUMAN	SubName: Full=cDNA FLJ53447, highly similar to Syntaxin-binding protein 2; - OS=Homo sapiens (Human).	62.7	3	3
284	B4DZ08_HUMAN	SubName: Full=cDNA FLJ51705, highly similar to Aconitate hydratase, mitochondrial (EC 4.2.1.3); - OS=Homo sapiens (Human).	83.4	8	8
285	B4DZW6_HUMAN	SubName: Full=Regulator of microtubule dynamics protein 1; SubName: Full=cDNA FLJ53118, highly similar to Protein FAM82B; - OS=Homo sapiens (Human).	32.3	2	2
286	B4E022_HUMAN	SubName: Full=Transketolase; SubName: Full=cDNA FLJ56274, highly similar to Transketolase (EC 2.2.1.1); - OS=Homo sapiens (Human).	62.8	11	11
287	B4E054_HUMAN	SubName: Full=cDNA FLJ58444, highly similar to Vacuolar ATP synthase subunit H (EC 3.6.3.14); - OS=Homo sapiens (Human).	52.7	4	4
288	B4E0K9_HUMAN	SubName: Full=cDNA FLJ54572, highly similar to Lysosomal alpha-mannosidase (EC 3.2.1.24); - OS=Homo sapiens (Human).	107.4	4	4
289	B4E0N6_HUMAN	SubName: Full=cDNA FLJ56280, highly similar to Endoplasmic reticulum-Golgi intermediate compartment protein 1; - OS=Homo sapiens (Human).	26.2	1	1
290	B4E0R1_HUMAN	RecName: Full=Integrin beta; - OS=Homo sapiens (Human).	77.3	7	7
291	B4E108_HUMAN	SubName: Full=cDNA FLJ61026, highly similar to Homo sapiens phosphofructokinase, liver (PFKL), transcript variant 1, mRNA; - OS=Homo sapiens (Human).	26.9	1	1
292	B4E1D8_HUMAN	SubName: Full=cDNA FLJ51597, highly similar to C4b-binding protein alpha chain; - OS=Homo	60.4	1	1

		sapiens (Human).			
293	B4E1F5_HUMAN	SubName: Full=cDNA FLJ57475, highly similar to Pulmonary surfactant-associated protein B; - OS=Homo sapiens (Human).	38.5	5	5
294	B4E1K7_HUMAN	SubName: Full=Stomatin-like protein 2; SubName: Full=cDNA FLJ61039, highly similar to Stomatin-like protein 2; - OS=Homo sapiens (Human).	33.3	1	1
295	B4E1X2_HUMAN	SubName: Full=cDNA FLJ51620, highly similar to Coatomer subunit delta; - OS=Homo sapiens (Human).	47.2	2	2
296	B4E216_HUMAN	SubName: Full=cDNA FLJ57339, highly similar to Complement C3; - OS=Homo sapiens (Human).	122.5	2	2
297	B4E261_HUMAN	SubName: Full=cDNA FLJ55646, highly similar to Adapter-relatedprotein complex 2 beta-1 subunit; - OS=Homo sapiens (Human).	76.2	4	2
298	B4E2S7_HUMAN	SubName: Full=Lysosome-associated membrane glycoprotein 2; SubName: Full=cDNA FLJ58780, highly similar to Homo sapiens lysosomal-associated membrane protein 2 (LAMP2), transcript variant LAMP2B, mRNA; - OS=Homo sapiens (Human).	39.8	2	2
299	B4E2T4_HUMAN	SubName: Full=cDNA FLJ54121, highly similar to Cysteine and glycine-rich protein 1; - OS=Homo sapiens (Human).	15.0	2	2
300	B4E2V5_HUMAN	SubName: Full=Erythrocyte band 7 integral membrane protein; SubName: Full=Uncharacterized protein; SubName: Full=cDNA FLJ52062, highly similar to Erythrocyte band 7 integral membrane protein; - OS=Homo sapiens (Human).	25.9	3	3
301	B4E2W0_HUMAN	SubName: Full=3-ketoacyl-CoA thiolase; SubName: Full=cDNA FLJ56214, highly similar to Trifunctional enzyme subunit beta, mitochondrial; - OS=Homo sapiens (Human).	48.8	7	7
302	B4E2Y1_HUMAN	SubName: Full=cDNA FLJ52879, highly similar to Peroxisome proliferator-activated receptordelta; - OS=Homo sapiens (Human).	38.8	1	1
303	B4E2Z3_HUMAN	SubName: Full=cDNA FLJ54090, highly similar to 4F2 cell-surface antigen heavy chain; - OS=Homo sapiens (Human).	55.9	2	2
304	B4E324_HUMAN	SubName: Full=cDNA FLJ60397, highly similar to Lysosomal protective protein (EC 3.4.16.5); -	54.2	3	3

		OS=Homo sapiens (Human).			
305	B4E363_HUMAN	SubName: Full=Phenylalanine--tRNA ligase alpha subunit; SubName: Full=cDNA FLJ50378, highly similar to Phenylalanyl-tRNA synthetase alpha chain (EC 6.1.1.20); - OS=Homo sapiens (Human).	54.1	1	1
306	B4E380_HUMAN	RecName: Full=Histone H3; - OS=Homo sapiens (Human).	12.9	2	2
307	B4E3A8_HUMAN	SubName: Full=cDNA FLJ53963, highly similar to Leukocyte elastase inhibitor; - OS=Homo sapiens (Human).	38.7	2	2
308	B4E3B6_HUMAN	SubName: Full=cDNA FLJ54408, highly similar to Heat shock 70 kDa protein 1; - OS=Homo sapiens (Human).	63.9	11	8
309	B4E3F7_HUMAN	SubName: Full=Muscleblind-like protein 2; SubName: Full=cDNA FLJ57455, moderately similar to Homo sapiens muscleblind-like 2 (Drosophila) (MBNL2), transcript variant 3, mRNA; - OS=Homo sapiens (Human).	23.0	1	1
310	B4E3M5_HUMAN	SubName: Full=cDNA FLJ57816, highly similar to Triple functional domain protein; - OS=Homo sapiens (Human).	174.8	2	1
311	B4E3Q4_HUMAN	SubName: Full=Adenosine deaminase CECR1; SubName: Full=cDNA FLJ58672, highly similar to Cat eye syndrome critical region protein 1; - OS=Homo sapiens (Human).	54.3	2	2
312	B5BU25_HUMAN	SubName: Full=U2 small nuclear RNA auxiliary factor 2 isoform b; - OS=Homo sapiens (Human).	53.1	2	2
313	B5MCP9_HUMAN	SubName: Full=40S ribosomal protein S7; - OS=Homo sapiens (Human).	21.3	1	1
314	B5MCX3_HUMAN	SubName: Full=Septin-2; - OS=Homo sapiens (Human).	36.9	5	5
315	B7Z1R5_HUMAN	SubName: Full=V-type proton ATPase catalytic subunit A; SubName: Full=cDNA FLJ51804, highly similar to Vacuolar ATP synthase catalytic subunit A, ubiquitous isoform (EC 3.6.3.14); - OS=Homo sapiens (Human).	64.7	7	7
316	B7Z238_HUMAN	SubName: Full=Bcl-2-like protein 13; SubName: Full=cDNA FLJ55839, highly similar to Bcl-2-like 13 protein; - OS=Homo sapiens (Human).	39.0	1	1
317	B7Z254_HUMAN	SubName: Full=Protein disulfide-isomerase A6; SubName: Full=cDNA FLJ58502, highly similar to Protein disulfide-isomerase A6 (EC 5.3.4.1); - OS=Homo sapiens (Human).	47.8	8	8

318	B7Z2E2_HUMAN	SubName: Full=cDNA FLJ54671, highly similar to Calcium-binding mitochondrial carrier protein Aralar2; - OS=Homo sapiens (Human).	62.2	1	1
319	B7Z2F4_HUMAN	RecName: Full=T-complex protein 1 subunit delta; - OS=Homo sapiens (Human).	42.3	1	1
320	B7Z361_HUMAN	SubName: Full=cDNA FLJ50772, highly similar to Reticulon-3; - OS=Homo sapiens (Human).	22.9	1	1
321	B7Z3Q4_HUMAN	SubName: Full=cDNA FLJ51873, highly similar to Alkyldihydroxyacetonephosphate synthase, peroxisomal (EC 2.5.1.26); - OS=Homo sapiens (Human).	63.8	4	4
322	B7Z438_HUMAN	SubName: Full=cDNA FLJ56352, highly similar to Succinyl-CoA ligase (GDP-forming) subunit alpha, mitochondrial (EC 6.2.1.4); - OS=Homo sapiens (Human).	26.5	1	1
323	B7Z478_HUMAN	SubName: Full=Proteasome (Prosome, macropain) subunit, beta type, 2, isoform CRA_b; SubName: Full=cDNA FLJ51890, highly similar to Proteasome subunit beta type 2 (EC 3.4.25.1); - OS=Homo sapiens (Human).	20.2	1	1
324	B7Z4K6_HUMAN	SubName: Full=Deoxyribonuclease-2-alpha; SubName: Full=cDNA FLJ51996, highly similar to Deoxyribonuclease-2-alpha (EC 3.1.22.1); - OS=Homo sapiens (Human).	33.6	2	2
325	B7Z4V2_HUMAN	RecName: Full=Chaperone protein DnaK A; AltName: Full=HSP70 A; AltName: Full=Heat shock 70 kDa protein A; AltName: Full=Heat shock protein 70 A; - OS=Homo sapiens (Human).	72.4	11	11
326	B7Z4Y1_HUMAN	SubName: Full=cDNA FLJ58031, highly similar to Tuftelin; - OS=Homo sapiens (Human).	46.4	1	1
327	B7Z4Y5_HUMAN	SubName: Full=cDNA FLJ51553, highly similar to HLA class II histocompatibility antigen, DMalpha chain; - OS=Homo sapiens (Human).	14.1	1	1
328	B7Z553_HUMAN	SubName: Full=cDNA FLJ51266, highly similar to Vitronectin; - OS=Homo sapiens (Human).	23.6	1	1
329	B7Z565_HUMAN	SubName: Full=cDNA FLJ54739, highly similar to Alpha-actinin-1; - OS=Homo sapiens (Human).	94.7	18	6
330	B7Z570_HUMAN	SubName: Full=cDNA FLJ53078, highly similar to Splicing factor, arginine/serine-rich 1; - OS=Homo sapiens (Human).	16.2	1	1
331	B7Z5C0_HUMAN	SubName: Full=DnaJ homolog subfamily A member 1; SubName: Full=cDNA FLJ52352, highly similar to DnaJ homolog subfamily A member 1; - OS=Homo sapiens (Human).	27.5	2	2
332	B7Z5E7_HUMAN	SubName: Full=cDNA FLJ51046, highly similar to 60 kDa heat shock protein, mitochondrial; -	55.0	13	13

		OS=Homo sapiens (Human).			
333	B7Z5N4_HUMAN	SubName: Full=cDNA FLJ51950, highly similar to Homo sapiens src family associated phosphoprotein 2 (SCAP2), mRNA; - OS=Homo sapiens (Human).	39.6	1	1
334	B7Z5P7_HUMAN	SubName: Full=Leupaxin; SubName: Full=cDNA FLJ51550, highly similar to Leupaxin; - OS=Homo sapiens (Human).	41.6	1	1
335	B7Z5V6_HUMAN	SubName: Full=cDNA FLJ57046, highly similar to Lysosomal alpha-glucosidase (EC 3.2.1.20); - OS=Homo sapiens (Human).	71.7	4	2
336	B7Z601_HUMAN	SubName: Full=cDNA FLJ57187, highly similar to Glycerol-3-phosphate dehydrogenase, mitochondrial (EC 1.1.99.5); - OS=Homo sapiens (Human).	55.7	8	8
337	B7Z6A4_HUMAN	SubName: Full=Surfeit 4, isoform CRA_c; SubName: Full=Surfeit locus protein 4; SubName: Full=Uncharacterized protein; SubName: Full=cDNA FLJ50656, highly similar to Surfeit locus protein 4; - OS=Homo sapiens (Human).	14.8	1	1
338	B7Z6A8_HUMAN	SubName: Full=Abhydrolase domain-containing protein 10, mitochondrial; SubName: Full=cDNA FLJ50858, highly similar to Homo sapiens abhydrolase domain containing 10 (ABHD10), mRNA; - OS=Homo sapiens (Human).	16.9	1	1
339	B7Z6B8_HUMAN	SubName: Full=2,4-dienoyl-CoA reductase, mitochondrial; SubName: Full=cDNA FLJ50204, highly similar to 2,4-dienoyl-CoA reductase, mitochondrial (EC 1.3.1.34); - OS=Homo sapiens (Human).	35.0	7	7
340	B7Z766_HUMAN	SubName: Full=cDNA FLJ54564, highly similar to 150 kDa oxygen-regulated protein (Orp150); - OS=Homo sapiens (Human).	94.1	2	2
341	B7Z7A9_HUMAN	RecName: Full=Phosphoglycerate kinase B; EC=2.7.2.3; - OS=Homo sapiens (Human).	41.4	9	9
342	B7Z7T2_HUMAN	SubName: Full=cDNA FLJ58709, highly similar to Homo sapiens neuropathy target esterase (NTE), mRNA; - OS=Homo sapiens (Human).	143.3	2	2
343	B7Z7X2_HUMAN	SubName: Full=cDNA FLJ52367, highly similar to Ras GTPase-activating-like protein IQGAP2; - OS=Homo sapiens (Human).	43.6	1	1
344	B7Z7Z9_HUMAN	SubName: Full=Shootin-1; SubName: Full=cDNA FLJ58712, highly similar to Mus musculus myosin,	56.3	1	1

		heavy polypeptide 9, non-muscle (Myh9), transcript variant 1, mRNA; - OS=Homo sapiens (Human).			
345	B7Z8D3_HUMAN	SubName: Full=Proteasome activator complex subunit 3; SubName: Full=cDNA FLJ57249, highly similar to Proteasome activator complex subunit 3; - OS=Homo sapiens (Human).	14.8	1	1
346	B7Z8T9_HUMAN	SubName: Full=cDNA FLJ52526, highly similar to Lysosomal acid phosphatase (EC 3.1.3.2); - OS=Homo sapiens (Human).	26.6	1	1
347	B7Z8Y6_HUMAN	SubName: Full=cDNA FLJ58394, highly similar to Platelet endothelial cell adhesion molecule; - OS=Homo sapiens (Human).	81.7	2	2
348	B7Z972_HUMAN	RecName: Full=Protein-L-isoaspartate O-methyltransferase; EC=2.1.1.77; - OS=Homo sapiens (Human).	20.7	1	1
349	B7Z992_HUMAN	SubName: Full=cDNA FLJ53698, highly similar to Gelsolin; - OS=Homo sapiens (Human).	78.8	12	12
350	B7ZAL5_HUMAN	SubName: Full=cDNA, FLJ79229, highly similar to Lactotransferrin (EC 3.4.21.-); - OS=Homo sapiens (Human).	73.1	6	6
351	B7ZB41_HUMAN	SubName: Full=cDNA, FLJ79405, highly similar to Homo sapiens solute carrier family 25, member 24, transcript variant 1, mRNA; - OS=Homo sapiens (Human).	53.3	9	9
352	B7ZBK6_HUMAN	SubName: Full=Aminolevulinate, delta-, dehydratase; SubName: Full=Delta-aminolevulinic acid dehydratase; Flags: Fragment; - OS=Homo sapiens (Human).	13.3	1	1
353	B7ZLF0_HUMAN	SubName: Full=Fibronectin 1; SubName: Full=Fibronectin 1, isoform CRA_g; - OS=Homo sapiens (Human).	239.5	10	10
354	B8XPJ7_HUMAN	SubName: Full=Soluble catechol-O-methyltransferase; - OS=Homo sapiens (Human).	24.5	4	4
355	B8XPR9_HUMAN	SubName: Full=MHC class I antigen; Flags: Fragment; - OS=Homo sapiens (Human).	31.6	3	1
356	B8ZZ35_HUMAN	SubName: Full=N-acetylgalactosaminidase, alpha-; Flags: Fragment; - OS=Homo sapiens (Human).	23.6	1	1
357	B8ZZ51_HUMAN	SubName: Full=Malate dehydrogenase, cytoplasmic; - OS=Homo sapiens (Human).	18.7	3	3
358	B8ZZU8_HUMAN	SubName: Full=Transcription elongation factor B (SIII), polypeptide 2 (18kDa, elongin B), isoform CRA_b; SubName: Full=Transcription elongation factor B polypeptide 2; - OS=Homo sapiens (Human).	12.5	1	1

359	B9EJA8_HUMAN	SubName: Full=Mannose receptor, C type 1-like 1; - OS=Homo sapiens (Human).	165.9	16	16
360	B9EJE3_HUMAN	SubName: Full=Putative uncharacterized protein; - OS=Homo sapiens (Human).	17.5	1	1
361	BGAL_HUMAN	RecName: Full=Beta-galactosidase; EC=3.2.1.23; AltName: Full=Acid beta-galactosidase; Short=Lactase; AltName: Full=Elastin receptor 1; Flags: Precursor; - OS=Homo sapiens (Human).	76.0	5	5
362	BIEA_HUMAN	RecName: Full=Biliverdin reductase A; Short=BVR A; EC=1.3.1.24; AltName: Full=Biliverdin-IX alpha-reductase; Flags: Precursor; - OS=Homo sapiens (Human).	33.4	3	3
363	BLVRB_HUMAN	RecName: Full=Flavin reductase (NADPH); Short=FR; EC=1.5.1.30; AltName: Full=Biliverdin reductase B; Short=BVR-B; EC=1.3.1.24; AltName: Full=Biliverdin-IX beta-reductase; AltName: Full=Green heme-binding protein; Short=GHBP; AltName: Full=NADPH-dependent diaphorase; AltName: Full=NADPH-flavin reductase; Short=FLR; - OS=Homo sapiens (Human).	22.1	4	4
364	BOLA2_HUMAN	RecName: Full=BolA-like protein 2; - OS=Homo sapiens (Human).	10.1	1	1
365	C0H5Y3_HUMAN	SubName: Full=Natural resistance-associated macrophage protein 1; SubName: Full=SLC11A1 protein; SubName: Full=Solute carrier family 11 (Proton-coupled divalent metal ion transporters), member 1, isoform CRA_a; - OS=Homo sapiens (Human).	47.3	1	1
366	C1KJL2_HUMAN	SubName: Full=MHC class I antigen; Flags: Fragment; - OS=Homo sapiens (Human).	21.0	2	0
367	C1TC_HUMAN	RecName: Full=C-1-tetrahydrofolate synthase, cytoplasmic; Short=C1-THF synthase; Includes: RecName: Full=Methylenetetrahydrofolate dehydrogenase; EC=1.5.1.5; Includes: RecName: Full=Methenyltetrahydrofolate cyclohydrolase; EC=3.5.4.9; Includes: RecName: Full=Formyltetrahydrofolate synthetase; EC=6.3.4.3; - OS=Homo sapiens (Human).	101.5	5	5
368	C6KXN3_HUMAN	SubName: Full=Lambda light chain of human immunoglobulin surface antigen-related protein; Flags: Fragment; - OS=Homo sapiens (Human).	24.7	4	4
369	C9J0D1_HUMAN	RecName: Full=Histone H2A; - OS=Homo sapiens (Human).	13.2	3	1
370	C9J0K6_HUMAN	SubName: Full=Sorcin; - OS=Homo sapiens (Human).	17.6	2	2
371	C9J3L8_HUMAN	SubName: Full=Translocon-associated protein subunit alpha; - OS=Homo sapiens (Human).	29.6	3	3
372	C9J815_HUMAN	SubName: Full=Apolipoprotein B receptor; - OS=Homo sapiens (Human).	113.0	5	5

373	C9J8F3_HUMAN	SubName: Full=Fructose-bisphosphate aldolase C; Flags: Fragment; - OS=Homo sapiens (Human).	16.3	1	1
374	C9J8H9_HUMAN	SubName: Full=ATP synthase subunit f, mitochondrial; - OS=Homo sapiens (Human).	5.7	1	1
375	C9J9K3_HUMAN	SubName: Full=40S ribosomal protein SA; Flags: Fragment; - OS=Homo sapiens (Human).	29.5	5	5
376	C9JAQ9_HUMAN	SubName: Full=U5 small nuclear ribonucleoprotein 200 kDa helicase; - OS=Homo sapiens (Human).	71.4	1	1
377	C9JBL0_HUMAN	SubName: Full=Nuclear autoantigen Sp-100; Flags: Fragment; - OS=Homo sapiens (Human).	22.0	1	1
378	C9JCN0_HUMAN	SubName: Full=Myoferlin; - OS=Homo sapiens (Human).	233.3	14	14
379	C9JDR0_HUMAN	SubName: Full=Sterol-4-alpha-carboxylate 3-dehydrogenase, decarboxylating; Flags: Fragment; - OS=Homo sapiens (Human).	28.1	1	1
380	C9JFR7_HUMAN	SubName: Full=Cytochrome c; Flags: Fragment; - OS=Homo sapiens (Human).	11.3	5	5
381	C9JGI3_HUMAN	SubName: Full=Thymidine phosphorylase; Flags: Fragment; - OS=Homo sapiens (Human).	46.1	9	9
382	C9JH92_HUMAN	SubName: Full=Quinone oxidoreductase; Flags: Fragment; - OS=Homo sapiens (Human).	21.9	1	1
383	C9JIS1_HUMAN	SubName: Full=Guanine nucleotide-binding protein G(I)/G(S)/G(T) subunit beta-2; Flags: Fragment; - OS=Homo sapiens (Human).	25.5	2	1
384	C9JJ34_HUMAN	SubName: Full=Ran-specific GTPase-activating protein; Flags: Fragment; - OS=Homo sapiens (Human).	18.8	1	1
385	C9JJ47_HUMAN	SubName: Full=AP-2 complex subunit mu; Flags: Fragment; - OS=Homo sapiens (Human).	28.8	1	1
386	C9JJK5_HUMAN	SubName: Full=Zyxin; Flags: Fragment; - OS=Homo sapiens (Human).	19.1	1	1
387	C9JL12_HUMAN	SubName: Full=Prolyl 4-hydroxylase subunit alpha-1; - OS=Homo sapiens (Human).	58.9	1	1
388	C9JMD7_HUMAN	SubName: Full=B-cell receptor-associated protein 31; Flags: Fragment; - OS=Homo sapiens (Human).	20.2	1	1
389	C9JPM4_HUMAN	SubName: Full=ADP-ribosylation factor 4; Flags: Fragment; - OS=Homo sapiens (Human).	14.5	5	3
390	C9JTK6_HUMAN	SubName: Full=Obg-like ATPase 1; Flags: Fragment; - OS=Homo sapiens (Human).	12.3	1	1
391	C9JTV7_HUMAN	SubName: Full=Ephexin-1; Flags: Fragment; - OS=Homo sapiens (Human).	22.0	1	1
392	C9JW96_HUMAN	SubName: Full=Prohibitin; Flags: Fragment; - OS=Homo sapiens (Human).	26.9	7	7
393	CA031_HUMAN	RecName: Full=Uncharacterized protein C1orf31; - OS=Homo sapiens (Human).	14.1	2	2
394	CAH1_HUMAN	RecName: Full=Carbonic anhydrase 1; EC=4.2.1.1; AltName: Full=Carbonate dehydratase I;	28.9	9	9

		AltName: Full=Carbonic anhydrase B; Short=CAB; AltName: Full=Carbonic anhydrase I; Short=CA-I; - OS=Homo sapiens (Human).			
395	CAH2_HUMAN	RecName: Full=Carbonic anhydrase 2; EC=4.2.1.1; AltName: Full=Carbonate dehydratase II; AltName: Full=Carbonic anhydrase C; Short=CAC; AltName: Full=Carbonic anhydrase II; Short=CA-II; - OS=Homo sapiens (Human).	29.2	9	9
396	CALX_HUMAN	RecName: Full=Calnexin; AltName: Full=IP90; AltName: Full=Major histocompatibility complex class I antigen-binding protein p88; AltName: Full=p90; Flags: Precursor; - OS=Homo sapiens (Human).	67.5	7	7
397	CATA_HUMAN	RecName: Full=Catalase; EC=1.11.1.6; - OS=Homo sapiens (Human).	59.7	16	16
398	CATD_HUMAN	RecName: Full=Cathepsin D; EC=3.4.23.5; Contains: RecName: Full=Cathepsin D light chain; Contains: RecName: Full=Cathepsin D heavy chain; Flags: Precursor; - OS=Homo sapiens (Human).	44.5	11	11
399	CATH_HUMAN	RecName: Full=Pro-cathepsin H; Contains: RecName: Full=Cathepsin H mini chain; Contains: RecName: Full=Cathepsin H; EC=3.4.22.16; Contains: RecName: Full=Cathepsin H heavy chain; Contains: RecName: Full=Cathepsin H light chain; Flags: Precursor; - OS=Homo sapiens (Human).	37.4	5	5
400	CATS_HUMAN	RecName: Full=Cathepsin S; EC=3.4.22.27; Flags: Precursor; - OS=Homo sapiens (Human).	37.5	5	5
401	CATZ_HUMAN	RecName: Full=Cathepsin Z; EC=3.4.18.1; AltName: Full=Cathepsin P; AltName: Full=Cathepsin X; Flags: Precursor; - OS=Homo sapiens (Human).	33.8	2	2
402	CAZA2_HUMAN	RecName: Full=F-actin-capping protein subunit alpha-2; AltName: Full=CapZ alpha-2; - OS=Homo sapiens (Human).	32.9	3	2
403	CBR1_HUMAN	RecName: Full=Carbonyl reductase [NADPH] 1; EC=1.1.1.184; AltName: Full=15-hydroxyprostaglandin dehydrogenase [NADP(+)]; EC=1.1.1.197; AltName: Full=NADPH-dependent carbonyl reductase 1; AltName: Full=Prostaglandin 9-ketoreductase; AltName: Full=Prostaglandin-E(2) 9-reductase; EC=1.1.1.189; - OS=Homo sapiens (Human).	30.4	3	3
404	CD47_HUMAN	RecName: Full=Leukocyte surface antigen CD47; AltName: Full=Antigenic surface determinant protein OA3; AltName: Full=Integrin-associated protein; Short=IAP; AltName: Full=Protein MER6;	35.2	1	1

		AltName: CD_antigen=CD47; Flags: Precursor; - OS=Homo sapiens (Human).			
405	CDC42_HUMAN	RecName: Full=Cell division control protein 42 homolog; AltName: Full=G25K GTP-binding protein; Flags: Precursor; - OS=Homo sapiens (Human).	21.2	3	2
406	CHCH3_HUMAN	RecName: Full=Coiled-coil-helix-coiled-coil-helix domain-containing protein 3, mitochondrial; - OS=Homo sapiens (Human).	26.1	2	2
407	CHID1_HUMAN	RecName: Full=Chitinase domain-containing protein 1; AltName: Full=Stabilin-1-interacting chitinase-like protein; Short=SI-CLP; Flags: Precursor; - OS=Homo sapiens (Human).	44.9	1	1
408	CK5P3_HUMAN	RecName: Full=CDK5 regulatory subunit-associated protein 3; AltName: Full=CDK5 activator-binding protein C53; AltName: Full=Protein HSF-27; - OS=Homo sapiens (Human).	56.9	2	2
409	CLH1_HUMAN	RecName: Full=Clathrin heavy chain 1; AltName: Full=Clathrin heavy chain on chromosome 17; Short=CLH-17; - OS=Homo sapiens (Human).	191.5	30	30
410	CLIC1_HUMAN	RecName: Full=Chloride intracellular channel protein 1; AltName: Full=Chloride channel ABP; AltName: Full=Nuclear chloride ion channel 27; Short=NCC27; AltName: Full=Regulatory nuclear chloride ion channel protein; Short=hRNCC; - OS=Homo sapiens (Human).	26.9	5	5
411	CNOT1_HUMAN	RecName: Full=CCR4-NOT transcription complex subunit 1; AltName: Full=CCR4-associated factor 1; AltName: Full=Negative regulator of transcription subunit 1 homolog; Short=NOT1H; Short=hNOT1; - OS=Homo sapiens (Human).	266.8	1	1
412	COPB_HUMAN	RecName: Full=Coatomer subunit beta; AltName: Full=Beta-coat protein; Short=Beta-COP; - OS=Homo sapiens (Human).	107.1	1	1
413	COR1A_HUMAN	RecName: Full=Coronin-1A; AltName: Full=Coronin-like protein A; Short=Clipin-A; AltName: Full=Coronin-like protein p57; AltName: Full=Tryptophan aspartate-containing coat protein; Short=TACO; - OS=Homo sapiens (Human).	51.0	2	2
414	COTL1_HUMAN	RecName: Full=Coactosin-like protein; - OS=Homo sapiens (Human).	15.9	5	5
415	COX41_HUMAN	RecName: Full=Cytochrome c oxidase subunit 4 isoform 1, mitochondrial; AltName: Full=Cytochrome c oxidase polypeptide IV; AltName: Full=Cytochrome c oxidase subunit IV isoform	19.6	2	2

		1; Short=COX IV-1; Flags: Precursor; - OS=Homo sapiens (Human).			
416	COX5B_HUMAN	RecName: Full=Cytochrome c oxidase subunit 5B, mitochondrial; AltName: Full=Cytochrome c oxidase polypeptide Vb; Flags: Precursor; - OS=Homo sapiens (Human).	13.7	3	3
417	CP27A_HUMAN	RecName: Full=Sterol 26-hydroxylase, mitochondrial; EC=1.14.13.15; AltName: Full=5-beta-cholestane-3-alpha,7-alpha,12-alpha-triol 27-hydroxylase; AltName: Full=Cytochrome P-450C27/25; AltName: Full=Cytochrome P450 27; AltName: Full=Sterol 27-hydroxylase; AltName: Full=Vitamin D(3) 25-hydroxylase; Flags: Precursor; - OS=Homo sapiens (Human).	60.2	7	7
418	CP2S1_HUMAN	RecName: Full=Cytochrome P450 2S1; EC=1.14.14.1; AltName: Full=CYPIIS1; - OS=Homo sapiens (Human).	55.8	1	1
419	CPNS1_HUMAN	RecName: Full=Calpain small subunit 1; Short=CSS1; AltName: Full=Calcium-activated neutral proteinase small subunit; Short=CANP small subunit; AltName: Full=Calcium-dependent protease small subunit; Short=CDPS; AltName: Full=Calcium-dependent protease small subunit 1; AltName: Full=Calpain regulatory subunit; - OS=Homo sapiens (Human).	28.3	2	2
420	CREG1_HUMAN	RecName: Full=Protein CREG1; AltName: Full=Cellular repressor of E1A-stimulated genes 1; Flags: Precursor; - OS=Homo sapiens (Human).	24.1	2	2
421	CS010_HUMAN	RecName: Full=UPF0556 protein C19orf10; AltName: Full=Interleukin-25; Short=IL-25; AltName: Full=Stromal cell-derived growth factor SF20; Flags: Precursor; - OS=Homo sapiens (Human).	18.8	2	2
422	CT027_HUMAN	RecName: Full=UPF0687 protein C20orf27; - OS=Homo sapiens (Human).	19.3	1	1
423	CUTA_HUMAN	RecName: Full=Protein CutA; AltName: Full=Acetylcholinesterase-associated protein; AltName: Full=Brain acetylcholinesterase putative membrane anchor; Flags: Precursor; - OS=Homo sapiens (Human).	19.1	2	2
424	CX6B1_HUMAN	RecName: Full=Cytochrome c oxidase subunit 6B1; AltName: Full=Cytochrome c oxidase subunit VIb isoform 1; Short=COX VIb-1; - OS=Homo sapiens (Human).	10.2	3	3
425	CX7A2_HUMAN	RecName: Full=Cytochrome c oxidase subunit 7A2, mitochondrial; AltName: Full=Cytochrome c oxidase subunit VIIa-liver/heart; Short=Cytochrome c oxidase subunit VIIa-L; Short=Cytochrome c	9.4	2	2

		oxidase subunit VIIaL; Flags: Precursor; - OS=Homo sapiens (Human).			
426	CYTB_HUMAN	RecName: Full=Cystatin-B; AltName: Full=CPI-B; AltName: Full=Liver thiol proteinase inhibitor; AltName: Full=Stefin-B; - OS=Homo sapiens (Human).	11.1	3	3
427	CYTC_HUMAN	RecName: Full=Cystatin-C; AltName: Full=Cystatin-3; AltName: Full=Gamma-trace; AltName: Full=Neuroendocrine basic polypeptide; AltName: Full=Post-gamma-globulin; Flags: Precursor; - OS=Homo sapiens (Human).	15.8	1	1
428	D2Y6Y7_HUMAN	SubName: Full=ATP synthase subunit 6; Flags: Fragment; - OS=Homo sapiens (Human).	5.1	1	1
429	D3DP13_HUMAN	SubName: Full=Fibrinogen beta chain, isoform CRA_e; - OS=Homo sapiens (Human).	39.7	2	2
430	D3DP16_HUMAN	SubName: Full=Fibrinogen gamma chain, isoform CRA_a; - OS=Homo sapiens (Human).	37.7	3	3
431	D3DUJ0_HUMAN	SubName: Full=AFG3 ATPase family gene 3-like 2 (Yeast), isoform CRA_a; Flags: Fragment; - OS=Homo sapiens (Human).	84.4	3	3
432	D3DV53_HUMAN	SubName: Full=S100 calcium binding protein A13, isoform CRA_a; Flags: Fragment; - OS=Homo sapiens (Human).	5.8	1	1
433	D3DVH1_HUMAN	SubName: Full=Succinate dehydrogenase complex, subunit C, integral membrane protein, 15kDa, isoform CRA_a; - OS=Homo sapiens (Human).	11.3	1	1
434	D3DW07_HUMAN	SubName: Full=Putative uncharacterized protein RP5-1022P6.2; - OS=Homo sapiens (Human).	45.2	1	1
435	D3YTB1_HUMAN	SubName: Full=60S ribosomal protein L32; Flags: Fragment; - OS=Homo sapiens (Human).	15.6	1	1
436	D5KJA2_HUMAN	SubName: Full=Dehydrogenase/reductase (SDR family) member 4 like 2A; - OS=Homo sapiens (Human).	15.2	2	2
437	D6CHE9_HUMAN	SubName: Full=Proteinase 3; SubName: Full=Proteinase 3 (Serine proteinase, neutrophil, Wegener granulomatosis autoantigen), isoform CRA_a; - OS=Homo sapiens (Human).	23.6	1	1
438	D6R937_HUMAN	SubName: Full=Endothelial monocyte-activating polypeptide 2; Flags: Fragment; - OS=Homo sapiens (Human).	16.6	1	1
439	D6R9B6_HUMAN	SubName: Full=40S ribosomal protein S3a; SubName: Full=Ribosomal protein S3A, isoform CRA_e; - OS=Homo sapiens (Human).	16.5	2	2

440	D6R9P3_HUMAN	SubName: Full=Heterogeneous nuclear ribonucleoprotein A/B; - OS=Homo sapiens (Human).	30.3	2	1
441	D6RA08_HUMAN	SubName: Full=Complement C1q subcomponent subunit B; Flags: Fragment; - OS=Homo sapiens (Human).	24.1	1	1
442	D6RAA2_HUMAN	SubName: Full=GTP-binding protein SAR1b; Flags: Fragment; - OS=Homo sapiens (Human).	11.5	1	1
443	D6RAA6_HUMAN	SubName: Full=Transmembrane protein 33; Flags: Fragment; - OS=Homo sapiens (Human).	25.2	2	2
444	D6RAW0_HUMAN	SubName: Full=Ubiquitin-conjugating enzyme E2 D3; Flags: Fragment; - OS=Homo sapiens (Human).	8.2	1	1
445	D6RBB5_HUMAN	SubName: Full=Microsomal glutathione S-transferase 2; - OS=Homo sapiens (Human).	8.4	1	1
446	D6RDU5_HUMAN	SubName: Full=Septin-11; Flags: Fragment; - OS=Homo sapiens (Human).	43.1	2	1
447	D6RE99_HUMAN	SubName: Full=Histidine triad nucleotide-binding protein 1; - OS=Homo sapiens (Human).	8.6	2	2
448	D6RF23_HUMAN	SubName: Full=Guanine nucleotide-binding protein subunit beta-2-like 1; - OS=Homo sapiens (Human).	11.2	2	2
449	D6RF44_HUMAN	SubName: Full=Heterogeneous nuclear ribonucleoprotein D0; Flags: Fragment; - OS=Homo sapiens (Human).	12.6	3	2
450	D6RFM5_HUMAN	SubName: Full=Succinate dehydrogenase [ubiquinone] flavoprotein subunit, mitochondrial; - OS=Homo sapiens (Human).	63.5	4	4
451	D6RG00_HUMAN	SubName: Full=Ubiquitin-conjugating enzyme E2 variant 1; - OS=Homo sapiens (Human).	10.1	1	1
452	D6RHZ5_HUMAN	SubName: Full=Protein transport protein Sec31A; - OS=Homo sapiens (Human).	96.4	1	1
453	D6RIZ4_HUMAN	SubName: Full=Major facilitator superfamily domain-containing protein 10; - OS=Homo sapiens (Human).	38.2	1	1
454	D6RJD1_HUMAN	SubName: Full=Clathrin light chain B; Flags: Fragment; - OS=Homo sapiens (Human).	13.1	1	1
455	D6W507_HUMAN	SubName: Full=HCG1990625, isoform CRA_a; - OS=Homo sapiens (Human).	16.6	2	2
456	D7GNM6_HUMAN	SubName: Full=MHC class I antigen; Flags: Fragment; - OS=Homo sapiens (Human).	31.7	6	1
457	DDRGK_HUMAN	RecName: Full=DDRGK domain-containing protein 1; Flags: Precursor; - OS=Homo sapiens (Human).	35.6	2	2

458	DEF1_HUMAN	RecName: Full=Neutrophil defensin 1; AltName: Full=Defensin, alpha 1; AltName: Full=HNP-1; Short=HP-1; Short=HP1; Contains: RecName: Full=HP 1-56; Contains: RecName: Full=Neutrophil defensin 2; AltName: Full=HNP-2; Short=HP-2; Short=HP2; Flags: Precursor; - OS=Homo sapiens (Human).	10.2	1	1
459	DHB11_HUMAN	RecName: Full=Estradiol 17-beta-dehydrogenase 11; EC=1.1.1.62; AltName: Full=17-beta-hydroxysteroid dehydrogenase 11; Short=17-beta-HSD 11; Short=17bHSD11; Short=17betaHSD11; AltName: Full=17-beta-hydroxysteroid dehydrogenase XI; Short=17-beta-HSD XI; Short=17betaHSDXI; AltName: Full=Cutaneous T-cell lymphoma-associated antigen HD-CL-03; Short=CTCL-associated antigen HD-CL-03; AltName: Full=Dehydrogenase/reductase SDR family member 8; AltName: Full=Retinal short-chain dehydrogenase/reductase 2; Short=retSDR2; Flags: Precursor; - OS=Homo sapiens (Human).	32.9	5	5
460	DHX9_HUMAN	RecName: Full=ATP-dependent RNA helicase A; Short=RHA; EC=3.6.4.13; AltName: Full=DEAH box protein 9; AltName: Full=Leukophysin; Short=LKP; AltName: Full=Nuclear DNA helicase II; Short=NDH II; - OS=Homo sapiens (Human).	140.9	6	6
461	DLRB1_HUMAN	RecName: Full=Dynein light chain roadblock-type 1; AltName: Full=Bithoraxoid-like protein; Short=BLP; AltName: Full=Dynein light chain 2A, cytoplasmic; AltName: Full=Dynein-associated protein Km23; AltName: Full=Roadblock domain-containing protein 1; - OS=Homo sapiens (Human).	10.9	1	1
462	DMBT1_HUMAN	RecName: Full=Deleted in malignant brain tumors 1 protein; AltName: Full=Glycoprotein 340; Short=Gp-340; AltName: Full=Hensin; AltName: Full=Salivary agglutinin; Short=SAG; AltName: Full=Surfactant pulmonary-associated D-binding protein; Flags: Precursor; - OS=Homo sapiens (Human).	260.6	1	1
463	DNJC3_HUMAN	RecName: Full=DnaJ homolog subfamily C member 3; AltName: Full=Endoplasmic reticulum DnaJ protein 6; Short=ERdj6; AltName: Full=Interferon-induced, double-stranded RNA-activated protein kinase inhibitor; AltName: Full=Protein kinase inhibitor of 58 kDa; Short=Protein kinase inhibitor p58; Flags: Precursor; - OS=Homo sapiens (Human).	57.5	1	1

464	DPP2_HUMAN	RecName: Full=Dipeptidyl peptidase 2; EC=3.4.14.2; AltName: Full=Dipeptidyl aminopeptidase II; AltName: Full=Dipeptidyl peptidase 7; AltName: Full=Dipeptidyl peptidase II; Short=DPP II; AltName: Full=Quiescent cell proline dipeptidase; Flags: Precursor; - OS=Homo sapiens (Human).	54.3	6	6
465	DPY30_HUMAN	RecName: Full=Protein dpy-30 homolog; AltName: Full=Dpy-30-like protein; Short=Dpy-30L; - OS=Homo sapiens (Human).	11.2	2	2
466	E4W6B6_HUMAN	SubName: Full=RPL27/NME2 fusion protein; Flags: Fragment; - OS=Homo sapiens (Human).	14.2	1	1
467	E5RFX7_HUMAN	SubName: Full=Proline synthase co-transcribed bacterial homolog protein; Flags: Fragment; - OS=Homo sapiens (Human).	15.3	1	1
468	E5RGJ2_HUMAN	SubName: Full=Protein EMC2; Flags: Fragment; - OS=Homo sapiens (Human).	13.5	1	1
469	E5RHJ4_HUMAN	SubName: Full=DBIRD complex subunit KIAA1967; Flags: Fragment; - OS=Homo sapiens (Human).	31.1	1	1
470	E5RHW4_HUMAN	SubName: Full=Erlin-2; Flags: Fragment; - OS=Homo sapiens (Human).	37.7	3	3
471	E5RI99_HUMAN	SubName: Full=60S ribosomal protein L30; Flags: Fragment; - OS=Homo sapiens (Human).	12.6	2	2
472	E5RJA0_HUMAN	SubName: Full=Acyl-protein thioesterase 1; - OS=Homo sapiens (Human).	15.1	1	1
473	E5RK61_HUMAN	SubName: Full=Protein FAM49B; Flags: Fragment; - OS=Homo sapiens (Human).	7.1	1	1
474	E5RK69_HUMAN	RecName: Full=Annexin; - OS=Homo sapiens (Human).	51.7	2	2
475	E7EMM4_HUMAN	SubName: Full=Acid ceramidase subunit beta; - OS=Homo sapiens (Human).	41.8	12	8
476	E7EQV9_HUMAN	RecName: Full=Ribosomal protein L15; Flags: Fragment; - OS=Homo sapiens (Human).	20.5	2	2
477	E7ERH2_HUMAN	SubName: Full=S-phase kinase-associated protein 1; Flags: Fragment; - OS=Homo sapiens (Human).	16.0	2	2
478	E7ERW8_HUMAN	SubName: Full=Protein diaphanous homolog 1; - OS=Homo sapiens (Human).	135.3	2	2
479	E7EUT4_HUMAN	RecName: Full=Glyceraldehyde-3-phosphate dehydrogenase; EC=1.2.1.12; - OS=Homo sapiens (Human).	31.5	8	8
480	E7EWI9_HUMAN	SubName: Full=Heterogeneous nuclear ribonucleoprotein A3; - OS=Homo sapiens (Human).	34.1	1	1
481	E9LUX2_HUMAN	SubName: Full=Hemoglobin alpha-2 chain variant; Flags: Fragment; - OS=Homo sapiens (Human).	7.7	3	1
482	E9PAU8_HUMAN	SubName: Full=Liver carboxylesterase 1; - OS=Homo sapiens (Human).	62.4	18	18
483	E9PCY7_HUMAN	SubName: Full=Heterogeneous nuclear ribonucleoprotein H, N-terminally processed; - OS=Homo	47.1	5	4

		sapiens (Human).			
484	E9PDQ8_HUMAN	SubName: Full=Succinyl-CoA ligase [GDP-forming] subunit beta, mitochondrial; - OS=Homo sapiens (Human).	41.4	4	4
485	E9PH29_HUMAN	SubName: Full=Thioredoxin-dependent peroxide reductase, mitochondrial; - OS=Homo sapiens (Human).	25.8	5	5
486	E9PHX3_HUMAN	SubName: Full=Neutrophil cytosol factor 2; - OS=Homo sapiens (Human).	54.4	5	5
487	E9PI87_HUMAN	SubName: Full=Oxidoreductase HTATIP2; - OS=Homo sapiens (Human).	22.0	1	1
488	E9PID9_HUMAN	SubName: Full=SID1 transmembrane family member 2; Flags: Fragment; - OS=Homo sapiens (Human).	12.4	1	1
489	E9PIQ8_HUMAN	SubName: Full=Stromal interaction molecule 1; Flags: Fragment; - OS=Homo sapiens (Human).	16.2	1	1
490	E9PJD9_HUMAN	SubName: Full=60S ribosomal protein L27a; - OS=Homo sapiens (Human).	10.1	2	2
491	E9PJK1_HUMAN	SubName: Full=CD81 antigen; - OS=Homo sapiens (Human).	18.0	1	1
492	E9PKD5_HUMAN	SubName: Full=26S protease regulatory subunit 6A; Flags: Fragment; - OS=Homo sapiens (Human).	32.7	2	2
493	E9PKH0_HUMAN	SubName: Full=Receptor-type tyrosine-protein phosphatase C; Flags: Fragment; - OS=Homo sapiens (Human).	67.6	2	2
494	E9PKW8_HUMAN	SubName: Full=Ubiquitin/ISG15-conjugating enzyme E2 L6; Flags: Fragment; - OS=Homo sapiens (Human).	7.5	1	1
495	E9PLX3_HUMAN	SubName: Full=Hepatitis B virus X-interacting protein; - OS=Homo sapiens (Human).	9.5	1	1
496	E9PN17_HUMAN	SubName: Full=ATP synthase subunit g, mitochondrial; - OS=Homo sapiens (Human).	8.4	2	2
497	E9PN51_HUMAN	SubName: Full=NADH dehydrogenase [ubiquinone] iron-sulfur protein 8, mitochondrial; Flags: Fragment; - OS=Homo sapiens (Human).	12.4	1	1
498	E9PN91_HUMAN	SubName: Full=Elongation factor 1-delta; - OS=Homo sapiens (Human).	11.6	2	2
499	E9PNT8_HUMAN	SubName: Full=Mitochondrial carrier homolog 2; Flags: Fragment; - OS=Homo sapiens (Human).	17.6	3	3
500	E9PP60_HUMAN	SubName: Full=GDP-L-fucose synthase; - OS=Homo sapiens (Human).	12.1	1	1
501	E9PP76_HUMAN	RecName: Full=Superoxide dismutase [Cu-Zn]; EC=1.15.1.1; Flags: Fragment; - OS=Homo sapiens	7.3	1	1

		(Human).			
502	E9PPM9_HUMAN	SubName: Full=Protein farnesyltransferase/geranylgeranyltransferase type-1 subunit alpha; Flags: Fragment; - OS=Homo sapiens (Human).	7.5	1	1
503	E9PPQ4_HUMAN	SubName: Full=Ferritin heavy chain; Flags: Fragment; - OS=Homo sapiens (Human).	6.7	2	2
504	E9PPS5_HUMAN	SubName: Full=NADH dehydrogenase [ubiquinone] flavoprotein 1, mitochondrial; Flags: Fragment; - OS=Homo sapiens (Human).	8.3	1	1
505	E9PR95_HUMAN	SubName: Full=Ester hydrolase C11orf54; Flags: Fragment; - OS=Homo sapiens (Human).	8.3	1	1
506	E9PSB0_HUMAN	SubName: Full=EH domain-binding protein 1-like protein 1; - OS=Homo sapiens (Human).	14.9	1	1
507	ECH1_HUMAN	RecName: Full=Delta(3,5)-Delta(2,4)-dienoyl-CoA isomerase, mitochondrial; EC=5.3.3.-; Flags: Precursor; - OS=Homo sapiens (Human).	35.8	4	4
508	ECHA_HUMAN	RecName: Full=Trifunctional enzyme subunit alpha, mitochondrial; AltName: Full=78 kDa gastrin-binding protein; AltName: Full=TP-alpha; Includes: RecName: Full=Long-chain enoyl-CoA hydratase; EC=4.2.1.17; Includes: RecName: Full=Long chain 3-hydroxyacyl-CoA dehydrogenase; EC=1.1.1.211; Flags: Precursor; - OS=Homo sapiens (Human).	82.9	13	13
509	ECHD1_HUMAN	RecName: Full=Ethylmalonyl-CoA decarboxylase; EC=4.1.1.94; AltName: Full=Enoyl-CoA hydratase domain-containing protein 1; AltName: Full=Methylmalonyl-CoA decarboxylase; Short=MMCD; EC=4.1.1.41; - OS=Homo sapiens (Human).	33.7	2	2
510	ECHM_HUMAN	RecName: Full=Enoyl-CoA hydratase, mitochondrial; EC=4.2.1.17; AltName: Full=Enoyl-CoA hydratase 1; AltName: Full=Short-chain enoyl-CoA hydratase; Short=SCEH; Flags: Precursor; - OS=Homo sapiens (Human).	31.4	4	4
511	EF1A1_HUMAN	RecName: Full=Elongation factor 1-alpha 1; Short=EF-1-alpha-1; AltName: Full=Elongation factor Tu; Short=EF-Tu; AltName: Full=Eukaryotic elongation factor 1 A-1; Short=eEF1A-1; AltName: Full=Leukocyte receptor cluster member 7; - OS=Homo sapiens (Human).	50.1	10	10
512	EF1B_HUMAN	RecName: Full=Elongation factor 1-beta; Short=EF-1-beta; - OS=Homo sapiens (Human).	24.7	2	2
513	EF2_HUMAN	RecName: Full=Elongation factor 2; Short=EF-2; - OS=Homo sapiens (Human).	95.3	6	6

514	EFHD2_HUMAN	RecName: Full=EF-hand domain-containing protein D2; AltName: Full=Swiprosin-1; - OS=Homo sapiens (Human).	26.7	5	5
515	EFTU_HUMAN	RecName: Full=Elongation factor Tu, mitochondrial; Short=EF-Tu; AltName: Full=P43; Flags: Precursor; - OS=Homo sapiens (Human).	49.5	10	10
516	EGLN2_HUMAN	RecName: Full=Egl nine homolog 2; EC=1.14.11.29; AltName: Full=Estrogen-induced tag 6; AltName: Full=HPH-3; AltName: Full=Hypoxia-inducible factor prolyl hydroxylase 1; Short=HIF-PH1; Short=HIF-prolyl hydroxylase 1; Short=HPH-1; AltName: Full=Prolyl hydroxylase domain-containing protein 1; Short=PHD1; - OS=Homo sapiens (Human).	43.6	1	1
517	ELAV1_HUMAN	RecName: Full=ELAV-like protein 1; AltName: Full=Hu-antigen R; Short=HuR; - OS=Homo sapiens (Human).	36.1	1	1
518	ENOA_HUMAN	RecName: Full=Alpha-enolase; EC=4.2.1.11; AltName: Full=2-phospho-D-glycerate hydro-lyase; AltName: Full=C-myc promoter-binding protein; AltName: Full=Enolase 1; AltName: Full=MBP-1; AltName: Full=MPB-1; AltName: Full=Non-neural enolase; Short=NNE; AltName: Full=Phosphopyruvate hydratase; AltName: Full=Plasminogen-binding protein; - OS=Homo sapiens (Human).	47.1	14	11
519	ENPP4_HUMAN	RecName: Full=Ectonucleotide pyrophosphatase/phosphodiesterase family member 4; Short=E-NPP 4; Short=NPP-4; EC=3.1.-.-; Flags: Precursor; - OS=Homo sapiens (Human).	51.6	2	2
520	EPDR1_HUMAN	RecName: Full=Mammalian ependymin-related protein 1; Short=MERP-1; AltName: Full=Upregulated in colorectal cancer 512gene 1 protein; Flags: Precursor; - OS=Homo sapiens (Human).	25.4	1	1
521	ERAP1_HUMAN	RecName: Full=Endoplasmic reticulum aminopeptidase 1; EC=3.4.11.-; AltName: Full=ARTS-1; AltName: Full=Adipocyte-derived leucine aminopeptidase; Short=A-LAP; AltName: Full=Aminopeptidase PILS; AltName: Full=Puromycin-insensitive leucyl-specific aminopeptidase; Short=PILS-AP; AltName: Full=Type 1 tumor necrosis factor receptor shedding aminopeptidase regulator; - OS=Homo sapiens (Human).	107.2	13	13

522	ERO1A_HUMAN	RecName: Full=ERO1-like protein alpha; Short=ERO1-L; Short=ERO1-L-alpha; EC=1.8.4.-; AltName: Full=Endoplasmic oxidoreductin-1-like protein; AltName: Full=Oxidoreductin-1-L-alpha; Flags: Precursor; - OS=Homo sapiens (Human).	54.4	4	4
523	ERP29_HUMAN	RecName: Full=Endoplasmic reticulum resident protein 29; Short=ERp29; AltName: Full=Endoplasmic reticulum resident protein 28; Short=ERp28; AltName: Full=Endoplasmic reticulum resident protein 31; Short=ERp31; Flags: Precursor; - OS=Homo sapiens (Human).	29.0	5	5
524	ERP44_HUMAN	RecName: Full=Endoplasmic reticulum resident protein 44; Short=ER protein 44; Short=ERp44; AltName: Full=Thioredoxin domain-containing protein 4; Flags: Precursor; - OS=Homo sapiens (Human).	46.9	9	9
525	ETFA_HUMAN	RecName: Full=Electron transfer flavoprotein subunit alpha, mitochondrial; Short=Alpha-ETF; Flags: Precursor; - OS=Homo sapiens (Human).	35.1	8	8
526	ETHE1_HUMAN	RecName: Full=Protein ETHE1, mitochondrial; EC=3.-.-.-; AltName: Full=Ethylmalonic encephalopathy protein 1; AltName: Full=Hepatoma subtracted clone one protein; Flags: Precursor; - OS=Homo sapiens (Human).	27.9	5	5
527	EVI5_HUMAN	RecName: Full=Ecotropic viral integration site 5 protein homolog; Short=EVI-5; AltName: Full=Neuroblastoma stage 4S gene protein; - OS=Homo sapiens (Human).	92.9	1	1
528	EZRI_HUMAN	RecName: Full=Ezrin; AltName: Full=Cytovillin; AltName: Full=Villin-2; AltName: Full=p81; - OS=Homo sapiens (Human).	69.4	7	4
529	F138A_HUMAN	RecName: Full=Protein FAM138A/B/C/F; AltName: Full=Retina-specific protein F379; - OS=Homo sapiens (Human).	9.2	1	1
530	F2Z2Y4_HUMAN	SubName: Full=Pyridoxal kinase; - OS=Homo sapiens (Human).	30.6	2	2
531	F2Z2Y8_HUMAN	SubName: Full=Toll-interacting protein; - OS=Homo sapiens (Human).	23.3	2	2
532	F5GWX2_HUMAN	SubName: Full=Heme-binding protein 1; - OS=Homo sapiens (Human).	14.7	1	1
533	F5GWY2_HUMAN	SubName: Full=Phosphoribosylaminoimidazolecarboxamide formyltransferase; - OS=Homo sapiens (Human).	58.6	3	3

Chapter 10 Appendices

534	F5GX11_HUMAN	SubName: Full=Proteasome subunit alpha type-1; - OS=Homo sapiens (Human).	26.5	3	3
535	F5GXN4_HUMAN	SubName: Full=Ras-related protein Rab-6A; Flags: Fragment; - OS=Homo sapiens (Human).	8.5	2	1
536	F5GXT8_HUMAN	SubName: Full=Diablo homolog, mitochondrial; Flags: Fragment; - OS=Homo sapiens (Human).	15.2	1	1
537	F5GZE5_HUMAN	SubName: Full=Septin-7; - OS=Homo sapiens (Human).	26.6	2	1
538	F5GZZ9_HUMAN	SubName: Full=Soluble CD163; - OS=Homo sapiens (Human).	120.2	5	5
539	F5H0T1_HUMAN	SubName: Full=Stress-induced-phosphoprotein 1; - OS=Homo sapiens (Human).	59.7	4	4
540	F5H1L4_HUMAN	SubName: Full=Thioredoxin reductase 2, mitochondrial; - OS=Homo sapiens (Human).	53.4	1	1
541	F5H1S8_HUMAN	SubName: Full=Malectin; Flags: Fragment; - OS=Homo sapiens (Human).	16.7	1	1
542	F5H265_HUMAN	SubName: Full=Ubiquitin; Flags: Fragment; - OS=Homo sapiens (Human).	16.8	2	2
543	F5H282_HUMAN	RecName: Full=T-complex protein 1 subunit alpha; - OS=Homo sapiens (Human).	36.4	1	1
544	F5H2R5_HUMAN	SubName: Full=Rho GDP-dissociation inhibitor 2; Flags: Fragment; - OS=Homo sapiens (Human).	9.8	1	1
545	F5H390_HUMAN	SubName: Full=Coronin-1B; - OS=Homo sapiens (Human).	31.0	2	2
546	F5H5E2_HUMAN	SubName: Full=Putative phospholipase B-like 2; - OS=Homo sapiens (Human).	61.8	2	2
547	F5H6N3_HUMAN	SubName: Full=Clathrin light chain A; - OS=Homo sapiens (Human).	17.7	2	2
548	F5H7F6_HUMAN	SubName: Full=Microsomal glutathione S-transferase 1; Flags: Fragment; - OS=Homo sapiens (Human).	8.9	1	1
549	F5H801_HUMAN	SubName: Full=2-oxoglutarate dehydrogenase, mitochondrial; - OS=Homo sapiens (Human).	110.5	6	6
550	F5H895_HUMAN	SubName: Full=Dolichyl-diphosphooligosaccharide--protein glycosyltransferase subunit DAD1; - OS=Homo sapiens (Human).	7.3	1	1
551	F6IQD3_HUMAN	SubName: Full=MHC class I antigen; Flags: Fragment; - OS=Homo sapiens (Human).	39.2	3	0
552	F6KPG5_HUMAN	SubName: Full=Albumin; Flags: Fragment; - OS=Homo sapiens (Human).	66.5	14	14
553	F6RFD5_HUMAN	SubName: Full=Destrin; - OS=Homo sapiens (Human).	15.4	1	1
554	F6UXX1_HUMAN	SubName: Full=Heterogeneous nuclear ribonucleoprotein Q; Flags: Fragment; - OS=Homo sapiens (Human).	20.2	2	1
555	F8VPF7_HUMAN	SubName: Full=Voltage-gated hydrogen channel 1; - OS=Homo sapiens (Human).	11.7	1	1

556	F8VQ14_HUMAN	SubName: Full=T-complex protein 1 subunit beta; - OS=Homo sapiens (Human).	44.8	2	2
557	F8VR50_HUMAN	SubName: Full=Actin-related protein 2/3 complex subunit 3; Flags: Fragment; - OS=Homo sapiens (Human).	9.7	1	1
558	F8VSD4_HUMAN	SubName: Full=Ubiquitin-conjugating enzyme E2 N; - OS=Homo sapiens (Human).	12.0	2	2
559	F8VTQ5_HUMAN	SubName: Full=Heterogeneous nuclear ribonucleoprotein A1; Flags: Fragment; - OS=Homo sapiens (Human).	16.5	2	2
560	F8VU65_HUMAN	SubName: Full=60S acidic ribosomal protein P0; Flags: Fragment; - OS=Homo sapiens (Human).	27.2	2	2
561	F8VVM2_HUMAN	SubName: Full=Phosphate carrier protein, mitochondrial; - OS=Homo sapiens (Human).	36.1	4	4
562	F8VVW6_HUMAN	SubName: Full=HLA class II histocompatibility antigen, DP beta 1 chain; - OS=Homo sapiens (Human).	14.9	2	1
563	F8VW92_HUMAN	SubName: Full=Tubulin beta chain; - OS=Homo sapiens (Human).	48.5	13	5
564	F8VWC5_HUMAN	RecName: Full=60S ribosomal protein L18; - OS=Homo sapiens (Human).	18.1	3	3
565	F8VZY5_HUMAN	SubName: Full=Keratin, type II cytoskeletal 7; Flags: Fragment; - OS=Homo sapiens (Human).	38.1	3	3
566	F8W031_HUMAN	SubName: Full=Uncharacterized protein; Flags: Fragment; - OS=Homo sapiens (Human).	29.2	5	4
567	F8W0P2_HUMAN	SubName: Full=HLA class II histocompatibility antigen, DR alpha chain; - OS=Homo sapiens (Human).	26.9	6	5
568	F8W181_HUMAN	RecName: Full=60S ribosomal protein L6; Flags: Fragment; - OS=Homo sapiens (Human).	25.9	2	2
569	F8W1A4_HUMAN	RecName: Full=Adenylate kinase C; Short=AK C; EC=2.7.4.3; AltName: Full=ATP-AMP transphosphorylase C; - OS=Homo sapiens (Human).	25.6	6	6
570	F8W1N5_HUMAN	SubName: Full=Nascent polypeptide-associated complex subunit alpha; Flags: Fragment; - OS=Homo sapiens (Human).	7.8	2	2
571	F8WAM2_HUMAN	SubName: Full=T-complex protein 1 subunit eta; Flags: Fragment; - OS=Homo sapiens (Human).	10.5	1	1
572	F8WAS3_HUMAN	SubName: Full=NADH dehydrogenase [ubiquinone] 1 alpha subcomplex subunit 5; - OS=Homo sapiens (Human).	7.8	1	1
573	F8WBG8_HUMAN	SubName: Full=Drebrin-like protein; - OS=Homo sapiens (Human).	13.7	1	1

574	F8WCC8_HUMAN	SubName: Full=Arylsulfatase A component C; - OS=Homo sapiens (Human).	44.9	1	1
575	F8WD51_HUMAN	SubName: Full=Uridine phosphorylase 1; - OS=Homo sapiens (Human).	9.3	1	1
576	F8WDL0_HUMAN	SubName: Full=AP-1 complex subunit beta-1; - OS=Homo sapiens (Human).	101.3	4	2
577	F8WEU4_HUMAN	SubName: Full=Cytochrome b5; - OS=Homo sapiens (Human).	14.2	1	1
578	FABP4_HUMAN	RecName: Full=Fatty acid-binding protein, adipocyte; AltName: Full=Adipocyte lipid-binding protein; Short=ALBP; AltName: Full=Adipocyte-type fatty acid-binding protein; Short=A-FABP; Short=AFABP; AltName: Full=Fatty acid-binding protein 4; - OS=Homo sapiens (Human).	14.7	4	4
579	FABP5_HUMAN	RecName: Full=Fatty acid-binding protein, epidermal; AltName: Full=Epidermal-type fatty acid-binding protein; Short=E-FABP; AltName: Full=Fatty acid-binding protein 5; AltName: Full=Psoriasis-associated fatty acid-binding protein homolog; Short=PA-FABP; - OS=Homo sapiens (Human).	15.2	5	5
580	FABPH_HUMAN	RecName: Full=Fatty acid-binding protein, heart; AltName: Full=Fatty acid-binding protein 3; AltName: Full=Heart-type fatty acid-binding protein; Short=H-FABP; AltName: Full=Mammary-derived growth inhibitor; Short=MDGI; AltName: Full=Muscle fatty acid-binding protein; Short=M-FABP; - OS=Homo sapiens (Human).	14.8	2	2
581	FAHD1_HUMAN	RecName: Full=Acylpyruvase FAHD1, mitochondrial; EC=3.7.1.5; AltName: Full=Fumarylacetoacetate hydrolase domain-containing protein 1; AltName: Full=YisK-like protein; Flags: Precursor; - OS=Homo sapiens (Human).	24.8	1	1
582	FIS1_HUMAN	RecName: Full=Mitochondrial fission 1 protein; AltName: Full=FIS1 homolog; Short=hFis1; AltName: Full=Tetratricopeptide repeat protein 11; Short=TPR repeat protein 11; - OS=Homo sapiens (Human).	16.9	1	1
583	FKBP2_HUMAN	RecName: Full=Peptidyl-prolyl cis-trans isomerase FKBP2; Short=PPIase FKBP2; EC=5.2.1.8; AltName: Full=13 kDa FK506-binding protein; Short=13 kDa FKBP; Short=FKBP-13; AltName: Full=FK506-binding protein 2; Short=FKBP-2; AltName: Full=Immunophilin FKBP13; AltName: Full=Rotamase; Flags: Precursor; - OS=Homo sapiens (Human).	15.6	1	1

584	FMNL_HUMAN	RecName: Full=Formin-like protein 1; AltName: Full=CLL-associated antigen KW-13; AltName: Full=Leukocyte formin; - OS=Homo sapiens (Human).	121.8	2	2
585	FRIL_HUMAN	RecName: Full=Ferritin light chain; Short=Ferritin L subunit; - OS=Homo sapiens (Human).	20.0	4	4
586	FUMH_HUMAN	RecName: Full=Fumarate hydratase, mitochondrial; Short=Fumarase; EC=4.2.1.2; Flags: Precursor; - OS=Homo sapiens (Human).	54.6	3	3
587	G1EMZ1_HUMAN	SubName: Full=MHC class II antigen; Flags: Fragment; - OS=Homo sapiens (Human).	10.9	3	1
588	G3V184_HUMAN	SubName: Full=ADP-ribosylation factor-like protein 2; SubName: Full=HCG23373, isoform CRA_b; - OS=Homo sapiens (Human).	18.0	1	1
589	G3V1A4_HUMAN	SubName: Full=Cofilin 1 (Non-muscle), isoform CRA_a; SubName: Full=Cofilin-1; - OS=Homo sapiens (Human).	16.8	5	5
590	G3V1N2_HUMAN	SubName: Full=HCG1745306, isoform CRA_a; SubName: Full=Hemoglobin subunit alpha; - OS=Homo sapiens (Human).	11.9	7	2
591	G3V1U9_HUMAN	SubName: Full=Tubulin alpha-1A chain; SubName: Full=Tubulin, alpha 3, isoform CRA_c; - OS=Homo sapiens (Human).	46.3	11	2
592	G3V2V6_HUMAN	SubName: Full=V-type proton ATPase subunit D; - OS=Homo sapiens (Human).	17.4	1	1
593	G3V3A0_HUMAN	SubName: Full=Alpha-1-antichymotrypsin; SubName: Full=Serpin peptidase inhibitor, clade A (Alpha-1 antiproteinase, antitrypsin), member 3, isoform CRA_a; - OS=Homo sapiens (Human).	23.4	3	3
594	G3V3U4_HUMAN	RecName: Full=Proteasome subunit alpha type; EC=3.4.25.1; - OS=Homo sapiens (Human).	11.6	4	4
595	G3V4X5_HUMAN	SubName: Full=Proteasome subunit alpha type-3; - OS=Homo sapiens (Human).	20.3	1	1
596	G3V4Y7_HUMAN	SubName: Full=Kinectin; - OS=Homo sapiens (Human).	68.9	2	2
597	G3V576_HUMAN	SubName: Full=Heterogeneous nuclear ribonucleoproteins C1/C2; - OS=Homo sapiens (Human).	25.2	5	5
598	G3V5W3_HUMAN	SubName: Full=Son of sevenless homolog 2; - OS=Homo sapiens (Human).	8.1	1	1
599	G3XAI1_HUMAN	SubName: Full=55 kDa erythrocyte membrane protein; SubName: Full=Membrane protein, palmitoylated 1, 55kDa, isoform CRA_a; - OS=Homo sapiens (Human).	49.8	1	1
600	G3XAN0_HUMAN	SubName: Full=40S ribosomal protein S20; SubName: Full=Ribosomal protein S20, isoform CRA_a;	7.2	1	1

		- OS=Homo sapiens (Human).			
601	G8FT56_HUMAN	SubName: Full=MHC class I antigen; Flags: Fragment; - OS=Homo sapiens (Human).	31.9	3	0
602	G9HTG4_HUMAN	SubName: Full=MHC class II antigen; Flags: Fragment; - OS=Homo sapiens (Human).	25.4	6	0
603	GALK1_HUMAN	RecName: Full=Galactokinase; EC=2.7.1.6; AltName: Full=Galactose kinase; - OS=Homo sapiens (Human).	42.2	1	1
604	GANAB_HUMAN	RecName: Full=Neutral alpha-glucosidase AB; EC=3.2.1.84; AltName: Full=Alpha-glucosidase 2; AltName: Full=Glucosidase II subunit alpha; Flags: Precursor; - OS=Homo sapiens (Human).	106.8	8	8
605	GAPR1_HUMAN	RecName: Full=Golgi-associated plant pathogenesis-related protein 1; Short=GAPR-1; Short=Golgi-associated PR-1 protein; AltName: Full=Glioma pathogenesis-related protein 2; Short=GliPR 2; - OS=Homo sapiens (Human).	17.2	3	3
606	GDIB_HUMAN	RecName: Full=Rab GDP dissociation inhibitor beta; Short=Rab GDI beta; AltName: Full=Guanosine diphosphate dissociation inhibitor 2; Short=GDI-2; - OS=Homo sapiens (Human).	50.6	8	8
607	GLRX1_HUMAN	RecName: Full=Glutaredoxin-1; AltName: Full=Thioltransferase-1; Short=TTase-1; - OS=Homo sapiens (Human).	11.8	2	2
608	GLRX3_HUMAN	RecName: Full=Glutaredoxin-3; AltName: Full=PKC-interacting cousin of thioredoxin; Short=PICOT; AltName: Full=PKC-theta-interacting protein; Short=PKCq-interacting protein; AltName: Full=Thioredoxin-like protein 2; - OS=Homo sapiens (Human).	37.4	1	1
609	GMFG_HUMAN	RecName: Full=Glia maturation factor gamma; Short=GMF-gamma; - OS=Homo sapiens (Human).	16.8	3	2
610	GPC5_HUMAN	RecName: Full=Glypican-5; Contains: RecName: Full=Secreted glypican-5; Flags: Precursor; - OS=Homo sapiens (Human).	63.7	1	1
611	GPX4_HUMAN	RecName: Full=Phospholipid hydroperoxide glutathione peroxidase, mitochondrial; Short=PHGPx; EC=1.11.1.12; AltName: Full=Glutathione peroxidase 4; Short=GPx-4; Short=GSHPx-4; Flags: Precursor; - OS=Homo sapiens (Human).	22.2	3	3
612	GRHPR_HUMAN	RecName: Full=Glyoxylate reductase/hydroxypyruvate reductase; EC=1.1.1.79; EC=1.1.1.81; - OS=Homo sapiens (Human).	35.6	1	1

613	GRP78_HUMAN	RecName: Full=78 kDa glucose-regulated protein; Short=GRP-78; AltName: Full=Endoplasmic reticulum lumenal Ca(2+)-binding protein grp78; AltName: Full=Heat shock 70 kDa protein 5; AltName: Full=Immunoglobulin heavy chain-binding protein; Short=BiP; Flags: Precursor; - OS=Homo sapiens (Human).	72.3	15	13
614	GSTP1_HUMAN	RecName: Full=Glutathione S-transferase P; EC=2.5.1.18; AltName: Full=GST class-pi; AltName: Full=GSTP1-1; - OS=Homo sapiens (Human).	23.3	4	4
615	GT251_HUMAN	RecName: Full=Procollagen galactosyltransferase 1; EC=2.4.1.50; AltName: Full=Glycosyltransferase 25 family member 1; AltName: Full=Hydroxylysine galactosyltransferase 1; Flags: Precursor; - OS=Homo sapiens (Human).	71.6	4	4
616	H0Y3Y6_HUMAN	SubName: Full=Serine/threonine-protein phosphatase PP1-beta catalytic subunit; Flags: Fragment; - OS=Homo sapiens (Human).	9.7	2	2
617	H0Y897_HUMAN	SubName: Full=Target of Nesh-SH3; Flags: Fragment; - OS=Homo sapiens (Human).	124.2	1	1
618	H0Y923_HUMAN	SubName: Full=Protein kinase C and casein kinase substrate in neurons protein 2; Flags: Fragment; - OS=Homo sapiens (Human).	6.4	1	1
619	H0Y9R4_HUMAN	SubName: Full=60S ribosomal protein L9; Flags: Fragment; - OS=Homo sapiens (Human).	10.1	1	1
620	H0YAE9_HUMAN	SubName: Full=Uncharacterized protein; Flags: Fragment; - OS=Homo sapiens (Human).	21.9	1	1
621	H0YB56_HUMAN	SubName: Full=Protein LYRIC; Flags: Fragment; - OS=Homo sapiens (Human).	24.5	1	1
622	H0YCX0_HUMAN	SubName: Full=Translationally-controlled tumor protein; Flags: Fragment; - OS=Homo sapiens (Human).	9.1	1	1
623	H0YCY8_HUMAN	SubName: Full=Dipeptidyl peptidase 1 light chain; Flags: Fragment; - OS=Homo sapiens (Human).	27.9	3	3
624	H0YD97_HUMAN	SubName: Full=Pyruvate dehydrogenase protein X component, mitochondrial; Flags: Fragment; - OS=Homo sapiens (Human).	20.7	1	1
625	H0YDG0_HUMAN	SubName: Full=Puromycin-sensitive aminopeptidase; Flags: Fragment; - OS=Homo sapiens (Human).	19.0	1	1
626	H0YDP7_HUMAN	SubName: Full=39S ribosomal protein L49, mitochondrial; Flags: Fragment; - OS=Homo sapiens (Human).	14.7	1	1

Chapter 10 Appendices

627	H0YDX6_HUMAN	SubName: Full=CD44 antigen; Flags: Fragment; - OS=Homo sapiens (Human).	19.6	2	2
628	H0YE04_HUMAN	SubName: Full=Signal peptidase complex subunit 2; Flags: Fragment; - OS=Homo sapiens (Human).	18.7	1	1
629	H0YEN5_HUMAN	SubName: Full=40S ribosomal protein S2; Flags: Fragment; - OS=Homo sapiens (Human).	21.1	4	4
630	H0YEU5_HUMAN	SubName: Full=Histone-binding protein RBBP4; Flags: Fragment; - OS=Homo sapiens (Human).	19.0	1	1
631	H0YGF3_HUMAN	SubName: Full=Pre-mRNA-processing factor 19; Flags: Fragment; - OS=Homo sapiens (Human).	5.2	1	1
632	H0YJ63_HUMAN	SubName: Full=Activator of 90 kDa heat shock protein ATPase homolog 1; Flags: Fragment; - OS=Homo sapiens (Human).	10.1	1	1
633	H0YJE4_HUMAN	SubName: Full=Dehydrogenase/reductase SDR family member 7; Flags: Fragment; - OS=Homo sapiens (Human).	17.9	1	1
634	H0YJE9_HUMAN	SubName: Full=26S protease regulatory subunit 10B; Flags: Fragment; - OS=Homo sapiens (Human).	8.7	1	1
635	H0YJN9_HUMAN	SubName: Full=Legumain; Flags: Fragment; - OS=Homo sapiens (Human).	9.8	1	1
636	H0YKU1_HUMAN	SubName: Full=Tropomodulin-3; Flags: Fragment; - OS=Homo sapiens (Human).	20.9	1	1
637	H0YKV0_HUMAN	SubName: Full=Isovaleryl-CoA dehydrogenase, mitochondrial; Flags: Fragment; - OS=Homo sapiens (Human).	15.8	1	1
638	H0YLA2_HUMAN	SubName: Full=Signal recognition particle 14 kDa protein; - OS=Homo sapiens (Human).	13.0	1	1
639	H0YLS6_HUMAN	RecName: Full=Proteasome subunit alpha type; EC=3.4.25.1; - OS=Homo sapiens (Human).	13.9	1	1
640	H0YM46_HUMAN	SubName: Full=Isocitrate dehydrogenase [NAD] subunit alpha, mitochondrial; Flags: Fragment; - OS=Homo sapiens (Human).	5.3	1	1
641	H0YNE9_HUMAN	SubName: Full=Ras-related protein Rab-8B; Flags: Fragment; - OS=Homo sapiens (Human).	21.9	4	1
642	H0YNX5_HUMAN	SubName: Full=Signal peptidase complex catalytic subunit SEC11A; Flags: Fragment; - OS=Homo sapiens (Human).	12.0	1	1
643	H0YNX7_HUMAN	SubName: Full=GTP cyclohydrolase 1 feedback regulatory protein; SubName: Full=GTP cyclohydrolase I feedback regulator, isoform CRA_a; - OS=Homo sapiens (Human).	7.8	1	1
644	H12_HUMAN	RecName: Full=Histone H1.2; AltName: Full=Histone H1c; AltName: Full=Histone H1d; AltName: Full=Histone H1s-1; - OS=Homo sapiens (Human).	21.4	3	3

645	H15_HUMAN	RecName: Full=Histone H1.5; AltName: Full=Histone H1a; AltName: Full=Histone H1b; AltName: Full=Histone H1s-3; - OS=Homo sapiens (Human).	22.6	3	3
646	H2A1A_HUMAN	RecName: Full=Histone H2A type 1-A; AltName: Full=Histone H2A/r; - OS=Homo sapiens (Human).	14.2	3	1
647	H2A1H_HUMAN	RecName: Full=Histone H2A type 1-H; AltName: Full=Histone H2A/s; - OS=Homo sapiens (Human).	13.9	3	1
648	H2AY_HUMAN	RecName: Full=Core histone macro-H2A.1; Short=Histone macroH2A1; Short=mH2A1; AltName: Full=Histone H2A.y; Short=H2A/y; AltName: Full=Medulloblastoma antigen MU-MB-50.205; - OS=Homo sapiens (Human).	39.6	6	6
649	H2B1B_HUMAN	RecName: Full=Histone H2B type 1-B; AltName: Full=Histone H2B.1; AltName: Full=Histone H2B.f; Short=H2B/f; - OS=Homo sapiens (Human).	13.9	3	1
650	H3BLU7_HUMAN	SubName: Full=Aflatoxin B1 aldehyde reductase member 2; Flags: Fragment; - OS=Homo sapiens (Human).	34.7	1	1
651	H3BM47_HUMAN	SubName: Full=Group XV phospholipase A2; Flags: Fragment; - OS=Homo sapiens (Human).	18.3	1	1
652	H3BMU1_HUMAN	SubName: Full=IST1 homolog; Flags: Fragment; - OS=Homo sapiens (Human).	23.4	1	1
653	H3BP04_HUMAN	SubName: Full=Cytochrome b-c1 complex subunit 2, mitochondrial; Flags: Fragment; - OS=Homo sapiens (Human).	19.5	3	3
654	H3BPF6_HUMAN	SubName: Full=Prefoldin subunit 5; Flags: Fragment; - OS=Homo sapiens (Human).	17.1	1	1
655	H3BPK3_HUMAN	SubName: Full=Hydroxyacylglutathione hydrolase, mitochondrial; Flags: Fragment; - OS=Homo sapiens (Human).	26.4	1	1
656	H3BQH0_HUMAN	SubName: Full=Calponin-2; Flags: Fragment; - OS=Homo sapiens (Human).	23.1	1	1
657	H3BQN4_HUMAN	RecName: Full=Fructose-bisphosphate aldolase; EC=4.1.2.13; - OS=Homo sapiens (Human).	39.3	6	6
658	H3BQZ7_HUMAN	SubName: Full=HCG2044799; SubName: Full=Uncharacterized protein; - OS=Homo sapiens (Human).	84.6	1	1
659	H3BR27_HUMAN	SubName: Full=RNA-binding motif protein, X chromosome, N-terminally processed; - OS=Homo sapiens (Human).	8.6	2	2
660	H3BTE6_HUMAN	SubName: Full=Erythrocyte membrane protein band 4.2; Flags: Fragment; - OS=Homo sapiens	59.8	2	2

		(Human).			
661	H3BTY8_HUMAN	SubName: Full=Eukaryotic translation initiation factor 3 subunit C; Flags: Fragment; - OS=Homo sapiens (Human).	9.5	1	1
662	H4_HUMAN	RecName: Full=Histone H4; - OS=Homo sapiens (Human).	11.4	3	3
663	H6SSQ1_HUMAN	SubName: Full=MHC class I antigen; Flags: Fragment; - OS=Homo sapiens (Human).	31.5	3	1
664	H6UYS7_HUMAN	SubName: Full=Alpha-synuclein transcript variant 12; SubName: Full=Alpha-synuclein transcript variant 15; SubName: Full=Alpha-synuclein transcript variant 6; SubName: Full=Alpha-synuclein transcript variant 9; - OS=Homo sapiens (Human).	10.0	1	1
665	H6VRF8_HUMAN	SubName: Full=Keratin 1; - OS=Homo sapiens (Human).	66.0	6	6
666	H6X377_HUMAN	SubName: Full=MHC class II antigen; Flags: Fragment; - OS=Homo sapiens (Human).	19.8	4	1
667	H7BXF3_HUMAN	SubName: Full=Transformer-2 protein homolog beta; Flags: Fragment; - OS=Homo sapiens (Human).	15.2	1	1
668	H7BXK9_HUMAN	SubName: Full=ATP-binding cassette sub-family B member 6, mitochondrial; Flags: Fragment; - OS=Homo sapiens (Human).	77.5	1	1
669	H7BZD1_HUMAN	SubName: Full=Glutaminase kidney isoform, mitochondrial; Flags: Fragment; - OS=Homo sapiens (Human).	12.6	1	1
670	H7BZI1_HUMAN	SubName: Full=Nucleobindin-1; Flags: Fragment; - OS=Homo sapiens (Human).	34.9	3	3
671	H7BZJ3_HUMAN	RecName: Full=Thioredoxin; Flags: Fragment; - OS=Homo sapiens (Human).	13.5	3	1
672	H7BZT4_HUMAN	SubName: Full=Uncharacterized protein; - OS=Homo sapiens (Human).	10.8	1	1
673	H7BZX2_HUMAN	SubName: Full=Metalloendopeptidase OMA1, mitochondrial; Flags: Fragment; - OS=Homo sapiens (Human).	37.8	1	1
674	H7C124_HUMAN	SubName: Full=Protein THEMIS2; Flags: Fragment; - OS=Homo sapiens (Human).	44.3	2	2
675	H7C131_HUMAN	SubName: Full=3-ketoacyl-CoA thiolase, peroxisomal; Flags: Fragment; - OS=Homo sapiens (Human).	30.3	5	5
676	H7C1C6_HUMAN	SubName: Full=Translocon-associated protein subunit delta; Flags: Fragment; - OS=Homo sapiens (Human).	13.1	1	1

677	H7C1K4_HUMAN	SubName: Full=Syndecan-1; Flags: Fragment; - OS=Homo sapiens (Human).	22.0	1	1
678	H7C2A0_HUMAN	SubName: Full=Glycerol kinase; Flags: Fragment; - OS=Homo sapiens (Human).	13.1	1	1
679	H7C2G3_HUMAN	SubName: Full=ES1 protein homolog, mitochondrial; Flags: Fragment; - OS=Homo sapiens (Human).	20.3	1	1
680	H7C2Y5_HUMAN	SubName: Full=DnaJ homolog subfamily B member 11; Flags: Fragment; - OS=Homo sapiens (Human).	19.3	1	1
681	H7C2Z6_HUMAN	SubName: Full=Grancalcin; Flags: Fragment; - OS=Homo sapiens (Human).	16.8	4	4
682	H7C342_HUMAN	SubName: Full=D-dopachrome decarboxylase; Flags: Fragment; - OS=Homo sapiens (Human).	5.7	1	1
683	H7C3M7_HUMAN	SubName: Full=FERM, RhoGEF and pleckstrin domain-containing protein 2; Flags: Fragment; - OS=Homo sapiens (Human).	23.7	1	1
684	H7C456_HUMAN	SubName: Full=Microtubule-associated protein 4; Flags: Fragment; - OS=Homo sapiens (Human).	31.6	1	1
685	H7C463_HUMAN	SubName: Full=Mitochondrial inner membrane protein; Flags: Fragment; - OS=Homo sapiens (Human).	68.1	7	7
686	H7C4F6_HUMAN	SubName: Full=Importin subunit alpha-4; Flags: Fragment; - OS=Homo sapiens (Human).	18.9	1	1
687	H7C531_HUMAN	SubName: Full=26S proteasome non-ATPase regulatory subunit 6; Flags: Fragment; - OS=Homo sapiens (Human).	16.0	1	1
688	H7C597_HUMAN	SubName: Full=Staphylococcal nuclease domain-containing protein 1; Flags: Fragment; - OS=Homo sapiens (Human).	26.2	1	1
689	H90B4_HUMAN	RecName: Full=Putative heat shock protein HSP 90-beta 4; - OS=Homo sapiens (Human).	58.2	3	1
690	H9E7B8_HUMAN	RecName: Full=Cytochrome c oxidase subunit 2; Flags: Fragment; - OS=Homo sapiens (Human).	24.8	1	1
691	H9KVC7_HUMAN	SubName: Full=Interferon-induced GTP-binding protein Mx1; Flags: Fragment; - OS=Homo sapiens (Human).	20.9	3	3
692	HBAZ_HUMAN	RecName: Full=Hemoglobin subunit zeta; AltName: Full=HBAZ; AltName: Full=Hemoglobin zeta chain; AltName: Full=Zeta-globin; - OS=Homo sapiens (Human).	15.6	4	3
693	HBD_HUMAN	RecName: Full=Hemoglobin subunit delta; AltName: Full=Delta-globin; AltName: Full=Hemoglobin delta chain; - OS=Homo sapiens (Human).	16.0	11	2

694	HCD2_HUMAN	RecName: Full=3-hydroxyacyl-CoA dehydrogenase type-2; EC=1.1.1.35; AltName: Full=17-beta-hydroxysteroid dehydrogenase 10; Short=17-beta-HSD 10; AltName: Full=3-hydroxy-2-methylbutyryl-CoA dehydrogenase; EC=1.1.1.178; AltName: Full=3-hydroxyacyl-CoA dehydrogenase type II; AltName: Full=Endoplasmic reticulum-associated amyloid beta-peptide-binding protein; AltName: Full=Mitochondrial ribonuclease P protein 2; Short=Mitochondrial RNase P protein 2; AltName: Full=Short-chain type dehydrogenase/reductase XH98G2; AltName: Full=Type II HADH; - OS=Homo sapiens (Human).	26.9	7	7
695	HEBP2_HUMAN	RecName: Full=Heme-binding protein 2; AltName: Full=Placental protein 23; Short=PP23; AltName: Full=Protein SOUL; - OS=Homo sapiens (Human).	22.9	1	1
696	HEXB_HUMAN	RecName: Full=Beta-hexosaminidase subunit beta; EC=3.2.1.52; AltName: Full=Beta-N-acetylhexosaminidase subunit beta; Short=Hexosaminidase subunit B; AltName: Full=Cervical cancer proto-oncogene 7 protein; Short=HCC-7; AltName: Full=N-acetyl-beta-glucosaminidase subunit beta; Contains: RecName: Full=Beta-hexosaminidase subunit beta chain B; Contains: RecName: Full=Beta-hexosaminidase subunit beta chain A; Flags: Precursor; - OS=Homo sapiens (Human).	63.1	7	6
697	HG2A_HUMAN	RecName: Full=HLA class II histocompatibility antigen gamma chain; AltName: Full=HLA-DR antigens-associated invariant chain; AltName: Full=Ia antigen-associated invariant chain; Short=Ii; AltName: Full=p33; AltName: CD_antigen=CD74; - OS=Homo sapiens (Human).	33.5	3	3
698	HM13_HUMAN	RecName: Full=Minor histocompatibility antigen H13; EC=3.4.23.-; AltName: Full=Intramembrane protease 1; Short=IMP-1; Short=IMPAS-1; Short=hIMP1; AltName: Full=Presenilin-like protein 3; AltName: Full=Signal peptide peptidase; - OS=Homo sapiens (Human).	41.5	1	1
699	HNRH3_HUMAN	RecName: Full=Heterogeneous nuclear ribonucleoprotein H3; Short=hnRNP H3; AltName: Full=Heterogeneous nuclear ribonucleoprotein 2H9; Short=hnRNP 2H9; - OS=Homo sapiens (Human).	36.9	2	2
700	HNRPM_HUMAN	RecName: Full=Heterogeneous nuclear ribonucleoprotein M; Short=hnRNP M; - OS=Homo sapiens (Human).	77.5	4	4

701	HPRT_HUMAN	RecName: Full=Hypoxanthine-guanine phosphoribosyltransferase; Short=HGPRT; Short=HGPRTase; EC=2.4.2.8; - OS=Homo sapiens (Human).	24.6	2	2
702	HS90A_HUMAN	RecName: Full=Heat shock protein HSP 90-alpha; AltName: Full=Heat shock 86 kDa; Short=HSP 86; Short=HSP86; AltName: Full=Renal carcinoma antigen NY-REN-38; - OS=Homo sapiens (Human).	84.6	13	7
703	HSPB1_HUMAN	RecName: Full=Heat shock protein beta-1; Short=HspB1; AltName: Full=28 kDa heat shock protein; AltName: Full=Estrogen-regulated 24 kDa protein; AltName: Full=Heat shock 27 kDa protein; Short=HSP 27; AltName: Full=Stress-responsive protein 27; Short=SRP27; - OS=Homo sapiens (Human).	22.8	3	3
704	HXK3_HUMAN	RecName: Full=Hexokinase-3; EC=2.7.1.1; AltName: Full=Hexokinase type III; Short=HK III; - OS=Homo sapiens (Human).	99.0	7	7
705	I1VE16_HUMAN	SubName: Full=SEC22 vesicle trafficking protein B; Flags: Fragment; - OS=Homo sapiens (Human).	4.1	1	1
706	I1VZV6_HUMAN	SubName: Full=Hemoglobin alpha 1; - OS=Homo sapiens (Human).	15.3	7	1
707	I2G9G1_HUMAN	SubName: Full=MHC class II antigen; - OS=Homo sapiens (Human).	29.4	3	3
708	I3L1P8_HUMAN	SubName: Full=Mitochondrial 2-oxoglutarate/malate carrier protein; Flags: Fragment; - OS=Homo sapiens (Human).	32.2	7	7
709	I3L397_HUMAN	SubName: Full=Eukaryotic translation initiation factor 5A-1; Flags: Fragment; - OS=Homo sapiens (Human).	16.1	2	2
710	I3L3D0_HUMAN	SubName: Full=Syntaxin-8; - OS=Homo sapiens (Human).	5.2	1	1
711	I3L3Q4_HUMAN	SubName: Full=Glyoxalase domain-containing protein 4; Flags: Fragment; - OS=Homo sapiens (Human).	25.5	1	1
712	I3L3Q7_HUMAN	SubName: Full=Complement component 1 Q subcomponent-binding protein, mitochondrial; Flags: Fragment; - OS=Homo sapiens (Human).	20.0	2	2
713	I3L471_HUMAN	SubName: Full=Phosphatidylinositol transfer protein alpha isoform; - OS=Homo sapiens (Human).	11.0	1	1
714	I3L4U1_HUMAN	SubName: Full=Basigin; Flags: Fragment; - OS=Homo sapiens (Human).	5.7	1	1
715	I3WTX1_HUMAN	SubName: Full=Allograft inflammatory factor 1 isoform 1; - OS=Homo sapiens (Human).	10.4	1	1

716	I6L965_HUMAN	SubName: Full=KRT18 protein; Flags: Fragment; - OS=Homo sapiens (Human).	42.1	1	1
717	I7HJT1_HUMAN	SubName: Full=HLA class II region expressed gene KE2; SubName: Full=Prefoldin subunit 6, isoform CRA_a; - OS=Homo sapiens (Human).	9.8	1	1
718	IGHA1_HUMAN	RecName: Full=Ig alpha-1 chain C region; - OS=Homo sapiens (Human).	37.6	4	4
719	IGHG1_HUMAN	RecName: Full=Ig gamma-1 chain C region; - OS=Homo sapiens (Human).	36.1	10	5
720	IGHG3_HUMAN	RecName: Full=Ig gamma-3 chain C region; AltName: Full=HDC; AltName: Full=Heavy chain disease protein; - OS=Homo sapiens (Human).	41.3	6	1
721	IGHG4_HUMAN	RecName: Full=Ig gamma-4 chain C region; - OS=Homo sapiens (Human).	35.9	6	1
722	IL21_HUMAN	RecName: Full=Interleukin-21; Short=IL-21; AltName: Full=Za11; Flags: Precursor; - OS=Homo sapiens (Human).	17.9	1	1
723	INF2_HUMAN	RecName: Full=Inverted formin-2; AltName: Full=HBEBP2-binding protein C; - OS=Homo sapiens (Human).	135.5	2	2
724	ITB1_HUMAN	RecName: Full=Integrin beta-1; AltName: Full=Fibronectin receptor subunit beta; AltName: Full=VLA-4 subunit beta; AltName: CD_antigen=CD29; Flags: Precursor; - OS=Homo sapiens (Human).	88.4	1	1
725	J3K000_HUMAN	SubName: Full=PEPD protein; - OS=Homo sapiens (Human).	54.5	1	1
726	J3KMX5_HUMAN	SubName: Full=40S ribosomal protein S13; - OS=Homo sapiens (Human).	16.7	2	2
727	J3KMY5_HUMAN	SubName: Full=Epididymal secretory protein E1; - OS=Homo sapiens (Human).	16.2	6	6
728	J3KPX7_HUMAN	SubName: Full=Prohibitin-2; - OS=Homo sapiens (Human).	33.4	7	7
729	J3KRC6_HUMAN	SubName: Full=Inositol-3-phosphate synthase 1; Flags: Fragment; - OS=Homo sapiens (Human).	23.6	1	1
730	J3KRE2_HUMAN	SubName: Full=Rho GDP-dissociation inhibitor 1; - OS=Homo sapiens (Human).	14.8	1	1
731	J3KSI4_HUMAN	SubName: Full=Mannose-P-dolichol utilization defect 1 protein; - OS=Homo sapiens (Human).	5.8	1	1
732	J3KSM3_HUMAN	SubName: Full=Proteasome subunit beta type-3; - OS=Homo sapiens (Human).	12.1	1	1
733	J3QL15_HUMAN	SubName: Full=60S ribosomal protein L19; Flags: Fragment; - OS=Homo sapiens (Human).	15.0	1	1
734	J3QL48_HUMAN	SubName: Full=Uncharacterized protein; Flags: Fragment; - OS=Homo sapiens (Human).	8.3	1	1

735	J3QLE5_HUMAN	SubName: Full=Small nuclear ribonucleoprotein-associated protein N; Flags: Fragment; - OS=Homo sapiens (Human).	17.5	1	1
736	J3QLI9_HUMAN	SubName: Full=Small nuclear ribonucleoprotein Sm D1; - OS=Homo sapiens (Human).	8.4	1	1
737	J3QLR8_HUMAN	SubName: Full=28S ribosomal protein S23, mitochondrial; - OS=Homo sapiens (Human).	17.5	1	1
738	J3QR48_HUMAN	SubName: Full=Importin subunit beta-1; Flags: Fragment; - OS=Homo sapiens (Human).	16.5	1	1
739	J3QRY4_HUMAN	SubName: Full=26S proteasome non-ATPase regulatory subunit 11; Flags: Fragment; - OS=Homo sapiens (Human).	21.2	1	1
740	J3QS45_HUMAN	SubName: Full=L-xylulose reductase; Flags: Fragment; - OS=Homo sapiens (Human).	10.8	1	1
741	K1C19_HUMAN	RecName: Full=Keratin, type I cytoskeletal 19; AltName: Full=Cytokeratin-19; Short=CK-19; AltName: Full=Keratin-19; Short=K19; - OS=Homo sapiens (Human).	44.1	8	6
742	K1C9_HUMAN	RecName: Full=Keratin, type I cytoskeletal 9; AltName: Full=Cytokeratin-9; Short=CK-9; AltName: Full=Keratin-9; Short=K9; - OS=Homo sapiens (Human).	62.0	2	1
743	K2C75_HUMAN	RecName: Full=Keratin, type II cytoskeletal 75; AltName: Full=Cytokeratin-75; Short=CK-75; AltName: Full=Keratin-6 hair follicle; Short=hK6hf; AltName: Full=Keratin-75; Short=K75; AltName: Full=Type II keratin-K6hf; AltName: Full=Type-II keratin Kb18; - OS=Homo sapiens (Human).	59.5	3	1
744	KAD1_HUMAN	RecName: Full=Adenylate kinase isoenzyme 1; Short=AK 1; EC=2.7.4.3; AltName: Full=ATP-AMP transphosphorylase 1; AltName: Full=Myokinase; - OS=Homo sapiens (Human).	21.6	1	1
745	KPYM_HUMAN	RecName: Full=Pyruvate kinase isozymes M1/M2; EC=2.7.1.40; AltName: Full=Cytosolic thyroid hormone-binding protein; Short=CTHBP; AltName: Full=Opa-interacting protein 3; Short=OIP-3; AltName: Full=Pyruvate kinase 2/3; AltName: Full=Pyruvate kinase muscle isozyme; AltName: Full=Thyroid hormone-binding protein 1; Short=THBP1; AltName: Full=Tumor M2-PK; AltName: Full=p58; - OS=Homo sapiens (Human).	57.9	14	14
746	KV101_HUMAN	RecName: Full=Ig kappa chain V-I region AG; - OS=Homo sapiens (Human).	12.0	1	1
747	KV301_HUMAN	RecName: Full=Ig kappa chain V-III region B6; - OS=Homo sapiens (Human).	11.6	2	1

748	LACTB_HUMAN	RecName: Full=Serine beta-lactamase-like protein LACTB, mitochondrial; EC=3.4.-.-; Flags: Precursor; - OS=Homo sapiens (Human).	60.7	3	3
749	LDHA_HUMAN	RecName: Full=L-lactate dehydrogenase A chain; Short=LDH-A; EC=1.1.1.27; AltName: Full=Cell proliferation-inducing gene 19 protein; AltName: Full=LDH muscle subunit; Short=LDH-M; AltName: Full=Renal carcinoma antigen NY-REN-59; - OS=Homo sapiens (Human).	36.7	8	7
750	LDHB_HUMAN	RecName: Full=L-lactate dehydrogenase B chain; Short=LDH-B; EC=1.1.1.27; AltName: Full=LDH heart subunit; Short=LDH-H; AltName: Full=Renal carcinoma antigen NY-REN-46; - OS=Homo sapiens (Human).	36.6	8	7
751	LEG1_HUMAN	RecName: Full=Galectin-1; Short=Gal-1; AltName: Full=14 kDa laminin-binding protein; Short=HLBP14; AltName: Full=14 kDa lectin; AltName: Full=Beta-galactoside-binding lectin L-14-I; AltName: Full=Galaptin; AltName: Full=HBL; AltName: Full=HPL; AltName: Full=Lactose-binding lectin 1; AltName: Full=Lectin galactoside-binding soluble 1; AltName: Full=Putative MAPK-activating protein PM12; AltName: Full=S-Lac lectin 1; - OS=Homo sapiens (Human).	14.7	4	4
752	LGUL_HUMAN	RecName: Full=Lactoylglutathione lyase; EC=4.4.1.5; AltName: Full=Aldoketomutase; AltName: Full=Glyoxalase I; Short=Glx I; AltName: Full=Ketone-aldehyde mutase; AltName: Full=Methylglyoxalase; AltName: Full=S-D-lactoylglutathione methylglyoxal lyase; - OS=Homo sapiens (Human).	20.8	2	2
753	LHPP_HUMAN	RecName: Full=Phospholysine phosphohistidine inorganic pyrophosphate phosphatase; Short=hLHPP; EC=3.1.3.-; EC=3.6.1.1; - OS=Homo sapiens (Human).	29.1	1	1
754	LKHA4_HUMAN	RecName: Full=Leukotriene A-4 hydrolase; Short=LTA-4 hydrolase; EC=3.3.2.6; AltName: Full=Leukotriene A(4) hydrolase; - OS=Homo sapiens (Human).	69.2	22	22
755	LMBD1_HUMAN	RecName: Full=Probable lysosomal cobalamin transporter; AltName: Full=HDAg-L-interacting protein NESI; AltName: Full=LMBR1 domain-containing protein 1; AltName: Full=Nuclear export signal-interacting protein; - OS=Homo sapiens (Human).	61.3	1	1
756	LMNB2_HUMAN	RecName: Full=Lamin-B2; Flags: Precursor; - OS=Homo sapiens (Human).	67.6	6	5

757	LOX5_HUMAN	RecName: Full=Arachidonate 5-lipoxygenase; Short=5-LO; Short=5-lipoxygenase; EC=1.13.11.34; - OS=Homo sapiens (Human).	77.9	11	11
758	LPPRC_HUMAN	RecName: Full=Leucine-rich PPR motif-containing protein, mitochondrial; AltName: Full=130 kDa leucine-rich protein; Short=LRP 130; AltName: Full=GP130; Flags: Precursor; - OS=Homo sapiens (Human).	157.8	5	5
759	LR16B_HUMAN	RecName: Full=Leucine-rich repeat-containing protein 16B; - OS=Homo sapiens (Human).	150.1	1	1
760	LRC59_HUMAN	RecName: Full=Leucine-rich repeat-containing protein 59; - OS=Homo sapiens (Human).	34.9	3	3
761	LRP1_HUMAN	RecName: Full=Prolow-density lipoprotein receptor-related protein 1; Short=LRP-1; AltName: Full=Alpha-2-macroglobulin receptor; Short=A2MR; AltName: Full=Apolipoprotein E receptor; Short=APOER; AltName: CD_antigen=CD91; Contains: RecName: Full=Low-density lipoprotein receptor-related protein 1 85 kDa subunit; Short=LRP-85; Contains: RecName: Full=Low-density lipoprotein receptor-related protein 1 515 kDa subunit; Short=LRP-515; Contains: RecName: Full=Low-density lipoprotein receptor-related protein 1 intracellular domain; Short=LRPICD; Flags: Precursor; - OS=Homo sapiens (Human).	504.3	9	9
762	LRRF1_HUMAN	RecName: Full=Leucine-rich repeat flightless-interacting protein 1; Short=LRR FLII-interacting protein 1; AltName: Full=GC-binding factor 2; AltName: Full=TAR RNA-interacting protein; - OS=Homo sapiens (Human).	89.2	2	2
763	LTOR1_HUMAN	RecName: Full=Ragulator complex protein LAMTOR1; AltName: Full=Late endosomal/lysosomal adaptor and MAPK and MTOR activator 1; AltName: Full=Lipid raft adaptor protein p18; AltName: Full=Protein associated with DRMs and endosomes; AltName: Full=p27Kip1-releasing factor from RhoA; Short=p27RF-Rho; - OS=Homo sapiens (Human).	17.7	3	3
764	LTOR3_HUMAN	RecName: Full=Ragulator complex protein LAMTOR3; AltName: Full=Late endosomal/lysosomal adaptor and MAPK and MTOR activator 3; AltName: Full=MEK-binding partner 1; Short=Mp1; AltName: Full=Mitogen-activated protein kinase kinase 1-interacting protein 1; AltName: Full=Mitogen-activated protein kinase scaffold protein 1; - OS=Homo sapiens (Human).	13.6	2	2

765	LYAG_HUMAN	RecName: Full=Lysosomal alpha-glucosidase; EC=3.2.1.20; AltName: Full=Acid maltase; AltName: Full=Aglucosidase alfa; Contains: RecName: Full=76 kDa lysosomal alpha-glucosidase; Contains: RecName: Full=70 kDa lysosomal alpha-glucosidase; Flags: Precursor; - OS=Homo sapiens (Human).	105.3	8	6
766	LYSC_HUMAN	RecName: Full=Lysozyme C; EC=3.2.1.17; AltName: Full=1,4-beta-N-acetylmuramidase C; Flags: Precursor; - OS=Homo sapiens (Human).	16.5	3	3
767	MANF_HUMAN	RecName: Full=Mesencephalic astrocyte-derived neurotrophic factor; AltName: Full=Arginine-rich protein; AltName: Full=Protein ARMET; Flags: Precursor; - OS=Homo sapiens (Human).	20.7	2	2
768	MAOM_HUMAN	RecName: Full=NAD-dependent malic enzyme, mitochondrial; Short=NAD-ME; EC=1.1.1.38; AltName: Full=Malic enzyme 2; Flags: Precursor; - OS=Homo sapiens (Human).	65.4	4	4
769	MGST3_HUMAN	RecName: Full=Microsomal glutathione S-transferase 3; Short=Microsomal GST-3; EC=2.5.1.18; AltName: Full=Microsomal GST-III; - OS=Homo sapiens (Human).	16.5	2	2
770	ML12A_HUMAN	RecName: Full=Myosin regulatory light chain 12A; AltName: Full=MLC-2B; AltName: Full=Myosin RLC; AltName: Full=Myosin regulatory light chain 2, nonsarcomeric; AltName: Full=Myosin regulatory light chain MRLC3; - OS=Homo sapiens (Human).	19.8	2	2
771	MOB1A_HUMAN	RecName: Full=MOB kinase activator 1A; AltName: Full=Mob1 alpha; Short=Mob1A; AltName: Full=Mob1 homolog 1B; AltName: Full=Mps one binder kinase activator-like 1B; - OS=Homo sapiens (Human).	25.1	1	1
772	MOES_HUMAN	RecName: Full=Moesin; AltName: Full=Membrane-organizing extension spike protein; - OS=Homo sapiens (Human).	67.8	12	9
773	MSRA_HUMAN	RecName: Full=Mitochondrial peptide methionine sulfoxide reductase; EC=1.8.4.11; AltName: Full=Peptide-methionine (S)-S-oxide reductase; Short=Peptide Met(O) reductase; AltName: Full=Protein-methionine-S-oxide reductase; Short=PMSR; Flags: Precursor; - OS=Homo sapiens (Human).	26.1	1	1
774	MTPN_HUMAN	RecName: Full=Myotrophin; AltName: Full=Protein V-1; - OS=Homo sapiens (Human).	12.9	2	2
775	MUC5A_HUMAN	RecName: Full=Mucin-5AC; Short=MUC-5AC; AltName: Full=Gastric mucin; AltName: Full=Lewis	526.3	10	5

		B blood group antigen; Short=LeB; AltName: Full=Major airway glycoprotein; AltName: Full=Mucin-5 subtype AC, tracheobronchial; AltName: Full=Tracheobronchial mucin; Short=TBM; Flags: Precursor; Fragments; - OS=Homo sapiens (Human).			
776	MYCBP_HUMAN	RecName: Full=C-Myc-binding protein; AltName: Full=Associate of Myc 1; Short=AMY-1; - OS=Homo sapiens (Human).	12.0	2	2
777	MYH9_HUMAN	RecName: Full=Myosin-9; AltName: Full=Cellular myosin heavy chain, type A; AltName: Full=Myosin heavy chain 9; AltName: Full=Myosin heavy chain, non-muscle IIa; AltName: Full=Non-muscle myosin heavy chain A; Short=NMMHC-A; AltName: Full=Non-muscle myosin heavy chain IIa; Short=NMMHC II-a; Short=NMMHC-IIA; - OS=Homo sapiens (Human).	226.4	20	20
778	NAAA_HUMAN	RecName: Full=N-acylethanolamine-hydrolyzing acid amidase; EC=3.5.1.-; AltName: Full=Acid ceramidase-like protein; AltName: Full=N-acylsphingosine amidohydrolase-like; Short=ASAH-like protein; Contains: RecName: Full=N-acylethanolamine-hydrolyzing acid amidase subunit alpha; Contains: RecName: Full=N-acylethanolamine-hydrolyzing acid amidase subunit beta; Flags: Precursor; - OS=Homo sapiens (Human).	40.0	2	2
779	NAGK_HUMAN	RecName: Full=N-acetyl-D-glucosamine kinase; Short=N-acetylglucosamine kinase; EC=2.7.1.59; AltName: Full=GlcNAc kinase; - OS=Homo sapiens (Human).	37.4	8	8
780	NAPSA_HUMAN	RecName: Full=Napsin-A; EC=3.4.23.-; AltName: Full=Aspartyl protease 4; Short=ASP4; Short=Asp 4; AltName: Full=Napsin-1; AltName: Full=TA01/TA02; Flags: Precursor; - OS=Homo sapiens (Human).	45.4	5	5
781	NB5R3_HUMAN	RecName: Full=NADH-cytochrome b5 reductase 3; Short=B5R; Short=Cytochrome b5 reductase; EC=1.6.2.2; AltName: Full=Diaphorase-1; Contains: RecName: Full=NADH-cytochrome b5 reductase 3 membrane-bound form; Contains: RecName: Full=NADH-cytochrome b5 reductase 3 soluble form; - OS=Homo sapiens (Human).	34.2	3	3
782	NCEH1_HUMAN	RecName: Full=Neutral cholesterol ester hydrolase 1; Short=NCEH; EC=3.1.1.-; AltName: Full=Arylacetamide deacetylase-like 1; - OS=Homo sapiens (Human).	45.8	7	7

Chapter 10 Appendices

783	NCF1_HUMAN	RecName: Full=Neutrophil cytosol factor 1; Short=NCF-1; AltName: Full=47 kDa autosomal chronic granulomatous disease protein; AltName: Full=47 kDa neutrophil oxidase factor; AltName: Full=NCF-47K; AltName: Full=Neutrophil NADPH oxidase factor 1; AltName: Full=Nox organizer 2; AltName: Full=Nox-organizing protein 2; AltName: Full=SH3 and PX domain-containing protein 1A; AltName: Full=p47-phox; - OS=Homo sapiens (Human).	44.6	3	3
784	NCPR_HUMAN	RecName: Full=NADPH--cytochrome P450 reductase; Short=CPR; Short=P450R; EC=1.6.2.4; - OS=Homo sapiens (Human).	76.6	8	8
785	NDKA_HUMAN	RecName: Full=Nucleoside diphosphate kinase A; Short=NDK A; Short=NDP kinase A; EC=2.7.4.6; AltName: Full=Granzyme A-activated DNase; Short=GAAD; AltName: Full=Metastasis inhibition factor nm23; AltName: Full=Tumor metastatic process-associated protein; AltName: Full=nm23-H1; - OS=Homo sapiens (Human).	17.1	4	4
786	NDUA4_HUMAN	RecName: Full=NADH dehydrogenase [ubiquinone] 1 alpha subcomplex subunit 4; AltName: Full=Complex I-MLRQ; Short=CI-MLRQ; AltName: Full=NADH-ubiquinone oxidoreductase MLRQ subunit; - OS=Homo sapiens (Human).	9.4	2	2
787	NNTM_HUMAN	RecName: Full=NAD(P) transhydrogenase, mitochondrial; EC=1.6.1.2; AltName: Full=Nicotinamide nucleotide transhydrogenase; AltName: Full=Pyridine nucleotide transhydrogenase; Flags: Precursor; - OS=Homo sapiens (Human).	113.8	6	6
788	NPM_HUMAN	RecName: Full=Nucleophosmin; Short=NPM; AltName: Full=Nucleolar phosphoprotein B23; AltName: Full=Nucleolar protein NO38; AltName: Full=Numatrin; - OS=Homo sapiens (Human).	32.6	3	3
789	NUP62_HUMAN	RecName: Full=Nuclear pore glycoprotein p62; AltName: Full=62 kDa nucleoporin; AltName: Full=Nucleoporin Nup62; - OS=Homo sapiens (Human).	53.2	1	1
790	O19678_HUMAN	SubName: Full=HLA-DRB4 protein; Flags: Fragment; - OS=Homo sapiens (Human).	25.4	6	0
791	O19763_HUMAN	SubName: Full=MHC class II antigen; Flags: Fragment; - OS=Homo sapiens (Human).	25.5	6	0
792	O60744_HUMAN	SubName: Full=Thioredoxin delta 3; Flags: Fragment; - OS=Homo sapiens (Human).	9.3	2	2
793	ODO2_HUMAN	RecName: Full=Dihydrolipoyllysine-residue succinyltransferase component of 2-oxoglutarate	48.7	4	4

		dehydrogenase complex, mitochondrial; EC=2.3.1.61; AltName: Full=2-oxoglutarate dehydrogenase complex component E2; Short=OGDC-E2; AltName: Full=Dihydrolipoamide succinyltransferase component of 2-oxoglutarate dehydrogenase complex; AltName: Full=E2K; Flags: Precursor; - OS=Homo sapiens (Human).			
794	ODPB_HUMAN	RecName: Full=Pyruvate dehydrogenase E1 component subunit beta, mitochondrial; Short=PDHE1-B; EC=1.2.4.1; Flags: Precursor; - OS=Homo sapiens (Human).	39.2	4	4
795	P79547_HUMAN	SubName: Full=MHC class II antigen; Flags: Fragment; - OS=Homo sapiens (Human).	10.9	4	0
796	PA1B2_HUMAN	RecName: Full=Platelet-activating factor acetylhydrolase IB subunit beta; EC=3.1.1.47; AltName: Full=PAF acetylhydrolase 30 kDa subunit; Short=PAF-AH 30 kDa subunit; AltName: Full=PAF-AH subunit beta; Short=PAFAH subunit beta; - OS=Homo sapiens (Human).	25.6	2	2
797	PARK7_HUMAN	RecName: Full=Protein DJ-1; EC=3.4.-.-; AltName: Full=Oncogene DJ1; AltName: Full=Parkinson disease protein 7; Flags: Precursor; - OS=Homo sapiens (Human).	19.9	1	1
798	PCBP1_HUMAN	RecName: Full=Poly(rC)-binding protein 1; AltName: Full=Alpha-CP1; AltName: Full=Heterogeneous nuclear ribonucleoprotein E1; Short=hnRNP E1; AltName: Full=Nucleic acid-binding protein SUB2.3; - OS=Homo sapiens (Human).	37.5	5	4
799	PCKGM_HUMAN	RecName: Full=Phosphoenolpyruvate carboxykinase [GTP], mitochondrial; Short=PEPCK-M; EC=4.1.1.32; AltName: Full=Phosphoenolpyruvate carboxylase; Flags: Precursor; - OS=Homo sapiens (Human).	70.7	9	9
800	PDC6I_HUMAN	RecName: Full=Programmed cell death 6-interacting protein; Short=PDCD6-interacting protein; AltName: Full=ALG-2-interacting protein 1; AltName: Full=Hp95; - OS=Homo sapiens (Human).	96.0	6	6
801	PDIA1_HUMAN	RecName: Full=Protein disulfide-isomerase; Short=PDI; EC=5.3.4.1; AltName: Full=Cellular thyroid hormone-binding protein; AltName: Full=Prolyl 4-hydroxylase subunit beta; AltName: Full=p55; Flags: Precursor; - OS=Homo sapiens (Human).	57.1	15	15
802	PDIA4_HUMAN	RecName: Full=Protein disulfide-isomerase A4; EC=5.3.4.1; AltName: Full=Endoplasmic reticulum resident protein 70; Short=ER protein 70; Short=ERp70; AltName: Full=Endoplasmic reticulum	72.9	9	9

		resident protein 72; Short=ER protein 72; Short=ERp-72; Short=ERp72; Flags: Precursor; - OS=Homo sapiens (Human).			
803	PDLI1_HUMAN	RecName: Full=PDZ and LIM domain protein 1; AltName: Full=C-terminal LIM domain protein 1; AltName: Full=Elfin; AltName: Full=LIM domain protein CLP-36; - OS=Homo sapiens (Human).	36.0	2	2
804	PEBP1_HUMAN	RecName: Full=Phosphatidylethanolamine-binding protein 1; Short=PEBP-1; AltName: Full=HCNPpp; AltName: Full=Neuropolypeptide h3; AltName: Full=Prostatic-binding protein; AltName: Full=Raf kinase inhibitor protein; Short=RKIP; Contains: RecName: Full=Hippocampal cholinergic neurostimulating peptide; Short=HCNP; - OS=Homo sapiens (Human).	21.0	6	6
805	PERE_HUMAN	RecName: Full=Eosinophil peroxidase; Short=EPO; EC=1.11.1.7; Contains: RecName: Full=Eosinophil peroxidase light chain; Contains: RecName: Full=Eosinophil peroxidase heavy chain; Flags: Precursor; - OS=Homo sapiens (Human).	81.0	2	2
806	PERM_HUMAN	RecName: Full=Myeloperoxidase; Short=MPO; EC=1.11.2.2; Contains: RecName: Full=Myeloperoxidase; Contains: RecName: Full=89 kDa myeloperoxidase; Contains: RecName: Full=84 kDa myeloperoxidase; Contains: RecName: Full=Myeloperoxidase light chain; Contains: RecName: Full=Myeloperoxidase heavy chain; Flags: Precursor; - OS=Homo sapiens (Human).	83.8	2	2
807	PEX14_HUMAN	RecName: Full=Peroxisomal membrane protein PEX14; AltName: Full=PTS1 receptor-docking protein; AltName: Full=Peroxin-14; AltName: Full=Peroxisomal membrane anchor protein PEX14; - OS=Homo sapiens (Human).	41.2	2	2
808	PFD2_HUMAN	RecName: Full=Prefoldin subunit 2; - OS=Homo sapiens (Human).	16.6	1	1
809	PGAM1_HUMAN	RecName: Full=Phosphoglycerate mutase 1; EC=3.1.3.13; EC=5.4.2.1; EC=5.4.2.4; AltName: Full=BPG-dependent PGAM 1; AltName: Full=Phosphoglycerate mutase isozyme B; Short=PGAM-B; - OS=Homo sapiens (Human).	28.8	3	3
810	PIGR_HUMAN	RecName: Full=Polymeric immunoglobulin receptor; Short=PIgR; Short=Poly-Ig receptor; AltName: Full=Hepatocellular carcinoma-associated protein TB6; Contains: RecName: Full=Secretory component; Flags: Precursor; - OS=Homo sapiens (Human).	83.2	3	3

811	PLBL1_HUMAN	RecName: Full=Phospholipase B-like 1; EC=3.1.1.-; AltName: Full=LAMA-like protein 1; AltName: Full=Lamina ancestor homolog 1; AltName: Full=Phospholipase B domain-containing protein 1; Flags: Precursor; - OS=Homo sapiens (Human).	63.2	4	4
812	PLCH1_HUMAN	RecName: Full=1-phosphatidylinositol 4,5-bisphosphate phosphodiesterase eta-1; EC=3.1.4.11; AltName: Full=Phosphoinositide phospholipase C-eta-1; AltName: Full=Phospholipase C-eta-1; Short=PLC-eta-1; AltName: Full=Phospholipase C-like protein 3; Short=PLC-L3; - OS=Homo sapiens (Human).	189.1	1	1
813	PLD3_HUMAN	RecName: Full=Phospholipase D3; Short=PLD 3; EC=3.1.4.4; AltName: Full=Choline phosphatase 3; AltName: Full=HindIII K4L homolog; AltName: Full=Hu-K4; AltName: Full=Phosphatidylcholine-hydrolyzing phospholipase D3; - OS=Homo sapiens (Human).	54.7	6	6
814	PLEC_HUMAN	RecName: Full=Plectin; Short=PCN; Short=PLTN; AltName: Full=Hemidesmosomal protein 1; Short=HD1; AltName: Full=Plectin-1; - OS=Homo sapiens (Human).	531.5	55	55
815	PLEK_HUMAN	RecName: Full=Pleckstrin; AltName: Full=Platelet 47 kDa protein; Short=p47; - OS=Homo sapiens (Human).	40.1	2	2
816	PLIN3_HUMAN	RecName: Full=Perilipin-3; AltName: Full=47 kDa mannose 6-phosphate receptor-binding protein; Short=47 kDa MPR-binding protein; AltName: Full=Cargo selection protein TIP47; AltName: Full=Mannose-6-phosphate receptor-binding protein 1; AltName: Full=Placental protein 17; Short=PP17; - OS=Homo sapiens (Human).	47.0	4	4
817	PLSL_HUMAN	RecName: Full=Plastin-2; AltName: Full=L-plastin; AltName: Full=LC64P; AltName: Full=Lymphocyte cytosolic protein 1; Short=LCP-1; - OS=Homo sapiens (Human).	70.2	21	21
818	PNPH_HUMAN	RecName: Full=Purine nucleoside phosphorylase; Short=PNP; EC=2.4.2.1; AltName: Full=Inosine phosphorylase; - OS=Homo sapiens (Human).	32.1	2	2
819	POTEI_HUMAN	RecName: Full=POTE ankyrin domain family member I; - OS=Homo sapiens (Human).	121.2	6	2
820	PPA5_HUMAN	RecName: Full=Tartrate-resistant acid phosphatase type 5; Short=TR-AP; EC=3.1.3.2; AltName: Full=Tartrate-resistant acid ATPase; Short=TrATPase; AltName: Full=Type 5 acid phosphatase; Flags:	36.6	5	5

		Precursor; - OS=Homo sapiens (Human).			
821	PPAC_HUMAN	RecName: Full=Low molecular weight phosphotyrosine protein phosphatase; Short=LMW-PTP; Short=LMW-PTPase; EC=3.1.3.48; AltName: Full=Adipocyte acid phosphatase; AltName: Full=Low molecular weight cytosolic acid phosphatase; EC=3.1.3.2; AltName: Full=Red cell acid phosphatase 1; - OS=Homo sapiens (Human).	18.0	1	1
822	PPIB_HUMAN	RecName: Full=Peptidyl-prolyl cis-trans isomerase B; Short=PPIase B; EC=5.2.1.8; AltName: Full=CYP-S1; AltName: Full=Cyclophilin B; AltName: Full=Rotamase B; AltName: Full=S-cyclophilin; Short=SCYLP; Flags: Precursor; - OS=Homo sapiens (Human).	23.7	3	3
823	PPT1_HUMAN	RecName: Full=Palmitoyl-protein thioesterase 1; Short=PPT-1; EC=3.1.2.22; AltName: Full=Palmitoyl-protein hydrolase 1; Flags: Precursor; - OS=Homo sapiens (Human).	34.2	3	3
824	PRDX1_HUMAN	RecName: Full=Peroxiredoxin-1; EC=1.11.1.15; AltName: Full=Natural killer cell-enhancing factor A; Short=NKEF-A; AltName: Full=Proliferation-associated gene protein; Short=PAG; AltName: Full=Thioredoxin peroxidase 2; AltName: Full=Thioredoxin-dependent peroxide reductase 2; - OS=Homo sapiens (Human).	22.1	7	5
825	PRDX4_HUMAN	RecName: Full=Peroxiredoxin-4; EC=1.11.1.15; AltName: Full=Antioxidant enzyme AOE372; Short=AOE37-2; AltName: Full=Peroxiredoxin IV; Short=Prx-IV; AltName: Full=Thioredoxin peroxidase AO372; AltName: Full=Thioredoxin-dependent peroxide reductase A0372; Flags: Precursor; - OS=Homo sapiens (Human).	30.5	6	5
826	PRDX5_HUMAN	RecName: Full=Peroxiredoxin-5, mitochondrial; EC=1.11.1.15; AltName: Full=Alu corepressor 1; AltName: Full=Antioxidant enzyme B166; Short=AOEB166; AltName: Full=Liver tissue 2D-page spot 71B; AltName: Full=PLP; AltName: Full=Peroxiredoxin V; Short=Prx-V; AltName: Full=Peroxisomal antioxidant enzyme; AltName: Full=TPx type VI; AltName: Full=Thioredoxin peroxidase PMP20; AltName: Full=Thioredoxin reductase; Flags: Precursor; - OS=Homo sapiens (Human).	22.1	6	6
827	PRDX6_HUMAN	RecName: Full=Peroxiredoxin-6; EC=1.11.1.15; AltName: Full=1-Cys peroxiredoxin; Short=1-Cys	25.0	5	5

		PRX; AltName: Full=24 kDa protein; AltName: Full=Acidic calcium-independent phospholipase A2; Short=aiPLA2; EC=3.1.1.-; AltName: Full=Antioxidant protein 2; AltName: Full=Liver 2D page spot 40; AltName: Full=Non-selenium glutathione peroxidase; Short=NSGPx; EC=1.11.1.9; AltName: Full=Red blood cells page spot 12; - OS=Homo sapiens (Human).			
828	PRG3_HUMAN	RecName: Full=Proteoglycan 3; AltName: Full=Eosinophil major basic protein homolog; AltName: Full=Prepro-major basic protein homolog; Short=Prepro-MBPH; Flags: Precursor; - OS=Homo sapiens (Human).	25.4	1	1
829	PROF1_HUMAN	RecName: Full=Profilin-1; AltName: Full=Epididymis tissue protein Li 184a; AltName: Full=Profilin I; - OS=Homo sapiens (Human).	15.0	6	6
830	PRS6B_HUMAN	RecName: Full=26S protease regulatory subunit 6B; AltName: Full=26S proteasome AAA-ATPase subunit RPT3; AltName: Full=MB67-interacting protein; AltName: Full=MIP224; AltName: Full=Proteasome 26S subunit ATPase 4; AltName: Full=Tat-binding protein 7; Short=TBP-7; - OS=Homo sapiens (Human).	47.3	1	1
831	PSA2_HUMAN	RecName: Full=Proteasome subunit alpha type-2; EC=3.4.25.1; AltName: Full=Macropain subunit C3; AltName: Full=Multicatalytic endopeptidase complex subunit C3; AltName: Full=Proteasome component C3; - OS=Homo sapiens (Human).	25.9	2	2
832	PSA5_HUMAN	RecName: Full=Proteasome subunit alpha type-5; EC=3.4.25.1; AltName: Full=Macropain zeta chain; AltName: Full=Multicatalytic endopeptidase complex zeta chain; AltName: Full=Proteasome zeta chain; - OS=Homo sapiens (Human).	26.4	2	2
833	PSME1_HUMAN	RecName: Full=Proteasome activator complex subunit 1; AltName: Full=11S regulator complex subunit alpha; Short=REG-alpha; AltName: Full=Activator of multicatalytic protease subunit 1; AltName: Full=Interferon gamma up-regulated I-5111 protein; Short=IGUP I-5111; AltName: Full=Proteasome activator 28 subunit alpha; Short=PA28a; Short=PA28alpha; - OS=Homo sapiens (Human).	28.7	5	5
834	PSME2_HUMAN	RecName: Full=Proteasome activator complex subunit 2; AltName: Full=11S regulator complex	27.4	4	4

		subunit beta; Short=REG-beta; AltName: Full=Activator of multicatalytic protease subunit 2; AltName: Full=Proteasome activator 28 subunit beta; Short=PA28b; Short=PA28beta; - OS=Homo sapiens (Human).			
835	PTBP1_HUMAN	RecName: Full=Polypyrimidine tract-binding protein 1; Short=PTB; AltName: Full=57 kDa RNA-binding protein PPTB-1; AltName: Full=Heterogeneous nuclear ribonucleoprotein I; Short=hnRNP I; - OS=Homo sapiens (Human).	57.2	1	1
836	PTN6_HUMAN	RecName: Full=Tyrosine-protein phosphatase non-receptor type 6; EC=3.1.3.48; AltName: Full=Hematopoietic cell protein-tyrosine phosphatase; AltName: Full=Protein-tyrosine phosphatase 1C; Short=PTP-1C; AltName: Full=Protein-tyrosine phosphatase SHP-1; AltName: Full=SH-PTP1; - OS=Homo sapiens (Human).	67.5	12	12
837	Q05CP4_HUMAN	SubName: Full=EIF2AK2 protein; Flags: Fragment; - OS=Homo sapiens (Human).	40.7	1	1
838	Q05CU9_HUMAN	SubName: Full=MNDA protein; Flags: Fragment; - OS=Homo sapiens (Human).	35.0	3	3
839	Q05DH1_HUMAN	RecName: Full=Proteasome subunit alpha type; EC=3.4.25.1; Flags: Fragment; - OS=Homo sapiens (Human).	26.7	3	3
840	Q06AH7_HUMAN	SubName: Full=Transferrin; - OS=Homo sapiens (Human).	76.9	10	10
841	Q08AS4_HUMAN	SubName: Full=HLA-DQA1 protein; - OS=Homo sapiens (Human).	27.9	4	1
842	Q08ES8_HUMAN	SubName: Full=Cell growth-inhibiting protein 34; - OS=Homo sapiens (Human).	20.1	2	2
843	Q0KKI6_HUMAN	SubName: Full=Immunoblobulin light chain; Flags: Fragment; - OS=Homo sapiens (Human).	24.0	5	5
844	Q0QEN7_HUMAN	RecName: Full=ATP synthase subunit beta; EC=3.6.3.14; Flags: Fragment; - OS=Homo sapiens (Human).	48.1	16	16
845	Q0QEY7_HUMAN	SubName: Full=Succinate dehydrogenase complex subunit B; Flags: Fragment; - OS=Homo sapiens (Human).	28.9	1	1
846	Q0QF37_HUMAN	RecName: Full=Malate dehydrogenase; EC=1.1.1.37; Flags: Fragment; - OS=Homo sapiens (Human).	31.9	15	15
847	Q0VGA5_HUMAN	SubName: Full=SARS protein; - OS=Homo sapiens (Human).	58.4	1	1
848	Q0VGD6_HUMAN	SubName: Full=HNRPR protein; Flags: Fragment; - OS=Homo sapiens (Human).	67.8	3	2

849	Q108N1_HUMAN	SubName: Full=Acyl-CoA synthetase long-chain family member 1 isoform a; Flags: Fragment; - OS=Homo sapiens (Human).	41.5	3	3
850	Q12898_HUMAN	SubName: Full=Adenine phosphoribosyltransferase; Flags: Fragment; - OS=Homo sapiens (Human).	3.5	1	1
851	Q14476_HUMAN	SubName: Full=G-gamma-hemoglobin gene from Greek HPFH mutant, .; Flags: Fragment; - OS=Homo sapiens (Human).	11.0	3	2
852	Q14485_HUMAN	SubName: Full=Delta-hemoglobin; Flags: Fragment; - OS=Homo sapiens (Human).	6.7	5	1
853	Q14730_HUMAN	SubName: Full=La 4.1 protein; Flags: Fragment; - OS=Homo sapiens (Human).	33.7	1	1
854	Q14887_HUMAN	SubName: Full=Mucin; Flags: Fragment; - OS=Homo sapiens (Human).	50.6	2	1
855	Q15136_HUMAN	SubName: Full=Protein kinase A-alpha; Flags: Fragment; - OS=Homo sapiens (Human).	23.9	1	1
856	Q1JQ76_HUMAN	RecName: Full=Ribosomal protein; Flags: Fragment; - OS=Homo sapiens (Human).	23.5	2	2
857	Q1JUQ3_HUMAN	SubName: Full=FK506 binding protein12; - OS=Homo sapiens (Human).	4.0	1	1
858	Q1RMG2_HUMAN	RecName: Full=Adenosylhomocysteinase; EC=3.3.1.1; - OS=Homo sapiens (Human).	33.8	1	1
859	Q1RMY8_HUMAN	SubName: Full=GNB1 protein; Flags: Fragment; - OS=Homo sapiens (Human).	36.3	2	1
860	Q2NLC8_HUMAN	SubName: Full=GSTK1 protein; Flags: Fragment; - OS=Homo sapiens (Human).	19.4	4	4
861	Q2Q9H2_HUMAN	RecName: Full=Glucose-6-phosphate 1-dehydrogenase; EC=1.1.1.49; Flags: Fragment; - OS=Homo sapiens (Human).	54.8	6	6
862	Q2TU34_HUMAN	RecName: Full=Fructose-1,6-bisphosphatase class 1 D; Short=FBPase class 1 D; EC=3.1.3.11; AltName: Full=D-fructose-1,6-bisphosphate 1-phosphohydrolase class 1 D; - OS=Homo sapiens (Human).	36.8	7	7
863	Q30131_HUMAN	SubName: Full=HLA DR-beta-III; Flags: Precursor; Fragment; - OS=Homo sapiens (Human).	27.2	6	1
864	Q32XH3_HUMAN	SubName: Full=Ribosomal protein L18a-like protein; - OS=Homo sapiens (Human).	15.8	1	1
865	Q330K1_HUMAN	SubName: Full=Mitochondrial import inner membrane translocase subunit TIM50; SubName: Full=TIM50L; SubName: Full=TIMM50 protein; - OS=Homo sapiens (Human).	27.6	1	1
866	Q38G99_HUMAN	SubName: Full=C-myc intron-binding protein 1; - OS=Homo sapiens (Human).	268.6	1	1
867	Q3LAB6_HUMAN	SubName: Full=MHC class II antigen; Flags: Fragment; - OS=Homo sapiens (Human).	20.8	6	2

Chapter 10 Appendices

868	Q3LAB7_HUMAN	SubName: Full=MHC class II antigen; Flags: Fragment; - OS=Homo sapiens (Human).	21.1	4	0
869	Q3LAC1_HUMAN	SubName: Full=MHC class II antigen; Flags: Fragment; - OS=Homo sapiens (Human).	21.3	4	0
870	Q3LR79_HUMAN	SubName: Full=Hemoglobin beta; Flags: Fragment; - OS=Homo sapiens (Human).	11.5	8	1
871	Q45KI0_HUMAN	SubName: Full=Trypsin I; Flags: Fragment; - OS=Homo sapiens (Human).	9.2	1	1
872	Q49AG2_HUMAN	SubName: Full=TMED5 protein; - OS=Homo sapiens (Human).	19.9	1	1
873	Q4G1A8_HUMAN	SubName: Full=CAMK2D protein; Flags: Fragment; - OS=Homo sapiens (Human).	38.9	1	1
874	Q4TZM4_HUMAN	SubName: Full=Hemoglobin beta chain; Flags: Fragment; - OS=Homo sapiens (Human).	11.0	7	1
875	Q4VXM1_HUMAN	SubName: Full=Methylenetetrahydrofolate dehydrogenase (NADP+ dependent) 1-like; SubName: Full=Monofunctional C1-tetrahydrofolate synthase, mitochondrial; Flags: Fragment; - OS=Homo sapiens (Human).	6.2	1	1
876	Q4VXN1_HUMAN	SubName: Full=Band 4.1-like protein 1; SubName: Full=Erythrocyte membrane protein band 4.1-like 1; Flags: Fragment; - OS=Homo sapiens (Human).	22.9	1	1
877	Q4W5I3_HUMAN	SubName: Full=Putative uncharacterized protein ABCG2; Flags: Fragment; - OS=Homo sapiens (Human).	66.8	1	1
878	Q53ET5_HUMAN	SubName: Full=ATPase, H+ transporting, lysosomal V0 subunit a isoform 1 variant; Flags: Fragment; - OS=Homo sapiens (Human).	95.7	1	1
879	Q53FJ5_HUMAN	SubName: Full=Prosaposin (Variant Gaucher disease and variant metachromatic leukodystrophy) variant; Flags: Fragment; - OS=Homo sapiens (Human).	58.1	9	9
880	Q53G25_HUMAN	SubName: Full=Ribosomal protein S5 variant; Flags: Fragment; - OS=Homo sapiens (Human).	23.0	2	2
881	Q53G71_HUMAN	SubName: Full=Calreticulin variant; Flags: Fragment; - OS=Homo sapiens (Human).	46.9	5	5
882	Q53G74_HUMAN	SubName: Full=Ribosomal protein L4 variant; Flags: Fragment; - OS=Homo sapiens (Human).	47.7	4	4
883	Q53G79_HUMAN	SubName: Full=Carnitine O-palmitoyltransferase II, mitochondrial variant; Flags: Fragment; - OS=Homo sapiens (Human).	64.7	5	5
884	Q53G83_HUMAN	SubName: Full=Ribosomal protein S3 variant; Flags: Fragment; - OS=Homo sapiens (Human).	26.7	4	4
885	Q53GN4_HUMAN	SubName: Full=WD repeat domain 1, isoform CRA_a; SubName: Full=WD repeat-containing protein	66.1	9	9

		1 isoform 1 variant; Flags: Fragment; - OS=Homo sapiens (Human).			
886	Q53HF2_HUMAN	SubName: Full=Heat shock 70kDa protein 8 isoform 2 variant; Flags: Fragment; - OS=Homo sapiens (Human).	53.5	13	10
887	Q53HP9_HUMAN	SubName: Full=Chromosome 14 open reading frame 159 variant; Flags: Fragment; - OS=Homo sapiens (Human).	44.2	2	2
888	Q53QE9_HUMAN	SubName: Full=Putative uncharacterized protein UGP2; Flags: Fragment; - OS=Homo sapiens (Human).	49.2	4	4
889	Q53T09_HUMAN	SubName: Full=Putative uncharacterized protein XRCC5; Flags: Fragment; - OS=Homo sapiens (Human).	64.2	1	1
890	Q562M5_HUMAN	SubName: Full=Actin-like protein; Flags: Fragment; - OS=Homo sapiens (Human).	11.6	3	1
891	Q562V5_HUMAN	SubName: Full=Actin-like protein; Flags: Fragment; - OS=Homo sapiens (Human).	11.4	2	1
892	Q567R0_HUMAN	SubName: Full=UQCRH protein; SubName: Full=Ubiquinol-cytochrome c reductase hinge protein, isoform CRA_c; - OS=Homo sapiens (Human).	9.9	1	1
893	Q567R6_HUMAN	RecName: Full=Single-stranded DNA-binding protein; - OS=Homo sapiens (Human).	17.3	2	2
894	Q56FN6_HUMAN	SubName: Full=MHC class II antigen; - OS=Homo sapiens (Human).	30.0	6	0
895	Q56FP5_HUMAN	SubName: Full=MHC class II antigen; - OS=Homo sapiens (Human).	30.1	6	0
896	Q59EW3_HUMAN	SubName: Full=RAB18, member RAS oncogene family variant; Flags: Fragment; - OS=Homo sapiens (Human).	14.4	1	1
897	Q59F83_HUMAN	SubName: Full=Major histocompatibility complex, class II, DM beta variant; Flags: Fragment; - OS=Homo sapiens (Human).	16.8	2	2
898	Q59FQ8_HUMAN	SubName: Full=Spinster variant; Flags: Fragment; - OS=Homo sapiens (Human).	36.4	1	1
899	Q59G96_HUMAN	SubName: Full=Dynamin 2 isoform 4 variant; Flags: Fragment; - OS=Homo sapiens (Human).	55.1	2	2
900	Q59GN1_HUMAN	RecName: Full=Proteasome subunit beta type; EC=3.4.25.1; Flags: Fragment; - OS=Homo sapiens (Human).	21.3	2	2
901	Q59GS3_HUMAN	SubName: Full=Proteasome 26S ATPase subunit 5 variant; Flags: Fragment; - OS=Homo sapiens	38.7	2	2

		(Human).			
902	Q59H47_HUMAN	SubName: Full=Guanylate binding protein 1, interferon-inducible, 67kD variant; Flags: Fragment; - OS=Homo sapiens (Human).	32.7	2	1
903	Q59H95_HUMAN	SubName: Full=Flightless I homolog variant; Flags: Fragment; - OS=Homo sapiens (Human).	125.2	1	1
904	Q5CAQ5_HUMAN	RecName: Full=Chaperone protein HtpG I; AltName: Full=Heat shock protein HtpG I; AltName: Full=High temperature protein G I; - OS=Homo sapiens (Human).	92.3	13	12
905	Q5HYB6_HUMAN	SubName: Full=Putative uncharacterized protein DKFZp686J1372; - OS=Homo sapiens (Human).	27.2	5	3
906	Q5HYD9_HUMAN	SubName: Full=Putative uncharacterized protein DKFZp686M0619; Flags: Fragment; - OS=Homo sapiens (Human).	11.9	1	1
907	Q5HYM2_HUMAN	SubName: Full=Putative uncharacterized protein DKFZp686O2462; Flags: Fragment; - OS=Homo sapiens (Human).	72.0	3	3
908	Q5J7W2_HUMAN	SubName: Full=Migration-inducing gene 9 protein; - OS=Homo sapiens (Human).	9.6	1	1
909	Q5JPE4_HUMAN	SubName: Full=Putative uncharacterized protein DKFZp667O202; - OS=Homo sapiens (Human).	20.4	1	1
910	Q5JPU2_HUMAN	SubName: Full=Pyruvate dehydrogenase (Lipoamide) alpha 1; SubName: Full=Pyruvate dehydrogenase E1 component subunit alpha, somatic form, mitochondrial; Flags: Fragment; - OS=Homo sapiens (Human).	13.8	1	1
911	Q5JQ44_HUMAN	SubName: Full=Putative uncharacterized protein DKFZp547A0616; Flags: Fragment; - OS=Homo sapiens (Human).	20.3	1	1
912	Q5JR06_HUMAN	SubName: Full=Ras homolog gene family, member C; SubName: Full=Rho-related GTP-binding protein RhoC; Flags: Fragment; - OS=Homo sapiens (Human).	10.3	3	3
913	Q5JR95_HUMAN	SubName: Full=40S ribosomal protein S8; SubName: Full=Ribosomal protein S8; - OS=Homo sapiens (Human).	21.9	3	3
914	Q5JTW5_HUMAN	SubName: Full=Propionyl Coenzyme A carboxylase, alpha polypeptide; Flags: Fragment; - OS=Homo sapiens (Human).	15.6	1	1
915	Q5JVH5_HUMAN	SubName: Full=Ribosomal protein 26 (RPS26) pseudogene; - OS=Homo sapiens (Human).	13.0	1	1

916	Q5JW01_HUMAN	SubName: Full=Engulfment and cell motility 2; SubName: Full=Engulfment and cell motility protein 2; Flags: Fragment; - OS=Homo sapiens (Human).	33.2	1	1
917	Q5JXH9_HUMAN	SubName: Full=Four and a half LIM domains 1; SubName: Full=Four and a half LIM domains protein 1; Flags: Fragment; - OS=Homo sapiens (Human).	17.8	1	1
918	Q5QPE4_HUMAN	SubName: Full=Sorting nexin 5; SubName: Full=Sorting nexin-5; Flags: Fragment; - OS=Homo sapiens (Human).	26.3	2	2
919	Q5QPM0_HUMAN	SubName: Full=RNA binding protein, autoantigenic (HnRNP-associated with lethal yellow homolog (Mouse)); SubName: Full=RNA-binding protein Raly; Flags: Fragment; - OS=Homo sapiens (Human).	18.7	2	2
920	Q5QTQ6_HUMAN	SubName: Full=MSTP010; SubName: Full=cDNA FLJ11394 fis, clone HEMBA1000592, highly similar to Sorting nexin-6; - OS=Homo sapiens (Human).	24.6	1	1
921	Q5R370_HUMAN	SubName: Full=Calcyclin binding protein; SubName: Full=Calcyclin-binding protein; - OS=Homo sapiens (Human).	21.2	1	1
922	Q5S4N1_HUMAN	SubName: Full=Putative uncharacterized protein; Flags: Fragment; - OS=Homo sapiens (Human).	40.2	2	2
923	Q5SQT6_HUMAN	SubName: Full=Inorganic pyrophosphatase; SubName: Full=Pyrophosphatase (Inorganic) 1; - OS=Homo sapiens (Human).	20.0	2	1
924	Q5SYT8_HUMAN	SubName: Full=Novel protein similar to Pre-B cell enhancing factor (PBEF); SubName: Full=Protein NAMPTL; Flags: Fragment; - OS=Homo sapiens (Human).	53.4	5	5
925	Q5T0R9_HUMAN	RecName: Full=Adenylyl cyclase-associated protein; Flags: Fragment; - OS=Homo sapiens (Human).	28.7	4	1
926	Q5T123_HUMAN	SubName: Full=SH3 domain binding glutamic acid-rich protein like 3; SubName: Full=SH3 domain-binding glutamic acid-rich-like protein 3; - OS=Homo sapiens (Human).	9.4	1	1
927	Q5T204_HUMAN	SubName: Full=Nicastrin; Flags: Fragment; - OS=Homo sapiens (Human).	30.0	3	3
928	Q5T6W5_HUMAN	SubName: Full=Heterogeneous nuclear ribonucleoprotein K; - OS=Homo sapiens (Human).	47.5	6	6
929	Q5T6W8_HUMAN	SubName: Full=Acidic (Leucine-rich) nuclear phosphoprotein 32 family, member B; SubName: Full=Acidic leucine-rich nuclear phosphoprotein 32 family member B; Flags: Fragment; - OS=Homo sapiens (Human).	17.9	1	1

930	Q5TB53_HUMAN	SubName: Full=SM-11044 binding protein (SMBP)(EP70-P-iso); SubName: Full=Transmembrane 9 superfamily member 3; Flags: Fragment; - OS=Homo sapiens (Human).	29.9	1	1
931	Q5TCU6_HUMAN	SubName: Full=Talin 1; SubName: Full=Talin-1; - OS=Homo sapiens (Human).	257.9	23	23
932	Q5VU21_HUMAN	SubName: Full=PAI-1 mRNA-binding protein variant; SubName: Full=SERPINE1 mRNA binding protein 1; SubName: Full=cDNA, FLJ92551, Homo sapiens PAI-1 mRNA-binding protein (PAI-RBP1), mRNA; - OS=Homo sapiens (Human).	42.4	1	1
933	Q5VXS2_HUMAN	SubName: Full=Ubiquitin-fold modifier 1; Flags: Fragment; - OS=Homo sapiens (Human).	8.5	1	1
934	Q5XTR9_HUMAN	SubName: Full=Hemoglobin delta-beta fusion protein; Flags: Fragment; - OS=Homo sapiens (Human).	3.9	3	1
935	Q60FE6_HUMAN	SubName: Full=Filamin A; - OS=Homo sapiens (Human).	277.3	65	65
936	Q67AU1_HUMAN	SubName: Full=MHC class II antigen; Flags: Fragment; - OS=Homo sapiens (Human).	10.8	1	1
937	Q68CW8_HUMAN	SubName: Full=Putative uncharacterized protein DKFZp434I2216; Flags: Fragment; - OS=Homo sapiens (Human).	6.0	1	1
938	Q68D64_HUMAN	SubName: Full=Putative uncharacterized protein DKFZp686E23276; Flags: Fragment; - OS=Homo sapiens (Human).	37.0	4	4
939	Q68DR3_HUMAN	SubName: Full=Putative uncharacterized protein DKFZp779H1622; Flags: Fragment; - OS=Homo sapiens (Human).	35.1	1	1
940	Q69YR1_HUMAN	SubName: Full=Putative uncharacterized protein DKFZp667C1917; Flags: Fragment; - OS=Homo sapiens (Human).	23.5	1	1
941	Q69YT6_HUMAN	SubName: Full=Putative uncharacterized protein DKFZp547B159; Flags: Fragment; - OS=Homo sapiens (Human).	21.2	1	1
942	Q6AW83_HUMAN	SubName: Full=Putative uncharacterized protein DKFZp686G08243; Flags: Fragment; - OS=Homo sapiens (Human).	15.5	1	1
943	Q6DC98_HUMAN	SubName: Full=LMNB1 protein; Flags: Fragment; - OS=Homo sapiens (Human).	38.1	6	5
944	Q6FG43_HUMAN	SubName: Full=FLOT2 protein; SubName: Full=Flotillin 2; SubName: Full=HCG1998851, isoform	41.7	4	4

		CRA_e; - OS=Homo sapiens (Human).			
945	Q6FGE5_HUMAN	SubName: Full=S100A10 protein; Flags: Fragment; - OS=Homo sapiens (Human).	11.2	1	1
946	Q6IBG5_HUMAN	SubName: Full=MYL6 protein; - OS=Homo sapiens (Human).	13.0	4	4
947	Q6IPN0_HUMAN	SubName: Full=RTN4 protein; - OS=Homo sapiens (Human).	36.9	5	5
948	Q6LBZ1_HUMAN	SubName: Full=MRNA for apolipoprotein E (apo E); Flags: Fragment; - OS=Homo sapiens (Human).	19.9	1	1
949	Q6LER7_HUMAN	SubName: Full=Alpha-galactosidase A; EC=3.2.1.22; Flags: Fragment; - OS=Homo sapiens (Human).	45.8	2	2
950	Q6NSD4_HUMAN	RecName: Full=Glutathione peroxidase; - OS=Homo sapiens (Human).	16.2	4	4
951	Q6P1N7_HUMAN	SubName: Full=TAPBP protein; SubName: Full=Tapasin; - OS=Homo sapiens (Human).	16.4	1	1
952	Q6PIX2_HUMAN	SubName: Full=SFPQ protein; Flags: Fragment; - OS=Homo sapiens (Human).	55.4	3	3
953	Q6UYC3_HUMAN	SubName: Full=Lamin A/C; SubName: Full=Prelamin-A/C; SubName: Full=Progerin; - OS=Homo sapiens (Human).	69.2	21	21
954	Q6VFQ6_HUMAN	SubName: Full=Hemoglobin beta chain; Flags: Fragment; - OS=Homo sapiens (Human).	4.5	3	2
955	Q6ZNK5_HUMAN	SubName: Full=FLJ00293 protein; Flags: Fragment; - OS=Homo sapiens (Human).	92.8	2	2
956	Q6ZR81_HUMAN	SubName: Full=cDNA FLJ46566 fis, clone THYMU3040829, moderately similar to Cold-inducible RNA-binding protein; - OS=Homo sapiens (Human).	15.3	1	1
957	Q70T18_HUMAN	SubName: Full=BBF2H7/FUS protein; Flags: Fragment; - OS=Homo sapiens (Human).	16.1	1	1
958	Q7KYN0_HUMAN	SubName: Full=HS24/P52 protein; Flags: Fragment; - OS=Homo sapiens (Human).	29.4	2	2
959	Q7Z4Q5_HUMAN	SubName: Full=Heterogeneous nuclear ribonucleoprotein U (Scaffold attachment factor A), isoform CRA_a; - OS=Homo sapiens (Human).	57.6	1	1
960	Q7Z4W8_HUMAN	SubName: Full=Heparin-binding protein HBp15; - OS=Homo sapiens (Human).	14.8	1	1
961	Q7Z612_HUMAN	SubName: Full=Acidic ribosomal phosphoprotein P1; - OS=Homo sapiens (Human).	11.4	1	1
962	Q861F4_HUMAN	SubName: Full=MHC class II antigen; Flags: Fragment; - OS=Homo sapiens (Human).	21.5	3	1
963	Q86TY5_HUMAN	SubName: Full=Full-length cDNA clone CS0DI041YE05 of Placenta of Homo sapiens (human); - OS=Homo sapiens (Human).	13.9	4	4
964	Q86UL7_HUMAN	SubName: Full=Putative uncharacterized protein TBXAS1; Flags: Fragment; - OS=Homo sapiens	35.6	3	3

		(Human).			
965	Q86YQ1_HUMAN	SubName: Full=Hemoglobin alpha-2; Flags: Fragment; - OS=Homo sapiens (Human).	9.7	4	1
966	Q86YQ4_HUMAN	SubName: Full=Alpha-1 globin; Flags: Fragment; - OS=Homo sapiens (Human).	9.5	4	1
967	Q86Z09_HUMAN	SubName: Full=FGA protein; Flags: Fragment; - OS=Homo sapiens (Human).	7.0	1	1
968	Q8HWG4_HUMAN	SubName: Full=MHC class II antigen; Flags: Fragment; - OS=Homo sapiens (Human).	10.8	4	0
969	Q8IUL9_HUMAN	SubName: Full=Hemoglobin beta chain variant Hb.Sinai-Bel Air; Flags: Fragment; - OS=Homo sapiens (Human).	11.5	8	1
970	Q8IWL5_HUMAN	SubName: Full=CLU; Flags: Fragment; - OS=Homo sapiens (Human).	16.3	1	1
971	Q8IZ29_HUMAN	SubName: Full=Tubulin, beta 2C; - OS=Homo sapiens (Human).	49.8	12	4
972	Q8IZI0_HUMAN	SubName: Full=Hemoglobin beta chain variant Hb-I_Toulouse; Flags: Fragment; - OS=Homo sapiens (Human).	11.5	8	1
973	Q8N730_HUMAN	SubName: Full=Peripheral-type Benzodiazepine Receptor; Flags: Fragment; - OS=Homo sapiens (Human).	6.7	1	1
974	Q8N9C4_HUMAN	SubName: Full=cDNA FLJ37765 fis, clone BRHIP2024742, highly similar to ATP-CITRATE; - OS=Homo sapiens (Human).	76.4	1	1
975	Q8NB80_HUMAN	SubName: Full=cDNA FLJ34106 fis, clone FCBBF3008073, highly similar to SPLICING FACTOR, ARGININE/SERINE-RICH 7; - OS=Homo sapiens (Human).	15.9	1	1
976	Q8TC97_HUMAN	SubName: Full=CTBS protein; - OS=Homo sapiens (Human).	11.7	2	2
977	Q8TES5_HUMAN	SubName: Full=FLJ00114 protein; Flags: Fragment; - OS=Homo sapiens (Human).	38.9	1	1
978	Q8WVH4_HUMAN	SubName: Full=Putative uncharacterized protein; Flags: Fragment; - OS=Homo sapiens (Human).	20.1	1	1
979	Q8WYJ5_HUMAN	SubName: Full=Protein kinase C inhibitor-2; - OS=Homo sapiens (Human).	13.9	2	2
980	Q93020_HUMAN	SubName: Full=GTP-binding regulatory protein Gi alpha-2 chain; Flags: Fragment; - OS=Homo sapiens (Human).	22.1	4	4
981	Q95379_HUMAN	SubName: Full=MHC class II HLA-DR2; Flags: Fragment; - OS=Homo sapiens (Human).	24.7	6	0
982	Q95HL2_HUMAN	SubName: Full=MHC class I antigen; Flags: Fragment; - OS=Homo sapiens (Human).	37.9	4	1

983	Q969I0_HUMAN	SubName: Full=KRT8 protein; Flags: Fragment; - OS=Homo sapiens (Human).	41.1	7	6
984	Q96B07_HUMAN	SubName: Full=EIF4A2 protein; - OS=Homo sapiens (Human).	21.0	1	1
985	Q96ET4_HUMAN	SubName: Full=Similar to calcyphosine; Flags: Fragment; - OS=Homo sapiens (Human).	18.4	1	1
986	Q96HX3_HUMAN	SubName: Full=Similar to ribophorin I; Flags: Fragment; - OS=Homo sapiens (Human).	64.5	10	10
987	Q96IR1_HUMAN	SubName: Full=RPS4X protein; Flags: Fragment; - OS=Homo sapiens (Human).	27.2	2	2
988	Q9BCN9_HUMAN	SubName: Full=MHC class II antigen; Flags: Fragment; - OS=Homo sapiens (Human).	20.2	6	1
989	Q9BS19_HUMAN	SubName: Full=HPX protein; - OS=Homo sapiens (Human).	28.6	1	1
990	Q9BVJ8_HUMAN	SubName: Full=HEXA protein; Flags: Fragment; - OS=Homo sapiens (Human).	47.1	9	8
991	Q9BZU1_HUMAN	SubName: Full=PNAS-20; - OS=Homo sapiens (Human).	9.0	1	1
992	Q9H9J7_HUMAN	SubName: Full=cDNA FLJ12692 fis, clone NT2RM4002623, weakly similar to ASPARTYL-TRNA SYNTHETASE (EC 6.1.1.12); - OS=Homo sapiens (Human).	52.6	1	1
993	Q9HBB2_HUMAN	SubName: Full=Cytoplasmic aconitate hydratase; SubName: Full=Iron regulatory protein 1; - OS=Homo sapiens (Human).	87.0	5	5
994	Q9HBQ7_HUMAN	SubName: Full=Cathepsin L, isoform CRA_b; - OS=Homo sapiens (Human).	16.8	2	2
995	Q9NP01_HUMAN	SubName: Full=Fibrillin 15; Flags: Fragment; - OS=Homo sapiens (Human).	56.5	1	1
996	Q9P1N8_HUMAN	SubName: Full=PRO0868; SubName: Full=cDNA FLJ51293, highly similar to Lamina-associated polypeptide 2, isoforms beta/gamma; - OS=Homo sapiens (Human).	12.1	1	1
997	Q9TQD9_HUMAN	SubName: Full=MHC class II antigen HLA-DR-beta 1; Flags: Fragment; - OS=Homo sapiens (Human).	27.2	6	0
998	Q9UEH5_HUMAN	SubName: Full=24-kDa subunit of complex I; EC=1.6.5.3; Flags: Fragment; - OS=Homo sapiens (Human).	25.4	2	2
999	Q9UF24_HUMAN	SubName: Full=Putative uncharacterized protein DKFZp586K0821; Flags: Fragment; - OS=Homo sapiens (Human).	22.2	3	3
1000	Q9UHS8_HUMAN	SubName: Full=PRO1975; - OS=Homo sapiens (Human).	44.1	9	9
1001	Q9UK54_HUMAN	SubName: Full=Hemoglobin beta subunit variant; Flags: Fragment; - OS=Homo sapiens (Human).	14.0	8	1

1002	Q9UNM1_HUMAN	SubName: Full=Chaperonin 10-related protein; Flags: Fragment; - OS=Homo sapiens (Human).	10.3	5	5
1003	Q9UPE4_HUMAN	SubName: Full=Putative mitochondrial inner membrane protein import receptor; - OS=Homo sapiens (Human).	47.3	1	1
1004	Q9UQT9_HUMAN	SubName: Full=Leucocyte antigen DR52 beta 1 chain; Flags: Fragment; - OS=Homo sapiens (Human).	10.8	4	0
1005	QCR9_HUMAN	RecName: Full=Cytochrome b-c1 complex subunit 9; AltName: Full=Complex III subunit 9; AltName: Full=Complex III subunit X; AltName: Full=Cytochrome c1 non-heme 7 kDa protein; AltName: Full=Ubiquinol-cytochrome c reductase complex 7.2 kDa protein; - OS=Homo sapiens (Human).	7.3	1	1
1006	R13AX_HUMAN	RecName: Full=Putative 60S ribosomal protein L13a-like MGC87657; - OS=Homo sapiens (Human).	12.1	1	1
1007	RAB10_HUMAN	RecName: Full=Ras-related protein Rab-10; - OS=Homo sapiens (Human).	22.5	4	2
1008	RAB14_HUMAN	RecName: Full=Ras-related protein Rab-14; - OS=Homo sapiens (Human).	23.9	4	3
1009	RAB1A_HUMAN	RecName: Full=Ras-related protein Rab-1A; AltName: Full=YPT1-related protein; - OS=Homo sapiens (Human).	22.7	6	3
1010	RAB21_HUMAN	RecName: Full=Ras-related protein Rab-21; Flags: Precursor; - OS=Homo sapiens (Human).	24.3	3	3
1011	RAB2A_HUMAN	RecName: Full=Ras-related protein Rab-2A; - OS=Homo sapiens (Human).	23.5	3	3
1012	RAB31_HUMAN	RecName: Full=Ras-related protein Rab-31; AltName: Full=Ras-related protein Rab-22B; - OS=Homo sapiens (Human).	21.6	4	4
1013	RAB5C_HUMAN	RecName: Full=Ras-related protein Rab-5C; AltName: Full=L1880; AltName: Full=RAB5L; - OS=Homo sapiens (Human).	23.5	4	4
1014	RAB7A_HUMAN	RecName: Full=Ras-related protein Rab-7a; - OS=Homo sapiens (Human).	23.5	9	9
1015	RAB9A_HUMAN	RecName: Full=Ras-related protein Rab-9A; - OS=Homo sapiens (Human).	22.8	1	1
1016	RAC2_HUMAN	RecName: Full=Ras-related C3 botulinum toxin substrate 2; AltName: Full=GX; AltName: Full=Small G protein; AltName: Full=p21-Rac2; Flags: Precursor; - OS=Homo sapiens (Human).	21.4	4	3
1017	RAN_HUMAN	RecName: Full=GTP-binding nuclear protein Ran; AltName: Full=Androgen receptor-associated	24.4	3	3

		protein 24; AltName: Full=GTPase Ran; AltName: Full=Ras-like protein TC4; AltName: Full=Ras-related nuclear protein; - OS=Homo sapiens (Human).			
1018	RINI_HUMAN	RecName: Full=Ribonuclease inhibitor; AltName: Full=Placental ribonuclease inhibitor; Short=Placental RNase inhibitor; AltName: Full=Ribonuclease/angiogenin inhibitor 1; Short=RAI; - OS=Homo sapiens (Human).	49.9	12	12
1019	RISC_HUMAN	RecName: Full=Retinoid-inducible serine carboxypeptidase; EC=3.4.16.-; AltName: Full=Serine carboxypeptidase 1; Flags: Precursor; - OS=Homo sapiens (Human).	50.8	7	7
1020	RL12_HUMAN	RecName: Full=60S ribosomal protein L12; - OS=Homo sapiens (Human).	17.8	3	3
1021	RL7_HUMAN	RecName: Full=60S ribosomal protein L7; - OS=Homo sapiens (Human).	29.2	3	3
1022	RLA2_HUMAN	RecName: Full=60S acidic ribosomal protein P2; AltName: Full=Renal carcinoma antigen NY-REN-44; - OS=Homo sapiens (Human).	11.7	2	2
1023	RMD3_HUMAN	RecName: Full=Regulator of microtubule dynamics protein 3; Short=RMD-3; Short=hRMD-3; AltName: Full=Cerebral protein 10; AltName: Full=Protein FAM82A2; AltName: Full=Protein FAM82C; AltName: Full=Protein tyrosine phosphatase-interacting protein 51; AltName: Full=TCPTP-interacting protein 51; - OS=Homo sapiens (Human).	52.1	6	6
1024	ROA0_HUMAN	RecName: Full=Heterogeneous nuclear ribonucleoprotein A0; Short=hnRNP A0; - OS=Homo sapiens (Human).	30.8	1	1
1025	ROA2_HUMAN	RecName: Full=Heterogeneous nuclear ribonucleoproteins A2/B1; Short=hnRNP A2/B1; - OS=Homo sapiens (Human).	37.4	4	4
1026	RS10_HUMAN	RecName: Full=40S ribosomal protein S10; - OS=Homo sapiens (Human).	18.9	1	1
1027	RS12_HUMAN	RecName: Full=40S ribosomal protein S12; - OS=Homo sapiens (Human).	14.5	2	2
1028	RS14_HUMAN	RecName: Full=40S ribosomal protein S14; - OS=Homo sapiens (Human).	16.3	1	1
1029	RS16_HUMAN	RecName: Full=40S ribosomal protein S16; - OS=Homo sapiens (Human).	16.4	1	1
1030	RS18_HUMAN	RecName: Full=40S ribosomal protein S18; AltName: Full=Ke-3; Short=Ke3; - OS=Homo sapiens (Human).	17.7	1	1

1031	RS19_HUMAN	RecName: Full=40S ribosomal protein S19; - OS=Homo sapiens (Human).	16.1	1	1
1032	RS25_HUMAN	RecName: Full=40S ribosomal protein S25; - OS=Homo sapiens (Human).	13.7	1	1
1033	RS28_HUMAN	RecName: Full=40S ribosomal protein S28; - OS=Homo sapiens (Human).	7.8	1	1
1034	RT36_HUMAN	RecName: Full=28S ribosomal protein S36, mitochondrial; Short=MRP-S36; Short=S36mt; - OS=Homo sapiens (Human).	11.5	1	1
1035	S10A4_HUMAN	RecName: Full=Protein S100-A4; AltName: Full=Calvasculin; AltName: Full=Metastasin; AltName: Full=Placental calcium-binding protein; AltName: Full=Protein Mts1; AltName: Full=S100 calcium-binding protein A4; - OS=Homo sapiens (Human).	11.7	2	2
1036	S10A8_HUMAN	RecName: Full=Protein S100-A8; AltName: Full=Calgranulin-A; AltName: Full=Calprotectin L1L subunit; AltName: Full=Cystic fibrosis antigen; Short=CFAG; AltName: Full=Leukocyte L1 complex light chain; AltName: Full=Migration inhibitory factor-related protein 8; Short=MRP-8; Short=p8; AltName: Full=S100 calcium-binding protein A8; AltName: Full=Urinary stone protein band A; - OS=Homo sapiens (Human).	10.8	4	4
1037	S10AB_HUMAN	RecName: Full=Protein S100-A11; AltName: Full=Calgizzarin; AltName: Full=Metastatic lymph node gene 70 protein; Short=MLN 70; AltName: Full=Protein S100-C; AltName: Full=S100 calcium-binding protein A11; - OS=Homo sapiens (Human).	11.7	3	3
1038	S15A3_HUMAN	RecName: Full=Solute carrier family 15 member 3; AltName: Full=Osteoclast transporter; AltName: Full=Peptide transporter 3; AltName: Full=Peptide/histidine transporter 2; - OS=Homo sapiens (Human).	63.5	2	2
1039	S27A3_HUMAN	RecName: Full=Long-chain fatty acid transport protein 3; Short=FATP-3; Short=Fatty acid transport protein 3; EC=6.2.1.-; AltName: Full=Solute carrier family 27 member 3; AltName: Full=Very long-chain acyl-CoA synthetase homolog 3; Short=VLCS-3; - OS=Homo sapiens (Human).	78.6	3	3
1040	SAMH1_HUMAN	RecName: Full=SAM domain and HD domain-containing protein 1; EC=3.1.4.-; AltName: Full=Dendritic cell-derived IFNG-induced protein; Short=DCIP; AltName: Full=Monocyte protein 5; Short=MOP-5; - OS=Homo sapiens (Human).	72.2	10	10

1041	SAP3_HUMAN	RecName: Full=Ganglioside GM2 activator; AltName: Full=Cerebroside sulfate activator protein; AltName: Full=GM2-AP; AltName: Full=Shingolipid activator protein 3; Short=SAP-3; Contains: RecName: Full=Ganglioside GM2 activator isoform short; Flags: Precursor; - OS=Homo sapiens (Human).	20.8	4	4
1042	SBP1_HUMAN	RecName: Full=Selenium-binding protein 1; AltName: Full=56 kDa selenium-binding protein; Short=SBP56; Short=SP56; - OS=Homo sapiens (Human).	52.4	10	10
1043	SCPDL_HUMAN	RecName: Full=Saccharopine dehydrogenase-like oxidoreductase; EC=1.-.-.-; - OS=Homo sapiens (Human).	47.1	2	2
1044	SCRB2_HUMAN	RecName: Full=Lysosome membrane protein 2; AltName: Full=85 kDa lysosomal membrane sialoglycoprotein; Short=LGP85; AltName: Full=CD36 antigen-like 2; AltName: Full=Lysosome membrane protein II; Short=LIMP II; AltName: Full=Scavenger receptor class B member 2; AltName: CD_antigen=CD36; - OS=Homo sapiens (Human).	54.3	2	2
1045	SEP15_HUMAN	RecName: Full=15 kDa selenoprotein; Flags: Precursor; - OS=Homo sapiens (Human).	17.8	1	1
1046	SEPT9_HUMAN	RecName: Full=Septin-9; AltName: Full=MLL septin-like fusion protein MSF-A; Short=MLL septin-like fusion protein; AltName: Full=Ovarian/Breast septin; Short=Ov/Br septin; AltName: Full=Septin D1; - OS=Homo sapiens (Human).	65.4	2	2
1047	SF3B1_HUMAN	RecName: Full=Splicing factor 3B subunit 1; AltName: Full=Pre-mRNA-splicing factor SF3b 155 kDa subunit; Short=SF3b155; AltName: Full=Spliceosome-associated protein 155; Short=SAP 155; - OS=Homo sapiens (Human).	145.7	1	1
1048	SFXN3_HUMAN	RecName: Full=Sideroflexin-3; - OS=Homo sapiens (Human).	36.0	4	4
1049	SG3A1_HUMAN	RecName: Full=Secretoglobin family 3A member 1; AltName: Full=Cytokine HIN-1; AltName: Full=High in normal 1; AltName: Full=Pneumo secretory protein 2; Short=PnSP-2; AltName: Full=Uteroglobin-related protein 2; Flags: Precursor; - OS=Homo sapiens (Human).	10.1	1	1
1050	SH3L1_HUMAN	RecName: Full=SH3 domain-binding glutamic acid-rich-like protein; - OS=Homo sapiens (Human).	12.8	3	3
1051	SIAE_HUMAN	RecName: Full=Sialate O-acetylesterase; EC=3.1.1.53; AltName: Full=H-Lse; AltName: Full=Sialic	58.3	2	2

		acid-specific 9-O-acetylesterase; Flags: Precursor; - OS=Homo sapiens (Human).			
1052	SIAS_HUMAN	RecName: Full=Sialic acid synthase; AltName: Full=N-acetylneuraminate synthase; EC=2.5.1.56; AltName: Full=N-acetylneuraminate-9-phosphate synthase; EC=2.5.1.57; AltName: Full=N-acetylneuraminic acid phosphate synthase; AltName: Full=N-acetylneuraminic acid synthase; - OS=Homo sapiens (Human).	40.3	2	2
1053	SNG2_HUMAN	RecName: Full=Synaptogyrin-2; AltName: Full=Cellugyrin; - OS=Homo sapiens (Human).	24.8	1	1
1054	SNX3_HUMAN	RecName: Full=Sorting nexin-3; AltName: Full=Protein SDP3; - OS=Homo sapiens (Human).	18.8	2	2
1055	SODC_HUMAN	RecName: Full=Superoxide dismutase [Cu-Zn]; EC=1.15.1.1; AltName: Full=Superoxide dismutase 1; Short=hSod1; - OS=Homo sapiens (Human).	15.9	3	3
1056	SPTA1_HUMAN	RecName: Full=Spectrin alpha chain, erythrocytic 1; AltName: Full=Erythroid alpha-spectrin; - OS=Homo sapiens (Human).	279.8	18	18
1057	SPTB1_HUMAN	RecName: Full=Spectrin beta chain, erythrocytic; AltName: Full=Beta-I spectrin; - OS=Homo sapiens (Human).	246.3	18	18
1058	STX11_HUMAN	RecName: Full=Syntaxin-11; - OS=Homo sapiens (Human).	33.2	2	2
1059	STX7_HUMAN	RecName: Full=Syntaxin-7; - OS=Homo sapiens (Human).	29.8	2	2
1060	SYWC_HUMAN	RecName: Full=Tryptophan--tRNA ligase, cytoplasmic; EC=6.1.1.2; AltName: Full=Interferon-induced protein 53; Short=IFP53; AltName: Full=Tryptophanyl-tRNA synthetase; Short=TrpRS; Short=hWRS; Contains: RecName: Full=T1-TrpRS; Contains: RecName: Full=T2-TrpRS; - OS=Homo sapiens (Human).	53.1	4	4
1061	TAGL2_HUMAN	RecName: Full=Transgelin-2; AltName: Full=Epididymis tissue protein Li 7e; AltName: Full=SM22-alpha homolog; - OS=Homo sapiens (Human).	22.4	9	9
1062	TALDO_HUMAN	RecName: Full=Transaldolase; EC=2.2.1.2; - OS=Homo sapiens (Human).	37.5	7	7
1063	TECTA_HUMAN	RecName: Full=Alpha-tectorin; Flags: Precursor; - OS=Homo sapiens (Human).	239.4	1	1
1064	TERA_HUMAN	RecName: Full=Transitional endoplasmic reticulum ATPase; Short=TER ATPase; AltName: Full=15S Mg(2+)-ATPase p97 subunit; AltName: Full=Valosin-containing protein; Short=VCP; - OS=Homo	89.3	13	13

		sapiens (Human).			
1065	TFR1_HUMAN	RecName: Full=Transferrin receptor protein 1; Short=TR; Short=TfR; Short=TfR1; Short=Trfr; AltName: Full=T9; AltName: Full=p90; AltName: CD_antigen=CD71; Contains: RecName: Full=Transferrin receptor protein 1, serum form; Short=sTfR; - OS=Homo sapiens (Human).	84.8	17	17
1066	THIL_HUMAN	RecName: Full=Acetyl-CoA acetyltransferase, mitochondrial; EC=2.3.1.9; AltName: Full=Acetoacetyl-CoA thiolase; AltName: Full=T2; Flags: Precursor; - OS=Homo sapiens (Human).	45.2	5	5
1067	TIGAR_HUMAN	RecName: Full=Fructose-2,6-bisphosphatase TIGAR; EC=3.1.3.46; AltName: Full=TP53-induced glycolysis and apoptosis regulator; - OS=Homo sapiens (Human).	30.0	1	1
1068	TIM13_HUMAN	RecName: Full=Mitochondrial import inner membrane translocase subunit Tim13; - OS=Homo sapiens (Human).	10.5	1	1
1069	TIM8A_HUMAN	RecName: Full=Mitochondrial import inner membrane translocase subunit Tim8 A; AltName: Full=Deafness dystonia protein 1; AltName: Full=X-linked deafness dystonia protein; - OS=Homo sapiens (Human).	11.0	1	1
1070	TIM9_HUMAN	RecName: Full=Mitochondrial import inner membrane translocase subunit Tim9; - OS=Homo sapiens (Human).	10.4	1	1
1071	TM173_HUMAN	RecName: Full=Transmembrane protein 173; AltName: Full=Endoplasmic reticulum interferon stimulator; Short=ERIS; AltName: Full=Mediator of IRF3 activation; Short=hMITA; AltName: Full=Stimulator of interferon genes protein; Short=hSTING; - OS=Homo sapiens (Human).	42.2	1	1
1072	TMM43_HUMAN	RecName: Full=Transmembrane protein 43; AltName: Full=Protein LUMA; - OS=Homo sapiens (Human).	44.8	3	3
1073	TMX1_HUMAN	RecName: Full=Thioredoxin-related transmembrane protein 1; AltName: Full=Thioredoxin domain-containing protein 1; AltName: Full=Transmembrane Trx-related protein; Flags: Precursor; - OS=Homo sapiens (Human).	31.8	1	1
1074	TOM40_HUMAN	RecName: Full=Mitochondrial import receptor subunit TOM40 homolog; AltName: Full=Protein Haymaker; AltName: Full=Translocase of outer membrane 40 kDa subunit homolog; AltName:	37.9	2	2

		Full=p38.5; - OS=Homo sapiens (Human).			
1075	TOM5_HUMAN	RecName: Full=Mitochondrial import receptor subunit TOM5 homolog; - OS=Homo sapiens (Human).	6.0	1	1
1076	TPIS_HUMAN	RecName: Full=Triosephosphate isomerase; Short=TIM; EC=5.3.1.1; AltName: Full=Triose-phosphate isomerase; - OS=Homo sapiens (Human).	30.8	11	11
1077	TRI25_HUMAN	RecName: Full=E3 ubiquitin/ISG15 ligase TRIM25; EC=6.3.2.19; EC=6.3.2.n3; AltName: Full=Estrogen-responsive finger protein; AltName: Full=RING finger protein 147; AltName: Full=Tripartite motif-containing protein 25; AltName: Full=Ubiquitin/ISG15-conjugating enzyme TRIM25; AltName: Full=Zinc finger protein 147; - OS=Homo sapiens (Human).	70.9	2	2
1078	TWF2_HUMAN	RecName: Full=Twinfilin-2; AltName: Full=A6-related protein; Short=hA6RP; AltName: Full=Protein tyrosine kinase 9-like; AltName: Full=Twinfilin-1-like protein; - OS=Homo sapiens (Human).	39.5	3	3
1079	TXD12_HUMAN	RecName: Full=Thioredoxin domain-containing protein 12; EC=1.8.4.2; AltName: Full=Endoplasmic reticulum resident protein 18; Short=ER protein 18; Short=ERp18; AltName: Full=Endoplasmic reticulum resident protein 19; Short=ER protein 19; Short=ERp19; AltName: Full=Thioredoxin-like protein p19; AltName: Full=hTLP19; Flags: Precursor; - OS=Homo sapiens (Human).	19.2	1	1
1080	TXD17_HUMAN	RecName: Full=Thioredoxin domain-containing protein 17; AltName: Full=14 kDa thioredoxin-related protein; Short=TRP14; AltName: Full=Protein 42-9-9; AltName: Full=Thioredoxin-like protein 5; - OS=Homo sapiens (Human).	13.9	2	2
1081	TXTP_HUMAN	RecName: Full=Tricarboxylate transport protein, mitochondrial; AltName: Full=Citrate transport protein; Short=CTP; AltName: Full=Solute carrier family 25 member 1; AltName: Full=Tricarboxylate carrier protein; Flags: Precursor; - OS=Homo sapiens (Human).	34.0	2	2
1082	UBA1_HUMAN	RecName: Full=Ubiquitin-like modifier-activating enzyme 1; AltName: Full=Protein A1S9; AltName: Full=Ubiquitin-activating enzyme E1; - OS=Homo sapiens (Human).	117.8	9	9
1083	UBP5_HUMAN	RecName: Full=Ubiquitin carboxyl-terminal hydrolase 5; EC=3.4.19.12; AltName:	95.7	1	1

		Full=Deubiquitinating enzyme 5; AltName: Full=Isopeptidase T; AltName: Full=Ubiquitin thioesterase 5; AltName: Full=Ubiquitin-specific-processing protease 5; - OS=Homo sapiens (Human).			
1084	UFC1_HUMAN	RecName: Full=Ubiquitin-fold modifier-conjugating enzyme 1; Short=Ufm1-conjugating enzyme 1; - OS=Homo sapiens (Human).	19.4	1	1
1085	URP2_HUMAN	RecName: Full=Fermitin family homolog 3; AltName: Full=Kindlin-3; AltName: Full=MIG2-like protein; AltName: Full=Unc-112-related protein 2; - OS=Homo sapiens (Human).	75.9	4	4
1086	USMG5_HUMAN	RecName: Full=Up-regulated during skeletal muscle growth protein 5; AltName: Full=Diabetes-associated protein in insulin-sensitive tissues; AltName: Full=HCV F-transactivated protein 2; - OS=Homo sapiens (Human).	6.5	1	1
1087	VASP_HUMAN	RecName: Full=Vasodilator-stimulated phosphoprotein; Short=VASP; - OS=Homo sapiens (Human).	39.8	1	1
1088	VAT1_HUMAN	RecName: Full=Synaptic vesicle membrane protein VAT-1 homolog; EC=1.-.-.-; - OS=Homo sapiens (Human).	41.9	7	7
1089	VATB2_HUMAN	RecName: Full=V-type proton ATPase subunit B, brain isoform; Short=V-ATPase subunit B 2; AltName: Full=Endomembrane proton pump 58 kDa subunit; AltName: Full=HO57; AltName: Full=Vacuolar proton pump subunit B 2; - OS=Homo sapiens (Human).	56.5	10	10
1090	VATC1_HUMAN	RecName: Full=V-type proton ATPase subunit C 1; Short=V-ATPase subunit C 1; AltName: Full=Vacuolar proton pump subunit C 1; - OS=Homo sapiens (Human).	43.9	3	3
1091	VATF_HUMAN	RecName: Full=V-type proton ATPase subunit F; Short=V-ATPase subunit F; AltName: Full=V-ATPase 14 kDa subunit; AltName: Full=Vacuolar proton pump subunit F; - OS=Homo sapiens (Human).	13.4	2	2
1092	VATG1_HUMAN	RecName: Full=V-type proton ATPase subunit G 1; Short=V-ATPase subunit G 1; AltName: Full=V-ATPase 13 kDa subunit 1; AltName: Full=Vacuolar proton pump subunit G 1; AltName: Full=Vacuolar proton pump subunit M16; - OS=Homo sapiens (Human).	13.7	1	1
1093	VDAC1_HUMAN	RecName: Full=Voltage-dependent anion-selective channel protein 1; Short=VDAC-1; Short=hVDAC1; AltName: Full=Outer mitochondrial membrane protein porin 1; AltName:	30.8	8	7

			MW	#peptides count	#unique peptide
		Full=Plasmalemmal porin; AltName: Full=Porin 31HL; AltName: Full=Porin 31HM; - OS=Homo sapiens (Human).			
1094	VDAC2_HUMAN	RecName: Full=Voltage-dependent anion-selective channel protein 2; Short=VDAC-2; Short=hVDAC2; AltName: Full=Outer mitochondrial membrane protein porin 2; - OS=Homo sapiens (Human).	31.5	7	7
1095	VDAC3_HUMAN	RecName: Full=Voltage-dependent anion-selective channel protein 3; Short=VDAC-3; Short=hVDAC3; AltName: Full=Outer mitochondrial membrane protein porin 3; - OS=Homo sapiens (Human).	30.6	4	3
1096	VIME_HUMAN	RecName: Full=Vimentin; - OS=Homo sapiens (Human).	53.6	21	21
1097	VP13C_HUMAN	RecName: Full=Vacuolar protein sorting-associated protein 13C; - OS=Homo sapiens (Human).	422.1	1	1
1098	VPP3_HUMAN	RecName: Full=V-type proton ATPase 116 kDa subunit a isoform 3; Short=V-ATPase 116 kDa isoform a3; AltName: Full=Osteoclastic proton pump 116 kDa subunit; Short=OC-116 kDa; Short=OC116; AltName: Full=T-cell immune regulator 1; AltName: Full=T-cell immune response cDNA7 protein; Short=TIRC7; AltName: Full=Vacuolar proton translocating ATPase 116 kDa subunit a isoform 3; - OS=Homo sapiens (Human).	92.9	11	11
1099	VPS18_HUMAN	RecName: Full=Vacuolar protein sorting-associated protein 18 homolog; Short=hVPS18; - OS=Homo sapiens (Human).	110.1	1	1
1100	ZNF90_HUMAN	RecName: Full=Zinc finger protein 90; AltName: Full=Zinc finger protein HTF9; - OS=Homo sapiens (Human).	69.0	1	1
MW: molecular weight; #peptides count: sum of peptide count; #unique peptide: sum of unique peptide					